REPORT DOCUMENTATION PAGE

Public reporting burden for this collection of information is estimated to average 1 hour per response, including the time for reviewing instructions, searching existing data sources, gathering and maintaining the data needed, and completing and reviewing the collection of information. Send comment regarding this burden estimates or any other aspect of this collection of information, including suggestions for reducing this burden, to Washington Headquarters Services, Directorate for information Operations and Reports, 1215 Jefferson Davis Highway, Suite 1204, Arlington, VA 22202-4302, and to the Office of Management and Budget, Paperwork Reduction Project (0704-0188), Washington, DC 20503.

1. AGENCY USE ONLY *(Leave blank)*	2. REPORT DATE Sept 1997	3. REPORT TYPE AND DATES COVERED Final

4. TITLE AND SUBTITLE Fifth International Workshop on Computational Electronics	5. FUNDING NUMBERS DAAH04-96-1-0337
6. AUTHOR(S) Wolfgang Porod (principal investigator)	

7. PERFORMING ORGANIZATION NAMES(S) AND ADDRESS(ES) University of Notre Dame Notre Dame, IN 46556	8. PERFORMING ORGANIZATION REPORT NUMBER

9. SPONSORING / MONITORING AGENCY NAME(S) AND ADDRESS(ES) U.S. Army Research Office P.O. Box 12211 Research Triangle Park, NC 27709-2211	10. SPONSORING / MONITORING AGENCY REPORT NUMBER ARO 36171.1-EL-CF

11. SUPPLEMENTARY NOTES

The views, opinions and/or findings contained in this report are those of the author(s) and should not be construed as an official Department of the Army position, policy or decision, unless so designated by other documentation.

12a. DISTRIBUTION / AVAILABILITY STATEMENT Approved for public release; distribution unlimited.	12 b. DISTRIBUTION CODE

13. ABSTRACT The Fifth International Workshop on Computational Electronics (IWCE-5) was held on the campus of the University of Notre Dame, May 28-30, 1997. As in previous IWCE meetings, the workshop covered all aspects of advanced simulation of electronic transport in semiconductors and semiconductor devices, particularly those which use large computational resources. More specifically, IWCE-5 focused on the following three major themes: (i) Device Simulation, (ii) Optoelectronics, and (iii) Quantum Simulation. IWCE-5 attracted 168 registered participants, and featured 15 invited speakers, 40 oral presentations, and 75 poster papers. As a novelty, IWCE-5 included an evening session with hands-on software demonstrations.

14. SUBJECT TERMS	15. NUMBER IF PAGES
DTIC QUALITY INSPECTED	16. PRICE CODE

17. SECURITY CLASSIFICATION OR REPORT UNCLASSIFIED	18. SECURITY CLASSIFICATION OF THIS PAGE UNCLASSIFIED	19. SECURITY CLASSIFICATION OF ABSTRACT UNCLASSIFIED	20. LIMITATION OF ABSTRACT UL

FINAL REPORT

TO THE

ARMY RESEARCH OFFICE

FOR SUPPORT OF THE

FIFTH INTERNATIONAL WORKSHOP
ON COMPUTATIONAL ELECTRONICS
Notre Dame, May 28 - 30, 1997

CONFERENCE CHAIR

Wolfgang Porod

DEPARTMENT OF ELECTRICAL ENGINEERING

UNIVERSITY OF NOTRE DAME

SUBMITTED ON
SEPTEMBER 30, 1997
TO THE
U.S. ARMY RESEARCH OFFICE
ATTN: Information Control and Analysis (Library)
P.O. Box 12211
RESEARCH TRIANGLE PARK, NC 27709-2211

ABSTRACT

The Fifth International Workshop on Computational Electronics (IWCE-5) was held on the campus of the University of Notre Dame, May 28-30, 1997. As in previous IWCE meetings, the workshop covered all aspects of advanced simulation of electronic transport in semiconductors and semiconductor devices, particularly those which use large computational resources. More specifically, IWCE-5 focused on the following three major themes: (i) Device Simulation, (ii) Optoelectronics, and (iii) Quantum Simulation. IWCE-5 attracted 168 registered participants, and featured 15 invited speakers, 40 oral presentations, and 75 poster papers. As a novelty, IWCE-5 included an evening session with hands-on software demonstrations.

Sponsorship for IWCE-5 was provided by the National Science Foundation, the Office of Naval Research, the Army Research Office, and the Notre Dame Department of Electrical Engineering and the College of Engineering. These funds were used for invited speakers (travel, registration, and lodging), partial student travel support, publication and mailing costs (including the abstract booklet and the forthcoming proceedings), conference facilities, and for local support (supplies and travel to NCCE at the Beckman Institute for W. Porod). A registration fee was charged for each participant to cover the costs for conference materials and meals, including a reception and the conference banquet.

The Army Research Office provided partial support for IWCE-5 in the amount of $6,000 which was used primarily for the support of invited speakers.

Fifth International Workshop on Computational Electronics

The Fifth International Workshop on Computational Electronics (IWCE-5) was held in the Center for Continuing Education on the campus of the University of Notre Dame from May 28-30, 1997. The workshop is intended to be an international forum for the discussion on the current trends and the future directions of computational electronics. As in previous IWCE's, this meeting covered all aspects of advanced simulation of electronic transport in semiconductors and semiconductor devices, particularly those which use large computational resources. The conference consisted of sessions with invited and contributed presentations, and poster papers. Session topics included:

- Device Simulation I, II & III

- Optoelectronics

- Modeling for ULSI

- Thermal Effects

- Molecular Structures

- Mathematical Models

- High Performance Computing

- Quantum Simulation I & II, and Quantum Structures

- Software Development and Software Demonstration

The emphasis of the contributions was on interdisciplinary aspects of Computational Electronics, encompassing Applied Physics, Engineering and Applied Mathematics. There were no parallel sessions, in keeping with the tradition of previous IWCE's. Participation of graduate students, including student poster papers, was strongly encouraged.

An International Advisory Committee helped in giving shape to IWCE-5, including the nomination of session topics and invited speakers. The Program Committee selected contributed and poster papers from among the submitted abstracts.

The conference venue was the Center for Continuing Education on the Notre Dame campus. All meals were provided on site (included in the registration fee) in order to provide a true workshop environment, allowing participants to stay together for discussions and interactions.

Invited Speakers

The main attraction of any meeting are its *Invited Speakers*. The selection process started with nominations made at the planning meeting held at the Beckman Institute in early Fall '96. *Invited Speakers* had to be internationally recognized experts in the field, and they were expected to help provide an introduction to the contributed papers in each session. After much deliberation (mostly by e-mail) by the Advisory and Program Committees, 15 speakers, including a dinner talk, were invited. The following individuals were *Invited Speakers* at IWCE-5:

- **Jeff D. Bude**, *Bell Labs, Lucent Technologies*

- **Emmanuel Crabbé**, *IBM*

- **David K. Ferry**, *Arizona State Univ.*

- **Wei-Ping Huang**, *University of Waterloo, Canada*

- **Gerhard Klimeck**, *Corporate R&D, Texas Instruments Inc.*

- **Günter Mahler**, *Oregon Center of Optics and Univ. Stuttgart, Germany*

- **Jerry Mar**, *Intel*

- **Shinji Onga**, *Toshiba, Japan*

- **Mark A. Ratner**, *Northwestern Univ.*

- **Kent Smith**, *Bell Laboratories, Lucent Technologies*

- **Christopher Snowden**, *Univ. Leeds, UK*

- **Shin-ichi Takagi**, *Toshiba, Japan*

- **Harold Trease**, *Los Alamos National Laboratory*

- **Peter Vogl**, *TU Munich*, Germany

- **Kiyoyuki Yokoyama**, *NTT, Japan*

IWCE-5 had a larger number of *Invited Speakers* (15) than previous IWCE's (typically, 10). This is due to a couple of invited sessions, as well as an extra evening session and the banquet talk. Also, the Japanese representation was increased with 3 *Invited Speakers*, as compared to only 1 at previous IWCE's. Financial support for *Invited Speakers* included registration and hotel expenses, and partial travel support.

Participation at IWCE-5:

IWCE-5 attracted 168 registered participants, and featured 15 invited speakers, 40 oral papers, and 75 poster presentations. Participation by Japanese and European researchers was particularly strong. This makes it the largest IWCE event so far.

Looking back at previous IWCE's, the first International Workshop on Computational Electronics was held on May 28-29, 1992, at the Beckman Institute of the University of Illinois at Urbana-Champaign and attracted some 100 US scientists and engineers. In 1993, the IWCE was held in Europe, at the University of Leeds (UK) with over 60 participants. The third workshop took place on May 18-20, 1994 in Portland, Oregon, and the fourth on October 30 - November 1, 1995 in Tempe, Arizona. The attendance at both events was again around 100 participants.

Student Support:

Approximately 15 student stipends were awarded to help support and encourage participation by graduate students in the workshop. The availability of limited student support was advertised and information given on how to apply for such support. The most important criterion for support was having an accepted paper at the workshop.

Dissemination of Results:

There are two venues for the dissemination of the workshop results:
    (1) published proceedings, and
    (2) the conference abstract booklet.

The *IWCE-5 Proceedings* will be published as a special issue of the journal *VLSI Design*, as was also done for the proceedings of the Tempe workshop. At the time of the writing of this report, the submitted final and revised papers had been forwarded to the editors of *VLSI Design* for type-setting and publication. Each workshop participant will receive a copy of the *Proceedings* as part of the registration cost. Interested individuals or libraries/institutions may purchase additional copies from *Gordon and Breach Science Publishers*.

Upon registration at the conference site, each participant received the IWCE-5 workshop-booklet which contained all abstracts and the conference program.

IWCE-5 Chronology and Dates:

- Summer, 1996   Preliminary Announcement distributed at various conferences

- Aug. 8, 1996   Preliminary Announcement (sent by e-mail)

- Sep. 30 & Oct. 1, '96   NCCE planning meeting at the Beckman Institute

- Nov. 27, 1996   First Call for Papers (sent by e-mail)

- Jan. 6, 1997   Call for Papers (sent by e-mail and brochure mailed)

- Feb. 6, 1997   Last Call for Papers (sent by e-mail)

- Feb. 14, 1997   Deadline for abstracts

- Mar. 31, 1997   Notification of acceptance (sent by e-mail and regular mail)

- Apr. 16, 1997   Instructions for manuscript preparation (sent by e-mail)

- Apr. 29, 1997   Reminder for early registration cutoff (sent by e-mail)

- Apr. 30, 1997   Early registration cutoff, last day to guarantee room

- **May 28-30, 1997**   **Workshop** (manuscripts collected and reviewed for proceedings)

- June 3, 1997   Notification of manuscript acceptance (sent by regular mail)

- July 15, 1997   Final (revised) manuscripts due for proceedings

- July 31, 1997   Manuscripts sent to Editor of *VLSI Design*

IWCE-5 WorldWideWeb Site:

In order to facilitate communication with prospective IWCE-5 participants, a WWWpage was maintained for the workshop. This site contains information about conference mailings, the workshop program, and travel information to Notre Dame. This page may be found at URL:

http://www.nd.edu/~iwce97/

Sponsorship:

Partial financial sponsorship was provided from the following agencies and institutions:

- National Science Foundation (Dr. George Lea)

- Office of Naval Research (Dr. Larry Cooper)

- Army Research Officer (Dr. Michael Stroscio)

- National Center for Computational Electronics (NCCE)

- Notre Dame Department of Electrical Engineering and College of Engineering
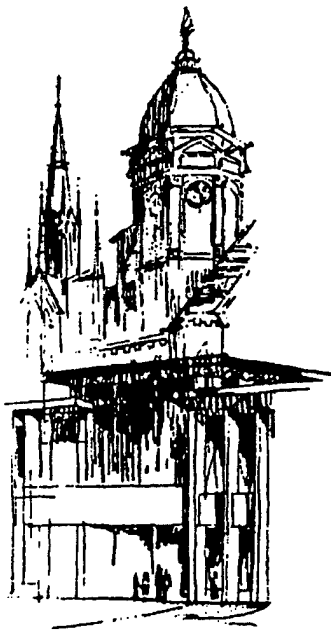
Technical co-sponsorship was provided by the IEEE Electron Devices Society.

Conference Budget:

Sponsor funds were used for invited speakers (travel, registration, and lodging), partial student travel support, publication and mailing costs (including the abstract booklet and the forthcoming proceedings), conference facilities, and for local support (supplies and travel to NCCE at the Beckman Institute for W. Porod).

No sponsor funds were budgeted for food and beverages. A registration fee was charged for each participant to cover the costs for conference materials and meals, including a reception and the conference banquet

Conference Program

Fifth International Workshop on Computational Electronics

IWCE-5

Notre Dame, Indiana
May 28-30, 1997

All sessions and social events will be held at the Center for Continuing Education (CCE) on the campus of the University of Notre Dame.

TUESDAY, May 27   **Registration and Reception**

4:00 - 9:00 pm   Registration

7:00 - 9:00 pm   Reception (food and drinks will be available)

Sponsors:

- National Science Foundation
- Office of Naval Research
- Army Research Office
- Univ. Notre Dame College of Engineering
- Univ. Notre Dame Department of Electrical Engineering
- Technical Co-Sponsorship, IEEE Electron Devices Society

IWCE-5 Committees:

Chairman:

Wolfgang Porod   Univ. Notre Dame

Program Committee:

Jeff Bude   Lucent
Bob Dutton   Stanford Univ.
Chihiro Hamaguchi   Osaka Univ., Japan
Steve Goodnick   Arizona State Univ.
Steve Laux   IBM
Craig Lent   Univ. Notre Dame
Mark Lundstrom   Purdue Univ.
Hiroshi Mizuta   Hitachi Cambridge, UK
Umberto Ravaioli   Univ. Illinois
Chris Ringhofer   Arizona State Univ.
Chris Snowden   Univ. Leeds, UK

Advisory Committee:

G. Baccarani   Univ. Bologna, Italy
Herb Bennett   NIST
Felix Buot   NRL
Larry Cooper   ONR
W. M. Coughran, Jr. Lucent
David Ferry   Arizona State Univ.
Wolfgang Fichtner   ETH Zurich, Switzerland
Max Fischetti   IBM
Bill Frensley   Univ. Texas at Dallas
Masao Fukuma   NEC, Japan
Hal Grubin   SRA
Karl Hess   Univ. Illinois
Gerald Iafrate   ARO
Joseph W. Jerome   Northwestern Univ.
Thomas Kerkhoven   Univ. Illinois
Tom McGill   Cal Tech
Donald J. Rose   Duke Univ.
Kent Smith   Lucent
Christopher Stanton Univ. Florida
Mike Stroscio   ARO
Al F. Tasch   Univ. Texas at Austin
Peter Vogl   TU Munich, Germany
Kiyoyuki Yokoyama   NTT, Japan
Naoki Yokoyama   Fujitsu, Japan

7:00 - 8:00   BREAKFAST

8:15 - 8:30   Welcome and Opening Remarks
- Daniel Costello, Chair of Electrical Engineering
- Jeffrey Kantor, Vice President and Associate Provost
- Karl Hess, Director, National Center for Computational Electronics

8:30 a.m.   Session *"Device Simulation I"* Chair: *Massimo Fischetti*

8:30 - 9:00   WeA1   Merits and Faults of Sub-Micron Device Simulation from a Designer Perspective (Invited), **Emmanuel Crabbé**, *IBM*

9:00 - 9:30   WeA2   Two-Dimensional Carrier Transport in Si MOSFETs (Invited), **Shin-ichi Takagi**, *Toshiba, Japan*

9:30 - 10:00   WeA3   Monte Carlo Simulations of Impact Ionization Feedback (Invited), **Jeff D. Bude**, *Bell Labs, Lucent Technologies*

10:00 - 10:30   COFFEE BREAK

10:30 a.m.   Session *"Device Simulation II"* Chair: Christine Maziar

10:30 - 10:45   WeA4   Numerical Simulation of MOSFETs Using Nonequilibrium Quantum Field Theory, **Dejan Jovanovic, Ulvi Erdogan, Chris Bowen**, and **Roger Lake**, *Texas Instruments*

10:45 - 11:00   WeA5   Inclusion of Quantum Confinement Effects in Self-Consistent Monte Carlo Device Simulations, **R. W. Kelsall** and **A. J. Lidsey**, *Univ. Leeds, UK*

11:00 -11:15   WeA6   Two Dimensional Modeling of HEMTs Using Multigrids with Quantum Corrections, **Eric A. B. Cole, Tobias Boettcher**, and **Christopher M. Snowden**, *Univ. Leeds, UK*

11:15 - 11:30   WeA7   p-Si Monte Carlo Simulator for Deep Submicron MOS Devices, **N. A. Bannov, W. C. Holton**, and **K. W. Kim**, *North Carolina State Univ.*

11:30 - 11:45   WeA8   MOMENTS: The Modular Monte Carlo Environment for Charge Transport Simulation - Overview and Applications, **Mark Peskin** and **Christine Maziar**, *Univ. Texas at Austin*

11:45 - 12:00   WeA9   High-Field Hole Transport in Strained Si and SiGe by Monte Carlo Simulation: Full Band versus Analytic Band Model, **F. M. Bufler, P. Graf**, and **B. Meinerzhagen**, *Univ. Bremen, Germany*

12:00 - 1:30		LUNCH

1:30 p.m.   Session *"Modeling for ULSI"* Chair: *Ting-wei Tang*

1:30 - 2:00   WeP1   Hierarchical Simulation for ULSI Process Design - From Atomistic to Conventional Process CAD (Invited), **S. Onga, T. K. Okada, H. Takada, T. Koyanagi**, *Toshiba, Japan*, **E. Kan** and **R. W. Dutton**, *Stanford Univ.*

2:00 - 2:15   WeP2   Necessary Roughness of MOS Interface for Device Simulation, **Edwin C. Kan, Heng-Chih Lin**, and **Robert W. Dutton**, *Stanford Univ.*

2:15-2:30   WeP3   Non-Uniformity Effects in Ultra-Thin Tunneling Oxides, **D. Z.-Y. Ting, Erik S. Daniel**, and **T. C. McGill**, *Cal Tech*

2:30 - 2:45   COFFEE BREAK

2:45 p.m.   Session *"Thermal Effects"* Chair: *Umberto Ravaioli*

2:45 - 3:15   WeP4   Modeling of Thermal Effects in Semiconductor Structures (Invited), **Christopher Snowden**, *Univ. Leeds, UK*

3:15 - 3:30   WeP5   Carrier Thermal Conductivity: Analysis and Application to Sub-micron-Device Simulation, **A. Greiner** and **L. Reggiani**, *Univ. Lecce, Italy*, **T. Kuhn**, *Univ. Münster*, Germany, **L. Varani**, *Univ. Montpellier, France*, **P. Golinelli**, *Univ. Modena, Italy*, **M. C. Vecchi**, *Univ. Bologna, Italy*

3:30 - 3:45   WeP6   Heat Dissipation from Quantum Structures, **V. V. Mitin, G. Paulavicius, N. Bannov**, *Wayne State Univ.*, and **M. A. Stroscio**, *U.S. Army Research Office*

3:45 - 4:00   COFFEE BREAK

4:00 p.m.   Session *"Molecular Structures"* Chair: *Craig Lent*

4:00 - 4:30   WeP7   Molecular Wires: Conductance, Geometric Dependence, Energetics, Electron Repulsion and Their Relationship to Intramolecular Electron Transfer (Invited), **Mark A. Ratner**, *Northwestern Univ.*

4:30 - 4:45   WeP8   Simulation of Molecular Electronic Devices, **Weidong Tian** and **Supriyo Datta**, *Purdue Univ.*

4:45 - 5:00   WeP9   Drift-Diffusion Equations Describe an Important Biological System: Ionic Channels in Membranes, **R. S. Eisenberg**, *Rush Medical Center, Chicago*

5:00 - 6:30		POSTER VIEWING (food and drinks will be available)
6:30 p.m.		Session *"Software Development"* Chair: *Henry Harbury*

6:30 - 7:00   WeE1   The NEMO Project or Writing Research Software in a Large Group (Invited), **Gerhard Klimeck, Dan Blanks, Roger Lake, R. Chris Bowen, Manhua Leng, Chenjing L. Fernando, William R. Frensley, Dejan Jovanovic,** and **Paul Sotirelis,** *Corporate R&D, Texas Instruments Inc.* and *School of Engineering, Univ. of Texas at Dallas*

7:00 - 7:30   Software Demo Previews (short presentations)

7:30 - 9:00   Software Demos (food and drinks will be available)

Bob Dutton et al., *Stanford Univ.*	Device and Process Simulation Tools
Bill Frensley, *UT Dallas*	Interactive Modeling and Design Tools
Neil Goldsman et al., *Univ. Maryland*	Spherical Harmonics and Hydrodynamic Simulation Tools
Harold Grubin, *Scientific Res. Assoc.*	PC Windows Interactive Modeling of Quantum Devices
Gerhard Klimeck, Dejan Jovanovic, Roger Lake, et al., *TI*	NEMO - Nanotechnology Engineering MOdeling program
Steve Laux and Max Fischetti, *IBM*	DAMOCLES - Device Analysis using MOnte CarLo Et poisson Solver
Craig Lent et al., *Univ. Notre Dame*	AQUINAS - A QUantum Interconnected Network Array Simulator
Mark Lundstrom and Umberto Ravaioli, Purdue and Illinois	"Simulation Hub," an Online Simulation Laboratory
Hans Kosina and Christian Troger, *Techn. Univ. Vienna*	SPIN - Schrödinger Poisson Solver Including Non-Parabolicity
Michael Obrecht, Siborg Systems, Inc	MicroTec: Educational 2D Semiconductor Process/Device Simulator for a PC
Christoph Wasshuber, *Techn. Univ. Vienna*	SIMON - Single-Electron Device and Circuit Simulator

7:00 - 8:00		BREAKFAST

8:30 a.m. — Session *"Optoelectronics"* Chair: *Karl Hess*

8:30 - 9:00 ThA1 — Photonic Device Modeling for Telecommunication Purposes (Invited), **Kiyoyuki Yokoyama**, *NTT, Japan*

9:00 - 9:30 ThA2 — Modeling and Simulation of Semiconductor DFB Lasers: A Hierarchical Approach (Invited), **Wei-Ping Huang** and **Xun Li**, *University of Waterloo, Canada*

9:30 - 10:00 ThA3 — Numerical Methods for Semiconductor Laser Simulations (Invited), **R. K. Smith, M. A. Alam, G. A. Baraff, M. S. Hybertsen**, *Bell Laboratories, Lucent Technologies*

10:00 - 10:15 ThA4 — Theory and Modeling of Lasing Modes in Vertical Cavity Surface Emitting Lasers, **Benjamin Klein, Leonard F. Register, Karl Hess**, *Univ. Illinois at Urbana-Champaign*, and **Dennis G. Deppe**, *Univ. Texas at Austin*

10:15 - 10:45 — COFFEE BREAK

10:45 a.m. — Session *"Device Simulation III"* Chair: Steve Goodnick

10:45 - 11:15 ThA5 — Cellular Automaton Study of Time-Dynamics of Avalanche Breakdown in IMPATT Diodes (Invited), **G. Zandler**, *TU Munich, Germany*, **M. Saraniti**, *Arizona State Univ.*, **P. Vogl**, *TU Munich, Germany*, **P. Lugli**, *Univ. Rome, Italy*

11:15 - 11:30 ThA6 — 3D Parallel Finite Element Simulation of In-Cell Breakdown in Lateral-Channel IGBTs, **A. R. Brown, A. Asenov**, and **J. R. Barker**, *Univ. Glasgow, UK*

11:30 - 11:45 ThA7 — Comparison of Iteration Schemes for the Solution of the Multidimensional Schrödinger-Poisson Equations, **A. Trellakis, A. T. Galik, A. Pacelli**, and **U. Ravaioli**, *Univ. Illinois at Urbana-Champaign*

11:45 -12:00 ThA8 — Cellular Automata Studies of Vertical Silicon Devices, **M. Saraniti**, *Arizona State Univ.*, **G. Zandler**, *TU Munich, Germany*, and **S. Goodnick**, *Arizona State Univ.*

12:00 - 1:30 — LUNCH

1:30 p.m. — Session *"High Performance Computing"* Chair: *Bill Coughran*

1:30 - 2:00 ThP1 — Large Scale Distributed Parallel Computing (Invited), **Harold Trease**, *Los Alamos National Laboratory*

2:00 - 2:15 ThP2 — X3D Moving Grid Methods for Semiconductor Applications, **Denise George, David Cartwright, J. Tinka Gammel, Brian Kendrick, David Kilcrease, Andrew Kuprat, Harold Trease**, and **Robert Walker**, *Los Alamos National Laboratory*

2:15 - 2:30	ThP3	The Finite-Volume Scharfetter-Gummel Method for Steady Convection-Diffusion Equations, **Randolph E. Bank**, *UC San Diego*, **W. M. Coughran, Jr.**, and **Lawrence C. Cowsar**, *Bell Labs, Lucent Technologies*
2:30 - 2:45	ThP4	Multilevel Algorithms for Large-Scope Molecular Dynamics Simulations of Nanostructures on Parallel Computers, **Aiichiro Nakano**, **Rajiv K. Kalia**, and **Priya Vashishta**, *Louisiana State Univ.*
2:45 - 3:00	ThP5	Ensemble Monte Carlo and Full-Wave Electrodynamics Models Implemented Self-Consistently on a Parallel Processor Using Perfectly Matched Layer Boundary Conditions, **Ik-Sung Lim**, *Motorola*, **Robert O. Grondin** and **Samir El-Ghazaly**, *Arizona State Univ.*
3:00 - 3:30		COFFEE BREAK
3:30 p.m.		Session *"Mathematical Models"* Chair: *Joe Jerome*
3:30 - 3:45	ThP6	Applicability of the High Field Model: An Analytical Study via Asymptotic Parameters Defining Domain Decomposition, **Carlo Cercignani**, *Politecnico di Milano, Italy*, **Irene Gamba**, *Courant Institute, New York Univ.*, **Joseph Jerome**, *Northwestern Univ.*, and **Chi-Wang Shu**, *Brown Univ.*
3:45 - 4:00	ThP7	Smooth QHD Simulation of the Resonant Tunneling Diode, **Carl L. Gardner** and **Christian Ringhofer**, *Arizona State Univ.*
4:00 - 4:15	ThP8	Spherical Harmonic Analysis of a 0.05 μm Base BJT: Monte Carlo-Type Results but a Thousand Times Faster, **C.-H. Chang**, **C.-K. Lin**, **N. Goldsman**, and **I. D. Mayergoyz**, *Univ. Maryland*
4:15 - 4:30	ThP9	Numerical Examination of Photon Recycling as an Explanation of Observed Carrier Lifetime in Direct Bandgap Materials, **Joseph W. Parks, Jr.**, **Kevin F. Brennan**, *Georgia Tech*, and **Arlynn W. Smith**, *ITT Night Vision*
4:30 - 4:45	ThP10	A Semi-Classical Description of Electron Transport in Semiconductor Quantum Well Devices, **Gene A. Baraff**, *Lucent Technologies Bell Labaratories*
4:45 - 5:00	ThP11	Electronic Structure Calculations Using an Adaptive Wavelet Basis, **D. A. Richie**, **P. von Allmen**, **K. Hess**, and **R. Martin**, *Univ. Illinois at Urbana-Champaign*
5:00 - 7:00		POSTER VIEWING (snacks and drinks will be available)
7:00 - 9:00		BANQUET
	Dinner Talk	The Art, Science, and Challenges of Simulating Advanced Devices, **Jerry Mar**, *Intel* (Introduced by *Jerry Iafrate*)

| 7:00 - 8:00 | | BREAKFAST |

8:30 a.m. 　　　　　Session *"Quantum Simulation I"* Chair: *Chihiro Hamaguchi*

| 8:30 - 9:00 | FrA1 | Open Problems in Quantum Simulation in Ultra-Submicron Devices (Invited), **David K. Ferry**, *Arizona State Univ.*, and **John R. Barker**, *Univ. Glasgow, UK* |

| 9:00 - 9:15 | FrA2 | Theory of Electron Transport in Small Semiconductor Devices Using the Pauli Master Equation, **M. V. Fischetti**, *IBM Research Division* |

| 9:15 - 9:30 | FrA3 | Modeling of Nano-Scale Ballistic Field-Effect Transistors, **F. G. Pikus** and **K. K. Likharev**, *SUNY Stony Brook* |

| 9:30 - 9:45 | FrA4 | Quantum Transport in Open Nanostructures, **I. V. Zozoulenko** and **K.-F. Berggren**, *Linköping Univ., Sweden* |

| 9:45 - 10:00 | FrA5 | Application of the Wigner-Function Formulation to Mesoscopic Systems in Presence of the Electron-Phonon Interaction, **C. Jacoboni, A. Abramo, P. Bordone, R. Brunetti**, and **M. Pascoli**, *Univ. Modena, Italy* |

| 10:00 - 10:30 | | COFFEE BREAK |

10:30 a.m. 　　　　　Session *"Quantum Simulation II"* Chair: *Bill Frensley*

| 10:30 -11:00 | FrA6 | Quantum Networks: Dynamics of Open Nanostructures (Invited), **Günter Mahler**, *Oregon Center of Optics and Univ. Stuttgart, Germany* |

| 11:00 - 11:15 | FrA7 | A Generalized Monte Carlo Approach for the Analysis of Quantum-Transport Phenomena in Mesoscopic Systems: Interplay between Coherence and Relaxation, **Fausto Rossi**, *Univ. Modena, Italy*, **Stefano Ragazzi, Aldo Di Carlo**, and **Paolo Lugli**, *Univ. Roma, Italy* |

| 11:15 - 11:30 | FrA8 | Coherent Control of Light Absorption in Semiconductor Nanostructures, **W. Pötz and X. Hu**, *Univ. Illinois at Chicago* |

| 11:30 -11:45 | FrA9 | A New Computational Approach to Photon-Assisted Tunneling in Intense Driving Fields Based on a Fabry-Perot Analogy, **Mathias Wagner**, *Hitachi Cambridge, UK* |

| 11:45 -12:00 | FrA10 | Phase Space Boundary Conditions and Quantum Device Transport, **H. L. Grubin** and **J. R. Caspar**, *Scientific Research Associates, Inc.*, and **D. K. Ferry**, *Arizona State Univ.* |

12:00 - 1:30		LUNCH

1:30 p.m.   Session *"Quantum Structures"* Chair: *Hal Grubin*

1:30 -1:45   FrP1   Single-Electron Memories, **Christoph Wasshuber, Hans Kosina**, and **Siegfried Selberherr**, *TU Vienna, Austria*

1:45 - 2:00   FrP2   Electron-LA Phonon Interaction in a Quantum Dot, **T. Ezaki, N. Mori**, and **C. Hamaguchi**, *Osaka Univ., Japan*

2:00 - 2:15   FrP3   Numerical Analysis of Asymmetric Single Electron Turnstiles Using Monte Carlo Simulation, **Masaharu Kirihara** and **Kenji Taniguchi**, *Osaka Univ., Japan*

2:15 - 2:30   FrP4   Self-Consistent Calculation of the Ground State and the Capacitance of a 3D Si/SiO_2 Quantum Dot, **A. Scholze, A. Wettstein, A. Schenk**, and **W. Fichtner**, *ETH-Zürich, Switzerland*

2:30 - 2:45   FrP5   An Interband Tunneling Oscillator: Self-Oscillations of Trapped Hole Charge in a Double-Barrier Structure, **F. A. Buot**, *U.S. Naval Research Laboratory*

2:45 - 3:00   FrP6   Tunneling between Multimode Stacked Quantum Wires, **M. Macucci**, *Univ. Pisa, Italy*, **A. T. Galick** and **U. Ravaioli**, *Univ. Illinois at Urbana-Champaign*

3:00 - 3:15   FrP7   Ballistic Directional Coupler on the DQW-Basis, **A. N. Korshak, Z. S. Gribnikov, N. Z. Vagidov, S. I. Kozlovsky**, and **V. V. Mitin**, *Institute of Semiconductor Physics, Kiev, Ukraine and Wayne State Univ.*

CONFERENCE CLOSE

POSTER PRESENTATIONS

P1 Monte Carlo Simulation of Non-local Transport Effects in Strained Si on Relaxed $Si_{1-x}Ge_x$ Heterostructures, **F. Gámiz, J. B. Roldán**, and **J. A. López-Villanueva**, *Univ. Granada, Spain*

P2 A β-SiC MOSFET Monte Carlo Simulator Including Inversion Layer Quantization, **F. Gámiz, J. B. Roldán**, and **J. A. López-Villanueva**, *Univ. Granada, Spain*

P3 A Closed-Loop Evaluation and Validation of a Method for Determining the Dependence of the Electron Mobility on the Longitudinal-Electric Field in MOSFETs, **J. B. Roldán, F. Gámiz**, and **J. A. López-Villanueva**, *Univ. Granada, Spain*

P4 Quantum Distribution-Function Transport Equations in Non-Normal Systems and in Ultra-Fast Dynamics of Optically-Excited Semiconductors, **F. A. Buot**, *U.S. Naval Research Laboratory*

P5 Applicability of the High Field Model: A Preliminary Numerical Study, **Carlo Cercignani**, *Politecnico di Milano, Italy*, **Irene Gamba**, *Courant Institute, New York University*, **Joseph Jerome**, *Northwestern Univ.*, and **Chi-Wang Shu**, *Brown Univ.*

P6 Simulation of Bistable Laser Diodes with Inhomogeneous Excitation, **Gang Fang** and **Ting-wei Tang**, *Univ. Massachusetts*

P7 Intersubband Relaxation in Step Quantum Well Structures, **J. P. Sun, H. B. Teng, G. I. Haddad**, *Univ. Michigan*, and **M. A. Stroscio** and **G. J. Iafrate**, *U.S. Army Research Office*

P8 Symplectic Finite-Element Time-Domain Method for Optical Field Analysis, **T. Hirono, W. Lui**, and **K. Yokoyama**, *NTT, Japan*

P9 Resonances in Conductance through Tunable Attractors, **Yong S. Joe, Tian Xie**, and **Ronald M. Cosby**, *Ball State Univ.*

P10 A New Method to Overcome the Divergent Problem in Numerical Modeling of Power 6H-SiC Devices, **Edward H. S. Hsing** and **Jeffrey L. Gray**, *Purdue Univ.*

P11 Convergence Properties of the Bi-CGSTAB Method for the Solution of the 3D Poisson and 3D Electron Current Continuity Equations for Scaled Si MOSFETs, **D. Vasileska, W. J. Gross, V. Kafedziski**, and **D. K. Ferry**, *Arizona State Univ.*

P12 Wave-function Scarring Effects in Open Ballistic Quantum Cavities, **R. Akis** and **D. K. Ferry**, *Arizona State Univ.*

P13 Complete RF Analysis of Compound FETs based on Transient Monte Carlo Simulation, **S. Babiker, A. Asenov, N. Cameron, S. P. Beaumont**, and **J. R. Barker**, *Glasgow Univ., UK*

P14 Monte Carlo Calibrated Drift-Diffusion Simulation of Short Channel HFETs, **A. Asenov, S. Babiker, S. P. Beaumont**, and **J. R. Barker**, *Glasgow Univ., UK*
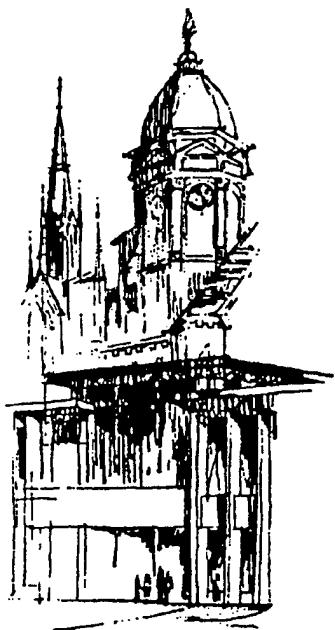
P15 RF Performance of Si/SiGe MODFETs: A Simulation Study, **S. Roy, A. Asenov, J. R. Barker**, and **S. P. Beaumont**, *Univ. Glasgow, UK*

P16 Ab-Initio Coulomb Scattering in Atomistic Device Simulation, **C. R. Arokianathan, J. H. Davies**, and **A. Asenov**, *Univ. Glasgow, UK*

P17 A New Approach for Obtaining Self-Consistent Solutions to the Coupled Schrödinger and Poisson System in Multiquantum Well Structures, **Fred Gelbard** and **Kevin J. Malloy**, *Univ. New Mexico*

P18 Numerical Evaluation of Iterative Schemes for Drift-Diffusion Simulation, **M. B. Patil, U. Ravaioli**, and **T. Kerkhoven**, *Univ. Illinois at Urbana-Champaign*

P19 Simulation of Si-MOSFETs with the Mutation Operator Monte Carlo Method and Evolutionary Optimization, **J. Jakumeit**, *Univ. Köln*, **A. Duncan, U. Ravaioli**, and **K. Hess**, *Univ. Illinois at Urbana-Champaign*

P20 A New HEMT Breakdown Model Incorporating Gate and Thermal Effects, **Lufti Albasha, Christopher M. Snowden**, and **Roger D. Pollard**, *Univ. Leeds, UK*

P21 Rate Equation Modelling of Nonlinear Dynamics in Directly Modulated Multiple Quantum Well Laser Diodes, **S. Bennett, C. M. Snowden**, and **S. Iezekiel**, *Univ. Leeds, UK*

P22 Temperature Dependence of the Electron and Hole Scattering Mechanisms in Silicon Analysed through a Full-Band, Spherical-Harmonics Solution of the BTE, **S. Reggiani, M. C. Vecchi**, and **M. Rudan**, *Univ. Bologna, Italy*

P23 Monte Carlo Simulation of Intersubband Hole Relaxation in a GaAs/AlAs Quantum Well, **R. W. Kelsall**, *Univ. Leeds, UK*

P24 VLSI Yield Prediction Using a Pattern-Recognition Based Critical Area Algorithm, **J. H. N. Mattick, R. W. Kelsall**, and **R. E. Miles**, *Univ. Leeds, UK*

P25 Bi-dimensional Simulation of the Simplified Hydrodynamic and Energy-Transport Models for Heterojunction Semiconductor Devices Using Mixed Finite Elements, **A. Marrocco** and **Ph. Montarnal**, *INRIA, Le Chesnay Cedex, France*

P26 Semiconductor Device Noise Computation Based on the Deterministic Solution of the Poisson and Boltzmann Transport Equations, **Alfredo J. Piazza** and **Can E. Korman**, *George Washington Univ.*

P27 Consistent Hydrodynamic and Monte-Carlo Simulation of SiGe HBTs Based on Table Models for the Relaxation Times, **B. Neinhüs, S. Decker, P. Graf, F. M. Bufler**, and **B. Meinerzhagen**, *Univ. Bremen, Germany*

P28 Additive Decomposition of the Drift-Diffusion Model, **Elizabeth J. Brauer, Marek Turowski**, and **James M. McDonough**, *Univ. Kentucky*

P29 Supersymmetric Quantum Mechanics (SUSY-QM) Applied to Quantum-Wire Devices, **William R. Grise**, *Morehead State Univ.*

P30 Monte Carlo Simulations of High Field Transport in Electroluminescent Devices, **M. Dür** and **S. M. Goodnick**, *Arizona State Univ.*, **M. Reigrotzki** and **R. Redmer**, *Univ. Rostock, Germany*

P31 Modeling of Radiation Fields in a Sub-Picosecond Photo-Conducting System, **K. A. Remley, A. Weisshaar, S. M. Goodnick**, and **V. K. Tripathi**, *Oregon State Univ.*

P32 New "Irreducible Wedge" for Scattering Rate Calculations in Full-Zone Monte Carlo Simulations, **John Stanley** and **Neil Goldsman**, *Univ. Maryland*

P33 A Self-Consistent Model for Quantum Well pin Solar Cells, **S. Ramey** and **R. Khoie**, *Univ. Nevada, Las Vegas*

P34 Hydrodynamic (HD) Simulations of N-Channel MOSFET's with a Computationally Efficient Inversion Layer Quantization Model, **Haihong Wang, Wei-Kai Shih, Susan Green, Scott Hareland, Christine Maziar**, and **Al Tasch**, *Univ. Texas at Austin*

P35 Study of Electron Velocity Overshoot in nMOS Inversion Layers, **W.-K. Shih, S. Jallepalli, M. Rashed, C. M. Maziar**, and **A. F. Tasch, Jr.**, *Univ. Texas at Austin*

P36 Study on Possible Double Peaks in Cutoff Frequency Characteristics of AlGaAs/GaAs HBTs by Energy Transport Simulation, **T. Okada** and **K. Horio**, *Shibaura Institute of Technology, Japan*

P37 Time Dependent Hydrodynamic Model of MESFET, **C. C. Lee, H. L. Cui, J. Cai**, and **R. Pastore**, *Stevens Institute of Technology*, **D. Woolard** and **D. Rhodes**, *U.S. Army Research Lab, Fort Monmouth*

P38 Shell-Filling Effects in Circular Quantum Dots, **M. Macucci**, *Univ. Pisa, Italy*, and **Karl Hess**, *Univ. Illinois at Urbana-Champaign*

P39 Modeling of Shot Noise in Resonant Tunneling Structures, **G. Iannaccone**, *Univ. Pisa, Italy*

P40 Impact Ionization and Hot-Electron Injection Derived Consistently from Boltzmann Transport, **Paul Hasler, Andreas G. Andreou, Chris Diorio, Bradley A. Minch**, and **Carver A. Mead**, *Cal Tech*

P41 Comparison of Variance Reduction Schemes for Monte Carlo Semiconductor Simulation, **Carl J. Wordelman**, *Univ. Illinois at Urbana-Champaign*, **Andrea Pacelli**, *Politecnico di Milano*, **Mark G. Gray** and **Thomas J. T. Kwan**, *Los Alamos National Lab*

P42 Edge Element Solution of Optical Dielectric Cavities, **A. T. Galick**, *Univ. Illinois at Urbana-Champaign*

P43 Inclusion of Bandstructure and Many-Body Effects in a Quantum Well Laser Simulator, **F. Oyafuso, P. von Allmen, M. Grupen**, and **K. Hess**, *Univ. Illinois at Urbana-Champaign*

P44 Coupled Free Carrier and Exciton Dynamics in Bulk and Quantum Well Semiconductor Materials, **M. Gulia**, *Univ. Modena, Italy*, **F. Compagnone**, *Univ. Roma, Italy*, **P. E. Selbman**, *Swiss Federal Inst. Lausanne*, **F. Rossi, E. Molinari**, *Univ. Modena, Italy*, and **P. Lugli**, *Univ. Roma, Italy*

P45 Optical and Electronic Properties of Semiconductor 2D Nanosystems: Self-Consistent Tight-Binding Calculations, **A. Di Carlo, S. Pescetelli, A. Reale, M. Paciotti,** and **P. Lugli,** *Univ. Roma, Italy*

P46 Transient Phenomena in High Speed Bipolar Devices, **Michael S. Obrecht, Edwin L. Heasell, Jiri Vlach,** and **Mohamed I. Elmasry,** *University of Waterloo, Canada*

P47 Interaction of 2D Electrons with Acoustic Phonons near the Semiconductor Surface and its Effect on 2D Electron Transport, **B. A. Glavin, V. I. Pipa, V. V. Mitin,** *Wayne State Univ.,* and **M. Stroscio,** *U.S. Army Research Office*

P48 Acoustic Phonon Modulation of the Electron Response in Tunnel-Coupled Quantum Wells, **G. Ya. Kis** and **F. T. Vasko,** *Institute of Semiconductor Physics, Kiev, Ukraine,* and **V. V. Mitin,** *Wayne State Univ.*

P49 Cathode Shape Influence on Subterahertz Oscillations of Ballistic Quantized Hole Current, **A. N. Korshak, Z. S. Gribnikov, N. Z. Vagidov, S. I. Kozlovsky,** and **V. V. Mitin,** *Institute of Semiconductor Physics, Kiev, Ukraine and Wayne State Univ.*

P50 Transverse Patterns in the Bistable Resonant Tunneling Systems under Ballistic Lateral Electron Transport, **V. A. Kochelap, B. A. Glavin,** and **V. V. Mitin,** *Institute of Semiconductor Physics, Kiev, Ukraine and Wayne State Univ.*

P51 SPIN - A Schrödinger Poisson Solver Including Non-Parabolic Bands, **Hans Kosina** and **Christian Troger,** *TU Vienna, Austria*

P52 Advantages of Semiconductor Device Simulator Combining Electromagnetic and Electron Transport Models, **S. M. Sohel Imtiaz, Samir M. El-Ghazaly,** and **Robert O. Grondin,** *Arizona State Univ.*

P53 Quantum Transport and Thermoelectric Properties of InAs/GaSb Superlattices, **J.-F. Lin** and **D. Z.-Y. Ting,** *National Tsing Hua Univ., Hsinchu, Taiwan*

P54 Multiband Quantum Transmitting Boundary Method for Non-Orthogonal Basis, **G.-C. Liang, Y. A. Lin, D. Z.-Y. Ting,** *National Tsing Hua Univ., Hsinchu, Taiwan,* and **Y.-C. Chang,** *Univ. of Illinois at Urbana-Champaign*

P55 Calibration of a One Dimensional Hydrodynamic Simulator with Monte Carlo Data, **O. Muscato, S. Rinaudo,** and **P. Falsaperla,** *Univ. di Catania and SGS-THOMSON, Catania, Italy*

P56 Hyperbolic Hydrodynamical Model of Carrier Transport in Semiconductor, **Angelo Marcello Anile,** *Univ. di Catania, Italy,* **Vittorio Romano,** *Politecnico di Bari, Taranto, Italy,* and **Giovanni Russo,** *Univ. di L'Aquila, Italy*

P57 A Hydrodynamical Model for Transport in Semiconductors without Free Parameters, **P. Falsaperla** and **M. Trovato,** *Univ. di Catania, Italy*

P58 Modeling of Poly-Silicon Carrier Transport with Explicit Treatment of Grains and Grain Boundaries, **Edwin C. Kan** and **Robert W. Dutton,** *Stanford Univ.*

P59 Formulation of the Boltzmann Equation as a Multi-Mode Drift-Diffusion Equation, **Kausar Banoo, Farzin Assad**, and **Mark Lundstrom**, *Purdue Univ.*

P60 Modeling of Hot Carrier Effects in Semiconductor Lasers, **Valery I. Tolstikhin** and **Theo G. van der Roer**, *TU Eindhoven, Netherlands*

P61 Quadratic Electron Wind in Electromigration, **Alfred M. Kriman, R. Frankovic**, and **G. H. Bernstein**, *SUNY Buffalo and Univ. Notre Dame*

P62 Semiclassical Many-Body Simulation, **Jae-Hyun Yu** and **Alfred M. Kriman**, *SUNY Buffalo and Univ. Notre Dame*

P63 On the Numerical Simulation of a Thermistor Device, **Charles Miller** and **Hong-Ming Yin**, *Univ. Notre Dame*

P64 A 3D Nonlinear Poisson Solver, **Gyula Veszely**, *TU Budapest, Hungary*

P65 Equilibrium Aspects of Quantum Dot Formation, **Istvan Daruka** and **Albert-Laszlo Barabasi**, *Univ. Notre Dame*

P66 An Alternative Geometry for Quantum Cellular Automata, **P. Douglas Tougaw, Paul Krause, Rachel Mueller**, and **Janelle Weidner**, *Valparaiso Univ.*

P67 Energy Dissipation in Quantum-Dot Cellular Automata, **John Timler** and **Craig S. Lent**, *Univ. Notre Dame*

P68 Electrostatic Formation of a Coupled Quantum Dot, **Per Hyldgaard, Henry K. Harbury**, and **Wolfgang Porod**, *Univ. Notre Dame*

P69 A Novel Method for Computing Particle Distributions, **Fred H. Schlereth**, *Syracuse Univ.*

P70 Nonperturbative Many Electron Approach Based on the Representation of Scattering States for Simulating Optoelectronic Devices Using Laser-Assisted Field Emission, **Andres J. Barrios, Valery G. Valeyev, Mark J. Hagmann**, and **Carolyne M. Van Vliet**, *Florida International Univ. and Bashkir State Univ., Russia*

P71 Electron Transport in One-Dimensional Magnetic Superlattices, **Zhen-Li Ji** and **D. W. L. Sprung**, *McMaster Univ., Canada*

P72 Boundary Conditions for the Modeling of Open-Circuited Devices in Non-Equilibrium, **Joseph W. Parks, Jr.** and **Kevin F. Brennan**, *Georgia Tech*

P73 Positron Slowing Down in Solids, **N. Bouarissa**, *Univ. Setif, Algeria*

P74 Modeling of Mid-Infrared Multi-Quantum Well Lasers, **A. D. Andreev**, *Ioffe Institute, St. Petersburg, Russia*

P75 Computation of Auger Recombination Rates in Semiconductor Quantum Wells, **A. D. Andreev**, *Ioffe Institute, St. Petersburg, Russia*

Conference Booklet Program & Abstracts

Fifth International Workshop on Computational Electronics

IWCE-5

Notre Dame, Indiana
May 28-30, 1997

All sessions and social events will be held at the Center for Continuing Education (CCE) on the campus of the University of Notre Dame.

TUESDAY, May 27	**Registration and Reception**
4:00 - 9:00 pm	Registration
7:00 - 9:00 pm	Reception (food and drinks will be available)

Sponsors:
- National Science Foundation
- Office of Naval Research
- Army Research Office
- Univ. Notre Dame College of Engineering
- Univ. Notre Dame Department of Electrical Engineering
- Technical Co-Sponsorship, IEEE Electron Devices Society

IWCE-5 Committees:

Chairman:

Wolfgang Porod | Univ. Notre Dame

Program Committee:

Jeff Bude | Lucent
Bob Dutton | Stanford Univ.
Chihiro Hamaguchi | Osaka Univ., Japan
Steve Goodnick | Arizona State Univ.
Steve Laux | IBM
Craig Lent | Univ. Notre Dame
Mark Lundstrom | Purdue Univ.
Hiroshi Mizuta | Hitachi Cambridge, UK
Umberto Ravaioli | Univ. Illinois
Chris Ringhofer | Arizona State Univ.
Chris Snowden | Univ. Leeds, UK

Advisory Committee:

G. Baccarani | Univ. Bologna, Italy
Herb Bennett | NIST
Felix Buot | NRL
Larry Cooper | ONR
W. M. Coughran, Jr. | Lucent
David Ferry | Arizona State Univ.
Wolfgang Fichtner | ETH Zurich, Switzerland
Max Fischetti | IBM
Bill Frensley | Univ. Texas at Dallas
Masao Fukuma | NEC, Japan
Hal Grubin | SRA
Karl Hess | Univ. Illinois
Gerald Iafrate | ARO
Joseph W. Jerome | Northwestern Univ.
Thomas Kerkhoven | Univ. Illinois
Tom McGill | Cal Tech
Donald J. Rose | Duke Univ.
Kent Smith | Lucent
Christopher Stanton | Univ. Florida
Mike Stroscio | ARO
Al F. Tasch | Univ. Texas at Austin
Peter Vogl | TU Munich, Germany
Kiyoyuki Yokoyama | NTT, Japan
Naoki Yokoyama | Fujitsu, Japan

7:00 - 8:00		BREAKFAST

8:15 - 8:30   Welcome and Opening Remarks
- Daniel Costello, Chair of Electrical Engineering
- Jeffrey Kantor, Vice President and Associate Provost
- Karl Hess, Director, National Center for Computational Electronics

8:30 a.m.   Session *"Device Simulation I"* Chair: *Massimo Fischetti*

8:30 - 9:00   WeA1   Merits and Faults of Sub-Micron Device Simulation from a Designer Perspective (Invited), **Emmanuel Crabbé**, *IBM*

9:00 - 9:30   WeA2   Two-Dimensional Carrier Transport in Si MOSFETs (Invited), **Shin-ichi Takagi**, *Toshiba, Japan*

9:30 - 10:00 WeA3   Monte Carlo Simulations of Impact Ionization Feedback (Invited), **Jeff D. Bude**, *Bell Labs, Lucent Technologies*

10:00 - 10:30   COFFEE BREAK

10:30 a.m.   Session *"Device Simulation II"* Chair: Christine Maziar

10:30 - 10:45 WeA4   Numerical Simulation of MOSFETs Using Nonequilibrium Quantum Field Theory, **Dejan Jovanovic, Ulvi Erdogan, Chris Bowen**, and **Roger Lake**, *Texas Instruments*

10:45 - 11:00 WeA5   Inclusion of Quantum Confinement Effects in Self-Consistent Monte Carlo Device Simulations, **R. W. Kelsall** and **A. J. Lidsey**, *Univ. Leeds, UK*

11:00 -11:15 WeA6   Two Dimensional Modeling of HEMTs Using Multigrids with Quantum Corrections, **Eric A. B. Cole, Tobias Boettcher**, and **Christopher M. Snowden**, *Univ. Leeds, UK*

11:15 - 11:30 WeA7   p-Si Monte Carlo Simulator for Deep Submicron MOS Devices, **N. A. Bannov, W. C. Holton**, and **K. W. Kim**, *North Carolina State Univ.*

11:30 - 11:45 WeA8   MOMENTS: The Modular Monte Carlo Environment for Charge Transport Simulation - Overview and Applications, **Mark Peskin** and **Christine Maziar**, *Univ. Texas at Austin*

11:45 - 12:00 WeA9   High-Field Hole Transport in Strained Si and SiGe by Monte Carlo Simulation: Full Band versus Analytic Band Model, **F. M. Bufler, P. Graf**, and **B. Meinerzhagen**, *Univ. Bremen, Germany*

12:00 - 1:30   LUNCH

1:30 p.m.   Session *"Modeling for ULSI"* Chair: *Ting-wei Tang*

1:30 - 2:00   WeP1   Hierarchical Simulation for ULSI Process Design - From Atomistic to Conventional Process CAD (Invited), **S. Onga, T. K. Okada, H. Takada, T. Koyanagi,** *Toshiba, Japan,* **E. Kan** and **R. W. Dutton,** *Stanford Univ.*

2:00 - 2:15   WeP2   Necessary Roughness of MOS Interface for Device Simulation, **Edwin C. Kan, Heng-Chih Lin,** and **Robert W. Dutton,** *Stanford Univ.*

2:15-2:30   WeP3   Non-Uniformity Effects in Ultra-Thin Tunneling Oxides, **D. Z.-Y. Ting, Erik S. Daniel,** and **T. C. McGill,** *Cal Tech*

2:30 - 2:45   COFFEE BREAK

2:45 p.m.   Session *"Thermal Effects"* Chair: *Umberto Ravaioli*

2:45 - 3:15   WeP4   Modeling of Thermal Effects in Semiconductor Structures (Invited), **Christopher Snowden,** *Univ. Leeds, UK*

3:15 - 3:30   WeP5   Carrier Thermal Conductivity: Analysis and Application to Sub-micron-Device Simulation, **A. Greiner** and **L. Reggiani,** *Univ. Lecce, Italy,* **T. Kuhn,** *Univ. Münster,* Germany, **L. Varani,** *Univ. Montpellier, France,* **P. Golinelli,** *Univ. Modena, Italy,* **M. C. Vecchi,** *Univ. Bologna, Italy*

3:30 - 3:45   WeP6   Heat Dissipation from Quantum Structures, **V. V. Mitin, G. Paulavicius, N. Bannov,** *Wayne State Univ.,* and **M. A. Stroscio,** *U.S. Army Research Office*

3:45 - 4:00   COFFEE BREAK

4:00 p.m.   Session *"Molecular Structures"* Chair: *Craig Lent*

4:00 - 4:30   WeP7   Molecular Wires: Conductance, Geometric Dependence, Energetics, Electron Repulsion and Their Relationship to Intramolecular Electron Transfer (Invited), **Mark A. Ratner,** *Northwestern Univ.*

4:30 - 4:45   WeP8   Simulation of Molecular Electronic Devices, **Weidong Tian** and **Supriyo Datta,** *Purdue Univ.*

4:45 - 5:00   WeP9   Drift-Diffusion Equations Describe an Important Biological System: Ionic Channels in Membranes, **R. S. Eisenberg,** *Rush Medical Center, Chicago*

5:00 - 6:30   POSTER VIEWING (food and drinks will be available)

6:30 p.m.   Session *"Software Development"* Chair: *Henry Harbury*

6:30 - 7:00   WeE1   The NEMO Project or Writing Research Software in a Large Group
                                   (Invited), **Gerhard Klimeck, Dan Blanks, Roger Lake,**
                                   R. Chris Bowen, Manhua Leng, Chenjing L. Fernando,
                                   William R. Frensley, Dejan Jovanovic, and **Paul Sotirelis,**
                                   Corporate R&D, Texas Instruments Inc. and
                                   School of Engineering, Univ. of Texas at Dallas

7:00 - 7:30   Software Demo Previews (short presentations)

7:30 - 9:00   Software Demos (food and drinks will be available)

Bob Dutton et al., *Stanford Univ.*	Device and Process Simulation Tools
Bill Frensley, *UT Dallas*	Interactive Modeling and Design Tools
Neil Goldsman et al., *Univ. Maryland*	Spherical Harmonics and Hydrodynamic Simulation Tools
Harold Grubin, *Scientific Res. Assoc.*	PC Windows Interactive Modeling of Quantum Devices
Gerhard Klimeck, Dejan Jovanovic, Roger Lake, et al., *TI*	NEMO - Nanotechnology Engineering MOdeling program
Steve Laux and Max Fischetti, *IBM*	DAMOCLES - Device Analysis using MOnte CarLo Et poisson Solver
Craig Lent et al., *Univ. Notre Dame*	AQUINAS - A QUantum Interconnected Network Array Simulator
Mark Lundstrom and Umberto Ravaioli, Purdue and Illinois	"Simulation Hub," an Online Simulation Laboratory
Hans Kosina and Christian Troger, *Techn. Univ. Vienna*	SPIN - Schrödinger Poisson Solver Including Non-Parabolicity
Michael Obrecht, Siborg Systems, Inc	MicroTec: Educational 2D Semiconductor Process/Device Simulator for a PC
Christoph Wasshuber, *Techn. Univ. Vienna*	SIMON - Single-Electron Device and Circuit Simulator

7:00 - 8:00		BREAKFAST

8:30 a.m.   Session *"Optoelectronics"* Chair: *Karl Hess*

8:30 - 9:00   ThA1   Photonic Device Modeling for Telecommunication Purposes (Invited), **Kiyoyuki Yokoyama**, *NTT, Japan*

9:00 - 9:30   ThA2   Modeling and Simulation of Semiconductor DFB Lasers: A Hierarchical Approach (Invited), **Wei-Ping Huang** and **Xun Li**, *University of Waterloo, Canada*

9:30 - 10:00   ThA3   Numerical Methods for Semiconductor Laser Simulations (Invited), **R. K. Smith, M. A. Alam, G. A. Baraff, M. S. Hybertsen**, *Bell Laboratories, Lucent Technologies*

10:00 - 10:15   ThA4   Theory and Modeling of Lasing Modes in Vertical Cavity Surface Emitting Lasers, **Benjamin Klein, Leonard F. Register, Karl Hess**, *Univ. Illinois at Urbana-Champaign*, and **Dennis G. Deppe**, *Univ. Texas at Austin*

10:15 - 10:45   COFFEE BREAK

10:45 a.m.   Session *"Device Simulation III"* Chair: Steve Goodnick

10:45 - 11:15   ThA5   Cellular Automaton Study of Time-Dynamics of Avalanche Breakdown in IMPATT Diodes (Invited), **G. Zandler**, *TU Munich, Germany*, **M. Saraniti**, *Arizona State Univ.*, **P. Vogl**, *TU Munich, Germany*, **P. Lugli**, *Univ. Rome, Italy*

11:15 - 11:30   ThA6   3D Parallel Finite Element Simulation of In-Cell Breakdown in Lateral-Channel IGBTs, **A. R. Brown, A. Asenov**, and **J. R. Barker**, *Univ. Glasgow, UK*

11:30 - 11:45   ThA7   Comparison of Iteration Schemes for the Solution of the Multidimensional Schrödinger-Poisson Equations, **A. Trellakis, A. T. Galik, A. Pacelli**, and **U. Ravaioli**, *Univ. Illinois at Urbana-Champaign*

11:45 -12:00   ThA8   Cellular Automata Studies of Vertical Silicon Devices, **M. Saraniti**, *Arizona State Univ.*, **G. Zandler**, *TU Munich, Germany*, and **S. Goodnick**, *Arizona State Univ.*

12:00 - 1:30   LUNCH

1:30 p.m.   Session *"High Performance Computing"* Chair: *Bill Coughran*

1:30 - 2:00   ThP1   Large Scale Distributed Parallel Computing (Invited), **Harold Trease**, *Los Alamos National Laboratory*

2:00 - 2:15   ThP2   X3D Moving Grid Methods for Semiconductor Applications, **Denise George, David Cartwright, J. Tinka Gammel, Brian Kendrick, David Kilcrease, Andrew Kuprat, Harold Trease**, and **Robert Walker**, *Los Alamos National Laboratory*

2:15 - 2:30	ThP3	The Finite-Volume Scharfetter-Gummel Method for Steady Convection-Diffusion Equations, **Randolph E. Bank**, *UC San Diego*, **W. M. Coughran, Jr.**, and **Lawrence C. Cowsar**, *Bell Labs, Lucent Technologies*
2:30 - 2:45	ThP4	Multilevel Algorithms for Large-Scope Molecular Dynamics Simulations of Nanostructures on Parallel Computers, **Aiichiro Nakano**, **Rajiv K. Kalia**, and **Priya Vashishta**, *Louisiana State Univ.*
2:45 - 3:00	ThP5	Ensemble Monte Carlo and Full-Wave Electrodynamics Models Implemented Self-Consistently on a Parallel Processor Using Perfectly Matched Layer Boundary Conditions, **Ik-Sung Lim**, *Motorola*, **Robert O. Grondin** and **Samir El-Ghazaly**, *Arizona State Univ.*
3:00 - 3:30		COFFEE BREAK
3:30 p.m.		Session *"Mathematical Models"* Chair: *Joe Jerome*
3:30 - 3:45	ThP6	Applicability of the High Field Model: An Analytical Study via Asymptotic Parameters Defining Domain Decomposition, **Carlo Cercignani**, *Politecnico di Milano, Italy*, **Irene Gamba**, *Courant Institute, New York Univ.*, **Joseph Jerome**, *Northwestern Univ.*, and **Chi-Wang Shu**, *Brown Univ.*
3:45 - 4:00	ThP7	Smooth QHD Simulation of the Resonant Tunneling Diode, **Carl L. Gardner** and **Christian Ringhofer**, *Arizona State Univ.*
4:00 - 4:15	ThP8	Spherical Harmonic Analysis of a 0.05 μm Base BJT: Monte Carlo-Type Results but a Thousand Times Faster, **C.-H. Chang, C.-K. Lin, N. Goldsman**, and **I. D. Mayergoyz**, *Univ. Maryland*
4:15 - 4:30	ThP9	Numerical Examination of Photon Recycling as an Explanation of Observed Carrier Lifetime in Direct Bandgap Materials, **Joseph W. Parks, Jr., Kevin F. Brennan**, *Georgia Tech*, and **Arlynn W. Smith**, *ITT Night Vision*
4:30 - 4:45	ThP10	A Semi-Classical Description of Electron Transport in Semiconductor Quantum Well Devices, **Gene A. Baraff**, *Lucent Technologies Bell Labaratories*
4:45 - 5:00	ThP11	Electronic Structure Calculations Using an Adaptive Wavelet Basis, **D. A. Richie, P. von Allmen, K. Hess**, and **R. Martin**, *Univ. Illinois at Urbana-Champaign*
5:00 - 7:00		POSTER VIEWING (snacks and drinks will be available)
7:00 - 9:00		BANQUET
	Dinner Talk	The Art, Science, and Challenges of Simulating Advanced Devices, **Jerry Mar**, *Intel* (Introduced by *Jerry Iafrate*)

7:00 - 8:00   BREAKFAST

8:30 a.m.   Session *"Quantum Simulation I"* Chair: *Chihiro Hamaguchi*

8:30 - 9:00   FrA1   Open Problems in Quantum Simulation in Ultra-Submicron Devices (Invited), **David K. Ferry**, *Arizona State Univ.*, and **John R. Barker**, *Univ. Glasgow, UK*

9:00 - 9:15   FrA2   Theory of Electron Transport in Small Semiconductor Devices Using the Pauli Master Equation, **M. V. Fischetti**, *IBM Research Division*

9:15 - 9:30   FrA3   Modeling of Nano-Scale Ballistic Field-Effect Transistors, **F. G. Pikus** and **K. K. Likharev**, *SUNY Stony Brook*

9:30 - 9:45   FrA4   Quantum Transport in Open Nanostructures, **I. V. Zozoulenko** and **K.-F. Berggren**, *Linköping Univ., Sweden*

9:45 - 10:00   FrA5   Application of the Wigner-Function Formulation to Mesoscopic Systems in Presence of the Electron-Phonon Interaction, **C. Jacoboni, A. Abramo, P. Bordone, R. Brunetti**, and **M. Pascoli**, *Univ. Modena, Italy*

10:00 - 10:30   COFFEE BREAK

10:30 a.m.   Session *"Quantum Simulation II"* Chair: *Bill Frensley*

10:30 -11:00   FrA6   Quantum Networks: Dynamics of Open Nanostructures (Invited), **Günter Mahler**, *Oregon Center of Optics and Univ. Stuttgart, Germany*

11:00 - 11:15 FrA7   A Generalized Monte Carlo Approach for the Analysis of Quantum-Transport Phenomena in Mesoscopic Systems: Interplay between Coherence and Relaxation, **Fausto Rossi**, *Univ. Modena, Italy*, **Stefano Ragazzi, Aldo Di Carlo**, and **Paolo Lugli**, *Univ. Roma, Italy*

11:15 - 11:30 FrA8   Coherent Control of Light Absorption in Semiconductor Nanostructures, **W. Pötz and X. Hu**, *Univ. Illinois at Chicago*

11:30 -11:45   FrA9   A New Computational Approach to Photon-Assisted Tunneling in Intense Driving Fields Based on a Fabry-Perot Analogy, **Mathias Wagner**, *Hitachi Cambridge, UK*

11:45 -12:00   FrA10   Phase Space Boundary Conditions and Quantum Device Transport, **H. L. Grubin** and **J. R. Caspar**, *Scientific Research Associates, Inc.*, and **D. K. Ferry**, *Arizona State Univ.*

12:00 - 1:30		LUNCH

1:30 p.m.   Session *"Quantum Structures"* Chair: *Hal Grubin*

1:30 -1:45	FrP1	Single-Electron Memories, **Christoph Wasshuber, Hans Kosina,** and **Siegfried Selberherr**, *TU Vienna, Austria*
1:45 - 2:00	FrP2	Electron-LA Phonon Interaction in a Quantum Dot, **T. Ezaki, N. Mori,** and **C. Hamaguchi,** *Osaka Univ., Japan*
2:00 - 2:15	FrP3	Numerical Analysis of Asymmetric Single Electron Turnstiles Using Monte Carlo Simulation, **Masaharu Kirihara** and **Kenji Taniguchi,** *Osaka Univ., Japan*
2:15 - 2:30	FrP4	Self-Consistent Calculation of the Ground State and the Capacitance of a 3D Si/SiO_2 Quantum Dot, **A. Scholze, A. Wettstein, A. Schenk,** and **W. Fichtner,** *ETH-Zürich, Switzerland*
2:30 - 2:45	FrP5	An Interband Tunneling Oscillator: Self-Oscillations of Trapped Hole Charge in a Double-Barrier Structure, **F. A. Buot,** *U.S. Naval Research Laboratory*
2:45 - 3:00	FrP6	Tunneling between Multimode Stacked Quantum Wires, **M. Macucci,** *Univ. Pisa, Italy,* **A. T. Galick** and **U. Ravaioli,** *Univ. Illinois at Urbana-Champaign*
3:00 - 3:15	FrP7	Ballistic Directional Coupler on the DQW-Basis, **A. N. Korshak, Z. S. Gribnikov, N. Z. Vagidov, S. I. Kozlovsky,** and **V. V. Mitin,** *Institute of Semiconductor Physics, Kiev, Ukraine and Wayne State Univ.*

CONFERENCE CLOSE

POSTER PRESENTATIONS

P1 Monte Carlo Simulation of Non-local Transport Effects in Strained Si on Relaxed $Si_{1-x}Ge_x$ Heterostructures, **F. Gámiz**, **J. B. Roldán**, and **J. A. López-Villanueva**, *Univ. Granada, Spain*

P2 A β-SiC MOSFET Monte Carlo Simulator Including Inversion Layer Quantization, **F. Gámiz**, **J. B. Roldán**, and **J. A. López-Villanueva**, *Univ. Granada, Spain*

P3 A Closed-Loop Evaluation and Validation of a Method for Determining the Dependence of the Electron Mobility on the Longitudinal-Electric Field in MOSFETs, **J. B. Roldán**, **F. Gámiz**, and **J. A. López-Villanueva**, *Univ. Granada, Spain*

P4 Quantum Distribution-Function Transport Equations in Non-Normal Systems and in Ultra-Fast Dynamics of Optically-Excited Semiconductors, **F. A. Buot**, *U.S. Naval Research Laboratory*

P5 Applicability of the High Field Model: A Preliminary Numerical Study, **Carlo Cercignani**, *Politecnico di Milano, Italy*, **Irene Gamba**, *Courant Institute, New York University*, **Joseph Jerome**, *Northwestern Univ.*, and **Chi-Wang Shu**, *Brown Univ.*

P6 Simulation of Bistable Laser Diodes with Inhomogeneous Excitation, **Gang Fang** and **Ting-wei Tang**, *Univ. Massachusetts*

P7 Intersubband Relaxation in Step Quantum Well Structures, **J. P. Sun**, **H. B. Teng**, **G. I. Haddad**, *Univ. Michigan*, and **M. A. Stroscio** and **G. J. Iafrate**, *U.S. Army Research Office*

P8 Symplectic Finite-Element Time-Domain Method for Optical Field Analysis, **T. Hirono**, **W. Lui**, and **K. Yokoyama**, *NTT, Japan*

P9 Resonances in Conductance through Tunable Attractors, **Yong S. Joe**, **Tian Xie**, and **Ronald M. Cosby**, *Ball State Univ.*

P10 A New Method to Overcome the Divergent Problem in Numerical Modeling of Power 6H-SiC Devices, **Edward H. S. Hsing** and **Jeffrey L. Gray**, *Purdue Univ.*

P11 Convergence Properties of the Bi-CGSTAB Method for the Solution of the 3D Poisson and 3D Electron Current Continuity Equations for Scaled Si MOSFETs, **D. Vasileska**, **W. J. Gross**, **V. Kafedziski**, and **D. K. Ferry**, *Arizona State Univ.*

P12 Wave-function Scarring Effects in Open Ballistic Quantum Cavities, **R. Akis** and **D. K. Ferry**, *Arizona State Univ.*

P13 Complete RF Analysis of Compound FETs based on Transient Monte Carlo Simulation, **S. Babiker**, **A. Asenov**, **N. Cameron**, **S. P. Beaumont**, and **J. R. Barker**, *Glasgow Univ., UK*

P14 Monte Carlo Calibrated Drift-Diffusion Simulation of Short Channel HFETs, **A. Asenov**, **S. Babiker**, **S. P. Beaumont**, and **J. R. Barker**, *Glasgow Univ., UK*

P15   RF Performance of Si/SiGe MODFETs: A Simulation Study, **S. Roy, A. Asenov, J. R. Barker**, and **S. P. Beaumont**, *Univ. Glasgow, UK*

P16   Ab-Initio Coulomb Scattering in Atomistic Device Simulation, **C. R. Arokianathan, J. H. Davies**, and **A. Asenov**, *Univ. Glasgow, UK*

P17   A New Approach for Obtaining Self-Consistent Solutions to the Coupled Schrödinger and Poisson System in Multiquantum Well Structures, **Fred Gelbard** and **Kevin J. Malloy**, *Univ. New Mexico*

P18   Numerical Evaluation of Iterative Schemes for Drift-Diffusion Simulation, **M. B. Patil, U. Ravaioli**, and **T. Kerkhoven**, *Univ. Illinois at Urbana-Champaign*

P19   Simulation of Si-MOSFETs with the Mutation Operator Monte Carlo Method and Evolutionary Optimization, **J. Jakumeit**, *Univ. Köln*, **A. Duncan, U. Ravaioli**, and **K. Hess**, *Univ. Illinois at Urbana-Champaign*

P20   A New HEMT Breakdown Model Incorporating Gate and Thermal Effects, **Lufti Albasha, Christopher M. Snowden**, and **Roger D. Pollard**, *Univ. Leeds, UK*

P21   Rate Equation Modelling of Nonlinear Dynamics in Directly Modulated Multiple Quantum Well Laser Diodes, **S. Bennett, C. M. Snowden**, and **S. Iezekiel**, *Univ. Leeds, UK*

P22   Temperature Dependence of the Electron and Hole Scattering Mechanisms in Silicon Analysed through a Full-Band, Spherical-Harmonics Solution of the BTE, **S. Reggiani, M. C. Vecchi**, and **M. Rudan**, *Univ. Bologna, Italy*

P23   Monte Carlo Simulation of Intersubband Hole Relaxation in a GaAs/AlAs Quantum Well, **R. W. Kelsall**, *Univ. Leeds, UK*

P24   VLSI Yield Prediction Using a Pattern-Recognition Based Critical Area Algorithm, **J. H. N. Mattick, R. W. Kelsall**, and **R. E. Miles**, *Univ. Leeds, UK*

P25   Bi-dimensional Simulation of the Simplified Hydrodynamic and Energy-Transport Models for Heterojunction Semiconductor Devices Using Mixed Finite Elements, **A. Marrocco** and **Ph. Montarnal**, *INRIA, Le Chesnay Cedex, France*

P26   Semiconductor Device Noise Computation Based on the Deterministic Solution of the Poisson and Boltzmann Transport Equations, **Alfredo J. Piazza** and **Can E. Korman**, *George Washington Univ.*

P27   Consistent Hydrodynamic and Monte-Carlo Simulation of SiGe HBTs Based on Table Models for the Relaxation Times, **B. Neinhüs, S. Decker, P. Graf, F. M. Bufler**, and **B. Meinerzhagen**, *Univ. Bremen, Germany*

P28   Additive Decomposition of the Drift-Diffusion Model, **Elizabeth J. Brauer, Marek Turowski**, and **James M. McDonough**, *Univ. Kentucky*

P29   Supersymmetric Quantum Mechanics (SUSY-QM) Applied to Quantum-Wire Devices, **William R. Grise**, *Morehead State Univ.*

P30 Monte Carlo Simulations of High Field Transport in Electroluminescent Devices,
M. Dür and **S. M. Goodnick**, *Arizona State Univ.*, **M. Reigrotzki** and
R. Redmer, *Univ. Rostock, Germany*

P31 Modeling of Radiation Fields in a Sub-Picosecond Photo-Conducting System,
K. A. Remley, A. Weisshaar, S. M. Goodnick, and **V. K. Tripathi**, *Oregon State Univ.*

P32 New "Irreducible Wedge" for Scattering Rate Calculations in Full-Zone Monte Carlo
Simulations, **John Stanley** and **Neil Goldsman**, *Univ. Maryland*

P33 A Self-Consistent Model for Quantum Well pin Solar Cells, **S. Ramey** and **R. Khoie**,
Univ. Nevada, Las Vegas

P34 Hydrodynamic (HD) Simulations of N-Channel MOSFET's with a Computationally
Efficient Inversion Layer Quantization Model, **Haihong Wang, Wei-Kai Shih, Susan
Green, Scott Hareland, Christine Maziar**, and **Al Tasch**, *Univ. Texas at Austin*

P35 Study of Electron Velocity Overshoot in nMOS Inversion Layers, **W.-K. Shih, S. Jallepalli,
M. Rashed, C. M. Maziar**, and **A. F. Tasch, Jr.**, *Univ. Texas at Austin*

P36 Study on Possible Double Peaks in Cutoff Frequency Characteristics of AlGaAs/GaAs
HBTs by Energy Transport Simulation, **T. Okada** and **K. Horio**,
Shibaura Institute of Technology, Japan

P37 Time Dependent Hydrodynamic Model of MESFET, **C. C. Lee, H. L. Cui, J. Cai**, and
R. Pastore, *Stevens Institute of Technology*, **D. Woolard** and **D. Rhodes**,
U.S. Army Research Lab, Fort Monmouth

P38 Shell-Filling Effects in Circular Quantum Dots, **M. Macucci**, *Univ. Pisa, Italy*, and
Karl Hess, *Univ. Illinois at Urbana-Champaign*

P39 Modeling of Shot Noise in Resonant Tunneling Structures, **G. Iannaccone**, *Univ. Pisa, Italy*

P40 Impact Ionization and Hot-Electron Injection Derived Consistently from Boltzmann Trans-
port, **Paul Hasler, Andreas G. Andreou, Chris Diorio, Bradley A. Minch**, and
Carver A. Mead, *Cal Tech*

P41 Comparison of Variance Reduction Schemes for Monte Carlo Semiconductor Simulation,
Carl J. Wordelman, *Univ. Illinois at Urbana-Champaign*, **Andrea Pacelli**, *Politecnico di
Milano*, **Mark G. Gray** and **Thomas J. T. Kwan**, *Los Alamos National Lab*

P42 Edge Element Solution of Optical Dielectric Cavities, **A. T. Galick**,
Univ. Illinois at Urbana-Champaign

P43 Inclusion of Bandstructure and Many-Body Effects in a Quantum Well Laser Simulator, **F.
Oyafuso, P. von Allmen, M. Grupen**, and **K. Hess**, *Univ. Illinois at Urbana-Champaign*

P44 Coupled Free Carrier and Exciton Dynamics in Bulk and Quantum Well Semiconductor
Materials, **M. Gulia**, *Univ. Modena, Italy*, **F. Compagnone**, *Univ. Roma, Italy*,
P. E. Selbman, *Swiss Federal Inst. Lausanne*, **F. Rossi, E. Molinari**,
Univ. Modena, Italy, and **P. Lugli**, *Univ. Roma, Italy*

P45 Optical and Electronic Properties of Semiconductor 2D Nanosystems: Self-Consistent Tight-Binding Calculations, **A. Di Carlo, S. Pescetelli, A. Reale, M. Paciotti**, and **P. Lugli**, *Univ. Roma, Italy*

P46 Transient Phenomena in High Speed Bipolar Devices, **Michael S. Obrecht, Edwin L. Heasell, Jiri Vlach**, and **Mohamed I. Elmasry**, *University of Waterloo, Canada*

P47 Interaction of 2D Electrons with Acoustic Phonons near the Semiconductor Surface and its Effect on 2D Electron Transport, **B. A. Glavin, V. I. Pipa, V. V. Mitin**, *Wayne State Univ.*, and **M. Stroscio**, *U.S. Army Research Office*

P48 Acoustic Phonon Modulation of the Electron Response in Tunnel-Coupled Quantum Wells, **G. Ya. Kis** and **F. T. Vasko**, *Institute of Semiconductor Physics, Kiev, Ukraine*, and **V. V. Mitin**, *Wayne State Univ.*

P49 Cathode Shape Influence on Subterahertz Oscillations of Ballistic Quantized Hole Current, **A. N. Korshak, Z. S. Gribnikov, N. Z. Vagidov, S. I. Kozlovsky**, and **V. V. Mitin**, *Institute of Semiconductor Physics, Kiev, Ukraine and Wayne State Univ.*

P50 Transverse Patterns in the Bistable Resonant Tunneling Systems under Ballistic Lateral Electron Transport, **V. A. Kochelap, B. A. Glavin**, and **V. V. Mitin**, *Institute of Semiconductor Physics, Kiev, Ukraine and Wayne State Univ.*

P51 SPIN - A Schrödinger Poisson Solver Including Non-Parabolic Bands, **Hans Kosina** and **Christian Troger**, *TU Vienna, Austria*

P52 Advantages of Semiconductor Device Simulator Combining Electromagnetic and Electron Transport Models, **S. M. Sohel Imtiaz, Samir M. El-Ghazaly**, and **Robert O. Grondin**, *Arizona State Univ.*

P53 Quantum Transport and Thermoelectric Properties of InAs/GaSb Superlattices, **J.-F. Lin** and **D. Z.-Y. Ting**, *National Tsing Hua Univ., Hsinchu, Taiwan*

P54 Multiband Quantum Transmitting Boundary Method for Non-Orthogonal Basis, **G.-C. Liang, Y. A. Lin, D. Z.-Y. Ting**, *National Tsing Hua Univ., Hsinchu, Taiwan*, and **Y.-C. Chang**, *Univ. of Illinois at Urbana-Champaign*

P55 Calibration of a One Dimensional Hydrodynamic Simulator with Monte Carlo Data, **O. Muscato, S. Rinaudo**, and **P. Falsaperla**, *Univ. di Catania and SGS-THOMSON, Catania, Italy*

P56 Hyperbolic Hydrodynamical Model of Carrier Transport in Semiconductor, **Angelo Marcello Anile**, *Univ. di Catania, Italy*, **Vittorio Romano**, *Politecnico di Bari, Taranto, Italy*, and **Giovanni Russo**, *Univ. di L'Aquila, Italy*

P57 A Hydrodynamical Model for Transport in Semiconductors without Free Parameters, **P. Falsaperla** and **M. Trovato**, *Univ. di Catania, Italy*

P58 Modeling of Poly-Silicon Carrier Transport with Explicit Treatment of Grains and Grain Boundaries, **Edwin C. Kan** and **Robert W. Dutton**, *Stanford Univ.*

P59 Formulation of the Boltzmann Equation as a Multi-Mode Drift-Diffusion Equation, **Kausar Banoo**, **Farzin Assad**, and **Mark Lundstrom**, *Purdue Univ.*

P60 Modeling of Hot Carrier Effects in Semiconductor Lasers, **Valery I. Tolstikhin** and **Theo G. van der Roer**, *TU Eindhoven, Netherlands*

P61 Quadratic Electron Wind in Electromigration, **Alfred M. Kriman**, **R. Frankovic**, and **G. H. Bernstein**, *SUNY Buffalo and Univ. Notre Dame*

P62 Semiclassical Many-Body Simulation, **Jae-Hyun Yu** and **Alfred M. Kriman**, *SUNY Buffalo and Univ. Notre Dame*

P63 On the Numerical Simulation of a Thermistor Device, **Charles Miller** and **Hong-Ming Yin**, *Univ. Notre Dame*

P64 A 3D Nonlinear Poisson Solver, **Gyula Veszely**, *TU Budapest, Hungary*

P65 Equilibrium Aspects of Quantum Dot Formation, **Istvan Daruka** and **Albert-Laszlo Barabasi**, *Univ. Notre Dame*

P66 An Alternative Geometry for Quantum Cellular Automata, **P. Douglas Tougaw**, **Paul Krause**, **Rachel Mueller**, and **Janelle Weidner**, *Valparaiso Univ.*

P67 Energy Dissipation in Quantum-Dot Cellular Automata, **John Timler** and **Craig S. Lent**, *Univ. Notre Dame*

P68 Electrostatic Formation of a Coupled Quantum Dot, **Per Hyldgaard**, **Henry K. Harbury**, and **Wolfgang Porod**, *Univ. Notre Dame*

P69 A Novel Method for Computing Particle Distributions, **Fred H. Schlereth**, *Syracuse Univ.*

P70 Nonperturbative Many Electron Approach Based on the Representation of Scattering States for Simulating Optoelectronic Devices Using Laser-Assisted Field Emission, **Andres J. Barrios**, **Valery G. Valeyev**, **Mark J. Hagmann**, and **Carolyne M. Van Vliet**, *Florida International Univ. and Bashkir State Univ., Russia*

P71 Electron Transport in One-Dimensional Magnetic Superlattices, **Zhen-Li Ji** and **D. W. L. Sprung**, *McMaster Univ., Canada*

P72 Boundary Conditions for the Modeling of Open-Circuited Devices in Non-Equilibrium, **Joseph W. Parks, Jr.** and **Kevin F. Brennan**, *Georgia Tech*

P73 Positron Slowing Down in Solids, **N. Bouarissa**, *Univ. Setif, Algeria*

P74 Modeling of Mid-Infrared Multi-Quantum Well Lasers, **A. D. Andreev**, *Ioffe Institute, St. Petersburg, Russia*

P75 Computation of Auger Recombination Rates in Semiconductor Quantum Wells, **A. D. Andreev**, *Ioffe Institute, St. Petersburg, Russia*

Merits and Faults of Sub-Micron Device Simulation from a Designer Perspective

Emmanuel Crabbé
IBM

(Abstract not available)

Two-dimensional Carrier Transport in Si MOSFETs

Shin-ichi Takagi

ULSI Research Laboratories, Toshiba Corporation

1, Komukai Toshiba-cho, Saiwai-ku, Kawasaki, Japan 210

TEL: 81-44-549-2075 FAX: 81-44-549-2268 Email: takagi@ull.rdc.toshiba.co.jp

Introduction   Carrier transport in the inversion layer of Si, which determines the drain current in MOSFETs, is known to be strongly influenced by 2-dimensional features of the carriers. In this paper we present the results of the systematic experiments on the mobility and the saturation velocity, v_{sat}, in the inversion layer, and the inversion-layer capacitance, C_{inv}, for the comprehensive understanding of these physical parameters. In addition, the analysis including the subband calculations is performed to explain the experimental results. Based on the knowledge of the 2-dimensional carrier transport properties, a subband engineering scenario for realizing higher performance Si MOSFETs is introduced.

Impact of 2-dimensional carriers on the performance in MOSFETs

(1) Low field mobility and saturation velocity   One of the 2-dimensional quantization effects on the inversion-layer mobility appears as its effective field (E_{eff}) dependence, which is the origin of the "universal curve", verified experimentally over a wide range of the substrate impurity concentration for n- and p-MOSFETs. However, the E_{eff} dependence, provided by phonon scattering and surface roughness scattering, has not been fully represented yet by the theoretical calculations, partly because the scattering parameters are not accurately known. While we have shown that the amount of the mobility calculated under the higher coupling with inter-valley phonons than in bulk can be in better agreement with the experimental values, the other experiments to directly evaluate the scattering parameters are required.

On the other hand, the value of v_{sat} in the inversion layer seems to have not been fully established yet experimentally. We have observed, using the resistive gate MOSFETs, that v_{sat} is dependent on the surface carrier concentration, N_s, though a careful attention should be paid to the uniformity of N_s along the channel in this structure. However, this dependence might be attributable not to the 2-dimensional properties of carriers in the inversion layer, but to an effect inherent to N_s itself like plasmon scattering, because v_{sat} in the inversion layer has been observed to be almost independent of E_{eff} under a fixed value of N_s.

(2) Inversion-layer capacitance   It is known that C_{inv} degrades the gate capacitance more significantly with reducing the oxide thickness. In order to quantitatively clarify the influence, we have experimentally evaluated C_{inv} as a function of N_s for n- and p-channel MOSFETs. As a result, the dominant contribution from the 2-dimensional quantization on C_{inv} at room temperature has been directly verified from the surface orientation dependence of C_{inv}. The values of C_{inv} are almost the same between electron and hole inversion layers. It has also been confirmed that C_{inv} can be accurately represented by determining $d\psi_s/dV_g$ through the self-consistent subband calculations. The gate capacitance is severely degraded, when the gate oxide thickness becomes thinner than 2 nm.

Subband engineering for higher performance MOSFETs

It is suggested from the analysis of mobility and C_{inv} that the optimum 2-dimensional electronic system to provide the higher performance has lighter effective mass parallel to Si/SiO$_2$ interface, which increases mobility, and heavier effective mass perpendicular to the interface, which maximizes C_{inv}. As for electrons in the Si inversion layer, the 2-fold valleys in the subbands on (100) surface can be the optimum system. Thus, a subband engineering to enhance the electron occupation in the 2-fold valleys on (100) surface can be an effective strategy for obtaining the higher current drive in Si MOSFETs. Two typical examples of this subband engineering are presented here.

(1) Strained Si MOSFETs   It is known that tensile strain in Si, which is typically seen in Si grown on relaxed SiGe, causes the band splitting between the 2- and the 4-fold valleys, which leads to higher electron occupation in the 2-fold valleys with lighter conductivity mass. The phonon-limited mobility calculations have revealed that the suppression of inter-valley scattering due to the band splitting and the increased occupation of the 2-fold valleys provide the mobility in strained Si MOSFETs of roughly twice as high as in conventional ones, which has already been observed experimentally. It has also been found that C_{inv} in the inversion layer of Si with tensile strain increases a little.

(2) Ultra-thin film SOI MOSFETs   When the SOI film in SOI MOSFETs is thinner than that of the inversion layer in conventional MOSFETs, the subband structure can be significantly modified by the thickness of the SOI film. The subband calculations have shown that C_{inv} and the resulting gate capacitance increases significantly with decreasing the SOI thickness. Furthermore, it has been found, thorough the phonon-limited mobility calculations, that the mobility with the SOI thickness of around 3 nm can be higher than that in conventional MOSFETs. This enhancement is attributable to the fact that, with decreasing the SOI thickness, the subband energy of the 4-fold valleys increases more rapidly than that of the 2-fold valleys and, consequently, the electron occupation of the 2-fold valleys becomes higher, because the inversion layer thickness of the 4-fold valleys is thicker than that of the 2-fold valleys.

Conclusion   The importance of the 2-dimensional features of carriers in the inversion layers on the current drive of MOSFETs has been examined through the experiments and the subband calculations. The effectiveness of a subband engineering, based on these results, for the higher performance has been presented.

Monte Carlo Simulations of Impact Ionization Feedback

Jeff D. Bude

Bell Labs, Lucent Technologies,
600 Mountain Avenue, Murray Hill, NJ 07974, USA

Abstract

Monte Carlo transport simulation is a widely recognized tool for detailed understanding of non-stationary transport in semiconductor devices. In particular, it is the only practical means for accurately obtaining the high energy tail of the electron energy distribution function, responsible for impact ionization, oxide degradation and gate currents in MOSFETs. Recently, Monte Carlo MOSFET simulations have demonstrated that impact ionization feedback, the coupled impact ionization of electrons and holes, can have a strong effect on the distribution function tail [1]. Although impact ionization feedback is recognized as an important current multiplication mechanism, its importance as a carrier heating mechanism has been largely overlooked. This work emphasizes the inclusion of impact ionization feedback in Monte Carlo device simulations, and its implications for carrier heating in sub-micron CMOS and EEPROM technologies. Examples will be given comparing simulated MOSFET gate currents and device degradation to experiment [1]-[2]. In addition, a new class of EEPROM devices have been created based on the physical understanding of the ionization feedback process provided by Monte Carlo simulation [3]. These optimized devices have shown strong potential for low voltage, low power, high performance non-volatile memories.

References

[1] J.D. Bude, 1995 Symposium on VLSI Technology p. 125, 1995

[2] J.D. Bude et al, IEDM Tech. Dig., p. 865, 1996.

[3] J.D. Bude et al, IEDM Tech. Dig., p. 989, 1995.

Numerical Simulation of MOSFETs using Nonequilibrium Quantum Field Theory

Dejan Jovanovic*, Ulvi Erdogan, Chris Bowen, and Roger Lake

Texas Instruments Inc., P.O. Box 655936, MS134, Dallas, TX 75265

Phone: (972)995-2374, FAX: (972)995-2836, e-mail: jovanov@ti.com

A complete two-dimensional nonequilibrium quantum mechanical approach for simulating scaled MOS-FETs is presented. We use nonequilibrium quantum field theory[1] and the Kohn-Sham framework[2] to self-consistently model carrier charge, the direct, exchange, and correlation potentials, and the high-bias quantum mechanical current. This technique, based upon contour ordered Green's functions, enables the detailed treatment of scattering, bandstructure and quantum transport with varying degrees of complexity as determined by the demands of simulated device. 2D quantum transmitting boundary conditions[3] are implemented at the source, drain, and, optionally, the gate to enable a complete treatment of transport under arbitrary biasing configurations. Transport through the complete subband spectrum is subsequently enabled by solving the retarded Green's function, $G^r_{i,j,i',j'}(k_x, E)$, in real-space using the recursive Green's function algorithm[4]. To expedite scattering calculations we also employ a novel recursive algorithm for the correlation function $G^<_{i,j,i',j'}(k_x, E)$. In contrast to quantum-corrected semiclassical simulators, our approach naturally includes the effects of subband quantization and coherent subband mixing which become increasingly important for $L_G < 50nm$. Furthermore, contemporary trends in device scaling (e.g. high channel doping, thin t_{ox}) give rise to leakage mechanisms based upon direct, Fowler-Nordheim, and inter-band tunneling. These phenomena are directly addressed within our approach at the most fundamental level. As examples, we will discuss simulation results for $L_G = 40nm$ bulk and $L_G = 20nm$ double-gate MOSFETs and evaluate devices based on silicide source/drain.

[1] L. P. Keldysh and G. Baym, *Quantum Statistical Mechanics*, Benjamin, 1962.
L. V. Keldysh, Zh. Eksp. Teor. Fiz. **47**, 1515 (1964).

[2] W. Kohn and L. J. Sham, Phys. Rev. **140** (4A), A1133 (1965).

[3] C. S. Lent and D. J. Kirkner, J. Appl. Phys. **67**, 6353 (1990).

[4] R. Haydock, *The Recursive Solution of the Schrödinger Equation*, Solid State Physics vol. 35, Academic Press, 215 (1980).

Inclusion of Quantum Confinement Effects in Self-Consistent Monte Carlo Device Simulations

R W Kelsall and A J Lidsey

Microwave and Terahertz Technology Group
Department of Electronic and Electrical Engineering
University of Leeds
Leeds LS2 9JT, UK

The methodology for developing semiconductor device simulations using Monte Carlo methods is now reasonably mature. The 2-dimensional self-consistent Poisson Solver / Ensemble Monte Carlo scheme is a standard approach which has been successfully applied to FETs - including Silicon MOSFETs and SiGe and III-V MODFETs - and to HBTs. Numerous enhancements to the basic model have been developed to increase accuracy and efficiency.

However, the standard Monte Carlo device simulation is semi-classical: electrons and holes are modelled as discrete particles, whilst scattering rates are calculated using quantum mechanical theory. It has long been appreciated that in certain situations - such as the MOSFET inversion layer and the MODFET channel layer - quantum confinement effects may be significant and the discrete particle model may be inadequate. Inclusion of quantum confinement effects requires, in principle, self-consistent solution of the 2-dimensional Poisson and Schrodinger equations, *and* the Monte Carlo transport algorithm; a task which appears far too computationally expensive for practical application. Consequently, previous attempts to incorporate quantum confinement have usually involved restricted solution of the Schrodinger equation and loss of self-consistency.

In this paper, we discuss our work on a 2-dimensional Monte Carlo / Poisson / Schrodinger MODFET simulator. The Schrodinger equation is solved in a series of 1-dimensional slices between source and drain, but self-consistency between the electrostatic potential and quantum-mechanical charge distribution is maintained. The scattering rates in the MODFET channel are calculated *at each position along the channel* using the quantum confined wavefunctions, and are re-calculated periodically throughout the simulation. The code permits different timesteps to be used for the Poisson, Schrodinger and scattering rate updates, in order to maximise efficiency whilst preserving simulation accuracy and stability. An important aspect of the simulation is the manner in which transitions from localised (quantum confined) to delocalised (classical-like) states are modelled. In our code, transitions between classical and quantum confined states are only permitted for electrons localised in the channel region, and a corresponding set of transition rates are calculated. We contrast this approach to alternative suggestions in which both initial and final states are assumed purely bulk-like or purely two-dimensional. The implications for modelling real space transfer and transconductance in MODFETs are discussed. Comparisons are drawn with alternative (non Monte Carlo) simulation schemes which include quantum confined carrier wavefunctions yet have no microscopic description of scattering phenomena.

Two dimensional modelling of HEMTs using Multigrids with quantum correction

Eric A.B. Cole[†], Tobias Boettcher[†][‡] and Christopher M. Snowden[‡]
Centre for Nano-Device Modelling, University of Leeds, Leeds LS2 9JT, UK.

† Department of Applied Mathematical Studies, University of Leeds.
‡ Department of Electronic and Electrical Engineering, University of Leeds.

Abstract

One method of modelling the HEMT in two dimensiomns is to solve the current continuity, energy transport and Poisson equations self-consistently with the Schrödinger equation. The addition of the task of solving the Schrödinger equation with the first three equations adds considerably to the time taken to reach convergence as well as to the complexity of the simulation.

Strong coupling exists between the Schrödinger equation

$$-\frac{\hbar^2}{2}\nabla.(\frac{1}{m}\nabla\xi_i) + V\xi_i = \lambda_i\xi_i$$

which has to be solved for the energy eigenvalues λ_i and eigenfunctions $\xi_i (i = 0, 1, 2...)$ and the Poisson equation

$$\nabla.(\epsilon_0\epsilon_r\nabla\psi) = -q(N_d - n)$$

which is solved for the electrostatic potential ψ. The potential V in the Schrödinger equation is given in terms of ψ while the electron density n in the Poisson equation is given in terms of the eigenstates of the Schrödinger equation: $n = n_2 + n_3$ where n_2 is the contribution from the sub-bands given from the Schrödinger equation and n_3 is the bulk electron density. Care must be taken to avoid double counting of the electrons in this expression for n, and a method is developed to enable n to be calculated using a relatively small number of eigensolutions. A method is developed whereby all the equations, apart from the Schrödinger equation, are solved using the multigrid method, with the Schrödinger equation being solved at each level to provide the electron concentration n. Considerable speed-up is achieved using this method. The methods are illustrated in terms of the one dimensional solution of the coupled Poisson-Schrödinger equations, and applied to the full two dimensional solution by solving the Schrödinger equation in one dimensional slices perpendicular to the layer interfaces.

p-Si Monte Carlo simulator for deep submicron MOS devices

N. A. Bannov, W. C. Holton, and K. W. Kim

Department of Electrical and Computer Engineering
North Carolina State University, Raleigh, NC 27695

We have developed a package of Monte Carlo particle programs for simulation of hole transport in silicon deep submicron devices. The main objective for building such a simulator is to make it accurate for simulation of p-channel silicon devices with gate length 50-500 nm, still keep it efficient and hence usable for routine device simulations. To achieve this objective, numerical models and individual physical processes affecting hole transport have been carefully selected.

The bulk simulator includes a full band structure model, all essential mechanisms of scattering (optical and acoustic phonon inelastic scatterring, Coulomb scattering, impact ionization), and statistical enhancement for high energy particles. We make a comparison of our simulator with other existing p-Si simulators: DAMOCLES, a simulator from AT&T, and a simulator from the University of Texas at Austin.

The simulator has been used for investigation of the temperature dependence of the hole impact ionization coefficient. Until recently there was a significant difference in the hole impact ionization rates reported by different authors. Two independent recent works [1,2] based on *ab initio* calculations gave almost the same result for this important transport parameter. We have used results of Refs. [1,2] to obtain the hole impact ionization coefficient as a function of electric field for several lattice temperatures. These functions can be used in drift-diffusion and other simulators of p-Si devices.

---

[1] T. Kunikiyo, M. Takenaka, M. Morifuji, K. Taniguchi, and C. Hamaguchi,
    J. Appl. Phys. **79**, 7718 (1996).
[2] M. Fischetti, N. Sano, S. Laux, and K. Natori, private communication.

MOMENTS: The Modular Monte Carlo Environment for Charge Transport Simulation
Overview and Applications

Mark Peskin and Christine Maziar

Microelectronics Research Center, The University of Texas at Austin
Austin, TX 78712, USA
(512)471-8838, (512)471-5625 (fax)
mpeskin@mail.utexas.edu

We present MOMENTS, a newly developed software library for Monte Carlo simulation of semiconductor devices. This library uses object-oriented design principles to provide a flexible, extensible toolset that allows rapid development of a wide variety of Monte Carlo simulation applications. MOMENTS has a modular design permitting the relatively straightforward construction of simulations with an unprecedented level of complexity. It allows concurrent simulation of multiple particle species (e.g. electrons and holes) with arbitrary interactions between species (e.g. generation-recombination and carrier-carrier scattering) in arbitrary geometries. Both analytic and numerical bandstructure representations, as well as mixtures thereof, are supported. MOMENTS also provides a number of novel capabilities that together work to address the tremendous computational demands that have tended to limit Monte Carlo simulation to the role of a specialized research tool. Most importantly, MOMENTS takes advantage of the parallelism inherent in the ensemble Monte Carlo approach. Particle populations can be divided into several simulation "contexts," each of which evolves independently in parallel. These independent contexts are then synchronized and allowed to interact at predetermined intervals. This scheme can support a wide variety of parallel architectures, including heterogeneous distributed systems, and allows active load balancing. Additionally, MOMENTS allows virtually every aspect of the simulation, including scattering events, self-scattering rates, bandstructure representations, and even interpolation schemes, to be varied freely across different regions of the simulation domain. This allows the greatest degree of computational complexity to be focused in regions of the domain where the greatest accuracy is desired, a capability heretofore limited to continuum-type (i.e. drift-diffusion and hydrodynamic) simulations.

To demonstrate some of the capabilities of MOMENTS, we will also present the results of detailed simulations of impact ionization in III-V compound avalanche photodiode (APD) structures. This will include results from what we believe is the first concurrent Monte Carlo simulation of interacting populations of both electrons and holes with full numerical bandstructure representations used for both carrier types. The degree of simulation detail provided by MOMENTS will allow us for the first time to fully quantify the mechanisms underlying the noise-suppression recently observed in III-V APDs with very thin multiplication layers[1,2]. A detailed understanding of this phenomenon is critical for directing the future evolution of high-performance APD design.

References

[1] K. A. Anselm et. al., IEEE Electron Device Lett. 17(3), 91 (1996)

[2] C. Hu et. al., Appl. Phys. Lett. 69(24), 3734 (1996)

High-Field Hole Transport in Strained Si and SiGe by Monte Carlo Simulation: Full Band Versus Analytic Band Models

F. M. Bufler, P. Graf, and B. Meinerzhagen

Institut für Theoretische Elektrotechnik und Mikroelektronik
Universität Bremen, FB 1, Postfach 33 04 40, D-28334 Bremen, Germany
email: bufler@item.uni-bremen.de   Phone: +49 421-218 2204   Fax: +49 421-218 4434

The progress in epitaxial growth techniques of unstrained and strained SiGe layers have led to intensified efforts to explore the potential performance enhancement in SiGe based devices. In particular, the practical feasibility of p-MOSFET's with a channel consisting of strained Si [1] or strained SiGe [2] has been recently demonstrated. Since field effect devices operate in the low-field and in the high-field regime, reliable modeling of hole transport is important for both cases. However, previous publications on hole transport in strained Si and SiGe covered only the low-field regime [3] or were restricted to strained SiGe and electric field strengths below 20 kV/cm [4]. Hence, there is still a need for investigations of high-field effects like velocity saturation where the consideration of the full band structure is often necessary for accurate results. On the other hand, there are important situations where full band Monte Carlo simulations still involve an unmanageable computational burden (e.g. prohibitive memory requirements) and analytic band structure approximations have to be used instead. This is the case for Monte Carlo simulations of devices with realistic Germanium profiles as well as for the surface quantization problem where the effective Schrödinger equation under the influence of the gate voltage has to be solved. The aim of this paper is therefore twofold: On one hand, we perform for the first time full band Monte Carlo simulations for strained Si and SiGe in the high-field regime. On the other hand, we present a simple analytic hole band model and evaluate its range of validity.

The full band model for strained Si or SiGe is obtained by nonlocal empirical pseudo potential calculations including spin-orbit interaction [5]. For the analytic band structure we neglect the warping of the three valence bands ν=1,2,3 and use a simple parametrization according to

$$(\epsilon - \epsilon_{0,\nu})(1 + \alpha_\nu(\epsilon - \epsilon_{0,\nu})) = \frac{\hbar^2}{2}\left(\frac{k_x^2}{m_{\|,\nu}} + \frac{k_y^2}{m_{\|,\nu}} + \frac{k_z^2}{m_{\perp,\nu}}\right)$$

because of the feasibility of this formula for applications. The parameters α_ν, $m_{\|,\nu}$ and $m_{\perp,\nu}$ are adapted to the full band structure. The scattering mechanisms included are optical phonons and acoustic phonons in the isotropic and elastic equipartition approximation. In SiGe both Si-type and Ge-type phonons are considered and alloy scattering is taken into account with the alloy scattering potential adjusted to mobility measurements in unstrained SiGe [6]. Exactly the same coupling constants are used with the full band and the analytic band model.

In Figs. 1, 2 and 3 the drift mobilities and drift velocities resulting from the full band and the analytic band model are compared with experimental data in the case of unstrained Si. Overall good agreement is achieved. Especially the full band model in Fig. 2 reproduces accurately the anisotropy of the velocity-field characteristics as well as the saturation drift velocity of Ref. [7]. Within the isotropic band approximation (unstrained case) also the analytic band model yields surprisingly good results and only significantly underestimates the drift velocity above 50 kV/cm. In Figs. 5 and 6 the high-field results for strained Si and SiGe are shown. While the value of the saturation drift velocity in unstrained Si is retained in strained Si, the drift velocity at lower fields is considerably improved due to the enhanced population of the light hole band. In contrast, all strain induced advantages are suppressed by alloy scattering in strained SiGe. But please keep in mind that no realistic estimate of the corresponding device performance can be based on Fig. 5 alone, because advantages like the possibility of modulation doping have to be considered for this purpose as well. The analytic band model again underestimates the drift velocity above 50 kV/cm and somewhat overestimates anisotropy.

In summary, we have computed the velocity-field characteristics of holes in strained Si and SiGe by full band Monte Carlo simulations. In addition, a simple analytic hole band model has been developed which agrees well with the full band results and is therefore well suited for transport investigations where the consideration of the full band structure is still prohibitive.

References

[1] D. K. Nayak et al., IEEE Trans. ED **43**, 1709 (1996)
[2] L. Risch et al., *Proc. ESSDERC* **26**, 465 (1996)
[3] M. V. Fischetti et al., J. Appl. Phys. **80**, 2234 (1996)
[4] J. M. Hinckley et al., Phys. Rev. B **41**, 2912 (1990)
[5] M. M. Rieger et al., Phys. Rev. B **48**, 14276 (1993)
[6] G. Busch et al., Helv. Phys. Acta **33**, 437 (1960)
[7] P. M. Smith et al., Appl. Phys. Lett. **39**, 332 (1981)
[8] M. A. Green, J. Appl. Phys. **67**, 2944 (1990)
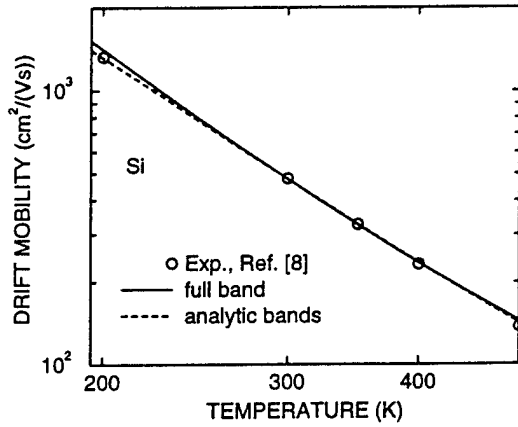[9] C. Canali et al., J. Phys. Chem. Solids **32**, 1707 (1971)

Fig. 1: Temperature dependence of Ohmic drift mobility for holes in unstrained Si: comparison of full band model, analytic band model and experimental results [8]
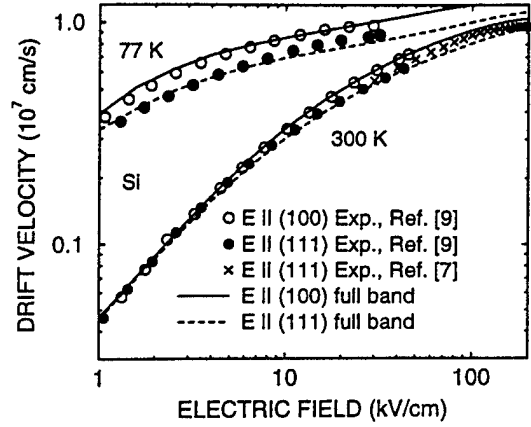

Fig. 2: Velocity-field characteristics of the full band model at 77 and 300 K in comparison with experimental results [9, 7]
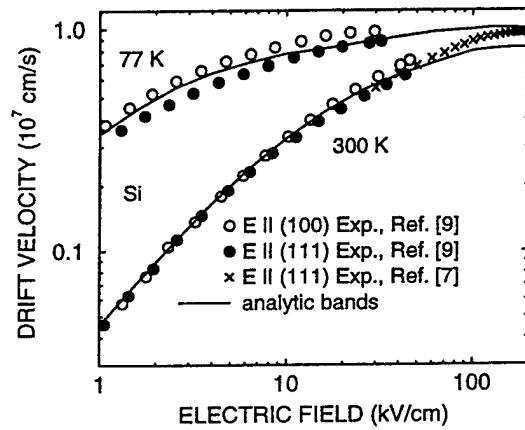

Fig. 3: Velocity-field characteristics of the analytic band model at 77 and 300 K in comparison with experimental results [9, 7]
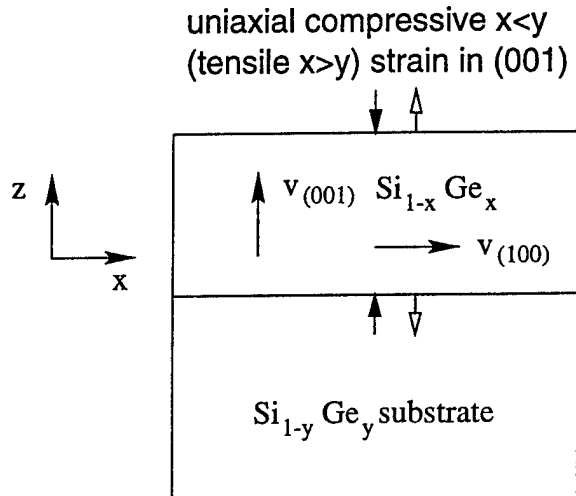

Fig. 4: Simplified cross section illustrating the relevant directions of the drift velocities v in a strained $Si_{1-x}Ge_x$ layer grown on a $Si_{1-y}Ge_y$ substrate
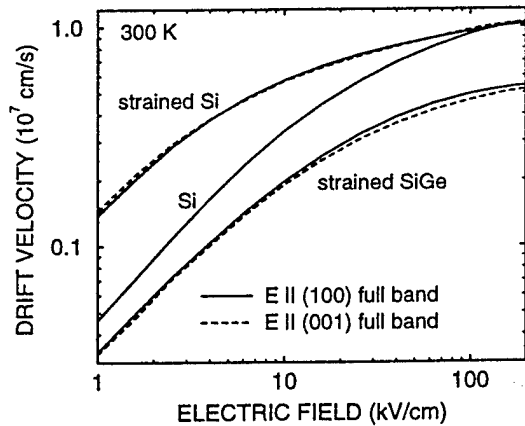
Fig. 5: Results of the full band model for the velocity-field characteristics at 300 K in strained Si grown on a $Si_{0.7}Ge_{0.3}$ substrate, in unstrained Si and in strained $Si_{0.6}Ge_{0.4}$ grown on a Si substrate
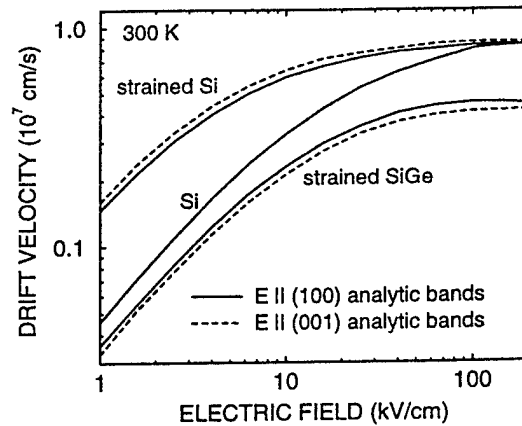
Fig. 6: Results of the analytic band model for the velocity-field characteristics at 300 K in strained Si grown on a $Si_{0.7}Ge_{0.3}$ substrate, in unstrained Si and in strained $Si_{0.6}Ge_{0.4}$ grown on a Si substrate

Hierarchical Simulation for ULSI Process Design
- From Atomistic to Conventional Process CAD

S.Onga, T.K.Okada, H.Takada, T.Koyanagi, E.Kan* and R.W.Dutton*

Toshiba Research and Development Center,

Toshiba Corporation, Kawasaki 210, Japan

*Center for Integrated Systems, Stanford University,

Stanford, CA 94305-4070

§ 1. Introduction

In the design phase of scaled devices, several innovative process/materials have been introduced, for instance, 1)adoption of special rapid thermal process for shallower junctions, 2)introduction of low oxygen concentration silicon wafers for high reliability thin oxides, 3)trench isolation to reduce field area, 4)novel materials such as ferroelectrics for larger spontaneous polarization and high reliability and many others. It has become much more significant than before, to specially pay attention to process induced stress, and/or residual stress in those devices, in order to eliminate crystalline defects caused by thermal stress, also in order to have a precise estimation of structure in the oxide layers, taking into account stress dependence of oxidation rate and so-forth. Moreover, deeper insight of atomistic level behavior also would be necessary for such ferroelectrics.

From this view point, a prototype composite process/structure/materials simulation system has been created. In this report, a general concept of composite process/structure/material/EOM simulator would be first presented, and some of rigorous mathematical derivation of molecular dynamic(MD) simulation part will be shown. Finally some typical example results will be reported.

§ 2. General concept of a composite process/structure/material simulator and process designing.

Figure1 shows a composite process/structure/material simulation system. Several parts in the figure such as the ab-initio, MD parts as well as their interfaces have been developed specifically for this prototype. For conventional fabrication processes, the optimization of two-dimensional TSUPREM4/DEPICT process steps have been essential. We have also originally developed a new subroutine for extraction of electrical, optical, monitoring steps(EOM)' for extraction of specific values extraction of critical material characteristics, for example, the Young Modulii C_{ij}, Diffusivity D.

Using well-calibrated TSUPREM/ABAQUS modules, precise estimation of structure and process sequence designing can be achieved, with special attention of oxidant diffusion, oxidation rate dependence in relation to stress distribution during oxidation, and residual stress variation as a parameter of cooling rate. For the task of atomistic studying of Si/SiO2 interface, MD simulator can be used effectively. We have examined best-fit configuration of SiO2 crystal to the Si substrate, minimizing the interface energy. Moreover, using the composite system, we can simulate structure and stress distribution for cases that use new material, even without having specific value such as C_{ij}, Diffusivity D in advance.
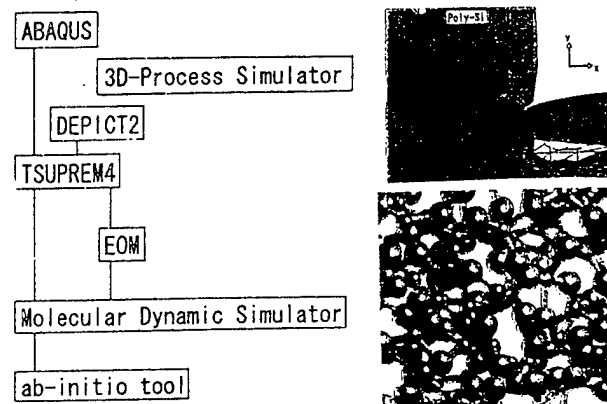
Fig. 1 General concept of hierarchical simulation using a composite pcess/structure/material simulator

WeP1

Necessary Roughness of MOS Interface for Device Simulation

Edwin C. Kan, Heng-Chih Lin and Robert W. Dutton

CIS-X 334, Stanford University, Stanford, CA 94305-4075

Phone: (415)723-9796, Fax: (415)725-7731, Email: kan@gloworm.stanford.edu

While planerization in VLSI layer technology is most common, modeling of MOS interface roughness [1] in the device simulation level (and to what degree the rough boundary can be smoothed without severe loss of accuracy in I-V characteristics since explicit treatment of interface roughness in Lagrangian description can cause serious gridding problems) is very useful for several MOS-based applications. Interface roughness may be purposely enlarged for enhancing tunneling efficiency [1,2], or may be unintentionally introduced due to physical process or process simulation. Surface characterization by AFM imaging (see an example in Fig. 1) can give surface resolution up to the angstrom range, which will virtually eliminate the uncertainty for initial interface geometry construction.

Si/SiO$_2$ interface roughness has four effects on MOSFET I-V characteristics, and the interface smoothing algorithms should conserve accuracy in these four aspects depending on simulation requirements:

- MOS capacitance (zeroth order in geometry): the areal magnification factor should not be extracted entirely from geometry since the carrier distribution does not follow the fine geometrical details of the interface (see Fig. 2). To maintain accuracy in capacitance extraction, the smoothing algorithms also need to consider the effects of degenerate carrier statistics and quantum capacitance (shift in threshold and enlarged thickness) due to carrier confinement in steep potential well [3]. A series of capacitance simulation on various RMS roughness levels will be shown in the conference.

- Surface mobility (first order in geometry): mobility degradation due to surface roughness has been summarized in [1]. The fine and unperiodical geometrical features should be smoothed out and an effective RMS value of roughness will be used in surface-roughness-scattering perturbation calculation.

- Tunneling efficiency (second order in geometry as curvature): Enhancement in oxide electric field will be well conserved if curvature is explicitly considered during smoothing.

- Stress-related: Owing to the lattice mismatch, flat Si/SiO$_2$ usually contains compressive stress in oxide and tensile stress in silicon. This situation will be more severe in the valleys and less in the tips. However, presently there is no good physical model or experimental measurement for stress estimation in the resolution considered here.

Tradeoffs between physical accuracy and gridding complexity for the smoothing algorithms (curvature based, spatial Fourier analyses, etc.) will be summarized in the conference.

[1] H.-C. Lin, E.C. Kan, T. Yamanaka and C.R. Helms, submitted to *VLSI Technology Symp.*, Kyoto, June 1997.
[2] Y. Fong, A.T.-T. Wu, and C. Hu, *IEEE Trans. ED*, vol.37, no.3, pp. 583-90, 1990.
[3] K.S. Krisch, J.D. Bude and L. Manchanda, *IEEE EDL*, vol. 17, no. 11, pp. 521-524, Nov. 1996.
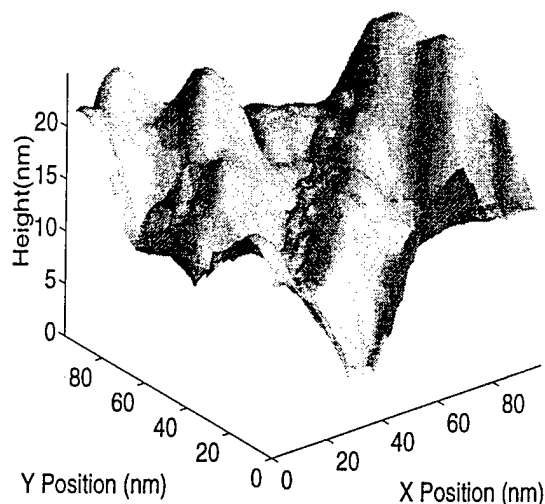
Fig. 1: 3D AFM image with size of 100nm × 100nm. The RMS roughness is 4.3nm. The surface is purposely roughened for improving tunneling efficiency.
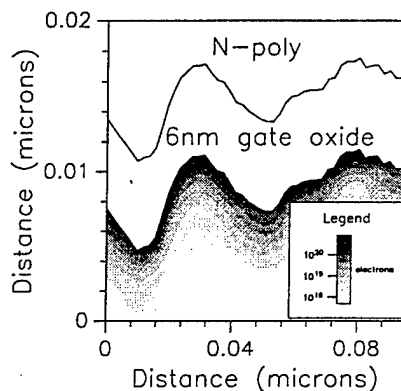

Fig. 2: Electron distribution simulated by the drift-diffusion model. The oxide geometry is constructed by a 2D cross section from Fig. 1.

Non-Uniformity Effects in Ultra-Thin Tunneling Oxides

D. Z.-Y. Ting† , Erik S. Daniel, and T. C. McGill
Thomas J. Watson, Sr. Laboratory of Applied Physics
Mail Stop 128-95
California Institute of Technology
Pasadena, California 91125

ABSTRACT

Advanced MOSFETS for ULSI and novel silicon-based devices require the use of ultra-thin tunneling oxides where non-uniformity is often present. We shall report on our theoretical study of how tunneling properties of ultra-thin oxides are affected by roughness at the silicon/oxide interface. The effect of rough interfacial topography is accounted for by using the planar supercell stack method (PSSM) which can accurately and efficiently compute scattering properties of 3D supercell strcutures. Our results indicate that while interface roughness effects can be substantial in the direct tunneling regime, they are less important in the Fowler-Nordheim regime.

† Corresponding Author. dzt@ssdp.caltech.edu
Also with Department of Physics, National Tsing Hua University, Hsinchu, Taiwan.

Modeling of Thermal Effects in Semiconductor Structures

Christopher M. Snowden *(Invited Paper)*

Microwave and Terahertz Technology Group, Department of Electronic and Electrical Engineering,
University of Leeds, Leeds. LS2 9JT. UK
Telephone: + 44 113 233 2001. FAX: + 44 113 233 2032. email: C.M. Snowden@elec-eng.leeds.ac.uk

Abstract

Introduction
Until relatively recently very little effort has been devoted to thermal considerations associated with most semiconductor devices, yet in many cases the thermal effects have a very strong impact on their performance. The high power densities associated with modern microwave transistors makes this class of active device particularly sensitive to temperature effects and dependent on good thermal management. This is especially true of the heterojunction bipolar transistor (HBT) which typically achieves power densities up to 3 times that of FETs. Compound semiconductors such as GaAs generally have a far lower thermal conductivity than Si, which can in turn lead to high operating temperatures and poor thermal stability. Another consequence of the thermal resistance and the associated thermal time constant of active devices is the contribution from dynamic thermal effects to the RF performance of microwave transistors (eg. intermodulation distortion).

Thermal and Electro-Thermal Modeling
This paper addresses the modeling of thermal effects in semiconductor structures. In particular, it examines the requirements for thermal and electro-thermal modelling and then considers the impact on transport modelling and finally large-scale thermal modelling of complete structures (eg: a full die). Self-heating has a significant impact on parameters such as mobility, generation-recombination and trap occupancy. A rigorous electro-thermal solution is described with a coupled thermal and transport model. This is achieved by utilizing a set of hydrodynamic equations derived from the Boltzmann transport mode (utilizing four moments), coupled to an accurate solution of the heat flow equation. The numerical solution of the heat flow equation requires careful consideration to obtain an accurate solution, with a third-order boundary condition. Ghione et al have suggested that to obtain accurate results for MESFETs, the simulation domain

for analysis should be extended horizontally for up to three times the source-drain contact spacing and to a depth of up to ten times the active layer thickness of the device [1]. Examples of full electro-thermal simulations will be given in the presentation.

A three-dimensional thermal analysis technique has been developed which allows full-scale analysis of large device structures. The steady-state heat flow equation $\nabla.\kappa(T)\nabla T=0$ is solved for a three-dimensional temperature distribution over the full die using the method of Liou [2] and Gao et al [3]. This method uses a double Fourier expansion method to speed up the solution. The heatsink is assumed to be attached to the bottom of the substrate (at $T = T_{mount}$), whilst all other surfaces except the heat sources (region below the emitter fingers) are assumed to be adiabatic. The heat sources are treated locally using the coupled electro-thermal model. A typical surface temperature distribution for an eight finger pHEMT device is shown in Figure 1. The 3D simulator utilized over 12,500 mesh points on the surface to obtain these results, achieving very good agreement with measured IR data. Typical results for a 1 Watt HBT show agreement in temperature of better than 5% across the whole structure. Modeled and simulated DC characteristics for this HBT are shown in Figure 2. This has in turn allowed the accurate prediction of the microwave performance of the amplifiers. A multi-cell thermal analysis scheme based on this work has been used to develop a new thermal resistance matrix scheme to allow the rapid evaluation of self-heating. Further details will be given in the presentation.

Figure 1 Surface temperature contours (°C) for a 8 finger pHEMT, obtained from a 3D simulation of (V_{DS} = 3 V, I_{DS} = 100 mA, die thickness is 200 microns, mounting temperature is 40 °C).
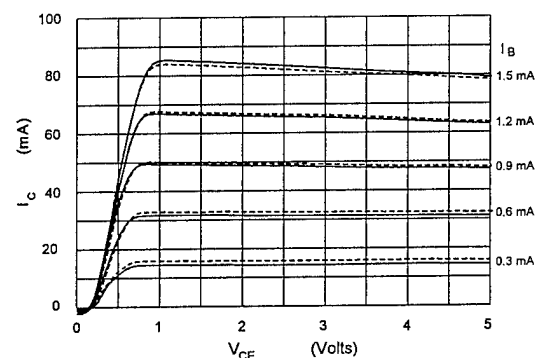
Figure 2 AlGaAs/GaAs HBT Characteristics --- measured,_____ modelled (full electro-thermal).

References
[1] G.Ghione et al, Alta Frequenza, Vol. LVII, 7:311-319, 1988.
[2] L.L. Liou et al, IEEE Trans. ED-40, No. 1, pp.35-42, 1993.
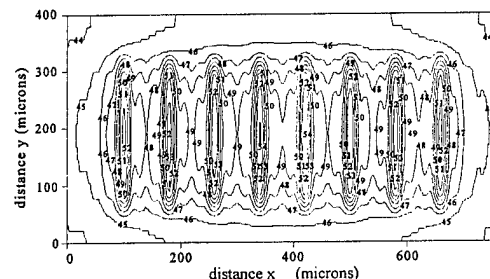[3] G-B Gao et al, IEEE Trans. , ED-36, No.5, pp.854-863, 1989.

Carrier Thermal Conductivity: Analysis and Application to Submicron-Device Simulation

A. Greiner and *L. Reggiani*, INFM, Dipartimento di Scienza dei Materiali
Università di Lecce, via Arnesano, 73100 Lecce, Italy
Fax: +39 (832) 320-525, e-mail: greiner@axpmat.unile.it
T. Kuhn, ITP II, Universität Münster, Münster, Germany
L. Varani, CNRS, Université Montpellier II, Montpellier, France
P. Golinelli, INFM, Università di Modena, Modena, Italy
M. C. Vecchi, DEIS, Università di Bologna, Bologna, Italy

Abstract. By using a correlation-function formalism, the kinetic coefficients of charge carriers in semiconductors are studied under a variety of different conditions. As a consequence of the fluctuation-dissipation theorem, these coefficients are determined by the spectrum of the fluctuations in the system.

For the case of linear response, the transitions from the classical to the degenerate regimes as well as from ballistic to diffusive conditions are discussed for different dimensionalities of the sample within an analytical model [1]. The result shows a universal character of the thermal conductance in the ballistic degenerate limit for a one-dimensional conductor.

Then, the method is generalized to high-field transport in nondegenerate semiconductors. Here, the correlation functions are determined by Monte Carlo calculations [2] under homogeneous conditions, which allows one to calculate the kinetic coefficients and, in particular, the thermal conductivity as a function of the carrier temperature. Such thermal conductivity obtained for silicon has been included into the hydrodynamic code HFIELDS [3] and applied to the simulation of an n^+nn^+ submicron device to calculate temperature and velocity profiles of the carriers.

The results are compared to calculations with HFIELDS applying a thermal conductivity $\kappa = (5/2 + c)(k_B/q)^2 \sigma T$ obtained from a simple Wiedemann-Franz law for different values of the power-law exponent c, as well as to full Monte Carlo simulations of the structure. It turns out that the thermal conductivity obtained by the generalized correlation-function formalism decays much more rapidly than the Wiedemann-Franz law as the temperature increases. The comparison with Monte Carlo simulations of the n^+nn^+ structures [4] shows that the correlation-function formalism is able to reproduce the Monte Carlo results for carrier velocity and temperature to a better extent than the power-law form of the Wiedemann-Franz law. Such result is traced back to the fact that the effect of the various timescales introduced by the fluctuations of the moments of the distribution function, which enter the definition of thermal conductivity, can not be reproduced by a single power-law exponent. The different timescales arising in the non-equilibrium case cause for example the asymmetry of the cross-correlation spectra [2].

To show the influence on the simulations of realistic devices, the concentration, velocity, and temperature profile of the carriers in short-channel MOS transistor have been calculated at different operating conditions.

References:

[1] A. Greiner *et al.*, Phys. Rev. Lett. **78**, p. 1114 (1997)
[2] P. Golinelli *et al.*, Phys. Rev. Lett. **77**, p. 1115 (1996)
[3] A. Forghieri *et al.*, IEEE Trans. on CAD of ICAS, CAD-7, pp. 231–242 (1988)
[4] A. Gnudi *et al.*, Europ. Trans. on Telecommunications and Related Techn., **1**, pp. 307–312 (1990)

Heat Dissipation from Quantum Structures

V. V. Mitin, G. Paulavicius, and N. Bannov

Department of Electrical and Computer Engineering
Wayne State University, Detroit, MI 48202

Michael A. Stroscio

U.S. Army Research Office
P.O. Box 12211, Research Triangle Park, North Carolina 27695-7911

When characteristic sizes of heterostructure devices approach nanodimensions, the physical picture for heat accumulation, transfer, and dissipation undergoes substantial modifications. While these processes in macrodevices are characterized by the thermal energy diffusion and are governed by the semiclassical thermoconductivity equation, heat accumulation and removal in nanodevices need to be described by coupled kinetic equations for phonons and electrons in which both electron quantization and phonon confinement are important.

We will review results of numerical simulation for thermal energy dissipation, transfer, and accumulation in several heterojunction nanostructures. We discuss the computational problems associated with solving the kinetic equations for the coupled electron–phonon system. We also consider a simplified and more efficient model for thermal energy removal from nanostructures.

Special attention will be paid to acoustic phonon radiation patterns due to electron–acoustic phonon interaction in double–barrier–quantum–well and quantum–wire based structures. A major feature of acoustic phonon emission from low dimensional structures is the lack of translational symmetry in the direction transverse with respect to quasi–free electron motion. This leads to violation of the transverse phonon wave vector component conservation in electron–phonon scattering. The characteristic energies of the emitted acoustic phonons correspond to $1-2\ meV$ for a $GaAs$ quantum well of $100-\mathring{A}$ width. This energy increases in proportion to the inverse of the thickness of the well. Such acoustic phonons propagate ballistically over macroscopic distances causing substantial deviation of spatially radiated energy distribution from that calculated using the conventional thermoconductivity equation.

We will also discuss optical phonon accumulation in quantum wells and wires due to stimulated phonon emission. The characteristic decay time of optical phonons ($8\ ps$ in $GaAs$) is significantly longer than the time of spontaneous emission of these phonons by electrons ($\approx 0.15\ ps$ in $GaAs$). Therefore, the optical phonon population grows with increasing electric current. For significant optical phonon populations, stimulated phonon emission becomes an important factor in electron–phonon kinetics. As a result, distribution functions of both, electrons and phonons, calculated self-consistently differ substantially from those obtained in the commonly used approximation which neglects nonequilibrium phonons.

Molecular Wires: Conductance, Geometric Dependence, Energetics, Electron Repulsion and Their Relationship to Intramolecular Electron Transfer

Mark A. Ratner
Department of Chemistry
Northwestern University
Evanston, Illinois 60208-3113

Abstract

Assembled electrode/molecule/electrode structures, using STM and mechanically controllable break junction techniques, permit experimental study of currents through single molecular wires. Computationally, this problem involves the interaction of discrete states of the molecular wire with the continuum states of the electrode. Utilizing a self energy formalism originally developed by Newns and Anderson for the chemisorption problem, and a tight binding model for the molecular wire, one can develop a computational algorithm to study the conductance of molecular wire circuits. The determining parameters are the metallic band width and Fermi energy, the molecular orbitals of the molecule, and the interaction strength at the molecule/electrode interface.

Results are given for characteristic molecular wire structures, and the variation of the conductance with geometry, molecular structure, binding motif and injection energy is studied. Control (three gate) structures are proposed, and their effects are noted. The effects of dephasing and vibrational interaction can also be relevant, changing the length dependence, the temperature dependence, and the appearance of coulomb blockade and staircase. The coulomb blockade and staircase features, themselves, will differ from those in characteristic quantum dot structures because of the sparse eigenvalue spectrum of characteristic molecular structures. Finally, comments on control of intramolecular currents will be ventured.

Simulation of Molecular Electronic Devices

Weidong Tian* and Supriyo Datta
School of Electrical and Computer Engineering
Purdue University
West Lafeyette, IN 47907
USA

ABSTRACT

Experimental measurements of the resistance of molecular wires has recently been reported. These molecules consist of one or more benzene rings with end groups designed to function as 'alligator clips' that attach to metallic contacts. Molecular nanostructures of this type require us to model electron transport problem at the atomic level. Unlike usual calculations in quantum chemistry which deal with isolated molecules, this problem involves an open system. We have developed a Green's function technique to handle the coupling between the molecule and the contacts through a self-energy function. This method can be used to analyze current flow through molecular electronic devices. Using a simple expression based on Friedel sum rule we show that the low-bias resistance of symmetric molecules can be understood in term of three parameters: (a) the normalized broadening factor $(\Gamma_e + \Gamma_o)/E_g$ where Γ_e, Γ_o are effective broadening for all even, odd states, E_g is HOMO-LUMO gap; (b) asymmetry factor Γ_e/Γ_o, and (c) the amount of charge transferred ΔN. Molecular resistance can be controlled by adjusting these three parameters. This viewpoint should be useful in interpreting and guiding new experiments in this fast-growing field of research.

*Corresponding author:
email: wtian@ecn.purdue.edu
mailing address: Weidong Tian
                   P.O.Box 039, EE Building
                   Purdue University
                   West Lafayette, IN 47906
                   USA
Telephone: 765-494-3365
Fax: 765-494-6441

DRIFT-DIFFUSION EQUATIONS DESCRIBE AN IMPORTANT BIOLOGICAL SYSTEM: IONIC CHANNELS IN MEMBRANES.

BOB EISENBERG, Dept. of Molecular Biophysics and Physiology, Rush Medical Center, Chicago IL 60612. Phone: (312)-942-6467. Fax: (312)-942-8711. Email: bob@aix550.phys.rpslmc.edu

Drift-diffusion equations, combined with Poisson's equation (*PDD*), are widely used in physical sciences to describe the flux of charge carriers through systems containing fixed charge (doping). An important class of biological molecules—proteins called ionic channels—conduct ions (like Na^+, K^+, Cl^-) through a narrow tunnel of fixed charge formed by the polar residues of the protein. Ionic channels open and close ('gate') to give currents that are a random telegraph signal. The properties of gating are complex and the structure(s) and mechanism(s) that produce gating are not known, but the flow of ions through open channels is much simpler, and obeys the *PDD* equations, as we shall see.

Channels are the main pathway by which substances move in and out of cells and so are of great biological and medical importance: they are responsible for signaling in the nervous system; for coordination of muscle contraction, including the coordination of cardiac muscle that allows the heart to function as a pump; and they are involved in transport in every cell and organ, for example, in the kidney, intestine and endocrine glands. A substantial fraction of all drugs used by physicians act directly or indirectly on channels.

Channels are studied one molecule at a time in hundreds, if not thousands of laboratories every day, using Neher & Sakmann's patch clamp method (for which they received the Nobel Prize). The concentrations of ions outside channels can be easily controlled and the shape of current voltage (*IV*) relations can be manipulated in this way. For all these reasons, channels are a popular object for experimentation: thousands of abstracts describing their properties are presented each year at the annual meeting of the Biophysical Society (!).

Channels are also an appealing and important object for theoretical work. Open channels are probably the simplest protein structures of general biological importance. Theories certainly should be able to predict the movement of ions through such a tunnel of fixed charge on the biological time scale of 100 μsec—10 sec. Ionic movement plays an important role in the function of all proteins, e.g., enzymes, and so a model that describes ionic movement in channels is likely to give important insight into protein function in general.

Five laboratories have shown that the *PDD* form an adequate model of *IV* relations of 6 different channel proteins in ~10 pairs of solutions in the range ±150 mV. The *IV* relations are *qualitatively* different in different channels—some are linear, some sublinear and some superlinear—because different channel proteins have qualitatively different profiles of fixed charge arising from their different sequences of amino acids.

The structures of two of these proteins (porin and its mutant G–119D) are known: the location of every atom has been determined by x-ray diffraction. The mutant has one extra negative charge. Measurements of *IV* relations allow the *PDD* model to estimate the additional charge as $-0.97e$, although this estimate will undoubtedly change as more work is done. (I hasten to add that no information about the proteins is used in the analysis except the length and diameter of the channel; parameters were not adjusted in any way.) We conclude that the *PDD* equations are an adequate model of the porin channel, when it is open.

It is surprising that the *PDD* equations work as well as they do, given their evident inadequacies. I imagine they work this well because the fixed charge density of channels is large ($\sim 3 \times 10^{21}$ cm^{-3}) compared to the concentration of ions outside the channel (2×10^{19} to 1×10^{21} cm^{-3}); because the biological range of voltages is quite limited; and because the *PDD* model uses effective parameters. Eisenberg, Chen, and Schuss have recently shown how the *PDD* equations can be derived in single file systems like channels. The *PDD* equations, or equations quite like them, describe the mean properties of ensembles of Langevin equations, each of which specifies the motion of a single ion (of a particular type moving from a given side of the channel), each of which is coupled to its own Poisson equation and boundary conditions.

The *PDD* equations are just a first description of open channels. More realistic models (using Monte Carlo simulations) are needed to provide insight with atomic resolution. It is likely that many critical functions of channels and enzymes will be best understood this way, but biologists cannot do the simulations themselves: much help is needed from physical scientists experienced in the simulations of computational electronics.

The NEMO Project
or
Writing Research Software in a Large Group

Gerhard Klimeck, Dan Blanks, Roger Lake, R. Chris Bowen, Manhua Leng[*],
Chenjing L. Fernando, William R. Frensley[*], Dejan Jovanovic, and Paul Sotirelis

Corporate R & D, Texas Instruments Incorporated, Dallas, TX 75265
[*] School of Engineering, The University of Texas at Dallas, Richardson, TX 75083

The nanoelectronic modeling (NEMO) program is the result of a 3 year development effort involving four universities and the corporate research lab of Texas Instruments to create a comprehensive quantum device modeling tool for layered semiconductor structures. Based on the non-equilibrium Green function formalism it includes the effects of quantum charging, bandstructure and incoherent scattering. The software has been written to address the diverse needs of two different user groups: (i) the engineer/experimentalist who desires a black-box design tool and (ii) the theorist who is interested in a detailed investigation of the physics. A hierarchy of models is available to the user which trade off accuracy with speed and memory requirements. Access to this comprehensive theoretical framework is accommodated by a command line interface (batch operation) or a graphical user interface (GUI). While the batch version provides the optimum speed, memory usage and portability, the GUI facilitates device prototyping and in-situ data analysis. The challenge in the software design was the simultaneous development/enhancement of the theory and the user-interface. We will describe our dynamic approach to satisfy both user and programmer requirements such as ease of use and ease of development. An issue addressed in particular is the user-friendly hierarchical entry of parameters and the design of a flexible interface which accepts rapidly changing theory modules with ever varying numbers and types of parameters. Our dynamic approach allows the theory and the GUI modules to share data structures such as device structure, material, and simulation parameters. These data structures may contain general data such as integer and real numbers, option lists, vectors, matrices and the labels for both batch and GUI operation.

Photonic Device Modeling for Telecommunication Purposes

Kiyoyuki Yokoyama

NTT Opto-electronics Laboratories
3-1 Morinosato Wakamiya, Atsugi, Kanagawa 243-01, Japan
Phone: 81-462-40-2803, Fax: 81-462-40-4532, e-mail: yoko@aecl.ntt.co.jp

We have witnessed remarkable and continuous progress of device fabrication technologies and computational capabilities. Both have been well matched to each other and have provided us with a comfortable high-technology-assisted society. At the workshop, the author would like to focus on key photonic devices and modeling of photonic devices for optical access networks. The devices are divided into two categories for the purpose of modeling. One is semiconductor devices. The other is nonsemiconductor devices, such as LiNbO3 and PLCs (Planar Lightwave Circuits). For the latter modeling, the main subject is solving Helmholtz equation which determines optical behavior. On the other hand, for the former, in addition to the optical equation, semiconductor basic equations must be solved simultaneously to describe the carrier behavior. Numerical difficulties arise in solving the two different wavelength natures of equations in the same space, i.e., the wavelength of electron behavior (~ 10 nm) and that of optical behavior (~ 1.3-1.55 μm).

The reason for demand for photonic devices is their very high performance without sacrificing cost increase. Advanced hybrid technologies, in which the two different kinds of device are combined (currently semiconductor and/or LiNbO3 devices on PLC platforms) , are commonly used to construct optical systems. Numerical simulations are indispensable for the development of key photonic devices as shown below.

○ Semiconductor Active Devices (LDs, SOAs, and Modulators)

    Crystal Design
        Strained value (including compression or tensile), well width, barrier material and its width, and number of multi-quantum-well structure, etc.
    Device Design
        Cavity length, active region width, grating structures and the facet treatment.
        Accurate wavelength design, high-speed operation, high-temperature operation, high-power operation, low threshold, chirp design and polarization control, etc.

○ Semiconductor Passive Devices (Waveguides, Spot Size Converters, Polarization Rotators)

        Mode and BPM analysis for buried heterostructure, ridge structure, and intentionally nonuniform waveguide structure, etc.

○ PLC (Star Coupler, Arrayed-Waveguide Grating Multiplexer, Optical Delay Equalizer)

        Functional design for a large scale of optical integration using BPM method

In my talk, a few examples of the modeling shown above and future work in this field will be addressed.

Modeling and Simulation of Semiconductor DFB Lasers: A Hierarchical Approach

Wei-Ping Huang and Xun Li
Department of Electrical and Computer Engineering
University of Waterloo
Waterloo, Ontario, Canada N2L 3G1

Laws governing the operation of semiconductor laser diodes are well-known, yet modeling and simulation of such devices still remain a challenging task as the devices involve complicated optical, carrier and thermal processes which are coupled with each other and interact with materials in a complex manner. Zero-dimensional models based on rate equations are commonly used and are quite successful in explaining behaviors of laser diodes. A merit of the 0D models is the simplicity in both governing equations and modal parameters. Consequently, they are frequently employed as a theoretical framework to interpret experimental results. More sophisticated 1D models account for the variations of carrier and photon densities along the cavity. This is necessary for DFB lasers, as the longitudinal spatial hole-burning is important. In both 0 and 1D models, most of the parameters are "effective" and their links to actual device geometry and material properties are not always clear. To overcome this short-coming, detailed physics-based 3D models were also developed. Such models solve wave equations for optical field, Poisson and drift-diffusion equations for carriers and heat transfer equations for temperature. Furthermore, rigorous physics-based models are used for optical gain and other material properties. In comparison with the 0/1D models, however, these physics-based models are complicated and computation intensive. From practical point of view, however, this type of simulators may not be very useful for purpose of design and characterization. Aside from the issue of efficiency, there is a question of complexity as well. More often than not, one is interested in only one or a few aspects of a laser and has accurate knowledge for limited number of modal parameters. Under this situation, it may be not practical or even necessary to run a full 3D simulator.

With the above arguments in mind, we have developed a multi-level model that incorporates the three, one and zero-dimensional as well as the material models into a vertically integrated hierarchy. At the lowest level, the material parameters such as optical gains can be calculated rigorously and then fitted into an analytical formula dependent on carriers, wavelength detunig and temperature. The material parameters can be passed on to the next level three-dimensional model which is capable of simulating the optical, carrier and thermal effects in a complex DFB/FP laser. Furthermore, this model can also produce the effective modal parameters to higher-level one and zero-dimensional models, which are much more efficient and simpler. In addition, we have investigated and developed methods for parameter extraction, especially for the higher level simulators. This hierarchical approach leads to a good balance between physics and applications and is expected to play an important role in computer-aided design of advanced semiconductor lasers. In this presentation, we will review the status of this simulator and give examples for its applications.

Numerical Methods for Semiconductor Laser Simulations

R. K. Smith, M. A. Alam, G. A. Baraff, M. S. Hybertsen
Bell Laboratories, Lucent Technologies
Murray Hill, NJ

Given the technological importance of optoelectronic devices, it is important to be able to do predictive modeling of new device designs before devices are actually fabricated. We present a new algorithm for obtaining convergence of the resulting non-linear optoelectronic equations. The robustness and efficiency of this new algorithm are greater than anything previously reported in the literature. These features are essential ingredients for any laser simulation tool since a large number of parameter variations are necessary to characterize any laser design.

The basic equations for multiple quantum well optoelectronic simulations consist of:

- An eigenvalue equation that determines the optical modes of the device. This equation provides the optical intensity distribution necessary for the computation of the modal gain.

- An additional set of eigenvalue equations necessary to describe the electronic states of multiple quantum well hetrostructures. An eight band effective mass Hamiltonian provides models for the both the gain and the spontaneous emission rate as well as the 2D quantum density distributions

- The classical drift diffusion equations that determine the electrostatic potential, and the 3D carrier distributions.

- A set of integral rate equations used to compute the number of photons within each mode and 2D quantum well densities.

The traditional approach to laser simulations is to solve each system of equations sequentially, using the resultant updated solutions as input into the next equation. The effectiveness of this approach is severely limited by the photon rate equations, which become almost singular near threshold. In this regime, small perturbations in the gain produce enormous changes in the photon number which, in turn, causes this method to become ill conditioned.

Our approach includes the explicit coupling between the drift diffusion equations and the integral rate equations. The basic assumption in this method is to fix the eigenvectors associated with the eigenvalue problems and construct the couplings to the remaining system via first order perturbation theory. We have also introduced a set of squared slack variables, designed to stabilize the photon rate equations. The slack variables play the role of Lagrange multipliers and allow the intermediate iterates to overshoot the singularity in the photon equations. The resulting system of nonlinear equations is very well conditioned, even near threshold, and can be solved by a newton method resulting in a quadratically convergent algorithm.

We have performed several simulations involving both single and multiple quantum well devices. The sensitivity of the results to changes in the model parameters will be presented. Complete light voltage curves can be generated in a matter of minutes on a workstation. The robustness and computational efficiency of this algorithm makes it well suited for laser design applications.

Theory and Modeling of Lasing Modes in Vertical Cavity Surface Emitting Lasers

Benjamin Klein*, Leonard F. Register*, Karl Hess*, and Dennis G. Deppe[†]

* Beckman Institute, University of Illinois at Urbana-Champaign

[†] Microelectronics Research Center, University of Texas at Austin

We formulate the problem of lasing in an open optical cavity with a gain source, in particular lasing in a vertical cavity surface emitting laser, in terms of a *frequency-dependent* eigenvalue problem in required *gain amplitudes*. The frequency-dependent operator for this eigenvalue problem is a product of the (fixed) normalized spatial distribution of the gain source and the Green's functions between source coordinates. These gain eigenvalues are in general complex quantities, while the gain that the laser can produce is ostensibly real. Therefore, lasing only occurs when one of the frequency-dependent gain eigenvalues crosses the real axis, with the real part of the gain eigenvalue determining the threshold condition. This restriction allows calculation of the frequencies at which lasing can occur and the corresponding threshold conditions, as well as the corresponding field patterns. Two methods can be used to solve for the gain eigenvalues: the first is by directly solving the eigenvalue problem; the second is by iteratively solving for the smallest gain eigenvalue. This latter method corresponds the approach used by Deppe et al. to study the lasing modes of VCSELs (C. C. Lin and D. G. Deppe, J. Lightwave Tech. **13**, 575 [1995] and references therein). Illustrative results obtained using both methods will be presented.

Cellular Automaton Study of Time-Dynamics of Avalanche Breakdown in IMPATT Diodes

G. Zandler[+], M. Saraniti[++], P. Vogl[+], P. Lugli[†]

[+]Walter Schottky Institute, Technical University of Munich,
D-85748 Garching, FRG
[++]Electrical Engineering Department, Arizona State University,
Tempe, AZ 85287-6206
[†]Electrical Engineering Department, University of Rome, Tor Vergata,
00133 Rome, Italy

We have recently developed simulation tools for high field carrier dynamics in modern nanometer devices that offer a computational speed comparable to standard hydrodynamic simulators yet the accuracy of the full Boltzmann equation.

A novel scheme that we have deleloped is the cellular automaton technique. It may be considered a discrete variant of the Monte Carlo technique and is based on (i) optimized mesh size discretization of phase space, (ii) reduction of particle motion to spatially local, deterministic scattering rates, (iii) usage of pre-calculated, hierarchical scattering tables, (iv) restriction of all dynamical variables to a discrete and finite range. We have combined this method for solvng the Boltzmann equation with statistical particle weighting and a multi-grid Poisson solver.

We show a movie that illustrates these techniques and gives new physical insight into the highly complex carrier dynamics in GaAs avalanche p-i-n (IMPATT) diodes. We find that the impact ionization in reverse bias p-i-n diodes with ultrathin (less than 100 nm) intrinsic regions is triggered by Zener tunneling that eventually leads to the generation of hot electrons in the *low-field* i-n junction region. Subsequently, hot holes impact ionize in the high field regime. Since holes have smaller scattering rates and higher masses than electrons, the holes accumulate on the p-side, screen the electric field and delay the avalanche process. This screening effect can even stabilize the avalanche process above the breakdown voltage. The calculations predict significantly more minority carriers on the n-side than on the p-side. Consequently, the observed luminescence in these devices originates mainly from the n-region.

Corresponding author: P. Vogl, Tel. ++49-89-289-12750, Fax ++49-89-289-12737,
vogl@wsi.tu-muenchen.de

3D parallel finite element simulation of in-cell breakdown in lateral-channel IGBTs

A.R. Brown, A. Asenov[*] and J.R. Barker
Device Modelling Group
Department of Electronics and Electrical Engineering
University of Glasgow, Glasgow G12 8LT, Scotland, UK
[*]Tel: ++44 141 330 5233, Fax: ++44 141 330 4907, E-mail: A.Asenov@elec.gla.ac.uk

IGBTs are among the leaders in the power device market, combining a low on-state voltage typical of bipolar devices with MOS gated switching. Modern IGBTs have a cellular structure such as that shown in Fig.1. The optimisation of the device cell is an ongoing issue. Current density, for example, can be increased by reducing the cell-to-cell separation. Unfortunately in lateral channel IGBTs the minimum cell-to-cell separation is restricted by cell-to-cell punchthrough which limits the current density. Although vertical-channel non-punchthrough devices have been demonstrated the lateral channel devices with punchthrough stopper are still the preferred technological choice. The stopper concentration, however, should be carefully designed so as not to compromise the overall device breakdown. The calculation of the in-cell breakdown in the stopper design process requires an accurate 3D solution of the Poisson equation with fine resolution around the metallurgical pn-junction.
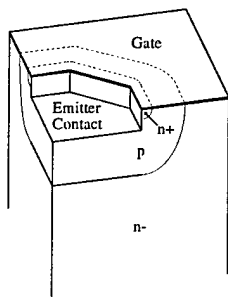
Fig.1. Schematic view of an octagonal IGBT cell
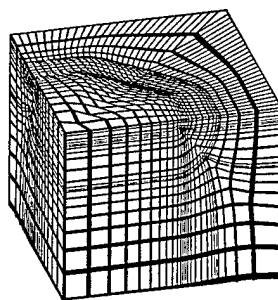
Fig.2 Finite element topologically rectangular 3d grid used in the breakdown voltage calculations
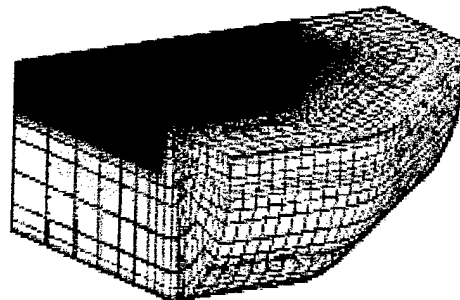
Fig.3 The grid at the metallurgical pn-junction of the p^+ emitter region

In this paper we describe the calculation of the in-cell IGBT breakdown using a parallel finite element 3D solution of the Poisson equation on an array of processors. The Poisson solver is part of a general purpose device simulator in development. The finite element discretization results in a topologically rectangular grid based on tri-linear distorted bricks. The grid conforms to the gate and emitter contact topology as well as to the metallurgical pn-junctions in the device (Fig.2). A detailed view of the grid around the metallurgical pn-junction of the p^+ emitter region is shown in Fig.3. The uniformly small step in the direction normal to the junction curvature provides the accuracy in the Poisson solution required for breakdown calculations. Using a spatial device decomposition approach[1] the 3D topologically rectangular grid is distributed over the 2D array of processors of an 8-node Power PC based Parsytec X-plorer. Both parallel four colour Block Newton-SOR and parallel BiCGSTAB solvers were developed and tested. Results on the comparative performance of both methods will be presented. The breakdown voltage is estimated using a search procedure which calculates the maximum ionisation integrals around the maximum junction field point of the reverse biased p^+ emitter region and updates the reverse bias until the ionisation integral becomes close to unity. Results for the dependence of the breakdown voltage on the device geometry and the doping profile will be presented.

1. A.R. Brown, A. Asenov, S. Roy and J.R. Barker, Parallel 3D finite element power semiconductor device simulator based on topologically rectangular grid, Simulation of Semiconductor Devices and Processes Vol. 6, Eds. H. Ryssel and P. Pichler, Springer Verlac, pp.336-339 (1995)

Cellular automata studies of vertical Silicon devices

M. Saraniti*, G. Zandler[†], S. Goodnick*.[‡]

February 12, 1997

Abstract

Recent developments in the cellular automaton (CA) significantly reduce the gap in computational speed between particle-based simulation techniques and moment-based approaches such as the hydrodynamic method. We discuss a scheme to include the full semiconductor band-structure into the CA and have developed new and efficient carrier tracking algorithms in phase-space. New schemes will be shown, that optimize the use of computer memory for the storage of tables representing the transition rates.

We present systematic theoretical CA studies of novel nanometer size Si devices, namely vertically grown MOSFETs with channel lengths between 35 and 120 nm. These devices consist of a p-layer, sandwiched between two n-doped layers that form the source and drain dopings. The active channel length is determined by the width of the p-layer that is controlled by the epitaxial CVD process that is used to grow these structures. The CA simulations predict drain and transfer characteristics as well as transit time frequencies as a function of gate length. These results are in excellent agreement with available experimental data even though the simulations neglect interface roughness scattering and are based on the nominal device geometry (such as oxide thickness). Impact ionization is shown to be of minor importance. Since the vertical growth modus allows arbitrary doping profiles along the channel, we have explored the potential of this additional degee of freedom and optimized this doping profile in order to maximize the output conductance.

*Electrical Engineering Department, Arizona State University, Tempe (AZ) 85287-6206.
[†]Physik Department and Walter Schottky Institut, TU-München, Garching , Germany.
[‡]Corresponding Author: M. Saraniti, e-mail: saraniti@asu.edu, phone: (602)965 2030, fax: (602)965 8118

Comparison of iteration schemes for the solution of the multidimensional Schrödinger-Poisson equations *

A. Trellakis, A. T. Galick, A. Pacelli[†] and U. Ravaioli

Beckman Institute, University of Illinois at Urbana-Champaign, Urbana, Illinois 61801, USA
† Dipartimento di Elettronica e Informazione and CEQSE-CNR, Politecnico di Milano,
Piazza Leonardo da Vinci 32-20133 Milano, Italy

As the dimensions of semiconductor devices continue to shrink, the influence of quantum effects on their electronic properties is expected to increase in the future, until finally for nano-scale structures these effects become the dominant factor. Consequently there is considerable interest in the numerical simulation of such structures, not only for exploring possible future device architectures but also for maintaining reliability for scaled-down present-day devices.

A typical calculation in performing these tasks is the computation of electron states in the cross-section of a quantum wire, which involves the self-consistent solution of a nonlinear Poisson equation coupled to Schrödinger's equation. This system of coupled nonlinear PDEs is usually solved by an iterative approach, as for example adaptive underrelaxation of the quantum electron density. The problem with this commonly used method is the inherent instability of the outer iteration caused by the strong nonlinear coupling between both equations, which can easily result in oscillations in the total electric charge leading to relatively slow convergence.

To address this problem we applied quantum mechanical perturbation theory to derive an approximate expression describing the dependence of the quantum electron density on changes of the electrostatic potential. The use of this approximation moves most nonlinearities into Poisson's equation and at the same time decreases the coupling to Schrödinger's equation considerably. This procedure eliminates the oscillations in the total electric charge and makes the outer iteration stable without employing underrelaxation.

We compare the two iteration methods by calculating the two-dimensional bound electron states within the cross-sections of GaAs-AlGaAs based quantum wires. Since the model devices contain material discontinuities, both Schrödinger's equation as well as Poisson's equation were discretized using a box integration finite difference approach. Additionally, we employ a non-uniform rectangular mesh condensed around the wire region to minimize computational effort.

The size of the matrices involved here demands the use of sparse solvers for both equations. The eigenvalue problem for Schrödinger's equation is solved using Chebyshev-Arnoldi iteration, which allows one to solve only for the lowest physically relevant eigenvalues in the energy spectrum. The nonlinear Poisson equation is solved using Newton-Raphson iteration with inexact line search. Since solving the nonlinear Poisson equation with Newton's method requires the solution of a linear Poisson equation at each iteration step, a version of the preconditioned conjugate gradient method involving red-black reordering is employed for inverting the Laplacian.

To compare the convergence of our new method with a fast adaptive underrelaxation scheme, we start both iterations from the same simple initial condition, which enforces local charge neutrality only. We find that for our new solution scheme the outer iteration is stable, and the residual in the quantum electron density decreases uniformly by almost one order of magnitude each step, which is a 6-fold increase in convergence speed compared to underrelaxation. This result holds for wide range of temperatures and gate potentials, also after including exchange correlation effects.

Corresponding Author:
Umberto Ravaioli, 3255 Beckman Institute, 405 N. Mathews Avenue, Urbana, IL 61801
FAX: (217) 244-4333 - e-mail: ravaioli@uiuc.edu

Large Scale Disributed Parallel Computing

Harold Trease

Los Alamos National Laboratory
Los Alamos, NM 87545

The purpose of this presentation is to review the area that we at Los Alamos call "large scale distributed parallel computing". Over the past 15 years we have been incorporating parallel computing into our day-to-day code development to produce engineering calculations that could not be done without the use of parallel computers. For the most part I will concentrate on the techniques that we use for grid based codes that solve computational physics problems involving hydrodynamics, heat/radiation transport, continuum mechanics, and particle transport.

X3D Moving Grid Methods for Semiconductor Applications

Denise George*, David Cartwright, J. Tinka Gammel, Brian Kendrick,
David Kilcrease, Andrew Kuprat, Harold Trease, and Robert Walker

Los Alamos National Laboratory

3D grain growth modeling and 3D topographic simulation have in common the requirement of accurately representing time dependent surface motion in a 3D volume. Problems involving fixed surfaces such as electrostatic interconnect modeling can benefit from adaptive grid methods to reduce solution error from iteration to iteration. The X3D grid toolbox provides a set of capabilities including initial grid generation of complex multimaterial geometries and grid optimization that preserves material interfaces. X3D data structures and toolbox methods are designed as objects in order to be user accessible and extensible. X3D commands can be issued from within an application driver program, and the example applications use this feature to perform, as needed, grid reconnection, node merging and smoothing. Additionally, all X3D data structures are available to the application driver via calls to utility routines. Thus when an application detects a non-routine event such as a topological change in a material region under deformation, a special purpose user routine can easily be incorporated into the system. These design features promote the separation of the physical based simulation from the grid maintenance chores, but allow full access to the grid data structures when required.

To model evolution of 3D metallic grain microstructure under mean curvature motion, movement of the grain surface (interface) triangles is done using an implicit implementation of the Moving Finite Element method. Nodes interior to the grains are moved using a smoothing scheme that guarantees positive element volumes. High level routines detect major topological events such as the collapse of a grain as well as the need to refine and de-refine the grid representing the evolving grains. X3D grid maintenance calls are employed to actually refine and derefine the grid. These grid maintenance calls automatically restrict grid reconnections to preserve grain interfaces until the final annihilation step which is ordered by the high level routine. For validation of this method, comparisons to other numerical grain evolution techniques are presented.

To simulate topographic etch and deposition, TopoSim3D, uses the X3D toolbox, which allows separation of the chemical and physical processes from grid generation and maintenance operations. As material is deposited or etched away, the corresponding material interface changes at each time step. The interface triangles are moved based on the flux of incident material and a sticking probability which is determined from the surface chemistry kinetics. As in grain growth modeling, the X3D grid maintenance calls are used to refine, reconnect and smooth the interface surface during the time evolution. TopoSim3D uses the X3D data structures to help avoid folding problems and detect topological events such as a pinch-off. Simulation results of deposition on an overhang structure with different sticking coefficients are given.

Electrostatic problems involve finding a potential in a 3D physical region bounded by highly complex boundaries which may include sharp corners and other nonsmooth features that lead to singularities in the solution. Efficient solution of this problem requires an iterative approach whereby the potential is first computed on an equally spaced grid, and then analyzed for quality. The grid is then adapted where quality is poor (i.e., near challenging portions of the boundary), and after several iterations, a uniform level of error is achieved throughout the domain. We demonstrate this iterative approach by employing a finite volume tetrahedral solver with the X3D grid code to compute a potential field at each iteration. Mesh adaption at each iteration is effected by use of the X3D smoothing capability that analyzes solution errors and moves the grid to equilibrate error.

* Denise George
dgeorge@lanl.gov
MS B221
Los Alamos National Laboratory
(505) 667-6248
fax: (505) 665-5757

The Finite-Volume Scharfetter-Gummel Method for Steady Convection-Diffusion Equations

RANDOLPH E. BANK*   W. M. Coughran, Jr.[†‡]   Lawrence C. Cowsar[†]

The classical Scharfetter-Gummel (SG) scheme for discretizing drift-diffusion and energy-transport models has proven itself to be the workhorse for device modeling codes. It is well defined in one spatial dimension but is subject to variations in two and higher dimensions, for both finite elements and finite volume (box) approaches. This class of discretizations is also sensitive to the mesh geometry and the direction of the advection in the continuity equations. With our methodology, we demonstrate various properties of finite-volume SG discretizations for a well-behaved mesh and how to stabilize things when the mesh is poor.

To focus our discussion, we consider the model convection-diffusion equation in two space dimensions. We demonstrate that the finite-volume SG discretization of this equation

- converges to the continuous solution;

- gives rise to an *M-matrix* on meshes without obtuse angles;

- obeys a maximum principle on meshes without obtuse angles;

- may be implemented in a simple way in existing finite-element-based simulators; and

- is the same discretization as the *Inverse-Average* finite-element schemes of Markowich and Zlámal (1988) and Xu and Zikatanov (1997).

The key tool in the analysis is a relation between the finite volume discretization and a Galerkin discretization with piecewise linear basis functions. From the flux in the finite volume scheme, we construct a new flux defined over the entire domain such that the new flux satisfies the standard Galerkin discretization when the flux in the finite volume scheme satisfies the finite-volume discretization.
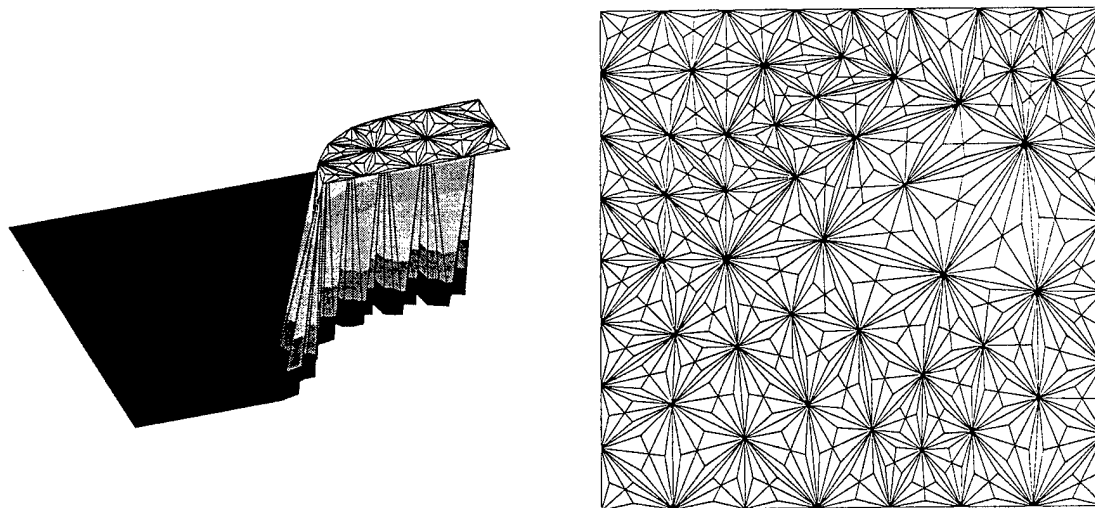
Figure 1: Stabilized SG calculation on a mesh with many obtuse angles

In the case of meshes with obtuse angles, the analysis suggests several ways to stabilize the method. These are widely applicable to general SG box schemes as described by Bank, Fichtner, and Rose (1983). We show how such stabilizations can be added to existing simulators. We contrast our approach with the DFUS scheme of Bank, Bürgler, Fichtner, and Smith (1988). Computational results will be shown.

*Department of Mathematics, University of California at San Diego, La Jolla, CA 92093, USA.
†Computing Sciences Research Center, Bell Labs, Lucent Technologies, Murray Hill, NJ 07974, USA.
‡Additional contact information for corresponding author: 908-582-6619, 908-582-5857 *(fax)*, wmc@research.bell-labs.com

Multilevel Algorithms for Large-Scope Molecular Dynamics Simulations of Nanostructures on Parallel Computers

Aiichiro Nakano,[*] Rajiv K. Kalia, and Priya Vashishta
Concurrent Computing Laboratory for Materials Simulations
Department of Computer Science, Department of Physics and Astronomy
Louisiana State University

Abstract

Molecular dynamics (MD) is a powerful tool for the atomistic understanding of long-range stress-mediated phenomena, phonon properties, and mechanical failure relevant to the operation and reliability of nanometer-size devices. For realistic modeling of nanostructures, however, the scope of simulations must be extended to larger system sizes, longer simulated times, and more complex realism. We have developed new multilevel algorithms and physical models encompassing multiple levels of abstraction: i) space-time multiresolution schemes; ii) hierarchical dynamics via a rigid-body/implicit-integration/normal-mode approach; iii) adaptive curvilinear-coordinate load balancing; iv) variable-valence MD based on electronegativity equalization; and v) multilevel preconditioned conjugate gradient method. Multimillion-atom MD simulations are performed on parallel computers to study fracture, local stress, and phonon properties in nanostructures consisting of ceramics (Si_3N_4, Al_2O_3) and semiconductors (GaAs). This work is supported by ARO, DOE, NSF, AFOSR, USC-LSU Multidisciplinary University Research Initiative, and Louisiana LEQSF.

[*] Corresponding author:
Department of Computer Science, Coates Hall, Louisiana State University
Baton Rouge, LA 70803-4020
Phone: (504) 388-1343
Fax: (504) 388-1465
Email: nakano@bit.csc.lsu.edu
URL: http://www.cclms.lsu.edu

Ensemble Monte Carlo and Full-Wave Electrodynamics Models Implemented Self-Consistently on a Parallel Processor Using Perfectly Matched Layer Boundary Conditions .

Ik-Sung Lim[1], Robert O. Grondin[2] and Samir El-Ghazaly[2]

We have been using a self-consistent formulation of full-wave electromagnetic solvers and ensemble Monte Carlo techniques to model ultrafast photoconductivity. Our simulations are running on a MASPAR machine. This paper will address aspects of this simulation which may interest workers who are simulating not only photoconductive systems but other systems as well which involve electrodynamics, waves and wave phenomomena and ensemble Monte Carlo transport models. In particular, we will report on the inclusion of perfectly matched layer approaches to absorbing boundary conditions for electromagnetic waves. These have in the past several years become widely used in computational electromagnetics codes because they reduce spurious numerical wave reflection off of an absorbing boundary by several orders of magnitude. We will also address the issue of computational cost and show that a full-wave electromagnetic approach is more competitive with a Poisson's equation approach than one might believe. We will report on how we have parallelized the ensemble Monte Carlo code. Lastly, our system has the feature that the active portion where the electrons and holes lie is in fact a small fraction of the total experimental system's volume. Unless care is exerted one either has a very significant load imbalance problem where only a small fraction of the processor array handles the ensemble Monte Carlo or alternatively potentially high communications overhead involved with reassigning processors as one switches between the ensemble Monte Carlo code and the electromagnetic solver. We have explored several different ways assigning the total computational task to the processor array.

[1] Motorola Inc., 2200 W. Broadway, Mesa AZ 85202

[2] Department of Electrical Engineering, Arizona State University, Tempe AZ 85287

APPLICABILITY OF THE HIGH FIELD MODEL: AN ANALYTICAL STUDY VIA ASYMPTOTIC PARAMETERS DEFINING DOMAIN DECOMPOSITION

Carlo Cercignani, Politecnico di Milano, Milano, Italy
Irene M. Gamba[1], Courant Institute, New York University, New York, NY 10012
Joseph Jerome[2], Department of Mathematics, Northwestern University, Evanston, IL 60208
Chi-Wang Shu, Division of Applied Mathematics, Brown University, Providence, RI 02912

In this paper, we present a mesoscopic–macroscopic model of self–consistent charge transport. It is based upon an asymptotic expansion of solutions of the Boltzmann transport equation (BTE). We identify two dimensionless parameters from the BTE. These parameters are, respectively, the quotient of reference scales for drift and thermal velocities, and the scaled mean free path. Such parameters induce domain dependent macroscopic approximations. Particular focus is placed upon the so–called high field model, defined by the regime where drift velocity dominates thermal velocity. This model incorporates kinetic transition layers, linking mesoscopic to macroscopic states. Reference scalings are defined by the background doping levels and distinct, experimentally measured mobility expressions, as well as locally determined ranges for the electric fields. The mobilities reflect a coarse substitute for reference scales of scattering mechanisms. See [2] for elaboration.

The high field approximation is a formally derived modification of the augmented drift-diffusion model originally introduced by Thornber some fifteen years ago [4]. We are able to compare our approach with the earlier kinetic approach of Baranger and Wilkins [1] and the macroscopic approach of Kan, Ravaioli, and Kerkhoven [3].

REFERENCES:

[1] H.U. Barenger and J.W. Wilkins, *Ballistic structure in the electron distribution function of small semiconducting structures: General features and specific trends,* Physical Review B, vol. 36, No 3, pp. 1487–1502 (1987).

[2] C. Cercignani, I.M. Gamba and C.D. Levermore, *High field approximations to Boltzmann-Poisson system boundary conditions in a semiconductor,* to appear in Applied Math. Letters.

[3] E.C. Kan, U. Ravaioli and T. Kerkhoven, *Calculation of velocity overshoot in submicron devices using an augmented drift-diffusion model,* Solid-State Electr. 34, No. 9, pp. 995–999 (1991).

[4] K.K. Thornber, *Current equations for velocity overshoot,* IEEE Electron Device Lett. No. 3, pp. 69–71 (1983).

---

[1]Presenting author
[2]Corresponding author: (847) 491 5575/ (847) 491 8906 (Fax)/jwj@math.nwu.edu

Smooth QHD Simulation of the Resonant Tunneling Diode

Carl L. Gardner and Christian Ringhofer
Department of Mathematics
Arizona State University
Tempe, AZ 85287-1804
Phone: 602-965-0226, FAX: 602-965-8119
gardner@asu.edu

The original $O(\hbar^2)$ quantum hydrodynamic equations have been remarkably successful in simulating the effects of electron tunneling through potential barriers including single and multiple regions of negative differential resistance and hysteresis in the current-voltage curves of resonant tunneling diodes. However, the model relies on an ad hoc replacement of derivatives of the potential with derivatives of the logarithm of the electron density in order to avoid infinite derivatives at heterojunctions.

Refs. [1] and [2] present an extension of the quantum hydrodynamic model that is mathematically rigorous for classical potentials with discontinuities—as are present at heterojunction barriers in quantum semiconductor devices. The effective stress tensor in this "smooth" QHD model actually cancels the leading singularity in the classical potential at a barrier and leaves a residual smooth effective potential with a lower potential height in the barrier region. The smoothing makes the barrier partially transparent to the electron flow and provides the mechanism for tunneling in the QHD model.

Smooth QHD simulations of the resonant tunneling diode exhibit enhanced negative differential resistance (NDR) when compared to simulations using the original $O(\hbar^2)$ QHD model. At room temperature, the smooth QHD simulations predict significant NDR for an GaAs/AlGaAs structure with 25 Å barriers and a 50 Å well even when the original QHD model simulations predict no NDR. An analysis is given of why NDR is enhanced in the smooth QHD model, based on an analysis of the smoothed potential.

[1] "Smooth Quantum Potential for the Hydrodynamic Model," C. L. Gardner and C. Ringhofer, *Physical Review* **E 53** (1996) 157–167.

[2] "Approximation of Thermal Equilibrium for Quantum Gases with Discontinuous Potentials and Application to Semiconductor Devices," C. L. Gardner and C. Ringhofer, accepted for publication in *SIAM Journal on Applied Mathematics* (1997).

Spherical Harmonic Analysis of a 0.05μm Base BJT: Monte Carlo-Type Results But A Thousand Times Faster

C.-H. Chang, C.-K. Lin, N. Goldsman and I. D. Mayergoyz
Department of Electrical Engineering, University of Maryland, College Park, MD 20742

The Spherical Harmonic (SH) method for solving the BTE has given rise to considerable controversy. Researchers developing the method have reported promising results[1,2]. On the other hand, strong advocates of the Monte Carlo (MC) method have expressed reservations as to the ability of the SH method to provide the distribution function[3]. Other researchers have called for a study of various methods, including the SH, especially under conditions of rapid spatial variations[4].

In this paper, we respond to these questions by performing a rigorous comparison between the SH and MC methods of solving the Boltzmann equation. *We find the SH and the MC methods give very similar results for the energy distribution function, using an analytical band-structure, at all points within the tested devices. However, the SH method can be as much as seven thousand times faster than the MC approach for solving an identical problem.*

We show some example results below. On the left is the electric field profile of the Si 0.05μm Base-BJT. It is important to note the range and rapid variation of the electric field, changing form $0 - 450kV/cm$ over a distance of $0.01\mu m$. We solve the BTE by both the SH and MC with this electric field as input. Both the SH and the MC simulations use the same input parameters[5]. On the right we show results at regular $0.05\mu m$ intervals for the energy distribution function calculated by both the SH and the MC methods. From the figure it is clear that the SH (lines) and MC (circles) methods give very similar answers. However, the SH approach required only 12 seconds on a DEC alpha 500, while the MC required more than 24 hours to accumulate reasonable statistics for the high energy tail and to surmount the large potential barrier at the emitter-base junction. We have developed a new numerical approach which calibrates the discretization to the density of states and facilitates rapid convergence of the SH method. (The MC could probably be optimized but our attempts at statistical enhancement proved unreliable when subjected to scrutiny.)

We explain the agreement between SH and MC by detailed analysis of the SH system of equations. Asymptotic analyses show that, due to high scattering rates, high order SH terms decay quickly enough to have minimal effect on the energy distribution function, even for abrupt large spatial variations. Furthermore, the Maxwellian boundary condition forces all but the zero order SH term to vanish at the contacts, thereby facilitating use of a low order SH expansion.
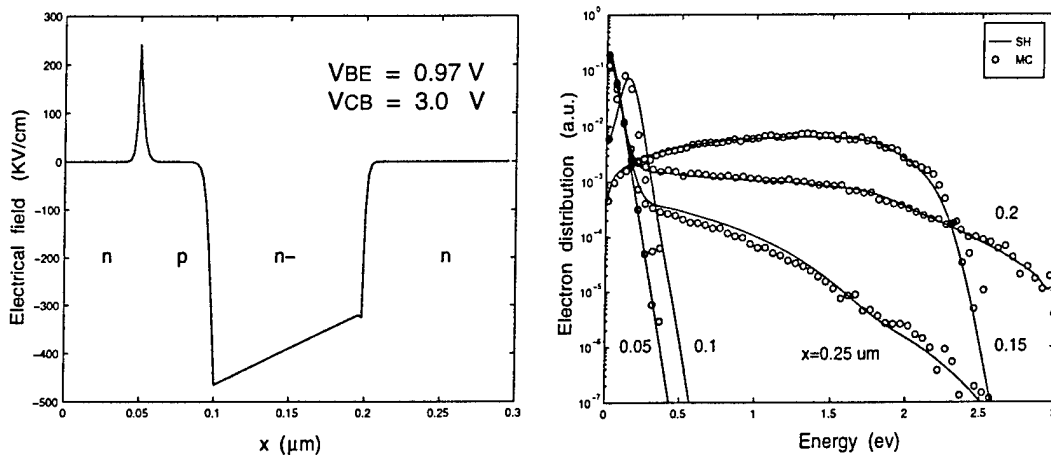
Figure 1: Comparison of energy distribution function calculated by SH and MC methods.

[1] W. Liang, N. Goldsman, I. Mayergoyz, P. Oldiges, *IEEE Trans. Elec. Dev.*, 44, pp. 257–276, 1997.
[2] A. Gnudi, D. Ventura, G. Baccarani, F. Odeh, *Sol.-State Elec.*, 36, pp. 575-581, 1993.
[3] J. Bude and M. Fischetti and S. Laux, Independent private communications, 1996.
[4] R. Dutton and K. Hess and U. Ravaioli, Independent private communications, 1996.
[5] C. Fiegna and E. Sangiorgi, *IEEE Trans. on Elec. Dev.*, 40, pp. 619-627, 1993.

Numerical Examination of Photon Recycling as an Explanation of Observed Carrier Lifetime in Direct Bandgap Materials

Joseph W. Parks Jr. and Kevin F. Brennan
Microelectronics Research Center
Georgia Institute of Technology
Atlanta, GA 30332

Arlynn W. Smith
ITT Night Vision, Roanoke, VA 24019

Abstract

Photon recycling is examined as an explanation for the observed large carrier lifetimes in an InP/InGaAs photodiode. This effect extends the effective carrier lifetime within a device by re-absorbing a fraction of the photons generated through radiative band-to-band recombination events. In order to predict the behavior of this carrier generation, photon recycling has been added to our two-dimensional macroscopic device simulator, STEBS-2D. A ray-tracing preprocessing step is used to map all of the possible trajectories and absorption of various wavelengths of emitted light from each originating node within the device. The macroscopic simulator uses these data to determine the spatial location of the re-absorbed radiation within the geometry of the device. By incorporating the ray tracer results with the total quantity and spectral content of recombined carriers at each node within the simulation, the recycled generation rate can be obtained. A practical application of this model is presented where the effects of photon recycling are used as a possible explanation of the discrepancy between the theoretically predicted and experimentally observed radiative recombination rate in a double heterostructure photodetector.

A SEMI-CLASSICAL DESCRIPTION OF ELECTRON TRANSPORT IN SEMICONDUCTOR QUANTUM WELL DEVICES

G.A. Baraff, Lucent Technologies Bell Laboratories Murray Hill, N.J. 07974

Carrier drift, diffusion, and thermionic emission for classical semiconductor devices (p-n junctions, heterostructures etc.) is most easily described using expressions derived from a Boltzmann transport equation point of view. This point of view is not particularly applicable to quantum well transport. It is shown here that by postulating a region of phase space that is forbidden to the mobile carriers and then altering the scattering probability so that no particles are scattered to the forbidden region, a Boltzmann equation based formalism emerges which does describe the mobile carrier component of quantum well transport in the limit of large carrier-carrier scattering.

The formalism that emerges from this postulate has the following feature: In the quantum well, left going carriers and right going carriers are considered to be separate populations, each with its own quasi-fermi energy, because at the high speeds which the carriers acquire upon enetering the well, scatterming from one population to the other is rather difficult. A pair of coupled Boltzmann equations and appropriate boundary conditions is set up, one for each population. These equations are then recast so that the two spatially dependent quasi-fermi energies are the unknowns. The final form is a pair of coupled first order differential equations, one for each quasi fermi energy, rather than the single second order differential equation of ordinary drift diffusion theory.

The use of two separate quasi fermi energies makes it possible to deal with a fundamental aspect of transport of mobile carriers across the wells, namely that carriers injected at z=0, traveling towards the right, have come out of a reservoir whose Fermi energy differs from that of the other reservoir which, at z=w, injects the carriers traveling towards the left. Equilibration of these two populations of traveling carriers will occur only via events which can transfer carriers from one population to the other. If the mechanisms for doing this are so weak that equilibration does not occur during the traversal time of the well, some measure of the Fermi level difference between the two reservoirs will persist into the well. This situation is analogous to that of electrons and holes in a p-n semiconductor junction. In a p-n junction under bias, the two types of carriers may have different quasi Fermi energies although, at some distance from the junction plane, carrier generation and recombination equilibrate the two populations. In the quantum well, the two types of carier (left going and right going) may have different quasi fermi energies although, at some distance from the well, the carriers are moving slowly enough that the two populations can equilibrate. Only one new parameter, the scattering time between the two populations, is needed in the new formalism. Even this one is unimportant if there is a healthy rate of transfer between the mobile states and any bound state population in the well.

Electronic Structure Calculations Using An Adaptive Wavelet Basis

D. A. Richie[1], P. von Allmen[1], K. Hess[1], R. Martin[2]

[1]*Beckman Institute for Advanced Science and Technology, University of Illinois, Urbana, Illinois 61801*

[2]*Department of Physics, University of Illinois, Urbana, Illinois 61801*

The use of a plane-wave basis has lead to very efficient methods for performing electronic structure calculations. One disadvantage is the large number of plane-waves needed to accurately represent the electronic orbitals in calculations with large numbers of atoms. For this reason there has been an interest in the use of localized basis sets for these types of calculations. Such considerations have lead us to consider the use of a compact orthonormal wavelet basis. Such a basis possesses many useful properties. One such property is their ability to allow one to construct a minimal basis set representation of a function by directing higher resolution only into the regions where it is needed. We use such a basis to perform self-consistent electronic structure calculations within the local density approximation. We present for the first time a truly adaptive wavelet method where by the minimal basis representation is determined automatically and the calculation is performed entirely upon this basis. Specifically, the basis set upon which each electronic orbital is expanded is iteratively refined throughout the calculation, resulting in a unique minimal basis set tailored to the needs of each electronic orbital. During the total energy minimization, the application of the hamiltonian is carried out entirely on such a minimal wavelet basis set. As an example we apply our method to bulk Ge and bulk Si.

Corresponding Author:
Karl Hess, 3247 Beckman Institute, 405 Mathews Ave., Urbana, IL 61801
Phone: (217)244-6362, FAX: (217)244-4333, email: k-hess@uiuc.edu

The Art, Science, and Challenge of Simulating Advanced Devices

Jerry Mar

Intel Corporation

Over the past years, scientific advances in modeling and computation have led to the development of superior, physics-based computer models, and simulation tools with significantly improved prediction capabilities. Despite this, critics still point out process/device simulation capabilities lag new technology development needs, and often are able to "predict" correct answers only after they are first "calibrated" with known experimental answers.

This talk will show why the lagging of modeling capabilities with next generation technology development requirements is a direct result of the usefulness of existing models. The talk will point out such model lags are inherent to aggressive growth industries like electronics, and will illustrate this point with examples. The difficulties and challenges of providing true predictability will also be discussed, as will methodologies for utilizing what is currently available - partial modeling capabilities of varying degrees of predictability. The talk will explore the art of combining such models with experimental data and tailored application methodologies, to aid the development of new technologies.

The talk will conclude with a look into the future, specifically at what might happen if technology changes begin leveling off.

Open Problems in Quantum Simulation in Ultra-Submicron Devices*

D. K. Ferry[1] and J. R. Barker[2]

[1]Center for Solid State Electronics Research
Arizona State University
Tempe, AZ 85287-6206

[2]Department of Electrical and Electronic Engineering
University of Glasgow
Glasgow G12 8QQ, United Kingdom

Quantum transport is becoming more significant as device size shrinks. For example, as device sizes are scaled below 0.1 μm, the number of impurities becomes quite small, so that they are no longer homogeneously distributed throughout the device volume. This leads to the need to discuss transport through an array of *quantum boxes*, in that self-energy corrections produced by locally high carrier densities will lead to *quantum dot* formation. Several issues must be considered in treating the transport through such devices, among which are: (1) electron correlation due to the small capacitances between such dots, and the possibility of single-electron effects in fluctuations of the overall device; (2) phase coherence within and among the array of quantum boxes; (3) the transition between semi-classical and fully quantum transport, including the ability or inability of the quantum potential to properly describe charge bunching and tunneling; (4) the role of the contacts, vis-à-vis the fabricated boundaries, and the actual versus internal boundaries; (5) the possible need to provide decoherence at the source and/or drain. We discuss a general quantum formulation, which allows separation of boundary regions from "internal" regions, as well as providing an approach that will allow studies of the above questions.

Theory of electron transport in small semiconductor devices using the Pauli master equation

M. V. Fischetti

IBM Research Division, T. J. Watson Research Center

P.O Box 218; Yorktown Heights, NY 10598, USA

e-mail: fischet@watson.ibm.com   Phone: (914) 945 3404;   FAX: (914) 945 3404

It is argued that the Pauli master equation (PME) can be used to simulate electron transport in very small electronic devices under steady-state conditions.

In order to justify the use of the PME and understand its limitations, it is convenient to consider the equation of motion for the density matrix, ρ, and use Van Hove's results[1]: In the weak-scattering limit, the PME describes correctly approach to equilibrium when the initial state $\rho(t = 0)$ is chosen from one of two classes of states: i) Those which are a superpositions of 'many' eigenstates of the unperturbed Hamiltonian, 'many' meaning that the initial states has amplitudes which vary slowly as a function of unperturbed energy, or ii), states which are a superpositions of 'very few' eigenstates of unperturbed Hamiltonian, 'very few' meaning that their amplitudes are nonzero only for a narrow range of unperturbed energy. Under these conditions the off-diagonal terms of the density matrix can be ignored. Moving to the problem of electron transport in open systems, one can paraphrase Van Hove, the role of the 'initial state' now being played by the conditions at the device/reservoir boundaries: The off-diagonal elements of the density matrix remain negligible when the 'reservoirs' inject either of two possible classes of states: Those in Van Hove's class i), corresponding to electrons which are spatially strongly localized, or those in class ii), corresponding to plane waves in the reservoirs. The first class is appropriate to the description of devices much larger that the electron wave-packets injected from the reservoirs. In this case, writing the equation of motion for ρ over a basis of plane waves, in the limit of small fields one recovers the Boltzmann transport equation (BTE), as done by Kohn and Luttinger[2]. The second class of states applies to devices smaller than the size of the wave-packets (presumably about 50 nm for heavily-doped Si reservoirs at 300 K). In this case one can represent ρ on a basis of eigenstates which are solutions of the self-consistent Poisson/Schrödinger problem with open boundary conditions[3] and the PME is recovered.

The use of the PME removes some of the approximations which render the BTE unsatisfactory (at least conceptually) at small length-scales, removing the idealized picture of electrons as point-like semiclassical objects, and the weak-field approximation. Therefore the PME allows the inclusion of tunneling, interference effects, arbitrary 'steep' potentials, and intra-collisional field effects. However, the PME is based on the same weak-scattering and long-time limits on which also the Boltzmann equation rests and cannot provide the complete solution of time dependent quantum transport problems. Moreover, under fast time-transients the PME violates (probability) current continuity, as noted by Frensley[3] and cannot be employed.

Results are given for the 'usual' one-dimensional examples (an $n - i - n$ diode, a single barrier tunnel structure, and a double-barrier resonant tunnel diode). A simple Monte Carlo algorithm is used to solve the PME. The algorithm draws heavily from conventional Monte Carlo schemes, differing mainly for the absence of drift-terms, since the effect of the electric field is absorbed into the eigenstates of the unperturbed Hamiltonian. Figures 1 and 2 show the results for an $n - i - n$ using a model 'semiconductor' (single parabolic band), including nonpolar scattering with optical phonons, obtained by solving self-consistently the Poisson, Schrödinger, and master equation. The results are compared with those obtained using the conventional Monte Carlo solution of the BTE. Of interest is the fact that, in addition to the similarity of the results shown in Fig. 1, the current densities predicted by the two profoundly different models are within 10% of each other.

References

[1] Léon Van Hove, Physica XXI, 517 (1955).
[2] W. Kohn and J. M. Luttinger, Phys. Rev. 108, 590 (1957).
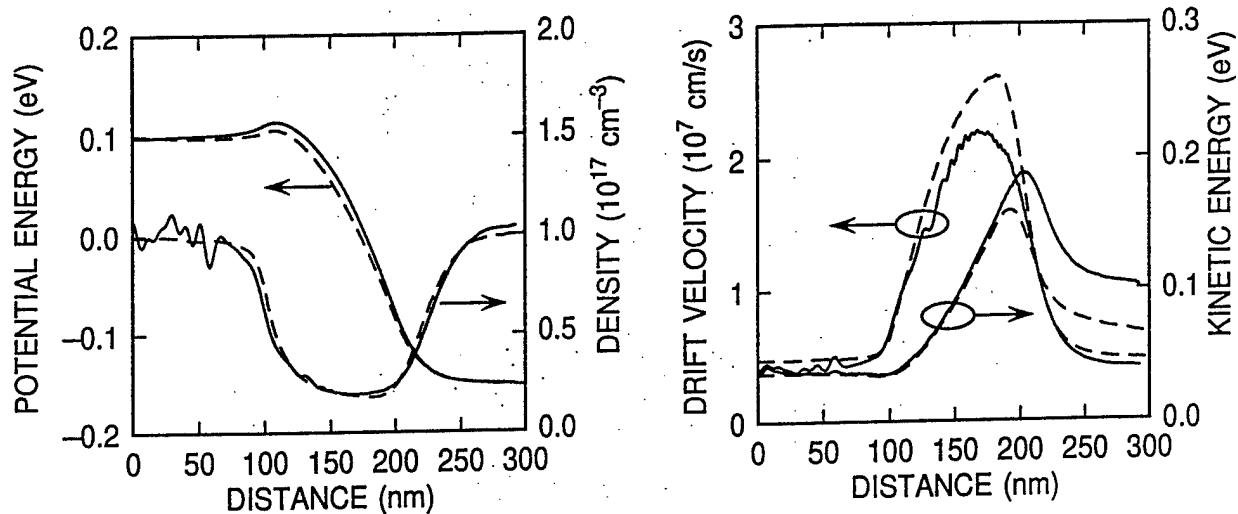[3] W. R. Frensley, Rev. Mod. Phys. 62, 754 (1990).

Figure 1: Calculated potential energy, and charge density (left), kinetic energy and drift-velocity (right) as a function of position inside a 100 nm $n-i-n$ diode. Scattering with optical phonons is included. The solid line represent the results obtained using the master equation, the dashed lines those obtained using a conventional Monte Carlo solution of the Boltzmann equation.
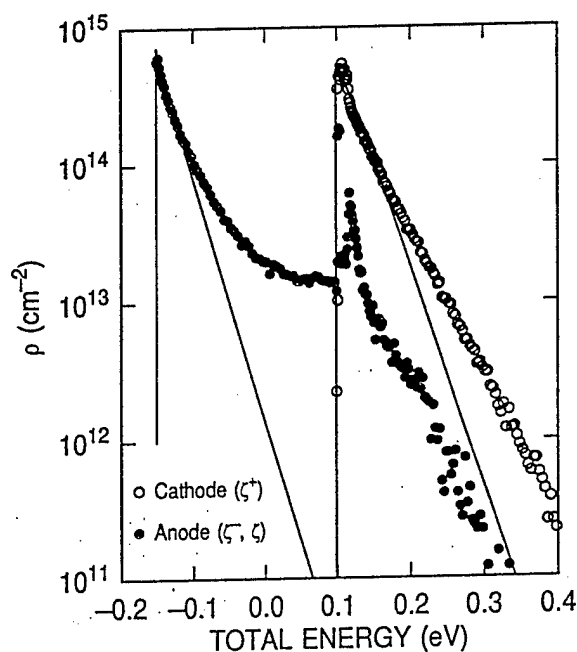

Figure 2: Occupation of states, (that is, diagonal elements of the density matrix ρ), as a function of total energy. The solid lines show the 'ballistic' distribution, open circles the distribution of states traveling from the cathode, solid circles the distribution of states traveling from the anode or non-current-carrying states.

Modeling of Nano-Scale Ballistic Field-Effect Transistors

F. G. Pikus* and K. K. Likharev

Department of Physics, State University of New York at stony Brook, Stony Brook, NY

11784-3800

(February 13, 1997)

The rapid progress in scaling down the field-effect transistors (FETs) has characterized the past three decades of the development of large scale digital electronic circuits, and continues at an almost the same rate - see, e.g., Ref. 1.

We present simple analytically solvable models for nano-scane field-effect transistors with the feature size of the order of 10 nm. One could argue that such devices will not present a practical interest for at least 10 years due to the fabrication problems. We believe, however, that an analysis of such FETs is long overdue, both because the recent progress of nanofabrication has brought us considerably closer to their practical implementation, and because it is very important to have a clear long-term prospective of the future development of such a VLSI technology workhorse as silicon-based FETs. This task seems even more urgent in view of the recent rapid progress in the development of their most prospective rivals, single-electron transistors (SETs) which apparently would allow to create memory circuits with 100 Gbits/cm^2 density, provided that a minimum feature size of 4 nm is available.[2]

The principal difference of our work from all earlier publications we know about is the different mechanism of electron transfer. Our basic point is that for the devices on our scale of interest (channel length L of the order of 10 nm), doping of the channel becomes both *unacceptable* and *unnecessary*. The first is because even at very large doping levels the number of dopant in the channel will be small and this leads to large statistical device-to-device variations of the basic parameters. The second follows from the fact that the channel length of such a device is comparable to the screening length, so that the necessary carriers may be delivered in to the channel from the highly doped source and drain.

We calculate the potential profile, electron density distribution, and electric current, for both 2D FET (using the so-called parabolic approximation) and 3D FET (where we employ a 1D model, simulating the gate with the effective charge density it induces in the channel). The assumptions bult into the model greatly simplify the computations, while preserving the essential physics.

Our results show that the Si ballistic MOSTFETs may be feasible as switching elements for DRAM even at the scale of 10 nm. However, using them in logical circuits is much more problemmatic, because of lack of the saturation regime and low voltage gain.

[*] FAX: (516) 632-8774, Phone: (516) 632-8345, E-mail: pikus@hana.physics.sunysb.edu

[1] See, e.g., A.W. Wieder, in: ”*Future Trends in Nanoelectronics*”, ed. by S. Luryi *et al.*, Kluwer, Dordrecht, 1995, p. 13.

[2] K.K. Likharev and A.N. Korotkov, in: ”*Proc. of 1995 In t. Semiconductor Device Research Symposium*” (Charlottesville, VA, Dec. 1995), p . 335.

Quantum transport in open nanostructures

I. V. Zozoulenko and K.-F. Berggren
Department of Physics (IFM), Linköping University,
S-581 83 Linköping, Sweden.
e-mail: `igorz@ifm.liu.se`, `kfber@ifm.liu.se`

We study electron transport in open square quantum dots with lateral dimensions typical for experiments. The multi-terminal conductance of the structure is calculated within the Landauer-Büttiker formalism. The scattering matrix is computed on the basis of the hybrid Green function technique[1], which is especially effective for wide or/and gradually modulated geometries and arbitrary high magnetic fields. In this approach, we use the local transverse energy modes as a basis. This allows great flexibility in modeling wide/smooth geometries within a function space of reasonable dimensionality. On the other hand the recursive Green-function technique is used in the (discretized) longitudinal direction to determine the transfer matrix, $\mathbf{T}$. This eliminates numerical instability problems from the calculations of $\mathbf{T}$. Our numerical analysis of the probability density distribution inside the dot enables us to map unambiguously the resonant states which mediate the transport through the structure.

In the present work we discuss the interplay between classical trajectories and quantum mechanical effects seen in a micrometer-size ballistic square dot[2]. At low magnetic fields the four terminal resistance is dominated by phenomena that depend on ballistic trajectories in a classical billiard. Superimposed on these classical effects are quantum interference effects manifested by highly periodic conductance oscillations as the Fermi wave vector, k_F, is varied. We show, that despite of the presence of lead openings, transport through the dot is effectively mediated by just a few (or even a single) eigenstates of the corresponding closed structure. In a single-mode regime in the leads the broadening of the resonant levels is typically smaller than the mean energy level spacing, Δ. Thus, at very low temperatures, transport measurement in a single-mode regime may probe a single resonant energy level of the dot. On the contrary, in the many-mode regime the broadening exceeds Δ and has essentially non-Lorentzian character. We demonstrate that in the latter case eigenlevel spacing statistics of the corresponding closed system is not relevant to the averaged transport properties of the dot. This conclusion seems to have a number of experimental as well as numerical verifications.

The calculated periodicity of the conduction oscillations in the open dot is related to the global shell structure in the density of states of the corresponding isolated square. The shell structure reflects periodic clustering of levels on the scale exceeding the mean level spacing separation. Each shell can be related to the certain family of the semi-classical periodic orbits in the square. However, particular arrangement of the leads may lead to the selective coupling between them, such that not all shells (or, alternatively, families of periodic orbits) mediate transport through the dot.

---

[1] I. V. Zozoulenko, F. A. Maaø, and E. H. Hauge, Phys. Rev. B **53**, 7975 (1996); ibid., 7987 (1996).

[2] I. V. Zozoulenko, R. Schuster, K.-F. Berggren, and K. Ensslin, accepted to Phys. Rev. B as a Rapid Communication.

Application of the Wigner-Function Formulation to Mesoscopic Systems in presence of the Electron-Phonon Interaction

C. Jacoboni, A. Abramo, P. Bordone, R.Brunetti and M. Pascoli

Istituto Nazionale per la Fisica della Materia,
Dipartimento di Fisica, Università di Modena, V. Campi 213/A, I-41100 Modena, Italy

A theoretical and computational analysis of the quantum dynamics of charge carriers in presence of electron-phonon (e-p) interaction based on the Wigner-function formulation is here applied to the study of transport in mesoscopic systems. The continuum quantum dynamical evolution of the scattering process is here accounted for, while the external fields are incorporated into the unperturbed Hamiltonian [1]. In particular, the following issues will be discussed.

a) Details of a single-electron propagation through a fixed potential profile (potential step and double-barrier have been considered) in presence of e-p scattering (Fig. 1); the case without field is also considered in order to illustrate the details of the quantum e-p interaction without any complications coming from the external field.

b) The existence of Wigner trajectories during e-p interaction has been demonstrated. The Wigner trajectory between two vertices of a phonon scattering process corresponds to the semiclassical trajectory where half of the phonon momentum q is transferred to the electron; at the second vertex the second half of q is transferred (in real processes) or the first half of q is given back to the phonon system (in virtual processes). The existence of such trajectories within e-p interactions open the possibility of using "traditional" Monte Carlo simulations for quantum transport without having to resort to the completed-scattering approximation.

c) It has been shown how to properly incorporate boundary conditions into a time dependent simulation of the electron Wigner function inside an open mesoscopic system (Fig.2). In such a formulation scattering with phonons inside the device does not alter the boundary conditions at finite positions even though the basis of extended scattering states is used.
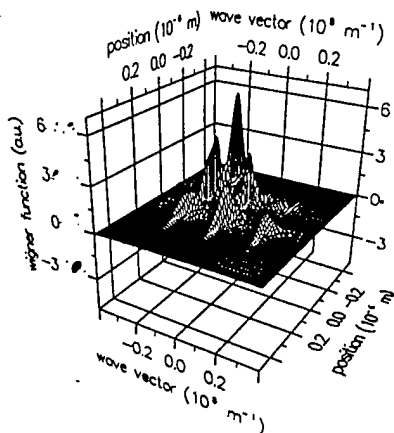
Fig. 1: Wigner function of an electron scattered by a phonon while crossing a double-barrier structure
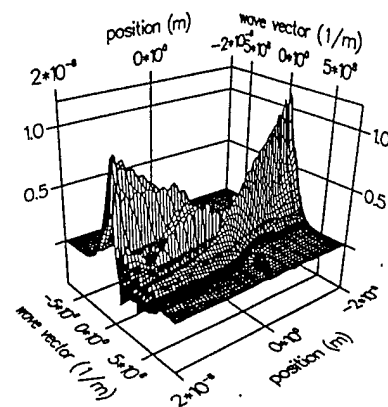
Fig. 2: Wigner function of electrons entering from the boundaries into a device with a potential step

1. R.Brunetti, C.Jacoboni, and M.Nedjalkov, in *Hot Carriers in Semiconductors*, Edited by K.Hess et al., Plenum Press, New York 1996, p.417.

Quantum Networks: Dynamics of Open Nanostructures

G. Mahler

Oregon Center of Optics, Dept. of Physics, University of Oregon, Eugene OR 97403
and
Institut für Theoretische Physik, Universität Stuttgart, 70550 Stuttgart, Germany

There is a growing interest in the analysis of non-classical states within "simple" quantum systems: Recent examples include the angular state density matrix of an electron in the H-atom, the vibrational state of a molecular wave packet, or the quantum state of photon fields (1). All these refer to single modes (subsystems); extensions to multi-mode systems have been undertaken for photon fields in a few cases. Nanostructures should constitute an interesting alternative route to multi-mode systems, the (separable) modes being represented here by subsets of localized electronic states (within quantum dots). Those quantum dots may be coupled via Coulomb interactions, but will presently not be allowed to exchange charge (no transport). Non-equilibrium dynamics is generated via external (classical) electromagnetic fields of selected frequencie s (2). As detection channels we use the luminescence fields. We explore the complexity of such composite systems by means of stochastic simulation of the electronic state and statistical analysis of the associated luminescence fields. In particular, we discuss characteristics of the quantum trajectories: In the classical limit these trajectories would reduce to a random walk defined on specific points in Hilbert space only. However, allowing for local and mutual coherence the system visits a significant part of its full Hilbert space, as can be inferred from multi-mode photon counting (3). With increasing network size the full state description becomes prohibitively complex, calling for appropriate data compression into some characteristic measures; pertinent examples will be discussed. Such investigations appear to be a natural extension of current trends in features proper. Quantum control would be a prerequisite for any application like quantum information processing.

(1) U. Leonhardt et al., Optics Commun. 127, 144 (1996)
(2) M. Keller, G. Mahler, J. mod. Optics 41, 2537 (1995); G. Mahler, M. Keller, R. Wawer, Z. Phys. B (1997), in press
(3) G. Mahler, R. Wawer, Superlattices & Microstructures 21, 7 (1997)

A GENERALIZED MONTE CARLO APPROACH FOR THE ANALYSIS OF QUANTUM-TRANSPORT PHENOMENA IN MESOSCOPIC SYSTEMS: INTERPLAY BETWEEN COHERENCE AND RELAXATION

Fausto Rossi*

Istituto Nazionale Fisica della Materia (INFM) and Dipartimento di Fisica, Università di Modena, I-41100 Modena, Italy

Stefano Ragazzi, Aldo Di Carlo, and Paolo Lugli

INFM and Dipartimento di Ingegneria Elettronica
Università di Roma "Tor Vergata", I-00133 Roma, Italy

The Monte Carlo (MC) method, which has been applied for more than 25 years for calculation of semiclassical charge transport in semiconductors, is the most powerful numerical tool for microelectronics device simulation [1]. However, it is well known that the present-day technology pushes device dimensions toward limits where the traditional semiclassical transport theory can no longer be applied, and a more rigorous quantum transport theory is required.

In this contribution, a generalized MC approach for the analysis of hot-carrier transport and relaxation phenomena in quantum devices is proposed. The method is based on a generalized MC solution of the set of kinetic equations describing the time evolution of the single-particle density matrix. Our approach can be regarded as an extension to open systems of the generalized MC method recently proposed for the analysis of the coupled coherent and incoherent carrier dynamics in photoexcited semiconductors [2]. This simulation scheme is based on a time-step separation between coherent and incoherent dynamics. The former, treated within a Wigner-function picture, accounts in a rigorous way for all quantum phenomena induced by the potential profile of the device as well as for the proper boundary conditions (which may be obtained within a selfconsistent Schrödinger-Poisson scheme). The latter, described within the basis given by the eigenstates of the potential profile (which includes the applied bias), accounts for all the relevant scattering mechanisms by means of a conventional MC simulation.

Compared to more academic quantum-kinetic approaches, whose application is still limited to highly simplified situations, the proposed simulation scheme can be applied to realistic cases, allowing on the one hand a proper description of quantum-interference phenomena induced by the potential profile and on the other hand maintaining all the well known advantages of the conventional MC method.

As a first application of the above algorithm, we will discuss the scattering-induced suppression of Bloch oscillations in semiconductor superlattices (see figure). As a second example, we will discuss the strong interplay between coherence and relaxation within a double-barrier structure, which clearly shows the failure of any pure coherent or incoherent approach in describing such quantum-transport regime.
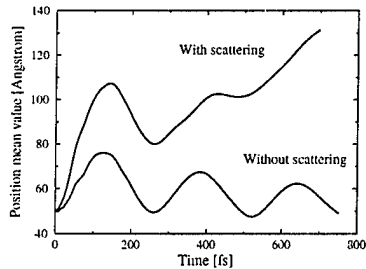
The figure shows the mean position of an electron wavepacket in a biased superlattice as obtained by means of our generalized Monte Carlo approach with and without scattering mechanisms. Bloch oscillations are suppressed when scattering is included.

[1] C. Jacoboni and P. Lugli, *The Monte Carlo Method for Semiconductor Device Simulation* (Springer, Wien, 1989).
[2] T. Kuhn and F. Rossi, Phys. Rev. Lett. **69**, 977 (1992); F. Rossi, S. Haas, and T. Kuhn, Phys. Rev. Lett. **72**, 152 (1994).

* Corresponding author. E-mail: rossi@unimo.it Tel: +39 (59) 586072 Fax: +39 (59) 367488

Coherent Control of Light Absorption in Semiconductor Nanostructures

W. Pötz and X. Hu
Physics Department
845 W. Taylor Str.
University of Illinois at Chicago, USA
Fax: (312) 996-9016; e-mail: wap@mozart.phy.uic.edu

It is shown theoretically that electron–hole pair generation in semiconductor heterostructures by sub–picosecond pump pulses can effectively be controlled by amplitude and phase of a coherent microwave field. This prediction is based on a microscopic theory of phase breaking in semiconductor multiband systems coupled to light fields.[1] This complex system of equations is solved numerically using spline fits and numerical integration, rather than Monte Carlo techniques.

In the simplest situation, we consider a sub–picosecond pump pulse applied to an asymmetric GaAs–AlGaAs double well. Net absorption of this light field is controlled by a dc microwave (MW) field which resonantly couples direct and indirect excitons. Depending on the pump pulse wavelength, the MW field can either be used to suppress or to enhance photoabsorption. Dependence of the net absorption on the phase of the MW field gives direct evidence of the importance of coherence. In particular, it is shown that the MW field–induced interband polarization is largely responsible for the predicted effect which is related to coherent "state trapping" which has been predicted in atomic three–level systems.[2] Here, however, we investigate the effect of the MW field directly on the pump pulse which couples electrons and holes. Moreover, excitonic effects cause significant deviations from the predicted behavior of the simple atomic three–level system considered in Ref. 2.

The possibility of coherent manipulation of charge transfer between wells, as well as net gain without inversion in semiconductor nanostructures will be discussed.

References

[1] W. Pötz, Phys. Rev. B **54**, 5647 (1996).

[2] M. O. Scully et al., Phys. Rev. Lett. **62**, 2813 (1989).

A New Computational Approach to Photon–Assisted Tunneling in Intense Driving Fields Based on a Fabry–Perot Analogy

Mathias Wagner

Hitachi Cambridge Laboratory, Madingley Road, Cambridge CB3 0HE, UK

Tel. +44 1223 467944, Fax. +44 1223 467942, wagner@phy.cam.ac.uk

Abstract

The subject of (in)coherent quantum transport in strongly driven heterostructures has recently gained much momentum with the advent of free–electron lasers, which are capable of providing intense radiation [1]. Here we report on a new approach to the notoriously complex problem of a theoretical description of quantum transport in intense laser fields that is based on an analogy with the Fabry–Perot interferometer in optics. In previous studies, the transfer–matrix method had been employed to calculate the reflection and transmission amplitudes of scattering states in driven heterostructures [2]. Due to the large size of the transfer matrix even for a one–dimensional system (the size is given by the highest order of photon processes one wishes to take into account), these calculations demand large computer resources. In contrast, the Fabry–Perot approach is rather modest in its computational demands and, moreover, much faster for not too complex heterostructures. In addition, it allows for the phenomenological inclusion of dephasing of the electronic wave function. Another advantage of the Fabry–Perot approach is that one builds up more complex structures from elementary building blocks such as single barriers, which often are more accessible to analytical treatments. For a single barrier in particular, analytical approximations can be used that have as input parameter only the strength of the driving field and the *dc transmission and reflection probabilities* [3], which may be obtained by other means. As a typical example we present results for a driven double–barrier diode. In the left panel of Fig. 1 we have plotted the transmission probabilities in the lowest few photonic sidebands for an electron incident one photon quantum below the energy of the (undriven) resonance. The ac driving field was taken to be uniform throughout the space, $F(t) = F \cos \omega t$. Clearly, the agreement with the much more CPU intensive transfer–matrix method, shown to the right, is excellent.

[1] B. J. Keay et. al., Phys. Rev. Lett. **75**, 4098 (1995).

[2] M. Wagner, Phys. Rev. Lett. **76**, 4010 (1996); A **51**, 798 (1995); B **49**, 16544 (1994).

[3] M. Wagner and W. Zwerger, Phys. Rev. B (RC, submitted).
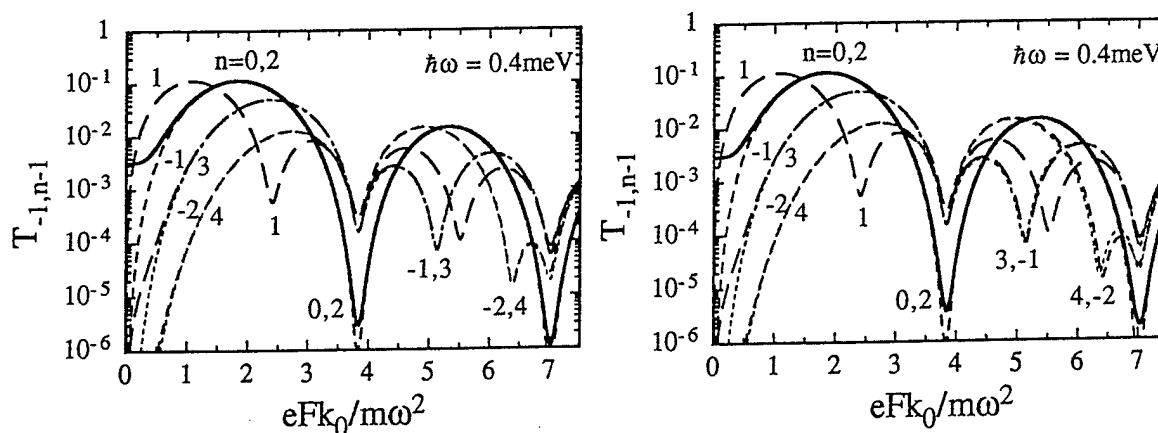
Fig. 1: Transmission probability via the lowest few photonic sidebands n through a driven double–barrier diode calculated using the Fabry–Perot approach (left), and the transfer–matrix method (right), as a function of the characteristic scaling parameter $eFk_0/m\omega^2$, where k_0 is the wave vector of the resonance and m the electron mass. In the Fabry–Perot approach, CPU time is reduced to about 1/30 in this case!

Phase Space Boundary Conditions and Quantum Device Transport

H. L. Grubin[*], J. R. Caspar[*] and D. K. Ferry[**]

[*]Scientific Research Associates, Inc. Glastonbury CT 06033
[**]Arizona State University, Tempe, AZ

Abstract

Devices interact with each other and with the environment. For classical devices assigning boundary conditions at the physical exit and entry regions of the device often satisfactorily treats this interaction. The situation with boundary conditions to quantum devices is more involved. To illustrate we consider one-space dimension structures whose details are unimportant, although they could include serially positioned RTDs, RTBTs, etc. We examine these structures within the framework of the coordinate representation, with the simplest description being that of a two dimensional phase space represented by the density matrix $\rho(x, x')$ driven by the Liouville potential energy $V(x)-V(x')$. The two-dimensional phase space is shown in the top left figure, where the shaded squares represent the phase spaces occupied by Liouville potentials for a specific pair of barrier groupings.
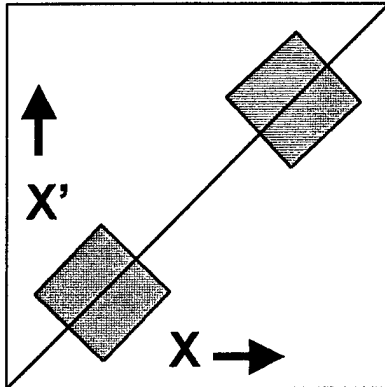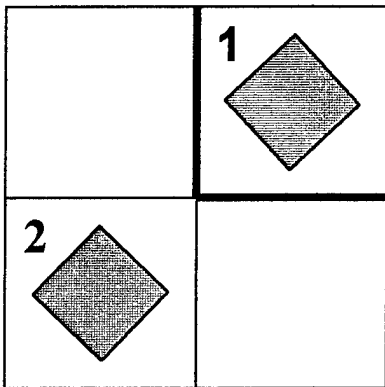
To treat the effect of device '2' on device '1', see left figure, the phase space is divided into four parts and the Liouville equation for device '1' is solved self-consistently. Modifying the boundary conditions on the bold lines of the figure represents the influence of device '2'. We examine this influence with device '1' as a single 200nm RTD. The figure at the bottom is a blow-up of density under equilibrium conditions, and illustrates the consequences of **modest** variations in the function boundary condition along the x-axis, with the principal variation occurring within 20 percent of the origin. The density distribution without boundary modification is displayed with open circles. With modest variations in the boundary conditions there is a qualitative alteration in the density profile with charge build- up within the barrier. The results suggest that device-device interaction may result in electrical characteristics of device '1' that are completely different than that of an isolated device. The effect is further enhanced as the device size is reduced and under bias, and demonstrates that the procedures discussed here may enable us to quantify the role of device separation on device independence.
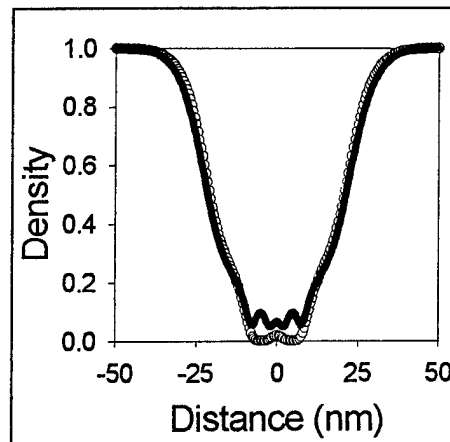
Single-Electron Memories

Christoph Wasshuber, Hans Kosina, and Siegfried Selberherr
Institute for Microelectronics, TU-Vienna
Gusshausstrasse 27-29/E360, A-1040 Wien, Austria, Europe
email: wasshuber@iue.tuwien.ac.at

One of the most promising applications of single-electronics is a single-electron memory chip. Such a chip would have orders of magnitude lower power consumption compared to state-of-the-art dynamic memories, and would allow integration densities beyond the tera bit chip. In order to reach this goal certain questions have to be solved: Is room temperature operation possible? How can single-electron memories be made random background charge independent? Is it possible to mass fabricate such single-electron devices?

Thus we studied various single-electron memory designs by simulation. Our main focus was on comparing operation temperature and random background charge independence. We examined already proposed memory designs, such as single-electron flip-flop [1], single-electron trap [2], Q_0-independent memory [3], and new variations which try to improve random background charge independence and manufacturability with todays process techniques.

Very often a single-electron transistor is used to read out the charge stored in a single-electron memory cell. Unfortunately, the single-electron transistor is strongly background charge dependent, and difficult to fabricate for room temperature operation. We show that the substitution of a single-electron transistor which consists of two tunnel junctions with a granular film batch which consists of many tunnel junctions solves many problems. Firstly, a granular film batch exhibits a similar Coulomb blockade and similar Coulomb oscillations as a single-electron transistor and thus can be substituted without change in functionality. Secondly, the individual grains of granular films which can have diameters in the nano-meter range provide with their minuteness a Coulomb blockade of up to 1eV and thus allow room temperature operation. Thirdly, the behavior of a batch which consists of hundreds and thousands of grains does not depend on individual grains, but on the ensemble characteristics. These are much easier to control in an industrial mass production and show much better independence to random background charges than the single-island single-electron transistor. Finally, the lateral dimensions of the granular film batch can be in the range achievable with todays e-beam lithography ($\sim$30 nm). Hence the necessity for highly advanced lithography is absent.

The conclusion of our simulations is, that a combination of granular film processes with state-of-the-art lithography allows the production of random background charge independent memory chips operating at room temperature.

[1] A. N. Korotkov, R. H. Chen, and K. K. Likharev. Possible performance of capacitively coupled single-electron transistors in digital circuits. *Journal of Applied Physics*, 78(4):2520–2530, August 1995.

[2] K. Nakazato and H. Ahmed. The multiple-tunnel junction and its application to single-electron memory and logic circuits. *Japanese Journal of Applied Physics*, 34(Part1, 2B):700–706, February 1995.

[3] K. K. Likharev and A. N. Korotkov. Analysis of Q_0-independent single-electron systems. In *Int. Workshop on Computational Electronics*, page 42, 1995.

Electron-LA phonon interaction in a quantum dot

T. Ezaki, N. Mori, and C. Hamaguchi

Department of Electronic Engineering, Osaka University Japan

2-1 Yamada-oka, Suita, Osaka 565, Japan.

Phone +81-6-879-7767, FAX +81-6-875-0506

E-mail: ezaki@ele.eng.osaka-u.ac.jp

Recent developments in microfabrication technology have made it possible to fabricate small quantum dots (QDs) where single or few electrons are confined three-dimensionally. In small QDs, atomic like discrete energy structures are realized, and the density of states is characterised by a delta function. In such systems, it is pointed out that relaxation of electrons from excited states to the ground state via electron-phonon interaction is reduced because of the conservation of energy and angular momentum during the transition between the discrete energy levels. When more electrons are added into a QD, electrons interact each other, and the energy levels are changed to form more complicated and dense structures. In such a case, we can expect a modification of the electron-phonon interaction. In the present work, we have calculated N-electron-states in a single QD by using an exact diagonalization method to estimate the energy relaxation time from excited states to the ground state via electron-LA phonon interaction.

We assume a simple model for quantum dots, where electrons are confined in a two-dimensional harmonic potential in x-y plane and an infinite square potential well along z direction. The N-electron Hamiltonian of the quantum dot including Coulomb interaction in the presence of a magnetic field is then given by the following form

$$\mathcal{H} = \sum_{i=1}^{N} \left\{ \frac{(p_i + eA(r_i))^2}{2m^*} + \frac{1}{2}m^*\omega_0^2(x_i^2 + y_i^2) + V(z_i) \right\} + \sum_{i<j} \frac{e^2}{4\pi\epsilon|r_i - r_j|}. \tag{1}$$

In the calculation, only the ground single-electron-state is taken into account along the z direction.

The transition probability due to electron-LA phonon interaction between excited states and the ground state in the N-electron QD are calculated by using the Fermi's golden rule. Since there are many intermediate N-electron-states between the higher energy states and the ground state in the QD with many electrons, various relaxation paths through such intermediate states can occur. In order to estimate the fastest relaxation time, we took all the intermediate states into consideration.

In figure 1, we show the calculated relaxation time from the excited states to the ground state of a two-electron QD with a parabolic confinement potential $\hbar\omega_0 = 1\,\text{meV}$ and well width $W = 50\,\text{nm}$ at $B = 0\,\text{T}$. The indices $(m, s; n)$ shown in the figure are quantum numbers of eigen states, indicating n-th state of N-electrons system with a total angular momentum $\hbar m$ and a total spin s. Open circles are relaxation time of direct transition from the excited state to the ground state, and solid circles represent the fastest relaxation process. The open and solid circles connected by the dashed line mean the transition from the same initial state. For example, the relaxation from the $(2, 0; 4)$ state to the ground state takes about 6 ns in the case of a direct process. On the other hand, the relaxation through the intermediate state of $(2, 0; 0)$ gives 1.5 ns because the relaxation is limited by the fast transitions

Figure 1: Relaxation time as a function of the energy difference between the initial state and the ground state.

of the two steps, between $(2, 0; 4)$ and $(2, 0; 0)$ ($\sim 0.9\,\text{ns}$) and between $(2, 0; 0)$ and the ground state ($\sim 0.6\,\text{ns}$). Relaxation time can therefore be accelerated through a certain intermediate state(s) between the initial and the final state (the ground state in the present case).

Numerical analysis of asymmetric single electron turnstiles using Monte Carlo simulation

Masaharu Kirihara and Kenji Taniguchi

Department of Electronics and Information systems, Osaka University

2-1 Yamada-Oka, Suita, Osaka, 565 Japan

Phone : +81-6-879-7781, Fax : +81-6-879-7792

In recent years there has been a growing interest in single electronics because of its potentiality for future integrated circuits with low power and high packing density. Several single electron devices such as a turnstile and an electron pump utilizing the discreteness of electronic charge have been proposed and their electrical characteristics have been studied extensively. In this paper, we first explain our Monte Carlo simulator to study their characteristics. Then, we describe a single electron winner-take-all (WTA) circuit using asymmetric turnstiles as one of the single electronic circuits.

A conventional circuit simulation is based on Kirchhoff's fundamental laws which cannot be used to simulate single electronic circuits because of the stochastic nature of tunnel events. We developed a single electron circuit simulator using a Monte Carlo method taking into account the following features inherent in single electron circuits; (1) electronic charge configuration in a network affects the electron tunneling rate and (2) the potential of each node changes discretely after a tunnel event.

The tunneling rate of an electron from a node to a neighboring one depends on the electrostatic energy difference ΔE and hence on the configuration of charges before and after a tunneling process. The average tunneling rate Γ is given by [1] $\Gamma = \Delta E/[e^2 R_T \{1 - \exp(-\Delta E/k_B T)\}]$. Due to the stochastic nature of the tunneling event, the probability density $p(t)$ that the next tunnel event occurs at time t after the previous one is given by $dp(t) = -\Gamma \exp(-\Gamma t)dt$. From this equation, one can evaluate the tunnel interval t by using a random number r distributed uniformly between 0 and 1, which is given by $t = -\ln(r)/\Gamma$.

The single electron turnstile[2] which consists of two tunnel junctions on each side of a central gate capacitor offers controlled transfer of single electronic charges one by one. In Ref. 2, a symmetric characteristic of the turnstile was reported because all the tunnel junction used have the same capacitance. However, if the tunnel junction capacitance of the left arm is smaller than that of the right, electronic charge transport becomes unidirectional.

A WTA circuit shown in Fig. 1 is composed of such unidirectional or asymmetric turnstiles. The circuit can find the largest data and identify its location from several input signals. The circuit in Fig. 1 consists of n asymmetric turnstiles as inputs, an inverter and an single electron transistor for discharging a load capacitor C_L. When k inputs are high, k electron charges are stored in the load capacitor C_L per one gate clock. No electronic charge transfer to the load capacitor occurs from low in-

put nodes through turnstiles because of their unidirectional nature. After several clock cycles, the voltage of the load capacitor increases up to high input level and then the output of the inverter falls down. The number of the clock cycles required for the output going to low level depends on the number of k; there exists a good correlation between the number of clock cycles required for switching the output and the number of high level inputs.

Figure 2 shows simulated characteristics of a 4-input single electron WTA circuit with $C_L = 25e/V_{DD}$. When all inputs are high level($k = 4$), the output goes to low after three clocks, while in the case of $k = 3$ four clocks needs. Further detailed simulations reveal that the clock frequency must be smaller than $10^{-4}(C_\Sigma R_{T\Sigma})^{-1}$Hz to ensure the error rate below 10^{-25} per gate.

References

[1] M. H. Devoret, and H. Grabert, in *Single Charge Tunneling*, edited by H. Grabert and M. H. Devoret (Plenum, New York, 1992), p. 12.

[2] L. J. Geerligs *et al.*, Phys. Rev. Lett. 64, 2691 (1990).

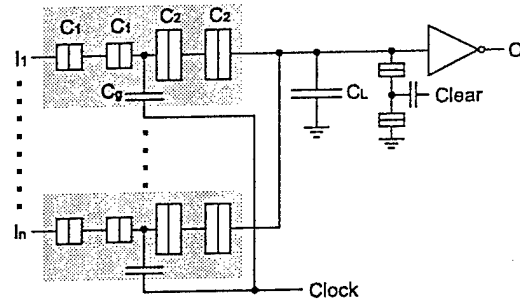Figure 1: Single electron WTA circuit. The circuits in shaded regions represent asymmetric turnstiles. The parameter sets are $C_1 = 3C_g$, $C_2 = 5C_g$, and $C_g = e/(6V_{DD})$ where V_{DD} is the supply voltage.
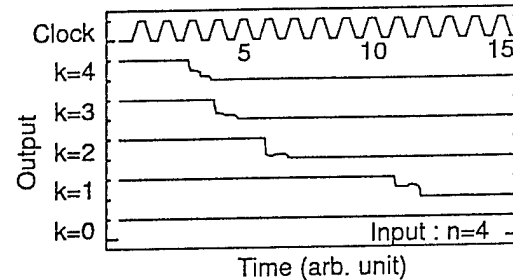

Figure 2: Output characteristics of a four inputs WTA simulated at $T = 0$. The clock signal swings quasi-statically from 0 to $5V_{DD}$.

Self-consistent calculations of the ground state and the capacitance of a 3D Si/SiO₂ quantum dot

A Scholze*, A Wettstein, A Schenk, W Fichtner

ETH–Zürich
Institut für Integrierte Systeme
Zürich, Switzerland

We perform self-consistent electronic structure calculations in the framework of inhomogeneously and anisotropically scaled local density functional theory of a fully 3D modeled Si/SiO₂ quantum dot. The electrons are laterally confined in the semiconductor/oxide heterojunction. The dot is defined by metallic gates atop of the device (Fig. 1). We solve the coupled Kohn-Sham–Poisson equation using a steepest descent approach. Weak coupling of the dot to the leads is assumed. Metallic gates are incorporated via Dirichlet boundary conditions to the Poisson equation. The Hamiltonian and the Poisson operator are discretized on a non-uniform tensor product mesh using the method of finite differences. Total charge densities (Fig. 2), total free energies (F), chemical potentials(μ) for different numbers of electrons in the dot, and the differential capacitances

$$\mu(N) = F(N) - F(N-1)$$

$$C_d(N) = \frac{q^2}{\mu(N+1) - \mu(N)}$$

for various dot sizes are calculated.

The self-consistent single particle potential is quasi parabolic and the single particle eigenvalue spectrum exhibits a shell structure familiar from the harmonic oscillator (HO). When adding electrons to the dot, the free energy increases almost linearly when adding to the same shell, however, the slope increases from shell to shell. Therefore, a minimum in the capacitance occurs, when a shell is filled. Since the shells for the 2D and the 3D HO are different, we observe different capacitance minima for different dot sizes (Fig. 4). The larger dot shows a minimum at electron 6, which corresponds to the filling of the second shell of a 2D HO. The smaller dot shows no pronounced minimum at this point. However, at the 8-th electron the second shell of a 3D HO is filled and a capacitance minimum occurs. For larger electron numbers this simple picture does not hold anymore. The filling of the third 2D shell at the 12-th electron shell is well pronounced for both dots and more minima occur for the smaller dot.

[1] M. Macucci *et al.*, Phys. Rev. B **44**, 17 354 (1993).
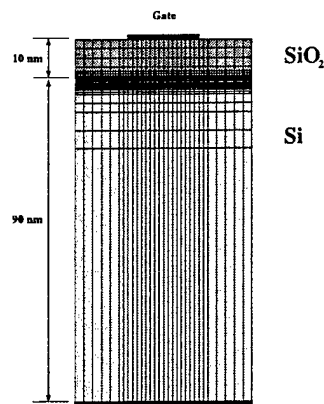
Figure 1

Gated Si/SiO₂ quantum dot and mesh.
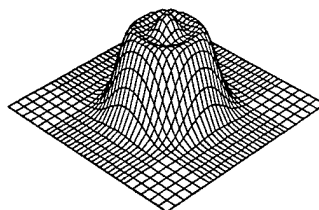
Figure 2

Self-consistent total charge density of 12 electrons (20 nm × 20 nm square gate).
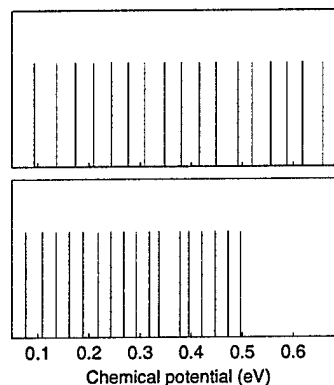
Figure 3

Chemical potential values for a 10 nm × 10 nm (upper) and an 20 nm × 20 nm (lower) dot.
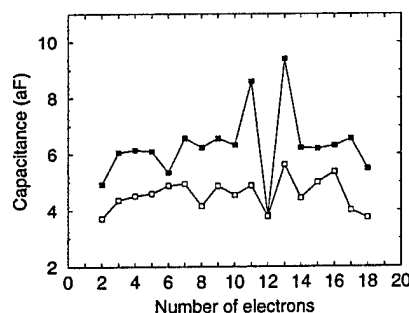
Figure 4

Differential capacitance for a 10 nm × 10 nm (lower curve) and an 20 nm × 20 nm (upper curve) dot.

AN INTERBAND TUNNELING OSCILLATOR: SELF-OSCILLATION OF TRAPPED HOLE CHARGE IN A DOUBLE-BARRIER STRUCTURE

F. A. Buot

Naval Research Laboratory, Washington, D.C. 20375-5320

Tel. (202)767-2644; FAX (202)767-0546; email: buot@estd.nrl.navy.mil

Abstract: It is shown that a polarization-induced limit cycle oscillation of trapped-hole-charge can occur in AlGaSb/InAs/AlGaSb double-barrier structure. A model for the quantum-transport-rate equations for Zener tunneling, polarization, and electron-hole recombination is used to analyze the behavior of this device structure. We show that the steady-state operation is unstable against the limit-cycle operation . An approximate analytical form of the limit cycle solution is obtained. The results show that the average values of the trapped hole charge in the AlGaSb barrier are slowly-varying function of the applied voltage, with the amplitude of the trapped-charge oscillation increasing with the applied bias at the drain. This result qualitatively agrees with the experimental measurements of the average current-voltage characteristic of this device structure. However, exact numerical results call for large-scale time-dependent numerical simulation of multi-band quantum transport equations which account for interband tunneling.

TUNNELING BETWEEN MULTIMODE
STACKED QUANTUM WIRES

M. Macucci (corresponding author)

Dipartimento di Ingegneria dell'Informazione, Università degli Studi di Pisa
Via Diotisalvi, 2
I-56126 Pisa, Italy
FAX +39 50 568522, e-mail: `massimo@mercurio.iet.unipi.it`

A. T. Galick and U. Ravaioli

Beckman Institute, University of Illinois
405 N Mathews, Urbana, IL 61801

The possibility of fabricating heterostructures containing weakly coupled 2DEGs (two-dimensional electron gases) has originated several proposals for possible devices exploiting controlled tunneling between such 2DEGs.

The basic idea, proposed by H. Sakakibara *et al.* (IEDM 93-411), consists in fabricating two stacked 2DEGs with different thicknesses, so that in normal conditions the ground states for the two wells will not be aligned. By applying a potential to a metallic gate obtained on top of the heterostructure, it is possible to alter the potential landscape and to line up the two ground states, so that tunneling will be possible. If we want to observe interference effects dependent on the length of the metallic gate, the situation is, however, more complex than what is discussed in the paper by Sakakibara *et al.*: while in a quantum wire the number of transverse modes is limited or we can even achieve monomode propagation, in a 2DEG the number of transverse modes is not limited and the continuous distribution of wavevectors will certainly wash out any interference effect.

Therefore, interference phenomena will be observable only in the case that the lateral size of the 2DEG is limited, thereby turning it into a wide quantum wire. We have been interested in evaluating the maximum lateral dimension and therefore the maximum number of propagating modes that allow the survival of some clear interference effect.

Our model consists in two stacked wires with a rectangular cross-section and a tunneling barrier separating them. We consider input and output regions where the wires are totally independent from each other and a coupling region, whose potential landscape is controlled by a metallic gate.

We solve the Schrödinger equation in each two-dimensional cross-section of the stacked wires and then compute the transmission coefficients between them as a function of gate bias, by means of a recursive Green's function technique. The eigenvalues and eigenvectors of the Schrödinger equation are computed with a recently developed optimized solver based on the iterative Arnoldi method.

We discuss the conditions needed for the observation of the interference effects which are dependent on the length of the gate along the direction of current flow, and we establish the minimum design requirements for devices based on this principle.

Ballistic Directional Coupler on the DQW-Basis

A. N. Korshak[1,2], Z. S. Gribnikov[1,2], N. Z. Vagidov[1], S. I. Kozlovsky[1], V. V. Mitin[2]

[1]*Institute of Semiconductor Physics, Kiev, Ukraine*
[2] *Department of ECE, Wayne State University, Detroit, MI 48202*

There are numerous theoretical suggestions and experimental intentions to create an effective directional electron ballistic coupler (DEBC) on the basis of a section of a double quantum WIRE with a connection through the tunnel barrier or through the ballistic window. This idea assumes a control of the interwire connection by a gate potential which varies a height of the tunnel barrier or a size of the window.

Here we turn to an idea of the DEBC on the basis of a symmetrical double quantum WELL (DQW) with a space-charge limited ballistic current in it [1]. Electrons are injecting into one of the two wells only (the down-well, Fig.1). While electrons propagate along the DQW, they pass from one well to the other ballistically due to the tunnel connection, which is assumed to be constant on the DQW-section. They can flow out through the independent anodes contacting each of the wells separately (the down- and up-wells, Fig.1).

Ideal coupler characteristics should provide a complete switching between the channels (that is between the anodes) and a conservation of the total current in the diode, $I_1 + I_2$. To satisfy these demands the diode should operate in a current saturation regime. Under this condition variations of the voltage across the diode base allow us to obtain an outcome current in one of the anodes only (see Fig.2).

A two-dimensional electric potential distribution in the diode base is calculated self-consistently with a solution of a one-dimensional ballistic transport problem in the single QW and DQW section for different shapes of the cathode and anodes.

Along with the DEBC other schemes of the anode and cathode contacts to the DQW are considered and N- and Z-shape IV-characteristics for these structures are obtained.

Reference: [1] Z. S. Gribnikov, A. N. Korshak, S. I. Kozlovsky, N. Z. Vagidov. Lithuanian Journ. of Physics, v. 36, no. 6, pp. 599-604 (1996).

Fig. 1

Fig.2
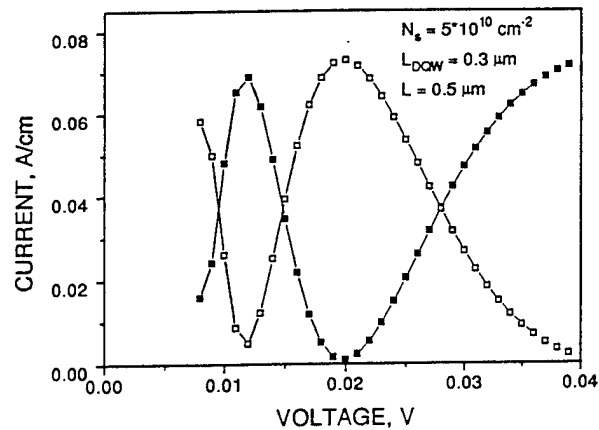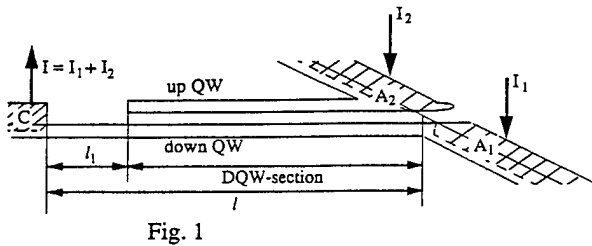
Title: Monte Carlo simulation of non-local transport effects in strained Si on relaxed $Si_{1-x}Ge_x$ heterostructures.

Authors: F.Gámiz, J.B.Roldán and J.A.López-Villanueva.
Address: Departamento de Electrónica y Tecnología de Computadores. Facultad de Ciencias. Universidad de Granada. 18071 Granada (SPAIN)
Phone: 34-58-246145 **Fax:** 34-58-243230 **E-mail:** paco@gcd.ugr.es ,, fgamiz@goliat.ugr.es

ABSTRACT:

When electron device dimensions shrink to the deep-submicrometer regime, the electron transit time becomes comparable to the energy-relaxation time. This implies that carriers do not travel in equilibrium with the lattice, and non-local transport effects, such as velocity-overshoot effects, become noticeable. Electron velocity overshoot in very short channel MOSFETs has been experimentally found to be responsible for a transconductance increase greater than the expected from local transport models. The microscopic nature of the Monte Carlo method allows to study these kind of non-local effects that could not be studied with other methods which use local transport models, such us the drift-diffusion model. We have developed a Monte Carlo simulation to study the electron transport properties of strained-Si on relaxed $Si_{1-x}Ge_x$ heterostructures. The steady and non-steady high-longitudinal field transport regimes have been described in depth to better understand the non-local transport effects that give rise to the transconductance enhancement experimentally observed. The different contributions of the conductivity-effective mass and the intervalley scattering rate reduction to the mobility enhancement as the Ge mole fraction rises have been discussed for several temperature, effective, and longitudinal-electric field conditions. Finally, electron-velocity-overshoot effects are also studied in deep-submicron strained-Si MOSFETs, where they show an improvement over the performance of their normal silicon counterparts. Figure 1 shows the time evolution of the electron velocity when a sudden longitudinal electric field is applied to a steady state electron distribution achieved under the influence of a smaller longitudinal electric field for different Ge mole fractions. Electron velocity overshoot, can be clearly observed: the higher the Ge mole fraction the higher the velocity. We have also simulated several $0.1 \mu m$ channel length MOSFETs for different Ge mole fractions.The inhomogeneous steady-state velocity distribution along the channel is shown in Figure 2. As can be observed, the electron velocity is higher than the saturation velocity.
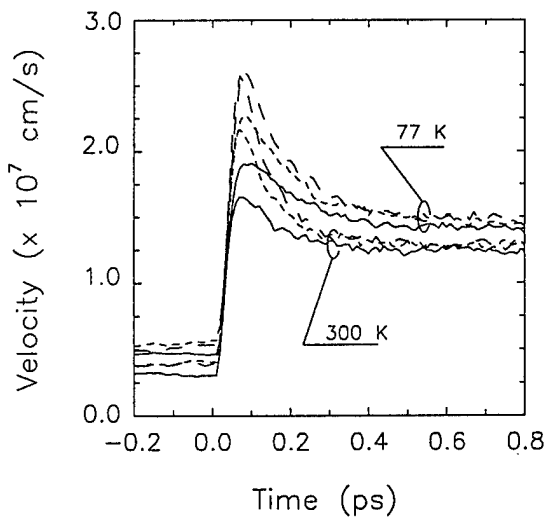
Figure 1
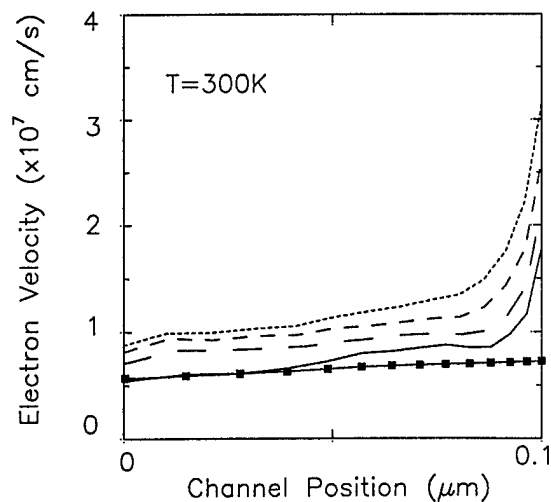
Figure 2

Title: A β-SiC MOSFET Monte Carlo simulator including inversion layer quantization.

Authors: F.Gámiz, J.B.Roldán and J.A.López-Villanueva.
Address: Departamento de Electrónica y Tecnología de Computadores. Universidad de Granada. Facultad de Ciencias. Avd.Fuentenueva s/n. 18071 GRANADA (SPAIN)
Fax: 34-58-243230   **Phone number:** 34-58-246145   **E-mail:** paco@gcd.ugr.es

ABSTRACT:

We have developed a β-SiC MOSFET Monte Carlo simulator considering inversion layer quantization. We have included acoustic, intervalley and polar-optical phonons, and Coulomb and surface roughness scattering mechanisms. We have studied the operation of these devices at room temperature, and have also analyzed in depth their high temperature features obtaining promising results. The reduction of the inversion layer centroid in SiC compared to Si, (Figure 1 Si-dashed line, SiC-solid line) enhances Coulomb (produced by interface charges) and surface roughness scattering (Figure 2 Si-dashed line, SiC-solid line). The high longitudinal-electric field homogenous transport regime SiC velocity curves are shown in Figure 3 for different transverse fields. There is a dependence of the peak velocity (whose value is higher than in silicon) on the transverse field. The energy- and momentum-relaxation times in SiC (Figure 4) are an order of magnitude lower than in Si, that means lower electron-velocity overshoot effects than in Si.
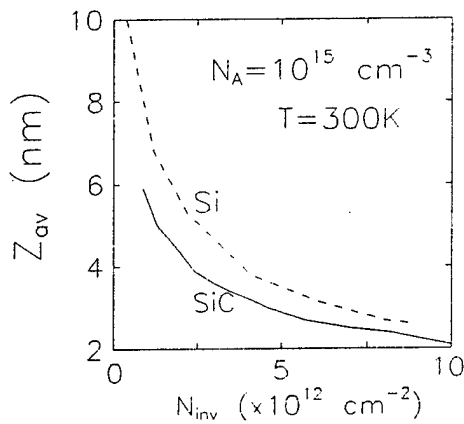
Figure 1
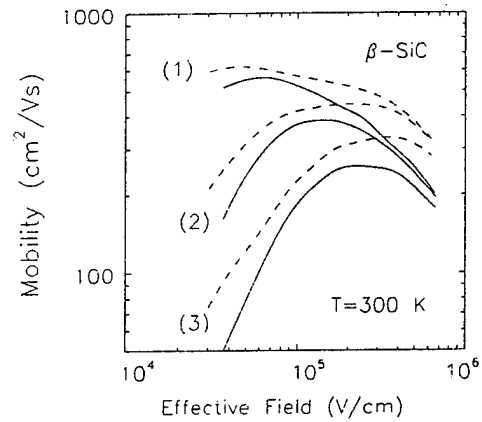
Figure 2
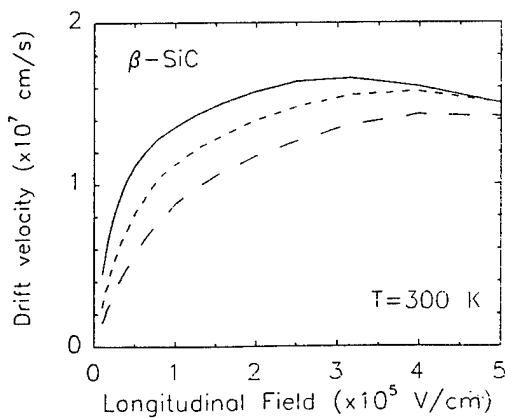
Figure 3
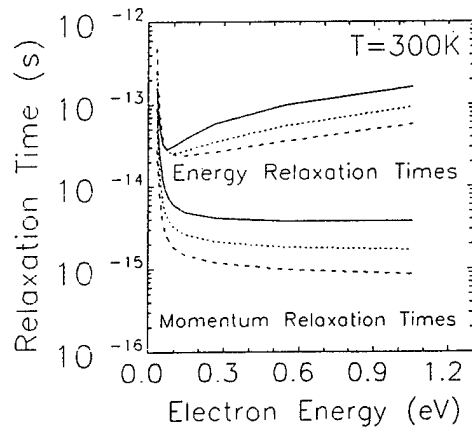
Figure 4

Title: A closed-loop evaluation and validation of a method for determining the dependence of the electron mobility on the longitudinal-electric field in MOSFETs.

Authors: J.B.Roldán, F.Gámiz and J.A.López-Villanueva.
Address: Departamento de Electrónica y Tecnología de Computadores. Universidad de Granada. Facultad de Ciencias. Avd.Fuentenueva s/n. <u>18071 GRANADA (SPAIN)</u>
Fax: 34-58-243230   **Phone number:** 34-58-246145   **E-mail:** paco@gcd.ugr.es

ABSTRACT:
We have developed a new iterative method to accurately determine the electron mobility in the channel of a submicron MOSFET. To do so, we have made use of a 2D drift-diffusion simulator including inversion layer quantization. Firstly, we calculated the low-field mobility and we employed this mobility curve to extract the dependence of the mobility on the longitudinal field. We compared many experimental I-V curves of a submicron MOSFETs to the curves obtained by our simulator within a self-consistent and iterative algorithm. The results are shown in Figure 1. The mobility data obtained were used to reproduce the experimental I-V curves (Figure 2). The mobility versus longitudinal-electric field curves were fitted using Equation 1 to estimate the values of the saturation velocity (v_{SAT}) and β parameters. Figure 3 and 4 show the velocity versus longitudinal field curves obtained using our method and the curves corresponding to Equation 1 for different values of v_{SAT} and β parameters. The best fit was given by $v_{SAT}=1.1 \times 10^7$ cm/s and $\beta=1$.

$$v(E_{|}, E_{\perp}) = \frac{\mu_0(E_{\perp}) E_{|}}{\left(1 + \left(\frac{\mu_0(E_{\perp}) \times E_{|}}{v_{sat}}\right)^{\beta}\right)^{\frac{1}{\beta}}} \qquad (1)$$
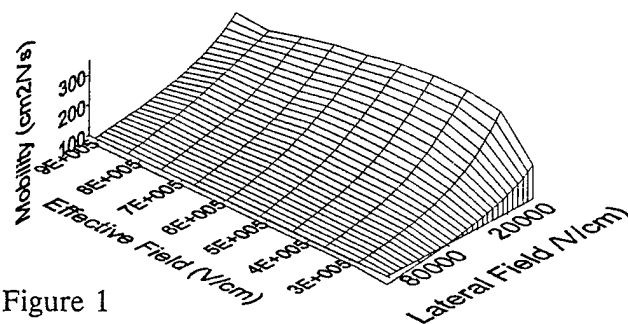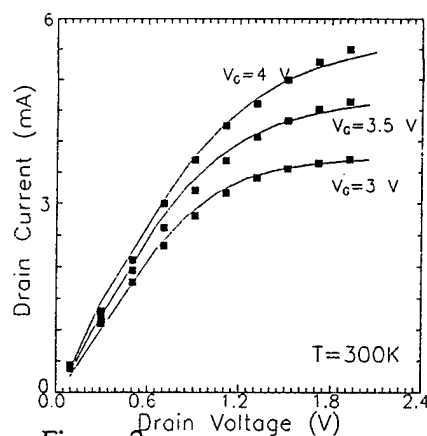
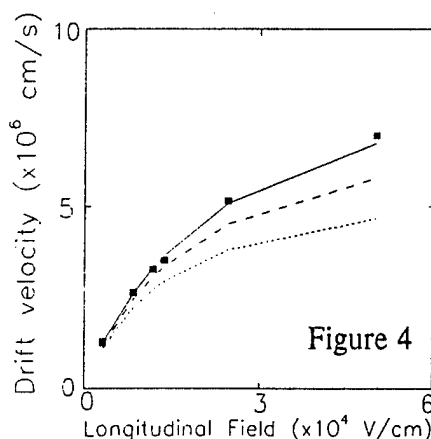Figure 1

Figure 2
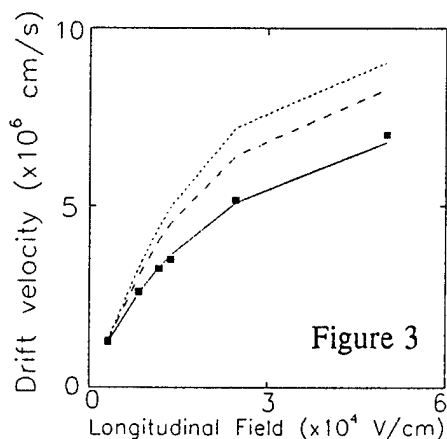
Figure 3

Figure 4

QUANTUM DISTRIBUTION-FUNCTION TRANSPORT EQUATIONS IN NON-NORMAL SYSTEMS AND IN ULTRA-FAST DYNAMICS OF OPTICALLY-EXCITED SEMICONDUCTORS

F. A. Buot

Naval Research Laboratory, Washington, D.C. 20375-5320

Tel. (202)767-2644; FAX (202)767-0546; email: buot@estd.nrl.navy.mil

Abstract: A major motivation for this work is the need to establish generalized quantum distribution-function (QDF) transport equations valid for non-normal, non-uniform, and non-stationary systems and optically-excited semiconductors that are free from approximations, as bases for computer simulations. To the authors knowledge, these have not been completely treated in the literature. This need becomes urgent with advances in material science, ultra-fast laser probes, nanofabrication, and the development of more powerful energy beams. The economic drive to produce faster devices and systems which are functionally more dense and have wider bandwidth will undoubtedly lead to the continued downsizing and tailoring of the nanostructures with different materials: insulators, semiconductors, metals, and superconductors. The derivation of the exact quantum distribution-function transport equations combines the Liouvillian super-Green's function technique and the lattice Weyl-Wigner formulation of the quantum theory of solids. A fully self-consistent generating super-functional is constructed which allows a purely 'algebraic' and straightforward application of quantum field-theoretical techniques in real time.

The derivation has extended previous results to non-normal systems: Bose superfluids, superconductors, and dense electron-hole liquids. Coupled quantum-transport equations, condensate, and pair-wavefunction 'effective-Schrodinger' equations are derived. For normal systems, these reduce to results given through the Keldysh time-contour technique. A self-consistent dynamical treatment of nonequilibrium and highly-coupled excitations in optically-excited semiconductors is given. Exact quantum distribution-function transport equations are given for phonons, plasmons, and photons. By transforming the Bethe-Salpeter equation into a multi-time evolution equation, QDF transport equations are obtained for electron-hole pairs and excitons. The virtue of quantum transport equations cast in phase space is that it allows the application of 'device-inflow' subsidiary boundary conditions for simulating femtosecond device-switching phenomena. These results provide the proper theoretical framework for the analyses of femtosecond-time scale dynamics in optoelectronics and quantum-confined nanometric systems under intense switching electromagnetic fields.

APPLICABILITY OF THE HIGH FIELD MODEL:
A PRELIMINARY NUMERICAL STUDY

Carlo Cercignani, Politecnico di Milano, Milano, Italy
Irene M. Gamba, Courant Institute, New York University, New York, NY 10012
Joseph Jerome[1], Department of Mathematics, Northwestern University, Evanston, IL 60208
Chi-Wang Shu[2], Division of Applied Mathematics, Brown University, Providence, RI 02912

In a companion presentation, we have discussed the theory of a mesoscopic/macroscopic model, which can be viewed as an augmented drift-diffusion model. Here, we describe how that model is used. The device we consider for this presentation is the one dimensional GaAs n^+-n-n^+ structure of length $0.8\mu m$. First, a full hydrodynamic (HD) model, proven reliable when compared with Monte Carlo simulations, is used to simulate the device via the ENO finite difference method (see [1]). As applied to the full device, the new model is outperformed by traditional drift-diffusion (DD). Indeed, when we plot the quantity $\eta = \mu_0 E / \frac{kT_0}{m}$, where μ_0 is the mobility constant and $E = -\Phi'$ is the electric field, we can see that the high field assumption $\eta > 1$ is satisfied only in the interval $[0.2, 0.5]$. When we run both the DD model and the new high field model in this restricted interval, with boundary conditions of concentration n and potential Φ provided by the HD results, we can clearly see that the new model outperforms the DD model, Figure 1. This indicates that the high field and DD models should be used only in parts of the device, connected by a transition kinetic regime. This will be a domain decomposition issue involving interface conditions and adequate numerical methods.
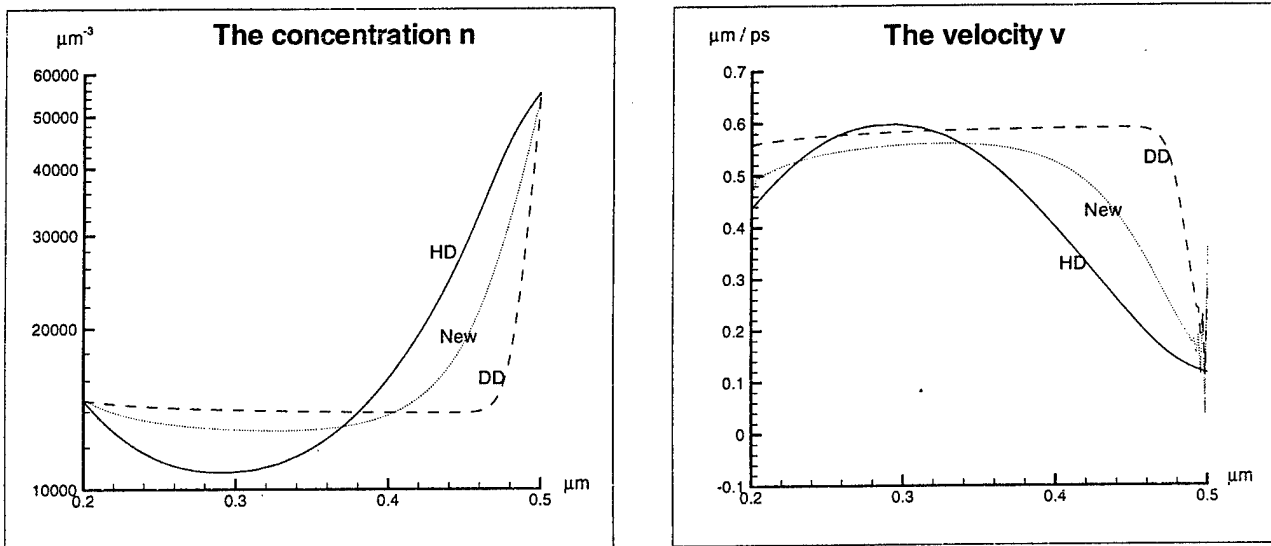

Fig. 1: The comparison of the drift-diffusion (DD) model (dashed line), the new high field model (dotted line), and the hydrodynamic (HD) model (solid line), in the sub-interval [0.2, 0.5] using the HD results as boundary conditions. Left: concentration n; right: velocity v.

REFERENCES:

[1] J.W. Jerome and C.-W. Shu, *Energy models for one-carrier transport in semiconductor devices*, in IMA Volumes in Mathematics and Its Applications, v59, W. Coughran, J. Cole, P. Lloyd and J. White, eds., Springer-Verlag, 1994, pp.185–207.

---

[1]Corresponding author: (847) 491 5575/ (847) 491 8906 (Fax)/jwj@math.nwu.edu
[2]Presenting author

Simulation of Bistable Laser Diodes with Inhomogeneous Excitation

Gang Fang and Ting-wei Tang

Department of Electrical and Computer Engineering
University of Massachusetts, Amherst, MA 01003, USA

In recent years, bistable Laser Diodes (BSLDs) have attracted much attention because of their potential applications in optical switching and wavelength conversion. The simulation of BSLDs involves large-signal analysis, which currently existing LD simulators (such as CLADISS [1]) cannot perform. Most studies of BSLDs are conducted using a set of rate equations that are expressed as a function of time only [2]. Such an approach has two main limitations. First, an approximation of distributed loss is required. Second, the spatial dependence of the gain saturation inside the cavity is not taken into account. Due to the highly nonuniform geometry of these devices, a few works have incorporated a spatial dependence into their models [3], but only the static behavior of BSLDs is studied. Most existing models use a single variable to represent the total photon density without considering the difference in wavelength. As a result, they are not suitable for studying the laser behavior under optical triggering where the wavelength of the optical input may not be close to that of the lasing light. Moreover, these models often do not include all pertinent physical processes which compete with each other to influence the dynamic characteristics of the device. Therefore a more sophisticated simulator is needed to assist the design as well as the understanding of the physics of BSLDs.

In this work, a comprehensive time-dependent one-dimensional (1-D) computer model is developed for the simulation of multi-section bistable laser diodes. Longitudinal spatial hole-burning, nonlinear gain, carrier-induced refractive index change (frequency chirp), and thermal effects are rigorously accounted for. Traveling-wave rate equations are solved for each longitudinal mode and the optical input. Special boundary conditions are introduced to handle the phase change. A reduced drift-diffusion equation is solved for the carrier density in the active region along the longitudinal direction. The gain model used is a function of wavelength, carrier density, photon density, and lattice temperature, which can be calibrated using experimental data or theoretical calculation. Previous space discretization scheme [4] has been improved for the matrix linear solver. A second-order implicit TR-BDF2 scheme [5] is adopted for time integration and is found to be very efficient.

To illustrate the capability of the simulator, a two-electrode Fabry-Perot cavity InGaAsP/InP laser diode incorporating an absorber region (Fig.1) is simulated. The static and dynamic characteristics of the device are investigated thoroughly. Special attention is paid to the all-optical set-reset operation by undershoot switching (Fig.2) where the BSLD is switched on by an optical pulse and switched off by an even higher optical pulse. It is found that both the height and shape (rise/fall time) of the optical input pulse affect the undershoot switching (Fig.3). The wavelength of the optical input also plays an important role (Fig.4).

References

[1] P. Vankwikelberge, G. Morthier, and R. Baets, *IEEE J. Quantum Electron.*, vol. 26, pp. 1728–1741, 1990
[2] H. Kawaguchi, *Optical and Quantum Electron.*, vol. 19, pp. S1–S36, 1987
[3] M.C. Perkins, R.F. Ormondroyd, and T.E. Rozzi, *IEE Proc. J*, vol. 133, pp. 283–292, 1986
[4] Y.L. Wong, and J.E. Carroll, *Solid-State Electron.*, vol. 30, pp. 13–19, 1987
[5] B.E. Bank, W.M. Coughan, W. Fichtner, E.H. Grosse, D.J. Rose, and R.K. Smith, *IEEE Trans. on CAD/ICAS*, vol. CAD-4, pp. 436–451, 1985
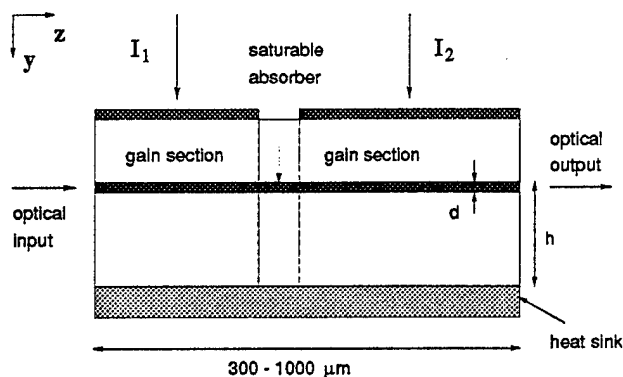
Figure 1: Longitudinal structure of a three-section laser diode
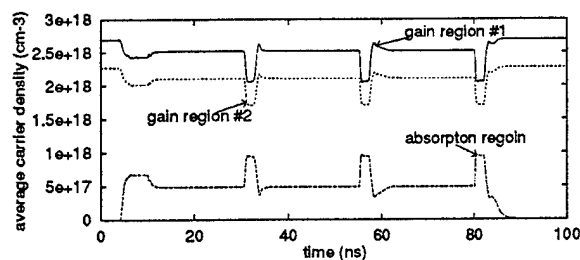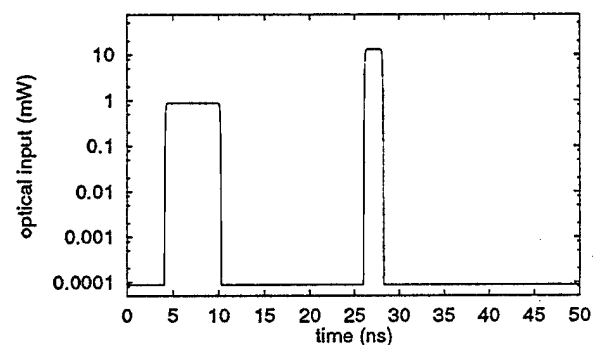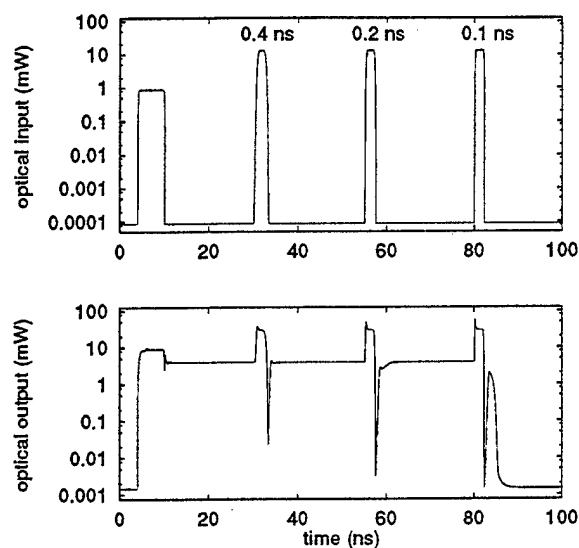

Figure 3: Examples of the set-reset operation : the effects of pulse shape on undershooting for $W_{in} = 13.12mW$, $\lambda_{in} = 1557.6nm$.
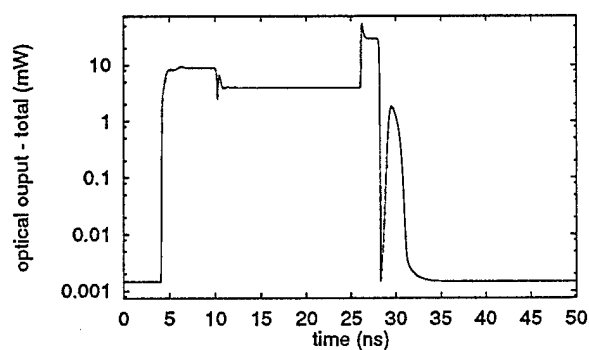

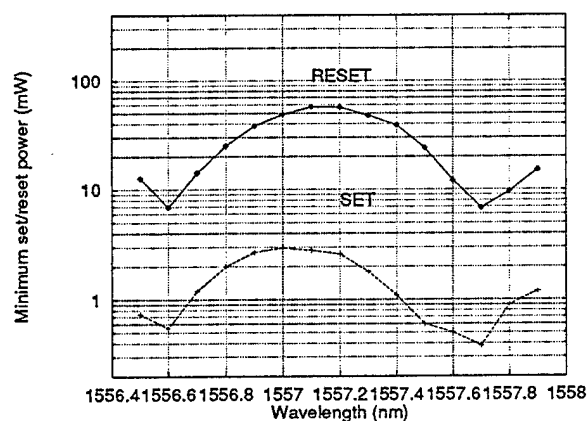Figure 2: The set-reset operation (undershoot shooting): optical input and optical output.

Figure 4: Influence of the wavelength of the optical signals on the set-reset operation

Intersubband Relaxation in Step Quantum Well Structures

J. P. Sun[†], H. B. Teng, G. I. Haddad
Solid State Electronics Laboratory
Department of Electrical Engineering and Computer Science
The University of Michigan, Ann Arbor, Michigan, 48109-2122

Michael A. Stroscio, G. J. Iafrate
U. S. Army Research Office
P. O. Box 12211
Research Triangle Park, North Carolina, 27709-2211

Abstract

Intersubband relaxation due to electron interactions with the localized phonon modes plays an important role for population inversion in quantum well laser structures designed for intersubband lasers operating at mid-infrared to submillimeter wavelengths. In this work, intersubband relaxation rates between subbands in step quantum well structures are evaluated numerically using Fermi's golden rule, in which the localized phonon modes including the asymmetric interface modes, symmetric interface modes, and confined phonon modes and the electron-phonon interaction Hamiltonians are derived based on the macroscopic dielectric continuum model, whereas the electron wave functions are obtained by solving the Schrödinger equation for the heterostructures under investigation. The sum rule for the relationship between the form factors of the various localized phonon modes and the bulk phonon modes is examined and verified for these structures. The intersubband relaxation rates due to electron scattering by the asymmetric interface phonons, symmetric interface phonons, and confined phonons are calculated and compared with the relaxation rates calculated using the bulk phonon modes and the Fröhlich interaction Hamiltonian for step quantum well structures with subband separations of 36 meV and 50 meV, corresponding to the bulk longitudinal optical phonon energy and interface phonon energy, respectively. Our results show that for preferential electron relaxation in intersubband laser structures, the effects of the localized phonon modes especially the interface phonon modes must be included for optimal design of these structures.

[†] Corresponding author:
Address: Dr. J. P. Sun
        EECS Department
        The University of Michigan
        Ann Arbor, MI 48109-2122

Phone: (313) 763-5489
Fax: (313) 647-1781
Email: jpsapo@engin.umich.edu

Symplectic finite-element time-domain method for optical field analysis

T. Hirono*, W. Lui, and K. Yokoyama

NTT Opto-electronics Laboratories
3-1, Morinosato Wakamiya, Atsugi-shi, Kanagawa, 243-01, Japan.
*) Facsimile: +81 462 40 2859, E-mail: tuhirono@aecl.ntt.co.jp

The symplectic finite-element time-domain method is applied to optical field analysis for the first time. This method accurately simulates wave propagation along a waveguide in 2- and 3-dimension.

Symplectic integrators for Hamiltonian systems preserve the symplectic structure of the phase space and conserve the volume in the phase space (Liouville's theorem). The integrators are expected to be suitable for long-term integration with high accuracy and their usefulness has been verified in the area of mechanics [1], especially in celestial mechanics [2].

We applied the 2nd order integrator to the optical field analysis. In our formulation, the Hamiltonian of the field, H, is

$$H = \int \{\frac{\pi^2}{2\varepsilon} + \frac{(\nabla \times A)^2}{2\mu}\} dxdydz \qquad (1)$$

where ε is the permittivity, μ is the permeability, A is the vector potential, and $-\pi$ is the electric displacement. (A, π) are the canonical variables. We use the gauge, in which the scalar potential is 0. The Hamiltonian is discretized by means of the finite element method.

Fig. 1 shows the example of full vectorial 3-dimentional simulation. The qualitative features of the wave-propagation are well simulated by this method.

[References]
[1] J. M. Sanz-Serna and M. P. Calvo, Numerical Hamiltonian Problems. London: Chapman & Hall, 1994.   [2] H. Yoshida,:   Celest. Mech., 56   pp. 27-43 (1993).
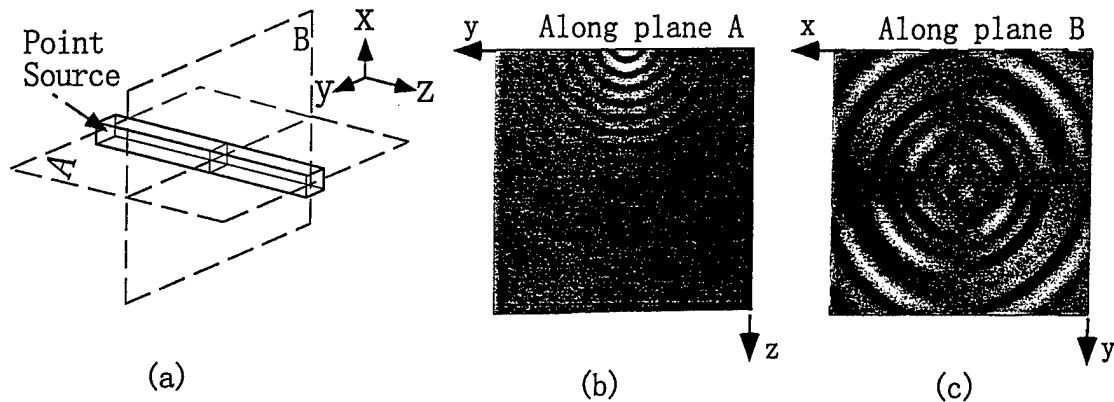

Fig. 1. (a) Schematic drawing of the simulated structure. The rectangular prism is a waveguide of which the permittivity is 10% larger than the environment. The wave, whose vector potential is polarized in the x-direction,   radiates from the point source. The space lattice is cubic and its spacing is one tenth of the wavelength. The time increment is one twentyth of the wave-period. (b) The amplitude of the x component of the vector potential in the y-z plane [i.e. plane A]. (c) The amplitude (x 200) of the y component of the vector potential in the x-y plane [i.e. plane B].

Resonances in Conductance through Tunable Attractors

Yong S. Joe, Tian Xie, and Ronald M. Cosby[1]
Department of Physics and Astronomy
Ball State University
Muncie, IN 47306 USA

Recent advances in nanometer-scale fabrication of GaAs heterostructures make it possible to study electron transport properties in various nanostructure devices. Current state-of-the-art techniques result in surface-independent probes or contacts that may be biased to introduce tunable scattering potentials in quantum nanosystems[2].

In this paper, we study the resonant conductance peaks of a quantum narrow channel containing a *finite-size* attractive impurity, called an *attractor*. By modulating the strength of the attractive impurity, it is possible for a single finite-size attractive impurity to produce a sequence of quasi-bound-states in the channel, and these states give rise to multiple resonant peaks *before* the first plateau in the conductance. We investigate the characteristics of these resonant peaks by introducing mode coupling and mean lifetime, which can be determined by the width of the tunneling peak. The effects of potential well strength, size, and location in the channel on the resonance peaks are discussed. Finally, we report the effects of resonant tunneling through multi-coupled attractors in series in a quantum nanosystem.

The calculation of the transport properties for these system is performed[3] using a tight-binding recursive Green's function method for coupled transverse modes[4], and the multichannel Landauer formula, where different confinement and modulation potentials are easily incorporated.

Submitted by Yong S. Joe
Tel:(317) 285-8879, Fax:(317) 265-5674
email:ysjoe@bsu-cs.bsu.edu

A NEW METHOD TO OVERCOME THE DIVERGENT PROBLEM IN NUMERICAL MODELING OF POWER 6H-SiC DEVICES

Edward H. S. Hsing and Jeffery L. Gray
School of Electrical and Computer Engineering
Purdue University, West Lafayette, IN47906, USA
Mailing Address: 3001 Sierra Road, San Jose, CA95132, USA
TEL: (408)433-6683; FAX: (408)986-1486
email: hsing@lsil.com; grayj@ecn.purdue.edu

Power devices made of 6H-SiC have gained much attention due to their superior characteristics as compared with Si power devices. Even though numerous experimental data on 6H-SiC devices have been generated, data from numerical modeling are seldom available. Computer simulation based on analytic or numerical approach with restricted current boundary condition had been tried to avoid numerical problem in convergence. Three reasons cause this difficulty. The first two, which are also common in Si power devices, are high bias operation and large device structure with significant dimensional difference among regions. The third one, which exists particularly in large energy bandgap material, i.e., 6H-SiC, is low intrinsic carrier concentration induced extremely huge carrier concentration change. This unique characteristic makes 6H-SiC power devices much more difficult to be simulated than Si power devices. Although smaller voltage step, denser mesh, and suitable value normalization can overcome part of the divergent problem, but more nodes and input steps means larger computer resource (CPU time and storage size) is needed for each case study. To overcome this trade-off, data recycling method is proposed and used in our device simulator, ADEPT, for power device simulation.

Data recycling method (DRM) is based on the idea that only extra node will be put to the place it is needed during calculation. Idea behind this method is very similar to the re-mesh pre-processing approach used in conventional simulators. Yet, re-mesh processing is only done once in the beginning of each case. It can not guarantee numerical convergence for all input conditions because it is based on the best guess from the initial trials. Should mesh assignment or voltage step is unsuitable, i.e., calculation is never converged after a certain number of iteration or floating point error happens, we have to redo everything and try different mesh and input assignment. In DRM, fewer nodes will be assigned first to try where more nodes are needed as bias increases. Calculated key variables (n, p, V, and T) will be stored and updated after each successful step. Node value where largest residual happens will be stored simultaneously. As iteration convergence is going to fail, stored data file will be modified automatically around problem area to include more nodes with values extracted from adjacent nodes. Program then starts again with modified data file as our initial guess and continue our incomplete work. This procedure can repeat itself until final goal achieved.

There are several advantages in this method. First, we do not have to assign many nodes, which may be way beyond requirement to do the job, in the beginning. Necessary nodes will be added to the critical location during calculation. This process can save significant computer resource in the early stage. Second, if calculation fails at some step, we do not have to restart simulation from the very beginning. It can save huge amount of CPU time if job is quite big. Third, with automatically failure detection and data correction by computer, non-stop calculation can be achieved. Basically, DRM performs like traditional re-mesh process, but it has higher efficiency and accuracy and more flexibility for different devices. This method can also be used for debugging issue based on generated intermediate data file. Should device characteristics not change a lot, we can use existent data for new simulation.

In our work, 6H-SiC p-i-n diodes with blocking capability larger than 1000V and UMOSFETs with breakdown voltage larger than 100V have been simulated by advanced device simulator, ADEPT, successfully. No restriction has to be applied to the samples for convergence concern. The ratio of number of node before and after DRM processing is ~4 for p-i-n diodes and ~8.5 for UMOSFETs. With models directly from experimental data, we can predict the behavior of different kinds of 6H-SiC power devices with high degree of accuracy.

Convergence Properties of the Bi-CGSTAB Method for the Solution of the 3D Poisson and 3D Electron Current Continuity Equations for Scaled Si MOSFETs

D. Vasileska, W. J. Gross, V. Kafedziski and D. K. Ferry

Center for Solid State Electronics Research
Arizona State University, Tempe, AZ 85287-6206, USA
tel: (602) 965-3452, fax: (602) 965-0000
e-mail: vasilesk@enws365.eas.asu.edu

We are studying the scaling of Si MOSFET's into the deep submicron regime (n-channel devices with 0.1 μm gate-length and 0.05-0.2 μm gate width, with both uniform and discrete dopant distribution in the channel). This requires high substrate doping levels which, in turn, lead to large potential and charge gradients. In this work, we investigate the convergence properties of a variant of the Conjugate Gradient Squared method (CGS), the so-called Bi-Conjugate Gradient Stabilized method (Bi-CGSTAB) [1]. While the solution of the three-dimensional (3D) Poisson equation for these devices is straightforward, the solution of the electron current continuity equation in the conventional 3D drift-diffusion simulators is nontrivial due to both the non-symmetry and poor conditioning of the coefficient matrix. For example, for the devices that we study, we find that CGS method suggested by Selberher *et al.* [2] for the solution of the electron current continuity equation leads to rather irregular convergence behavior and that the rounding errors result in severe cancellation effects in the solution. On the other hand, the Bi-CGSTAB method did not suffer from the above negative effects since it avoids the squaring of the residual polynomial.

The convergence properties of the Bi-CGSTAB method were compared to those obtained for the ILU method based on approximate (incomplete) decomposition of the original matrix into an LU product [3]. A variant of the ILU method (Stone's Strongly Implicit Procedure [4]) was also implemented for the solution of the Poisson equation. For both equations, we find that the Bi-CGSTAB method showed relatively smooth and superior convergence behavior when compared to the ILU methods. The use of the ILU(0) preconditioner in the Bi-CGSTAB method reduced the number of iterations by at least a factor of 2.

These results are demonstrated with simulations of the width dependence of the threshold voltage V_{th} in the subthreshold region for our MOSFETs. We find that V_{th} does not scale linearly with device width. An average shift of the threshold voltage of approximately 10 mV towards lower values is also observed when using a discrete impurity distribution in the active region of the device. The latter result is believed to be associated with the inhomogeneity of the channel potential barrier and is in agreement with the results reported by Wong and Taur [5].

[1] H. A. Van der Vorst, SIAM J. Sci. Stat. Comput. **13**, 631 (1992).
[2] S. Selberherr, M. Stiftinger, O. Heinreichsberger and K. P. Traar, Comp. Phys. Comm. **67**, 145 (1991).
[3] G. V. Gadiyak and M. S. Obrecht, in Simulation of Semiconductor Devices and Processes: Proceedings of the Second International Conference, Ed. by. K. Board and D. R. J. Owen (Pineridge Press, Swansea UK, 1986) 147.
[4] H. L. Stone, SIAM J. Numer. Anal. **5**, 530 (1968).
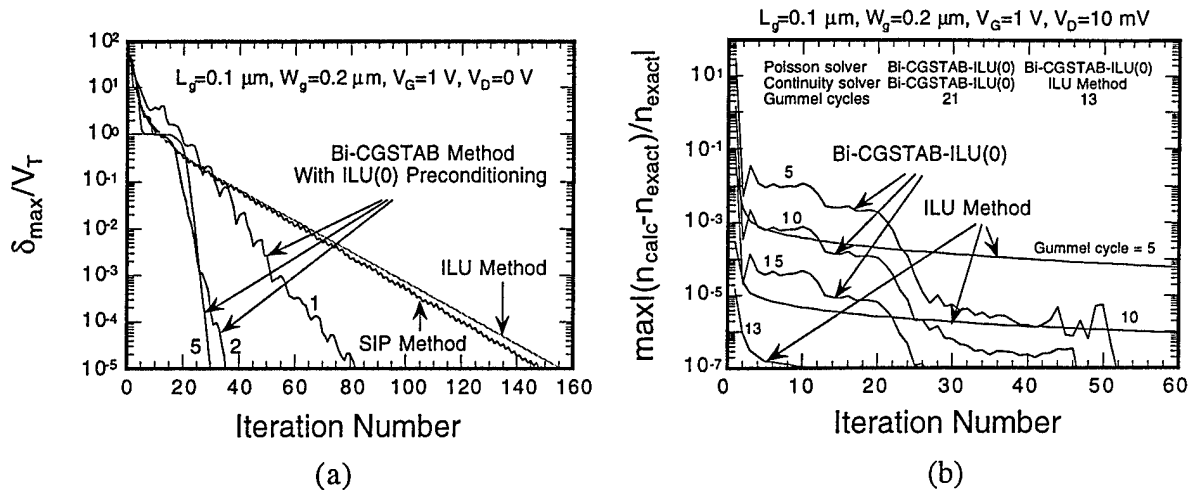[5] H.-S. Wong and Y. Taur, in IEDM Tech. Dig., 705 (1993).

(a)

(b)

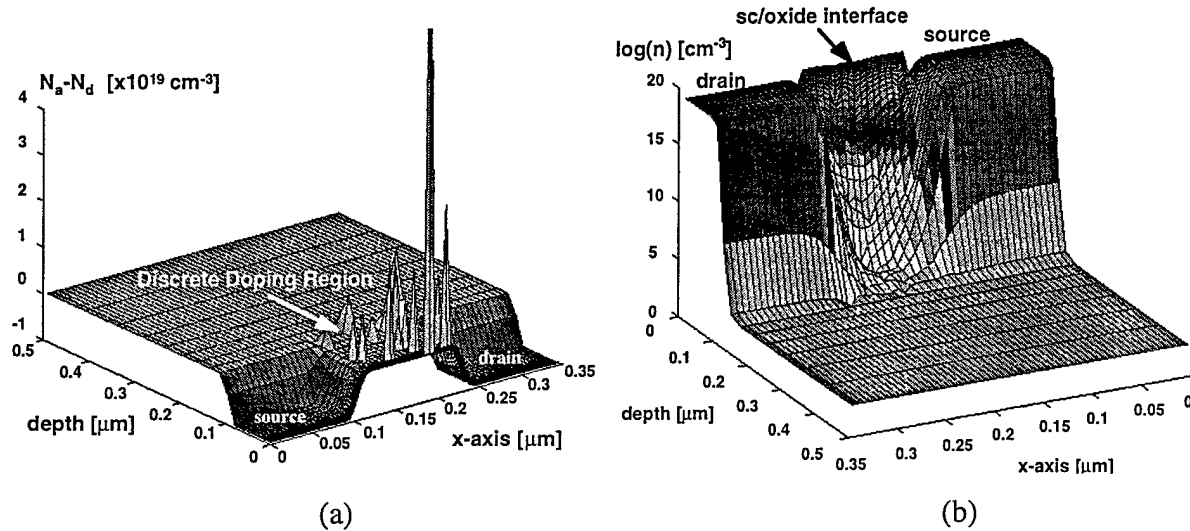Fig. 1 Convergence curves for the (a) 3D-Poisson and (b) electron current continuity equations.

(a)

(b)

Fig.2 Discrete impurity distribution under the gate (a) and calculated electron density (b) for a device with $N_a = 5 \times 10^{17}$ cm^{-3}, $t_{ox} = 3$ nm, $V_G = 0.7$ V and $V_D = 10$ mV.
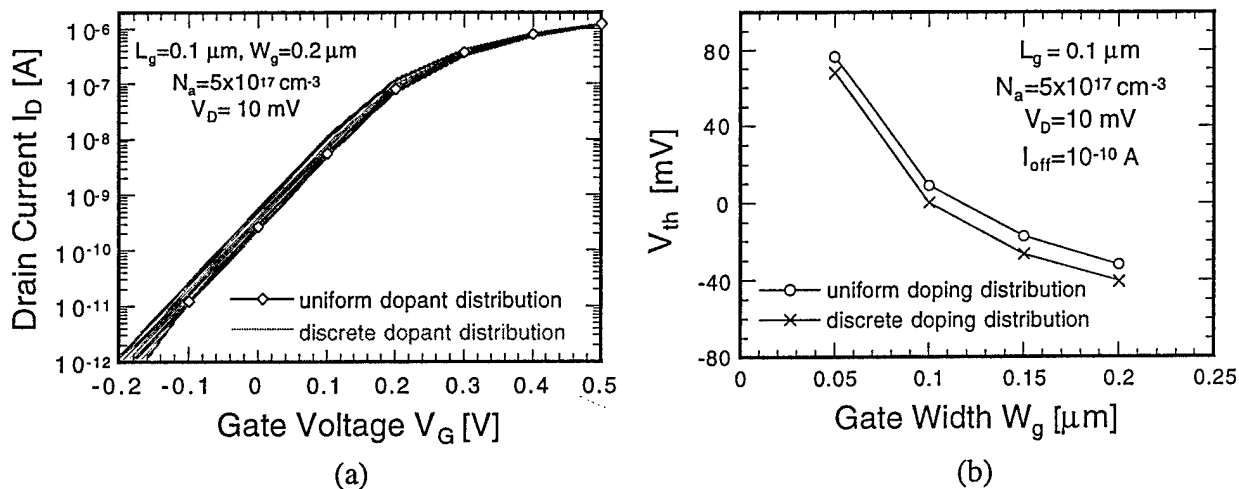

(a)

(b)

Fig.3 (a) $I_D - V_G$ characteristics for devices with uniform and discrete dopant distribution under the gate. (b) Width dependence of the threshold voltage for subthreshold conduction.

Wave-function Scarring Effects in Open Ballistic Quantum Cavities

R. Akis and D. K. Ferry[*]

Center for Solid State Electronics Research, and Center for Systems Science and Engineering,
Arizona State University, Tempe, AZ 85287-5706, USA

Numerical simulations have been carried out of the magneto-transport and corresponding wave-functions of two cavity structures whose classical counterparts are well known to be chaotic, the stadium and the Sinai billiard. In our method of calculation, the structures are enclosed in a waveguide and the Schrodinger equation is mapped onto a tight-binding lattice by replacing derivatives by finite differences. This yields a matrix equation that relates the wave-function on a slice with those from adjacent slices, which can then used to derive transfer matrices which allow us to translate across the entire structure. To overcome the numerical instabilities inherent in the transfer matrix approach, the problem is transformed [1] by using some clever matrix manipulations into a stable iterative procedure. Once the procedure is complete, one has the transmission coefficients that enter the Landauer formula to give the conductance and the wave-functions inside the cavities can be reconstructed by back substitution. In both structures studied, many of the resonance features in the transport appear to show **heavy scarring**, that is, the amplitude of the corresponding wave-functions are **highly** concentrated along underlying **periodic classical orbits**. For the stadium in particular, scars recur **periodically**, with periodicities in close correspondence to peaks in the power spectrum of the fluctuations. This leads to the conclusion that it is the corresponding periodic orbits, which are few in number, that dominate the transport. The power spectra we obtain are in good agreement with those obtained experimentally by Marcus *et al.* [2] for stadium structures. We find that the quantum nature of the input and output leads as well as their relative positions is crucial in exciting the particular orbits that are reflected in the scarred wave-functions.
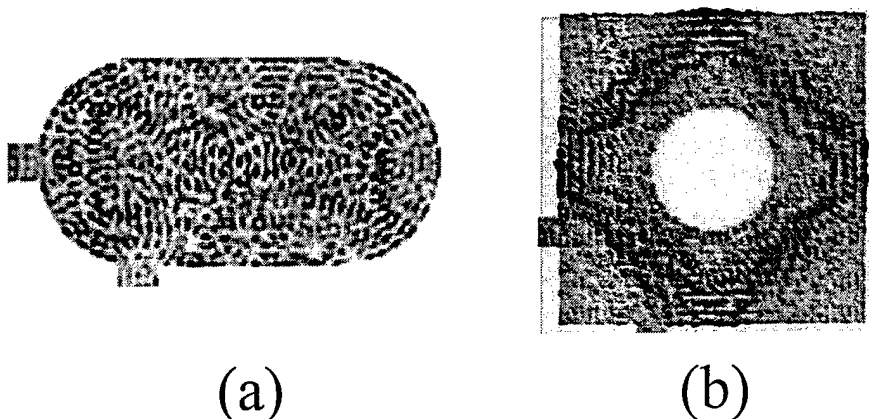
[1] T. Usuki, M. Saito, M. Takatsu, R. A. Keil, and N. Yokoyama, Phys. Rev. B, **52**, 8244 (1995).
[2] C.M. Marcus, A.J. Rimberg, R.M. Westervelt, P.F. Hopkins and A.C. Gossard, Phys. Rev. Lett. **69**, 506 (1992).

[*] mailing address as above, phone: 602-965-2570, fax: 602-965-8058, email: ferry@frodo.eas.asu.edu

Supporting Material

(a)   (b)

Figure: Two examples of wave-function scarring inside quantum cavities. The amplitude of the wave-function is plotted with darker shading indicating higher amplitude. (a) a "bow-tie" scar inside an open stadium shaped cavity. (b) a diamond scar inside a Sinai billiard structure, which consists of a square quantum dot with an anti-dot at the center. In both cases, the amplitude is enhanced along a path that a classical particle could take inside the structure. These paths can be classified as periodic orbits as they clearly retrace themselves. The closed, classical equivalents of these structures are known to be chaotic, which implies a situation where the number of periodic orbits is of measure zero in comparison to the numbers of non-retracing, phase space filling trajectories. For this reason, the somewhat surprising appearance of scarring features such as those shown here have generated much interest in the literature.

Complete RF analysis of compound FETs based on transient Monte Carlo simulation

S.Babiker, A. Asenov*, N. Cameron, S. P. Beaumont and J.R. Barker
Nanoelectronics Research Centre
Department of Electronics and Electrical Engineering
Glasgow University, Glasgow G12 8LT, Scotland, UK
*Tel: ++44 141 330 5233, Fax: ++44 141 330 4907, E-mail: A. Asenov@elec.gla.ac.uk

The remarkable RF performance of compound semiconductor FETs such as GaAs MESFETs and InGaAs HEMTs with channel length down to 0.1 μ is due to well pronounced velocity overshoot. The use of simulation for predictive analysis and design of such devices require in many cases the employment of full scale Ensemble Monte Carlo (EMC) technique. However most of the published EMC studies of compound FETs consider simplified device geometry and focus mainly on the transport physics and the effect of the enhanced channel velocity on the DC device characteristics. Far more important for the proper design of modern short channel compound FETs is the RF performance which is determined not only by the high field transport but also by the device geometry and the surface effects. The T- or Γ-shaped gate, the gate recess and the passivation in such devices critically affect the device parasitics and the overall RF device performance. Unfortunately very few EMC papers address RF performance issues.
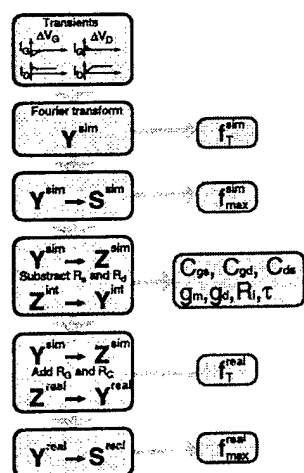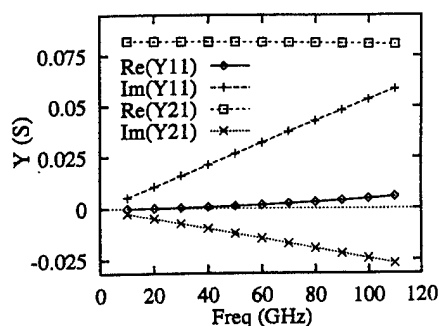

Fig. 1. Flow chart of the complete RF EMC analysis

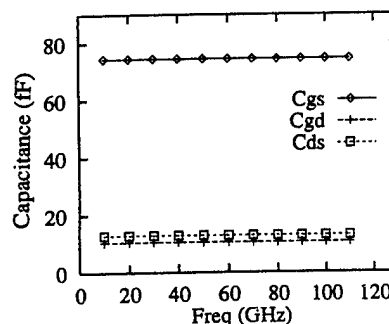Fig. 2 Y parameters extracted from EMC simulation of a 0.12 μm pHEMT. V_g=-0.2V, V_d=1.5V

Fig. 3 Capacitive components of the extracted small signal equivalent circuit. V_g=-0.2V, V_d=1.5V

In this paper for first time we describe a complete methodology to extract the RF performance of 'real' compound FETs from time domain EMC simulation which can be used for practical device design (Fig. 1). The methodology is based on transient finite element EMC simulation of realistic device geometries carried out with the Monte Carlo module of the Heterojunction compound 2d Finite element simulator H2F[1]. The extraction of the terminal current is based on the Ramo-Shockley theorem and employs all particles present in the simulated device. This allows stable extraction of the complex two port Y parameters (Fig.2). The proper description of the gate, contacts and recess shape provide reliable values for the small signal circuit components (Fig.3). The inclusion of the contact and the gate resistance, and eventually the inductive components associated with the contact pads, by post-processing the extracted y-parameters allows for realistic estimation of the RF performance of the devices under investigation. The small signal circuit component and RF performance figures of merit such as f_T and fmax extracted using MC simulation are in good agreement with those measured on real devices fabricated at the Glasgow Nanoelectronics Research Centre.

[1] S. Babiker, A. Asenov, J.R. Barker, and S. P. Beaumont, "Finite element Monte Carlo simulation of recess gate compound FETs", *Solid State Electronics*, Vol. 39, , pp. 629-635, 1996.

Monte Carlo calibrated drift-diffusion simulation of short channel HFETs

A. Asenov[*], S. Babiker, S. P. Beaumont and J.R. Barker
Nanoelectronics Research Centre
Department of Electronics and Electrical Engineering
Glasgow University, Glasgow G12 8LT, Scotland, UK
[*]Tel: ++44 141 330 5233, Fax: ++44 141 330 4907, E-mail: A. Asenov@elec.gla.ac.uk

Commercial device simulators like MEDICI are flexible, fast and work in a user friendly environment. Employing finite elements they can describe accurately the complex geometry of modern short gate heterojunction FETs (HFETs). Interface charge, surface states, and deep levels can be included in the simulation and the self heating can be treated through coupling to the heat flow equation. The transient algorithms are stable and allow for large time steps. Frequency domain analysis is also available. External circuit elements like contact and gate resistances, pad inductances and capacitances can be attached to the electrodes and hence included in the RF analysis. Unfortunately the local drift-diffusion (DD) approach, which is at the heart of such simulators, cannot predict the spatial overshoot effects responsible for the high performance of many short channel HFETs. Simplified hydrodynamic options usually offered as an extension to the DD engine slow down the simulations and often have convergence and parameter identification problems. The Monte Carlo (MC) approach, usually implemented in in-house software, is still computationally expensive and cannot match all the features of the commercial simulators, particularly their speed.
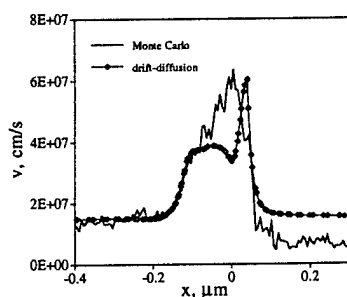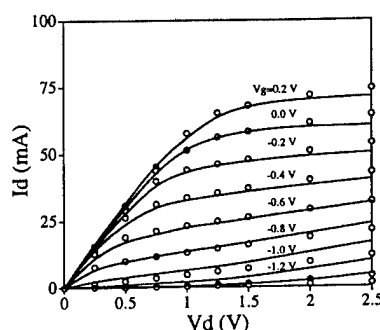

Fig. 1. Average velocity in the channel of 0.12 μ pHEMT

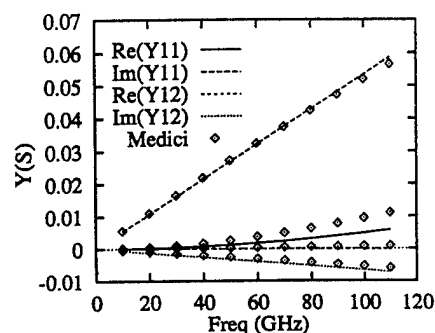Fig. 2 measured and DD simulated Id-Vd characteristics ($v_s = 2.8 \times 10^7$ cm/s)

Fig. 3 Y parameters extracted from MC and DD simulation

In this paper we describe a simple approach to the use of MC calibrated DD simulation in the design and optimisation of short channel HFETs. Our approach is based on the observation that in short channel 0.1 - 0.2 μ HFETs (e.g. pHEMTs) the velocity overshoot extends almost uniformly along the whole high field channel region. Thus the velocity profile obtained from MC simulation can be satisfactory emulated by increasing the saturation velocity v_s in a velocity saturation model used in DD simulations. This is illustrated in Fig. 1 for a 0.12 μ pHEMT with 22 nm gate-to-channel separation. The velocity profile from DD simulation with v_s forced to 2.8×10^7 cm/s is in good agreement with the MC result in the source region and in the channel. In the drain region, where most of the particles in the MC simulation are in the L-valley, the DD simulation overestimate the velocity but this hardly affects the RF device performance. Not surprisingly drift diffusion simulations incorporating enhanced saturation velocity and with contact resistances properly included are a good match to the measured dc output characteristics of the above pHEMT (Fig.2). The complex two port Y parameters extracted from time domain MC and DD simulation are also in good agreement (Fig.3). The calibrated DD simulation can be used confidently to investigate the design changes which do not affect the field profile in the channel but are important for the RF device performance including the gate and contact shapes, self-aligning, the cap layer, and the recess design etc. The small signal parameters f_T and f_{max} extracted from MC and DD simulation are also in good agreement. Examples of self aligned gamma-gate HFET technology DD simulation will be provided.

P14

RF performance of Si/SiGe MODFETs: A simulation study

S.Roy, A. Asenov[*], S. Babiker, J.R. Barker, and S. P. Beaumont
Nanoelectronics Research Centre
Department of Electronics and Electrical Engineering
Glasgow University, Glasgow G12 8LT, Scotland, UK
[*]Tel: ++44 141 330 5233, Fax: ++44 141 330 4907, E-mail: A. Asenov@elec.gla.ac.uk

Recent theoretical and experimental studies show that low field mobility and velocity overshoot are enhanced in Si layers grown pseudomorphically on relaxed SiGe substrates. The strain removes the six-fold degeneracy of the Si conduction band, resulting in an improved conduction band offset with higher in plane effective mobility and low in-plane effective masses for two of the valleys - and reduced inter valley scattering. Modulation doped field effect transistors (MODFETs) based on this material system have been demonstrated, and show significant potential for RF applications. The compatibility between SiGe and conventional Si technology makes such MODFETs attractive for Si MMICs design and microwave signal processing applications integrated on conventional Si chips.
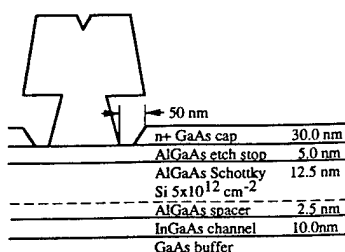

Fig. 1(a) Vertical layer struct-
ure of a 0.12 μm pHEMT

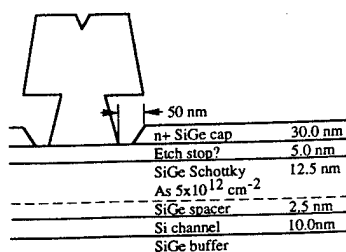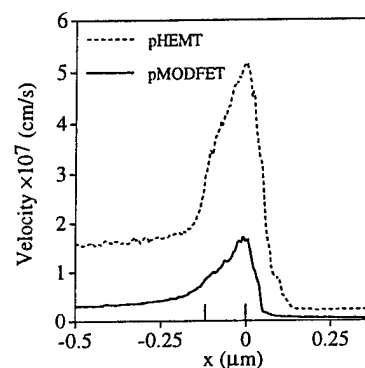Fig. 1(b) Vertical layer struct-
ure of a 0.12 μm pMODFET

Fig. 3 Comparison between average velocity in the channel of a 0.12 μm pHEMT and pMODFET. Vd=1.5V, Vg=0V.

A Monte Carlo simulation based RF analysis is used to study the microwave performance potential of Si/SiGe pseudomorphic MODFETs in comparison with state of the art InGaAs channel pseudomorphic HEMTs. To allow a fair comparison we consider similar layer structures (Fig.1 a,b) while realising that in the Si/SiGe case this may pose some unresolved growth problems. Both devices have δ-doping separated by a 2.5 nm spacer from the channel, a T shape recess gate with 50 nm recess offset and heavily doped cap layers. An effective δ-doping of 5×10^{12} cm^{-3} is considered in the both cases. The gate-to-channel separation is 22nm and the gate length is 0.12μm. This corresponds to the dimensions of real pHEMT fabricated at the Glasgow Nanoelectronics Research Centre and used for validation and calibration of the RC MC analysis technique (described in an accompanying paper). The average velocity in the channel of the both devices is compared in Fig. 3 for a drain voltage of 1.5 V and gate voltage of 0.0 V. Peak velocity in the pMODFET, at the drain end of the strained Si channel, is approximately a third of that in the pHEMT. The extracted small signal equivalent circuit parameters, cut off frequency f_T and maximum oscillation frequency f_{max}, as well as the minimum intrinsic noise figures for the two simulated devices, will be compared. The effect of contact and gate resistances on 'real' device performance will be studied. The possible performance enhancements associated with the realisation of self-aligned gamma-gate technology in the case of Si/SiGe MODFETs will be also investigated.

[1] S.Babiker, A. Asenov[*], N. Cameron, S. P. Beaumont and J.R. Barker, "Complete RF analysis of compound FETs based on transient Monte Carlo simulation", submitted for IWCE'97.

Ab-initio Coulomb scattering in atomistic device simulation

C. R. Arokianathan*, J. H. Davies and A. Asenov
Device Modelling Group
Department of Electronics and Electrical Engineering
University of Glasgow, Glasgow G12 8QQ, Scotland, UK
*Tel: ++44 141 330 4792, Fax: ++44 141 330 6010, E-mail: clint@elec.gla.ac.uk

As devices shrink to dimensions of order 0.1 μm, their properties begin to differ from their larger counterparts as the atomistic nature of their constituent charges begins to exert its influence. The simulation of such devices requires a full-scale 3D treatment, including the individual impurities and carriers. This presents a severe computational load, both for Poisson's equation and because the equation of motion must be integrated through a complex potential landscape (Fig. 1). The rapid variation of the potential in space may create difficulties with mesh-based calculations.

We have studied several methods for the solution of Poisson's equation and the integration of the equation of motion to evaluate their efficiency and accuracy. For Poisson's equation we compared a mesh-based solution with an near-exact potential based on Ewald summation [1]. The equation of motion was integrated either with a high-order adaptive Runge-Kutta scheme, which included the impurities alone, or using Brownian dynamics [2] with a low-order Euler method, which also includes phonons.

These methods were tested by calculating the mobility of electrons in a slab with randomly distributed impurities. The results are summarized in Fig. 2 and compared with the Conwell-Weisskopf formula. Phonon scattering was added using Mattheisen's rule where necessary. We conclude that the simpler mesh-based solution of Poisson's equation does not introduce significant errors, and reproduces well the expected mobility as a function of doping. The Brownian method is tolerant of errors introduced during integration of the equation of motion, because it tends to restore the system to equilibrium.

The Brownian method on a mesh was implemented in a simple simulation of an 80 nm dual-gate MESFET. Fig. 3 shows that the results of this atomistic simulation agree well with drift-diffusion results from MEDICI, at low source-drain voltage.
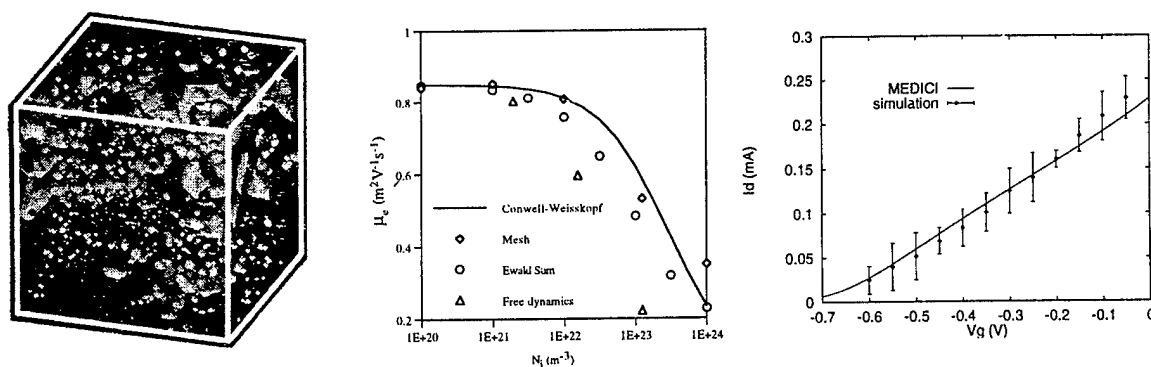

Fig 1. Random potential in a uniformly doped slab.

Fig 2. Mobility as a function of doping concentration

Fig 3. Transfer characteristic of a 80 nm dual-gate MESFET.

1. D. J. Adams and G. Dubey, *J. Comp. Phys.* **72**, 156 (1987).
2. C. Arokianathan, A. Asenov and J. H. Davies, *J. Appl. Phys.* **80** 226 (1996).

A New Approach for Obtaining Self-Consistent Solutions to the Coupled Schrödinger and Poisson System in Multiquantum Well Structures

Fred Gelbard and Kevin J. Malloy
Center for High Technology Materials and
Department of Electrical and Computer Engineering
EECE Building, Room 125
University of New Mexico
Albuquerque, New Mexico 87131-6081
(505) 277-1445
(505) 277-6433 (fax)
malloy@chtm.eece.unm.edu

Numerous numerical solution algorithms have been reported for solving Schrödinger's Equation. Some of these approaches have been extended to obtaining self-consistent solutions by coupling the Schrödinger solver to a Poisson solver. A common method of iteration is to employ these solvers successively. Thus, beginning with an assumed initial potential profile, Schrödinger's Equation is solved. Then using this solution to determine the charge distribution, a new potential profile is computed by solving Poisson's Equation. This process of successively solving Schrödinger's and Poisson's Equation is repeated in the hope that convergence will be obtained. As attractive as this approach may be, for many multiquantum well structures convergence is a problem, particularly for nonzero space charge or electric fields. Therefore, a relaxation method approach was developed and will be presented.

In this work, convergence problems for self-consistent solutions are the primary focus. The limitations of successive substitution algorithms and a previously reported relaxation algorithm are analyzed and compared to our proposed relaxation algorithm. Error norms for the eigenvalues, eigenvectors and potential profile are presented for one-dimensional structures.

Numerical Evaluation of Iterative Schemes for Drift-Diffusion Simulation

M.B. Patil[†], U. Ravaioli and T. Kerkhoven

Beckman Institute, University of Illinois at Urbana-Champaign, Urbana, Illinois, 61801
[†]on leave from Indian Institute of Technology, Kanpur, India

Abstract

A major problem for the development of drift-diffusion solvers for 3-D applications is the difficulty in adapting existing 2-D schemes. The traditional approaches based on Newton iteration [1] are in general too expensive because of the size of the matrices involved. It is therefore important to develop effective iterative procedures for practical 3-D applications [2].

We introduce an iterative scheme to solve the drift-diffusion device simulation problem, which combines the Gummel iteration with the "pointwise iteration", and then we compare its convergence behavior with other iteration strategies, for different test cases. Besides the traditional Gummel scheme [1], we have implemented also a multigrid iteration as discussed in [3,4].

In Gummel's method the equations are solved in a decoupled manner: Poisson's equation is solved at all grid points, followed by electron and hole continuity equations. This procedure is repeated until convergence is obtained. The coupling between grid points, arising from discretization, is maintained in Gummel's scheme while solving each equation separately, whereas the three equations are somewhat loosely coupled through the updated values of potential and carrier densities. In practice, the Gummel method is found to be efficient if the coupling between the equations is weak; otherwise, the convergence is unacceptably slow.

In the "pointwise iteration", the three equations are solved simultaneously at a given grid point treating the variables at adjacent grid points as constants. Thus, the coupling between the equations is maintained at each grid point, whereas the grid points are coupled to each other only loosely through the update of values at the neighbors. This approach is therefore complementary to Gummel's scheme. The pointwise iteration does not need a large matrix to be stored as the equations are solved simultaneously at one point each time; this makes the iteration very attractive from the memory point of view. This iteration has been used as the smoothing procedure in nonlinear multigrid solution of the device equations [3]. Also, in the Alternate Block Factorization [5] and ILU/Knot [6] methods, the idea of coupling the three equations at each grid point has been used, although not explicitly as an iteration.

The combined "Gummel-Pointwise" iteration simply consists of the following steps: (a) perform one Gummel iteration, (b) perform M times the pointwise iteration. We use in our experiments values of M between 1 and 25. A larger value of M improves the result of the Pointwise iteration but obviously makes step (b) computationally more expensive. The combined iteration significantly improves the convergence properties of the simple Gummel approach in all cases. In terms of required CPU time, we find that the combined iteration is faster for some 2-D examples, and that it becomes more and more advantageous as the size of the problem grows, because the cost of the pointwise iteration varies only linearly with the number of grid points. Therefore, the proposed "Gummel-Pointwise" iteration becomes very attractive for 3D simulation, as illustrated by examples. We also found that the nonlinear multigrid scheme that we implemented is generally not as effective as the combined iteration. The "Gummel-Pointwise" is in addition much simpler to implement than a multigrid scheme.

1. S. Selberherr, *Analysis and Simulation of Semiconductor Devices*, New York: Springer-Verlag, 1984.
2. G. Heiser, C. Pommerell, and W. Fichtner, "Three-dimensional semiconductor device simulation," *IEEE Trans. Computer-Aided Design*, vol. 10, no. 10, pp. 1218-1230, 1991.
3. R. Constapel and M. Berger, "A multigrid approach for device simulation using local linearization," in *Proc. NASECODE 6 Conf.*, pp. 355-359, 1989.
4. J. Molenaar and P. W. Hemker, "A multigrid approach for the solution of the 2D semiconductor equations," *Impact of Computing in Science and Engineering*, vol. 2, pp. 219-243, 1990.
5. R. E. Bank, T. F. Chan, W. M. Coughran, Jr., and R. K. Smith, "The alternate-block factorization procedure for systems of partial differential equations," *BIT*, vol. 29, pp. 938-954, 1989.
6. C. S. Rafferty, M. R. Pinto, and R. W. Dutton, "Iterative methods in semiconductor device simulation," *IEEE Trans. Electron Devices*, vol. 32, no. 10, pp. 2018-2027, 1985.

Corresponding Author:
Umberto Ravaioli, 3255 Beckman Institute, 405 N. Mathews Avenue, Urbana, IL 61801
FAX: (217) 244-4333 - e-mail: ravaioli@uiuc.edu

Simulation of Si-MOSFETs with the Mutation Operator Monte Carlo method and evolutionary optimization

J. Jakumeit

II. Phys. Inst., Universität Köln, Zülpicher Str. 77, 50937 Köln, Germany

A. Duncan, U. Ravaioli, K. Hess

Beckman Institute, University of Illinois, Urbana, IL 61801, USA

In the last two years we have developed a new approach to study gate and substrate currents in Si-MOSFETs, which is based on a mixture of evolutionary optimization algorithms (EA) [1] and a new type of Monte Carlo (MC) technique, the Mutation Operator Monte Carlo method (MOMC) [2]. The goal is to develop an algorithm for the investigation of hot electron effects in Si-MOSFETs, which is less complex and computational expensive than a full band Monte Carlo program (FBMC), yet gives more precise information than "lucky electron" or "electron temperature" models and can thus be used as a mediator between precise theory and experimental results.

The first step of our approach is the MOMC, which calculates electron distributions by starting with an arbitrary distribution and changing this distribution by physical mutation until a stationary condition is reached. The physical mutation can be seen as a time step of a standard MC-simulation. The electron distributions along the 0.8 μm long channel of a Si-MOSFET was calculated by a one-dimensional MOMC. The electron density and potential distribution along the channel are necessary inputs, which can be calculated, for instance, by a drift-diffusion program. Based on this input the MOMC calculates electron distributions which are comparable to FBMC-results within minutes on a modern workstation. From the distributions, substrate and gate currents can be calculated, which are reasonably close to experimental results. Besides the computational efficiency, a further advantage of the MOMC compared to standard MC techniques is the good resolution of the high energy tail of the distribution without the necessity of any statistical enhancement.

In a second step the EA can be used for a further optimization of the MOMC-results in combination with measurement results. The EA searches for electron distributions, which fit a given substrate current, by means of random mutation, physical mutation and selection of distributions. Our results demonstrate that the EA is able to improve unrealistic parts of the distribution, which may originate from an oversimplified model in the physical mutation of the MOMC, or a slightly unrealistic electron density and potential along the channel as input. This feature of the EA allows one to use simplified but computationally efficient models for the physical mutation and for the calculation of the input data. The latter can be calculated by drift diffusion programs or even simple analytical models, which not always yield realistic electron densities and potentials along the channel.

[1] J. Jakumeit, Appl. Phys. Lett. **66**, 1995, p. 1812

[2] J. Jakumeit, U. Ravaioli, K. Hess, J. Appl. Phys. **80**, 1996, p. 5061.

Corresponding Author:
Umberto Ravaioli, 3255 Beckman Institute, 405 N. Mathews Avenue, Urbana, IL 61801
FAX: (217) 244-4333 - e-mail: ravaioli@uiuc.edu

A New HEMT Breakdown Model Incorporating Gate and Thermal Effects

Lutfi Albasha, Christopher M. Snowden and Roger D. Pollard
Microwave and Terahertz Technology Group
Department of Electronic and Electrical Engineering
University Of Leeds, Leeds, LS2 9JT, UK

Abstract

This paper presents for the first time a comprehensive physical model for the breakdown process in HEMTs. The model is integrated into in a fast quasi-two-dimensional physical simulation. The work is based on a full study of the complex interactions between the different breakdown mechanisms and the influence of design parameters. The model takes account of tunnelling effects in the region of the gate metallization.

Microwave circuits such as power amplifiers operate under large-signal conditions. Their ability to perform efficiently is limited by the device's breakdown characteristics which limit the transistor's performance and power output. Popular breakdown theories have not been adequate to independently explain the full picture of the breakdown process. Analytical models for avalanche breakdown were based on physical simulations of the active channel around the gate. The effects of the gate leakage and substrate conduction in HEMTs on this have not been addressed. This paper considers breakdown from a more comprehensive point of view. It has been observed that the pattern of the I_D-V_{DS} and V_{GS} characteristics has three distinctive regions with regard to breakdown. These can be divided into pre-pinch-off, pinch-off and post-pinch-off.

In contrast to MESFETs, spurious substrate current occurs in HEMT buffer layers due to the lateral E_x field component. This current is drawn around the depleted channel and reduces the magnitude of the field; this results in an increase in the breakdown voltage. The computational interpretation of the breakdown model presented in this paper is based on the interactions between the avalanche and gate leakage mechanisms. The relation that both processes simultaneously have with the device design parameters and power dissipation inside the device is incorporated into the model. An analytical model relates gate leakage to avalanche. The model is currently capable of explaining and simulating many of the behaviour patterns of the electrical characteristics of microwave devices under large-signals conditions at or prior to breakdown under the influence of varying bias voltages.

The model presented in this paper is based on the following numerical and physical assumptions: The gate leakage and tunnelling currents are based on a combination of the Padovani[1] and Rideout[2] equations. These equations involve complex functions of temperature, barrier height and semiconductor parameters. In order to maintain the numerical efficiency of the physical device simulator, new approximations are introduced for the first time in this paper which simplify the tunnelling functions and maintain the accuracy of the solution. The Thermionic, Thermionic-Field and Field gate currents are dependent on the lattice temperature and material specifications. The breakdown model presented in this paper also incorporates a thermal model which continuously computes the channel temperature and updates the gate leakage model.

The temperature of the channel, consequently, stimulates the appropriate gate current type. Figure 1 shows the effect of varying the temperature on the tunnelling current at various doping levels. An increase in the Thermionic-Field tunnelling current is observed with an increase in the doping concentration. The gate leakage, conventionally termed 'soft breakdown' is assumed in this model to always occur in devices prior to avalanche. The flow of electrons from the gate would then influence the impact ionization process. The extent of this effect is considered analytically.

[1] F.A. Padovani, R. Stratton,"Field and thermionic-field emission in schottky barriers,"*Solid-State Electronics*, Vol. 9, pp. 695-707, 1966
[2] C.R. Crowell, V.L. Ridout,"Normalised thermionic-field (T-F) emission in metal-semiconductor (schottky) barriers," *Solid-State Electronics*, Vol. 12, pp. 89-105, 1969
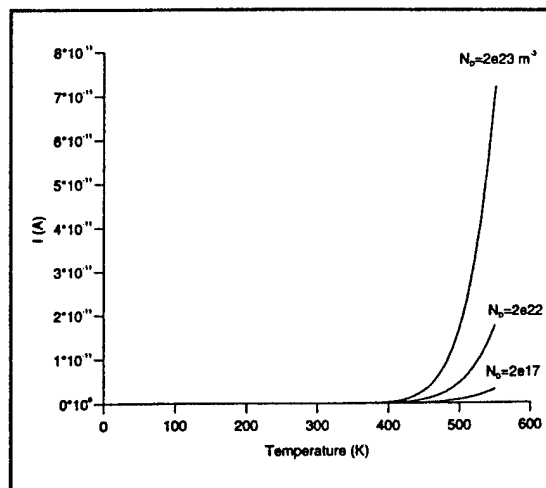
Figure 1 Tunnelling current Vs. channel temperature at various doping concentrations

Rate Equation Modelling of Nonlinear Dynamics in Directly Modulated Multiple Quantum Well Laser Diodes

S. Bennett, C.M. Snowden and S. Iezekiel

Department of Electronic and Electrical Engineering
University of Leeds
Leeds LS2 9JT
UK

Corresponding author: S. Iezekiel,
Phone +44 113 233 2000, Fax +44 113 233 2032, email: s.iezekiel@elec-eng.leeds.ac.uk

MQW laser diodes are widely used in many applications because of their superior performance characteristics over bulk laser diodes. These include higher modulation bandwidths and lower threshold currents, both of which are desirable for high speed optical links. Directly modulated laser diodes are operated under conditions that can lead to a wide variety of nonlinear responses, including intermodulation distortion, period doubling and chaotic behaviour. It is therefore vital to have an accurate model of nonlinear behaviour that is also numerically efficient, and for the most part rate equations are used by most workers. However, in contrast to a large volume of work using rate equations for nonlinear modelling of bulk structures, *little such work exists for MQW lasers*.

This paper presents a detailed theoretical (using rate equations) and experimental study of the nonlinear dynamics of both MQW Fabry-Perot and MQW distributed feedback laser diodes. In particular, the nonlinear dynamics of MQW FP and DFB laser diodes under single-tone and two-tone modulation have been investigated. In the FP MQW laser period doubling has been observed and in the DFB MQW laser both period doubling and tripling have been found. Period doubling was evident over a *wide range* of modulation frequencies in both lasers, and this is attributed to the large relaxation frequencies found in MQW laser diodes. Under two-tone modulation, it is noticed that nonlinear dynamics are enhanced and that chaotic behaviour is more widespread than for the single-tone case. In all cases, the computational results are compared to experimental data, and show good qualitative and quantitative agreement.

The paper concludes with a discussion of the applicability of rate equations to the nonlinear modelling of MQW laser diodes. The importance and relative influence of damping, the D and K factors and nonlinear gain suppression on such nonlinear behaviour as self pulsation and period doubling will be discussed. Particular emphasis will be placed on ease of use and application of rate equation models versus accuracy of predicted results.

Temperature Dependence of the Electron and Hole Scattering Mechanisms in Silicon Analysed through a Full-Band, Spherical-Harmonics Solution of the BTE

S. Reggiani, M. C. Vecchi and M. Rudan

Dipartimento di Elettronica, Università di Bologna, v. Risorgimento 2, 40136 Bologna, Italy
Corr. author: M. Rudan, Tel +39 (51) 64430-16, Fax 64430-73, e-mail: mrudan@deis.unibo.it

Abstract. By adopting the solution method for the BTE based on the spherical-harmonics expansion (SHE) [1], and using the full-band structure for both the electron and valence band of silicon [2], a number of scattering mechanisms have been investigated. In particular, the temperature dependence of such mechanisms has been modelled and implemented into the code (HARM) performing the SHE solution. Comparisons with the experimental mobility data show agreement over a wide range of temperatures. The analysis points out a number of factors from which the difficulties encountered in earlier investigations seemingly originate, particularly in the case of hole mobility.

The experiments show that the dependence of the electron mobility on temperature in intrinsic silicon differs from that of holes. In particular, at low temperatures ($T < 100$ K) it is $\mu_n \sim T^{-1.5}$, $\mu_p \sim T^{-2}$. On the other hand, at higher temperatures (up to 500 K) several investigators agree on that the mobility of both species of carriers is well described by a relation of the form $\mu_{n,p} = \mu_{max}(T/300)^\gamma$, with $2.2 < \gamma < 2.3$. The relative departure of the mobility laws in terms of the lattice temperature was initially ascribed to the different structure of the conduction and valence bands. However, after implementing the full-band structure in HARM, a quantitative agreement was found in a wide range of temperatures for the electron mobility only; on the contrary, the agreement of the hole mobility was acceptable at 300 K, whereas a difference of about 20% was found at 200 and 400 K.

Another effect whose temperature dependence proved relevant is the scattering with ionized impurities. To correctly describe such mechanism it is necessary to take the incomplete ionization into account, which becomes relevant when the total impurity concentration exceeds 10^{17} cm^{-3} and produces a significant lowering in the majority-carrier concentration with respect to that of the impurities. Incomplete ionization has been implemented into HARM, along with the description of the equilibrium carrier concentration in terms of Fermi statistics.

A final investigation is related to the phonon scattering, whose effect is modeled here following [3]. The values of the acoustical- and optical-phonon coupling constants were preliminarily fitted on the experimental data at 300 K. Then, a model for the temperature dependence of the acoustical-phonon coupling constant has been implemented into HARM and the values of its parameters have been derived from the experiments.

A number of runs have been carried out to test the model described above in a typical range of temperatures. The comparison with experimentally-fitted curves of electron and hole mobility reported by different investigators is shown in Figs. 1 and 2.

[1] A. Gnudi et al., Solid-State Electronics, **36**, 1993, p. 575.
[2] M. C. Vecchi et al., Proc. of the NUPAD V Conference, 1994.
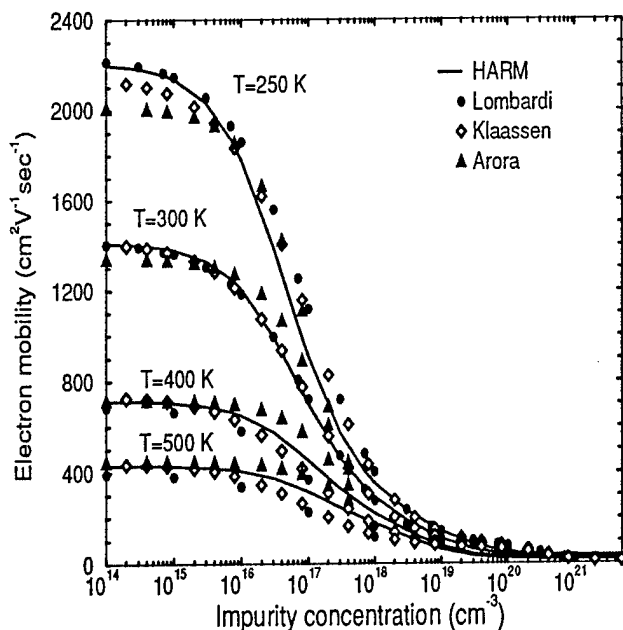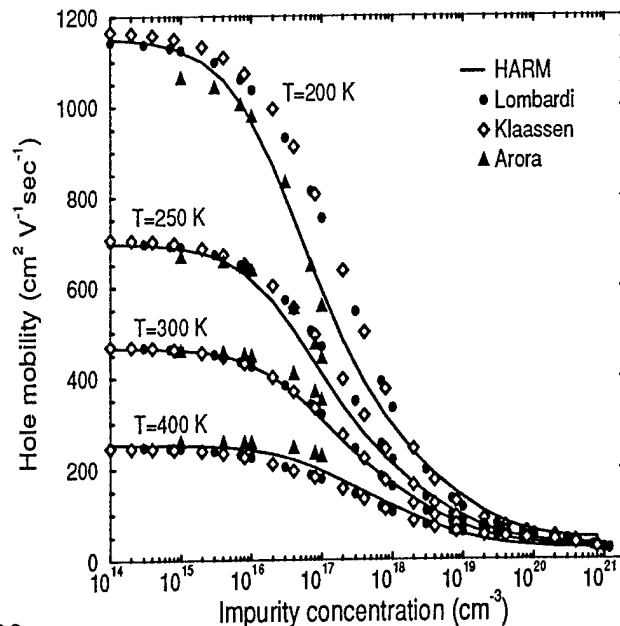[3] C. Jacoboni, L. Reggiani, Rev. of Modern Physics, **55**, 1983, p. 645.

Fig. 1

Fig. 2

Monte Carlo Simulations of Intersubband Hole Relaxation in a GaAs/AlAs Quantum Well

R W Kelsall

Microwave and Terahertz Technology Group
Department of Electronic and Electrical Engineering
University of Leeds
Leeds LS2 9JT, UK

Interest in intersubband transitions has been given new impetus by recent developments in "Quantum Cascade" or intersubband lasers for far-infra-red (FIR) operation[1]. Whilst the Quantum Cascade devices depend on electron intersubband transitions, p-type quantum well systems offer several advantages - high density of states, wide tunability and the possibility of normal incidence operation - and FIR emission has already been demonstrated in p-type germanium devices[2].

Design of FIR emitting devices requires detailed knowledge of the electronic bandstructure and transient carrier dynamics. The Monte Carlo method is an ideal simulation tool for these structures, since the time-dependent non-equilibrium carrier distribution function is intrinsically determined without recourse to any approximation, enabling accurate determination of intersubband lifetimes.

In this paper, an ensemble Monte Carlo code is used to simulate transient hole relaxation and energy loss phenomena in a GaAs/AlAs quantum well. The quantum confined valence bandstructure is calculated using an 8-band **k.p** scheme, to account for heavy-light hole mixing effects. The **k.p** wavefunctions are used to calculate hole-phonon scattering rates for the acoustic deformation potential, polar-optical, non-polar optical and piezoelectric interactions, via Fermi's Golden Rule. A total of 192 distinct intra- and inter-subband scattering processes are included in the simulation.

The k-space trajectories of up to 500,000 particles are simulated; cooling from a range of non-equilibrium carrier distributions is investigated. Transient de-population and re-population of the valence subbands is monitored, and the overall intersubband (phonon scattering) lifetimes evaluated. The transient hole energy loss rates are calculated, and resolved into components due to acoustic and optical phonon scattering. A crossover from optical to acoustic phonon dominated power loss is demonstrated, which is particularly clear when the initial distribution is mono-energetic.

The heavy-light hole mixing leads to severe distortion of the hole energy dispersion, resulting in off-zone-centre minima where the density of states has a mathematical (Van Hove) singularity. In practice, these singularities are removed by collision broadening, but strong scattering into these regions is still observed, which leads to "bottlenecks" in the hole cooling process.

Finally, possible FIR transitions and the conditions for laser operation are discussed.

1. J Faist, F Capasso, D L Sivco, C Sirtori, A L Hutchinson and A Y Cho *Science* **264** 553 (1994)
2. W Heiss et al *Semicond. Sci. Technol.* **5** SS638 (1994)

VLSI Yield Prediction Using a Pattern-Recognition Based Critical Area Algorithm

J H N Mattick, R W Kelsall and R E Miles

Microwave and Terahertz Technology Group
Department of Electronic and Electrical Engineering
University of Leeds
Leeds LS2 9JT, UK

Particle contamination remains one of the major causes of poor yield in VLSI circuits. Several yield predictions models have been suggested, and most are based on the concept of critical area (CA). The critical area of an integrated circuit represents the total area of all regions upon which, if a contaminant particle were to land, an electrical failure would result. Behind this simple definition lies considerable complexity. Firstly, the critical area is dependent on the exact particle size; and in any clean room a wide range of particle sizes are present in varying densities. Secondly, the critical area depends on which processing step is in progress during contamination: the mask layouts for diffusion, oxidation, and metallisation are all different, and thus failure will be caused by contamination in different regions of the chip. Thirdly, modern VLSI circuits are highly complex; accurate calculation of the critical area requires analysis of every feature on the chip. Whole-chip CA calculations have been performed using Monte Carlo techniques; however these require very long CPU times. In this paper, an alternative, pattern-recognition technique is presented, which combines accuracy with computational efficiency.

In the pattern recognition approach, the total wafer is divided into small regions each of which contain an identifiable mask feature: for Manhattan layouts, in which only $90°$ angles are used, all possible geometric features can be classified as one of 18 pre-defined patterns. For each pattern, an analytic formula for the associated critical area is obtained, as a function of pattern dimension and defect size. Formulae have been calculated for circular defects of arbitrary radius. The pattern recognition software converts a CAD system map of the layout into a list of pattern features. The critical area for each is calculated, and the chip CA given by the sum of all contributions. The software includes elimination of "double-counting" of CA contributions wherever a particle may overlap two or more adjacent features.

In this paper, the CA software is demonstrated for trial layout sections including CMOS multiplexers and shift registers. The CA calculations are based on analysis of the metallisation layout for susceptibility to short-circuit failures (which are typically an order of magnitude more probable than open circuit failures). In order to determine the overall short-circuit failure probability, CA calculations are performed for a whole range of defect sizes, and the results weighted according to the likely defect-size distribution in a clean room.

Bi-dimensional Simulation of the Simplified Hydrodynamic and Energy-Transport Models for Heterojunction Semiconductors Devices using Mixed Finite Elements

A. Marrocco [*]   Ph. Montarnal [†]

We study the application of the mixed finite elements method (MFE) for the simulation of the simplified hydrodynamic and energy-transport models. The two main points are firstly the use of entropic variables which gives a symmetric definite positive problem and secondly the coupled computation of the equations which requires a generalization of the MFE method for vector valued problems.

The drift-diffusion (DD) model, which is actually the most usual model in industrial simulation of electronic devices, is not sufficient for sub micrometer modeling. The two main contenders are the hydrodynamic and the energy transport models.

The mixed finite elements (MFE) method, which was first developed in the study of structural mechanics, is well adapted to these equations because it gives a exact conservation of the currents. For the DD equations this method was used by F. Brezzi, L.D. Marini and P. Pietra with the carrier concentration variables and by A. El Boukili, F. Hecht and A. Marrocco with the quasi-Fermi level variables. This last approach seems well adapted when considering heterojunctions. Indeed, the quasi-Fermi levels are continuous at the heterojunctions when densities are not.

We consider the stationary and bi-dimensional case and take a simplified hydrodynamic model or an energy transport model for the electrons coupled with a drift-diffusion model for the holes through the Poisson equation.
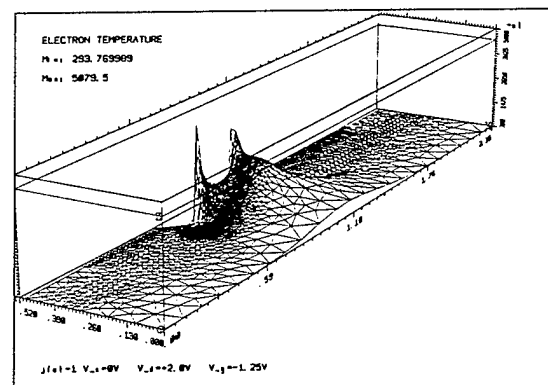
We express the problem in a conservative form. In order to obtain a symmetric positive definite system of elliptic equations, we introduce appropriate variables. We first use the electrostatic potential ϕ, the hole quasi-Fermi level φ_p, and for the electrons we introduce entropic variables v_1 and v_2 (functions of the electron quasi-Fermi levels φ_n and the electron temperature T_n) which lead to a particularly simple symmetrisation. We consider the usual "flow" variables like the electric displacement D, the hole current density J_p, the electron current density J_n and a "flow" function J_w which depends on J_n and on the thermal energy flow density S_n. Let us remark that we obtain a system of equations with the same mathematical properties as the DD model, the scalar equation for the electrons being replaced by a vector valued equation with unknowns v_1, v_2. The boundary conditions are non-homogeneous Dirichlet conditions on the contacts and homogeneous Neumann conditions on the interfaces.

We extend the numerical methods developed for the DD model at INRIA. The solution of the problem is obtained as the limit, when t goes to infinity, of a problem with artificial local time. We use block relaxation techniques as we consider sequentially the Poisson equation, the equation for the holes and the system of equations for the electrons. For each case "implicit-type" discretization for time and mixed finite elements for space are used.

For the computation of the two coupled equations for electrons , we extend the MFE method for a vector valued problem. We write the problem in his mixed-dual variational form. For the discretization we choose the Raviart-Thomas spaces of lowest order. We apply a Newton-Raphson algorithm to these non-linear discrete equations. Each Newton-Raphson step can easily be reduced to a linear problem involving only J_n and J_w as unknows (elimination of primal variables). The primal variables v_1 and v_2 are then recovered by explicit formula. Direct solver or GMRES algorithm with diagonal block pre-conditionning are used.

We have performed differents numericals tests: $n^+ - n - n^+$ diodes with homo and herero junctions, $p - n$ diode and a $GaAlAs$ JFET.

[*]INRIA, Projet M3N, B.P. 105, 78153 Le Chesnay Cedex, France, fax: 33 1 39 63 58 82, e_mail: americo.marrocco@inria.fr.

[†]INRIA, Projet M3N, fax: 33 1 39 63 58 82, e_mail: philippe.montarnal@inria.fr.

Semiconductor Device Noise Computation Based on the Deterministic Solution of the Poisson and Boltzmann Transport Equations

Alfredo J. Piazza and Can E. Korman

Department of Electrical Engineering and Computer Science

The George Washington University, Washington, DC 20052

Numerical simulation results of noise due to current fluctuations along an n^+ - n - n^+ diode are presented. The mathematical framework is based on the interpretation of the equations describing electron transport in the semiclassical transport model as stochastic differential equations (SDE). It was previously shown that the autocovariance funcion of current fluctuations can be obtained from the transient solution of the Boltzmann transport equation (BTE) with special initial conditions [1]. This aproach was succesfully employed for the computation of the noise spectral density in bulk silicon [2]. The results were in good agreement with those obtained using the Monte Carlo method. In this paper we build upon our previous development to compute the space dependent noise autocovariance function. In this case, the autocovariance function is obtained from the self-consistent transient solution of the Poisson and Boltzmann transport equations.

The solution method for the BTE is based on the Legendre polynomial method. The zero, first and second order Legendre polynomials are used, due to the particular form of the initial condition. The self-consistent solution of the Botzmann transport and Poisson equations is achieved by concurrently solving the corresponding discretized equations employing a Gummel-type iteration.

This paper describes the numerical algorithm, and presents results for the spectral density of current fluctuations along a device for different values of the applied potential. Noise due to acoustic and optical scattering and the effects of non-parabolicity are considered in the physical model.

[1] C. E. Korman and I. D. Mayergoyz, "Semiconductor noise in the framework of semiclassical transport," Phys. Rev. B 54, 24 (1996)

[2] A. J. Piazza and C. E. Korman, "Computation of the Spectral Density of Current Fluctuations in Bulk Silicon Based on the Solution of the Boltzmann Transport Equation," accepted for publication in *VLSI Design*

E-Mail: alfredo@seas.gwu.edu, FAX: (202) 994 0227.

Consistent Hydrodynamic and Monte-Carlo Simulation of SiGe HBTs Based on Table Models for the Relaxation Times

B. Neinhüs, S. Decker, P. Graf, F. M. Bufler, and B. Meinerzhagen

University of Bremen, Kufsteiner Strasse, Postfach 33 04 40, 28334 Bremen, Germany

Tel.: +49 421 218 4689, Fax.: +49 421 218 4434, E-mail: neinhus@item.uni-bremen.de

Among all SiGe device concepts SiGe-Heterojunction Bipolar Transistors (HBTs) have currently the highest potential for commercial applications. In order to support the design of SiGe-HBTs accurate and efficient device simulation tools are necessary. However, though even some of the commercially available simulators offer the capability of simulating heterojunction devices, reliable transport parameters for these devices are not available for most design tasks. The underlying reason for this dilemma is that the Ge content x is variable in SiGe devices which has added an additional dimension to the problem of determining transport parameters. For example, the relaxation times of a hydrodynamic (HD) model for SiGe HBTs $\tau(N, x, T_C, T_L)$ depend on four independent quantities instead of three namely the total doping density N, the Ge content x, the carrier temperature T_C and the lattice temperature T_L. Therefore the traditional approach of extracting transport parameters predominantly from experimental data that worked well for silicon for a long time is no longer feasible for SiGe devices, because reliable experimental data especially for strained SiGe are hardly available.

In order to overcome this problem the comprehensive and experimentally verified Monte–Carlo bulk transport model described in [2] was applied to generate transport parameters for the DD or HD device simulations at discrete mesh points of the 4D space spanned by N, x, T_C, T_L. To generate the smooth functions $\tau(N, x, T_C, T_L)$ that are needed for example for HD device simulations from the resulting table of transport data a flexible monotonicity preserving spline interpolation scheme has been developed. Compared to the traditional approach of using closed form analytic expressions with only few model parameters for $\tau(N, x, T_C, T_L)$ our spline approximation scheme has several advantages: For example it adapts itself automatically to model extensions like an extended range of N, x, T_C or T_L. Moreover it is easy to control the accuracy of the spline interpolation by just generating a denser table of transport data for the range of N, x, T_L, T_C, that is of highest interest.

In order to verify the validity of our modeling approach we have simulated the two–dimensional SiGe HBT structure shown in figure 1. The structure is very demanding for numerical device models because of its narrow base and piecewise constant profiles for N and x that give rise to abrupt junctions and steps in the valence and conduction band edges. Consequently this device is well suited for testing the modeling accuracy of classical device simulation in comparison to MONTE–CARLO device simulation. The structure has been simulated by three different models. The first model is the DD model. The second model is an extension of the Generalized HD Model reported in [3] to devices with position dependent band structure. Moreover the heat flux reduction that has been proven to be beneficial for ultra short MOSFETs [1] has been adopted. The third model is a newly developed MONTE–CARLO device model for SiGe hetero junction devices. Details of this MC model will be published elsewhere. Because all transport parameters of the DD and HD simulators have been derived from the SiGe MC bulk model and because the MC device model used exactly the same band structure and scattering models as the MC bulk simulator all three models are fully consistent under homogeneous material and field conditions. Moreover all three device models use exactly the same offsets for the valence and conduction band edges.

The results of the 2D simulations for $V_{BE} = 0.75$, $V_{CE} = 1V$ and 300K are summarized in figures 2-5 for the electric potential, the dynamic temperature, the drift velocity and the electron density. In all cases the results of the three models are shown along the vertical line at $y = 450$nm. It can be seen that at the base collector junction even in the MC model the drift velocity is more than a factor of two higher than the maximum drift velocity under homogeneous field conditions. Despite of this for Si–based devices extremely large velocity overshoot it can be clearly stated that the hydrodynamic results are in good agreement with the MC–results. Especially the electron density profile in the base and the space charge region, which is important for the transient behavior of the HBT, agrees well for the HD and the MC simulation. On the other hand the DD simulation deviates much more from the MC–reference which may lead to intolerable errors of the DD–model for agressively scaled SiGe HBTs in near future.

To our best knowledge the results reported in this paper represent the first 2D simulations of a SiGe HBT with fully consistent DD, HD and MC device models.

References

[1] BORK, I., JUNGEMANN, C., MEINERZHAGEN, B.,
    AND ENGL, W. L. Influence of heat flux on the
    accuracy of hydrodynamic models for ultrashort
    Si MOSFETs. In *NUPAD Tech. Dig.* (Honolulu,
    1994), vol. 5.

[2] BUFLER, F. M., GRAF, P., MEINERZHAGEN, B.,
    KIBBEL, H., AND FISCHER, G. A new comprehen-
    sive and experimentally verified electron transport
    model for strained SiGe. In *Proc. SISPAD* (Tokyo,
    1996), pp. 57-58.

[3] THOMA, R., EMUNDS, A., MEINERZHAGEN, B.,
    PEIFER, H. J., AND ENGL, W. L. Hydrodynamic
    equations for semiconductors with nonparabolic
    bandstructures. *IEEE Trans. Electron Devices ED-
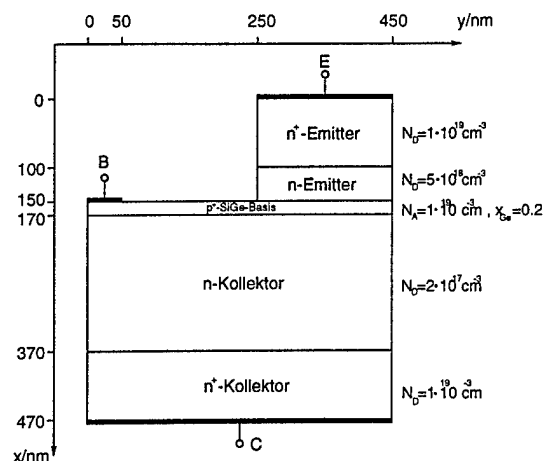   38* (1991), 1343-1352.
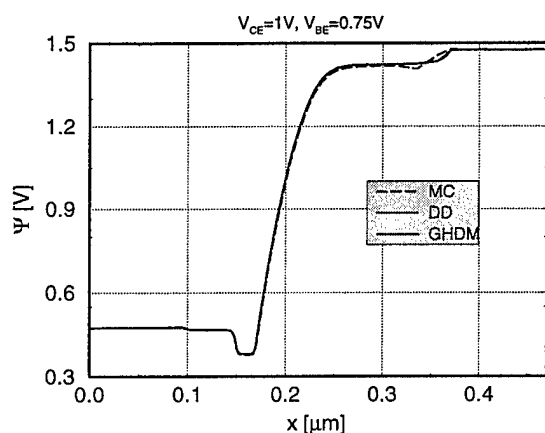
Figure 1: The 2D SiGe–HBT test structure

Figure 2: Comparison of the electrostatic potential profiles resulting from the DD, HD and MC models. All models are in good agreement.
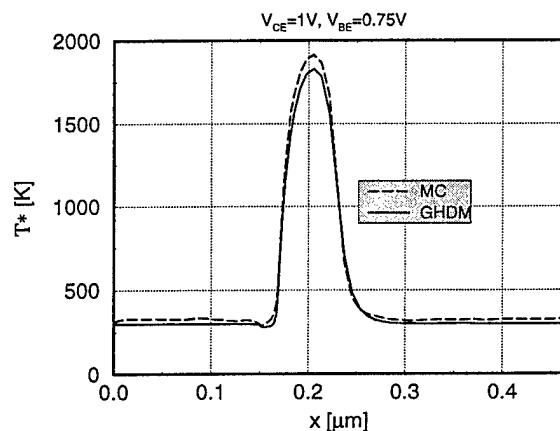
Figure 3: Comparison of the dynamic temperature profiles resulting from the HD and MC models. Both model are in good agreement.

Figure 4: Comparison of the electron densities resulting from the DD, HD and MC models. The HD and MC density distributions are in good agreement. The DD model deviates substantially.

Figure 5: Comparison of the drift velocity profiles resulting from the DD, HD and MC models. Please note the velocity overshoot which is extreme for Si-based devices.
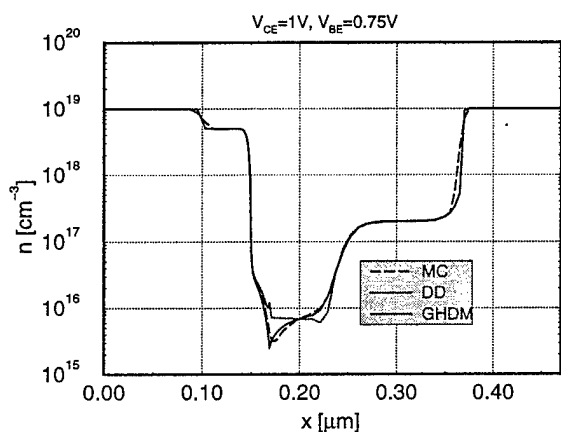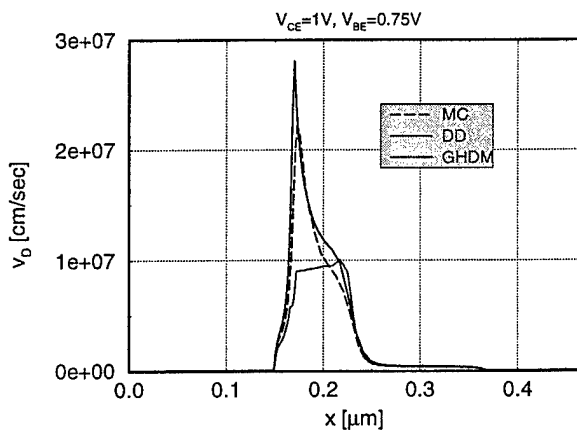
Additive Decomposition of the Drift-Diffusion Model

Elizabeth J. Brauer, Marek Turowski[*], James M. McDonough

University of Kentucky, 453 Anderson Hall, Lexington, KY 40506-0046, USA
Phone: (606) 257-4701, Fax: (606) 257-3092, Email: brauer@engr.uky.edu

This proposal describes a new numerical method for semiconductor device simulation. The numerical method, additive decomposition, has been successfully applied to Burgers' equation and the Navier-Stokes equations governing fluid flow by decomposing governing equations into large-scale and small-scale parts without averaging. The additive decomposition technique is well suited to problems with a large range of time and/or space scales, for example, thermal-electrical device simulation of power semiconductor devices with large physical size. Thermal-electrical effects have a large range of time scales since the electrical time constants are much faster than the thermal time constants. Furthermore, additive decomposition adds a level of parallelization for improved computational efficiency. Thus, semiconductor device simulation is a natural application of the additive decomposition numerical technique. Initially, we decompose the simplest device equations, the drift-diffusion model, to test the method.

Additive decomposition of the drift-diffusion model proceeds as follows. First, the basic variables: potential, electron density and hole density, are divided into large-scale and small-scale components:

$$\phi = \bar{\phi} + \phi^*, \qquad n = \bar{n} + n^*, \qquad p = \bar{p} + p^*. \tag{1}$$

The equations are decomposed into large-scale and small-scale equations:

$$\nabla^2 \bar{\phi} = \frac{q}{\varepsilon_s}\left(\bar{n} - \bar{p} - \bar{D} \right) \tag{2a}$$

$$\nabla^2 \phi^* = \frac{q}{\varepsilon_s}\left(n^* - p^* - D^* \right) \tag{2b}$$

$$\frac{\partial \bar{n}}{\partial t} = \nabla\left[D_n \nabla \bar{n} - \mu_n \bar{n} \nabla \bar{\phi} - \mu_n \cdot (1-\beta)\cdot\left(\bar{n}\nabla\phi^* + n^*\nabla\bar{\phi} \right) \right] - \bar{R} \tag{3a}$$

$$\frac{\partial n^*}{\partial t} = \nabla\left[D_n \nabla n^* - \mu_n n^* \nabla\phi^* - \mu_n \cdot \beta\cdot\left(\bar{n}\nabla\phi^* + n^*\nabla\bar{\phi} \right) \right] - R^* \tag{3b}$$

where (2a) is the large-scale Poisson's equation, (2b) is the small-scale Poisson's equation, (3a) is the large-scale current continuity equation for electrons, and (3b) is the small-scale current continuity equation for electrons. The decomposition of the current continuity equation for holes is similar to (3). The one large-scale equation is solved on the large-scale grid and the N small-scale equations are solved on the small-scale grid over a small section of the device centered around a large-scale grid point. There is a separate set of small-scale equations (for small-scale space or time points) for *each* large-scale grid point. Thus, the small-scale equations can be solved independently and in parallel. The large-scale solution ties up the total results over the whole simulation domain.

As a first approach, the new additive decomposition technique has been tested on the 1-D solution of the Poisson's equation inside the *p-i-n* diode for zero-current conditions, i.e., with zero or reverse bias. The distributions of ϕ, n, p have been calculated, and the space charge formation has been used as a measure of results quality. First, as a reference, a solution with the traditional method has been obtained, using a non-uniform grid with 40 points. Then, a large-scale solution has been computed on 9 grid points uniformly distributed. Small-scale results have been calculated in separate sections surrounding each large-scale point, including several small-scale grid points. After adding the large and small components, according to (1), the resulting space charge distribution was very close to the reference space charge distribution. The main advantage of the new method is that the matrix equations for sections with small-scale points can be solved independently, which allows for prospective parallel computations and smaller memory requirements.

---

[*] On leave from Dept. of Microelectronics and Computer Science, Technical University of Lodz, Poland.

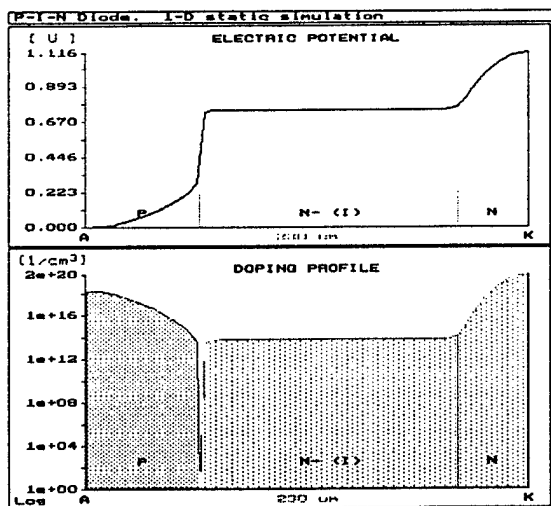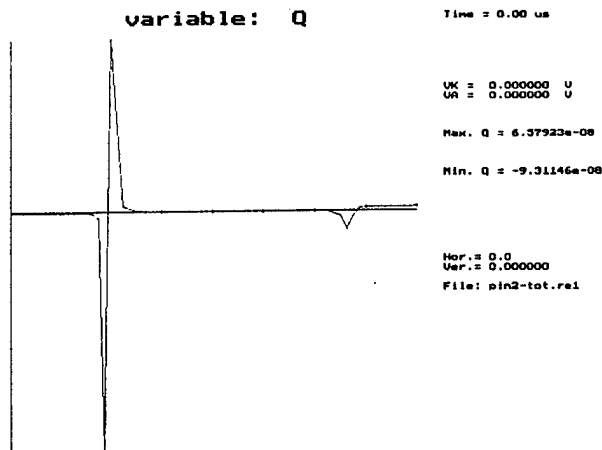Fig. 1. Potential distribution and doping profile of the *p-i-n* diode.

Fig. 2. Net charge calculated on non-uniform grid (40 points) using traditional method.
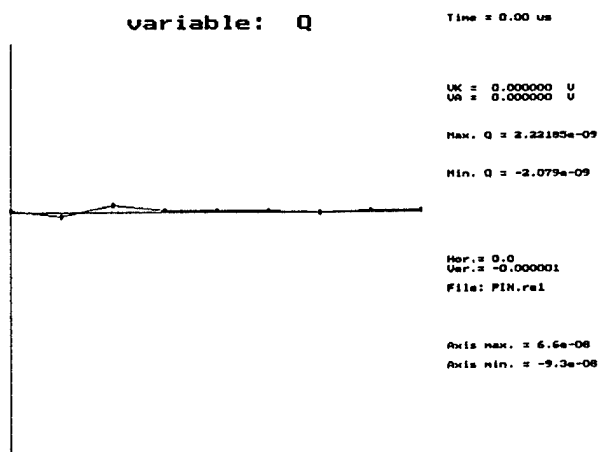

Fig. 3. Net charge calculated with large-scale grid with 9 points, uniform spacing.
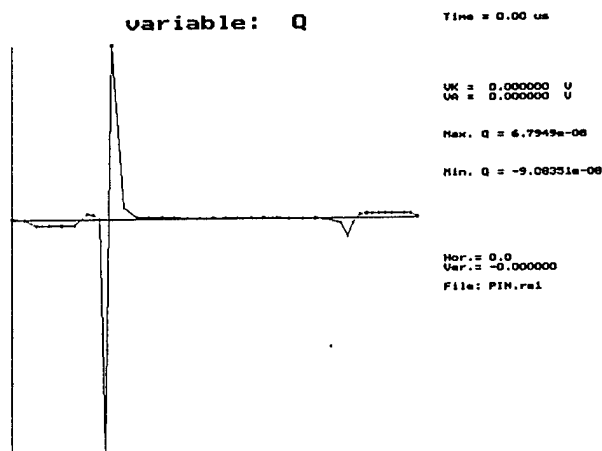

Fig. 4. Total net charge calculated by adding large-scale solution and small-scale solution. Note the similarity to the charge calculated with the traditional method in Fig. 2.

Supersymmetric Quantum Mechanics (SUSY-QM) applied to Quantum-wire devices

by
William R. Grise, Dept. of IET
Morehead State University
Morehead, KY 40351

Introduction

This paper explores the application of supersymmetric partner potentials to mesoscopic quantum waveguides and quantum modulated transistors (QMT). In particular, the use of SUSY-QM makes it possible to generate new, exactly or quasi-exactly solvable confining potentials for the transverse dimensions of such waveguides. The generation of a series of partner potentials makes it possible to tune the transmission coefficient which describes propagation through an electron waveguide in a manner different from that used in the QMT first described by Sols et al. [Sols et al., JAP-66, 3892, 1989]. This extra flexibility in adjusting the transmission properties of these devices will make it possible to synthesize more desirable current-voltage characteristics for electron waveguides.

SUSY Partner Potentials

Supersymmetric quantum mechanics (SUSY-QM) was originally developed in order to obtain a unified description of the basic interactions in particle and relativistic physics, i.e., the strong, electro-weak, and gravitational interactions [Cooper, Khare, Sukhatme, Phys. Rep. 251, 267, 1995]. SUSY ideas tie together both fermionic and bosonic degrees of freedom. As researchers studied SUSY, however, they discovered that SUSY-QM provides a ladder-operator technique useful in categorizing analytically solvable potentials and generating new classes of solvable potentials from other potentials. Briefly, SUSY-QM starts with the connection between the bound state wave functions and the potential. One then factorizes the Hamiltonian, as is done for instance with the harmonic oscillator, into the product of operators:

$$H_1 \psi_0(x) = -\nabla^2 \psi_0 + V_1(x)\psi_0(x). \text{ So: } V_1(x) = \frac{\psi_0''(x)}{\psi_0(x)}, \text{ where } \hbar = m = 1;$$

factorizing: $H_1 = A^+ A$, where $A = \nabla_x + W(x)$, $A^+ = -\nabla_x + W(x)$.

This gives: $V_1(x) = W^2(x) - \nabla_x W$, where W(x) is the superpotential. We now define a Hamiltonian $H_2 = AA^+$, reversing the order of the operators. It is easy to see that $H_2 = -\nabla_2 + V_2(x)$, where

$V_2(x) = W^2(x) + \nabla_x W(x)$. $V_2(x)$ is the supersymmetric partner potential to $V_1(x)$.

The energy eigenvalues, and wave functions of H_1 and H_2 are related in the following way:

$$E_n^{(2)} = E_{n+1}^{(1)}, \text{ and } \psi_n^{(2)} = \left[E_{n+1}^{(1)} \right]^{-\frac{1}{2}} \cdot A \psi_{n+1}^{(1)}, \text{ while } \psi_{n+1}^{(1)} = \left[E_n^{(2)} \right]^{-\frac{1}{2}} \cdot A^+ \psi_n^{(2)}.$$

To summarize, once all eigenfunctions of H_1 are known, then the eigenfunctions of H_2 are found by applying the operator A to the $\psi^{(1)}$. Furthermore, a series of potentials, V_1, ..., V_n, each corresponding to H_1, ..., H_n, all of which are different, can be shown to have the same spectra except that H_{n+1} has one fewer bound state than H_n. [Cooper, Khare, and Sukhatme, 1995]

Application to Quantum Wire Devices

This distribution of eigenvalues can be used to tune or modulate the transmission through a quantum wire, via the choice of partner potentials. This paper first investigates the case of transmission through a quantum wire whose confining potential along the length of the device switches between the hard-wall boundary and its superpotential, given by $V_2 = \frac{\pi^2}{2L^2} \cdot \left[2 \csc^2\left(\frac{\pi x}{L}\right) - 1 \right]$. Comparisons are made between this tuning mechanism and others such as alternating stub widths [Sols et al., 1989]. Finally, other selected partner potentials and their effect on transmission are investigated.

Monte Carlo Simulations of High Field Transport in Electroluminescent Devices

M. Dür and S. M. Goodnick

Department of Electrical Engineering, Arizona State University

Tempe, AZ 85287-5706 *

M. Reigrotzki and R. Redmer

Universität Rostock, D-18051 Rostock, Germany

February 13, 1997

Abstract

Hot electron excitation of luminescent impurities is an essential element of electroluminescent device performance. Therefore, an understanding of high field carrier transport in phosphor materials is important in modeling the behavior of such systems. Here we present full bandstructure Monte Carlo simulations of high field transport and optical excitation in wide bandgap semiconductor phosphor materials such as ZnS and SrS. The simulations include a nonlocal empirical pseudopotential bandstructure and all the pertinent electron scattering mechanisms. Band-to-band impact ionization is calculated directly from the nonlocal bandstructure using a special k-point integration scheme [1]. Impact excitation of luminescent centers is calculated for model wave functions representing luminescent impurities such as Mn and Ce. Both threshold phenomena are crucial to the operation of electroluminescent devices. We find good agreement between the simulated onset of impact excitation of typical luminescent impurities and the turn on of luminescence in actual devices. Our results reveal the expected trends in impact excitation yield with temperature, as well. Comparison of ZnS to cubic GaN indicates that there are more electrons above the threshold for impact excitation due to the lower density of states for GaN, and less in the case of SrS if identical deformation potentials are assumed.

[1] M. Reigrotzki et al., J. Appl. Phys. 80, 5054 (1996).

*Corresponding Author: M. Dür, e-mail: duer@asu.edu, phone: (602)965 3749, fax: (602)965 8118

Far Field Radiation in Sub-Picosecond Systems

K.A. Remley, A. Weisshaar, S.M. Goodnick and V.K. Tripathi
Department of Electrical and Computer Engineering

Oregon State University
Corvallis, Oregon, USA 97331

February 13, 1997

FDTD and Monte Carlo methods are combined to simulate the terahertz radiation fields from a coplanar photoconducting structure. The simulation tool under consideration [1] allows calculation of potentials, particle distributions, current densities, and the near field electromagnetic fields anywhere in the computational domain. To model the far field radiation, it is not efficient or, in many cases, physically possible at present to use the FDTD technique directly because of the excessive computational burden.

A technique is proposed using the time-domain near-to-far-field transformation [2] [3]. This technique incorporates an equivalent source methodology commonly used by microwave and RF engineers for the analysis of radiation from, for example, horn antennas [4]. Equivalent surface currents are found from the tangential electric and magnetic fields on a virtual surface (or aperture) in the vicinity of the actual source of radiation. These equivalent surface currents are used as new sources of radiation in a homogeneous problem space. Computational results showing the far field radiation are in agreement with published experimental results.

References

[1] S. Goodnick, S. Pennathur, U. Ranawake, P. Lenders, and V. Tripathi, "Parallel implementation of a Monte Carlo particle simulation coupled to Maxwell's equations," *Intl. J. of Num. Modelling*, vol. 8, pp. 205–219, 1995.

[2] K. S. Kunz and R. Luebbers, *The Finite Difference Time Domain Method for Electromagnetics*. Boca Raton: CRC Press, 1993.

[3] A. Taflove, *Computational Electrodynamics The Finite-Difference Time-Domain Method*. Boston: Artech House, 1995.

[4] C. Balanis, *Advanced Engineering Electromagnetics*. New York: Wiley, 1989.

New "Irreducible Wedge" for Scattering Rate Calculations in Full-zone Monte Carlo Simulations

John Stanley and Neil Goldsman
Department of Electrical Engineering
University of Maryland, College Park, MD, 20742

Carrier transport investigations based on full-zone band structure require accurate and efficient methods of computing singular integrals over the Brillouin zone. For example, in Monte Carlo simulations, net (integrated) scattering rates and scattering rate densities (in k-space) are needed to determine scattering event occurrences and post-scattering states for carriers [1].

To facilitate the implementation of accurate Brillouin zone integration codes for diamond-type semiconductors such as Si we have constructed a new "irreducible wedge" to be used in conjunction with tetrahedral k-space interpolations. This new wedge, defined by the vertices (000), (100), (110), and $(\frac{1}{2}\frac{1}{2}\frac{1}{2})$ (normalized to $|X| = 1$), spans portions of the first two Brillouin zones and contains the equivalent of 1/48 of a Brillouin zone volume. Simple symmetry arguments may be used to establish the equivalency of this new wedge with the standard irreducible wedge.

In contrast to the standard irreducible wedge [2], this new wedge allows a regular tetrahedral discretization in which there is essentially no distinction between boundary element and interior element contributions to integrals. That is, the new wedge may be precisely filled with a regular array of tetrahedral elements, while for the standard wedge, one inevitably finds elements intersecting the LUWK boundary plane to have portions extending outside the wedge. The presence of such "overhang," while posing no significant difficulties for element interpolations, can have a troublesome impact on the evaluation of integrals. The reason for this is as follows. Assuming a tetrahedral interpolation scheme, first note that evaluating interior element contributions to Brillouin zone integrals is relatively straightforward (at least for the case where energy is interpolated only to linear order); tetrahedral element integrals reduce to simple surface integrals over planar triangles contained within the element. The difficulty for boundary elements not conforming to the wedge boundary arises from the need to include only that portion of the (constant energy or post-scattering state) surface which lies within the tetrahedron and also within the wedge. Clearly, no such difficulties occur for interior elements or for boundary elements conforming to the wedge boundary.

To illustrate the quality of integration provided by the new wedge, the figure below shows the results of a density of states calculation for the lowest ten (4 valence plus 6 conduction) bands in Si using a local, 113 plane-wave pseudopotential calculation [3] (without spin-orbit coupling included). The mesh used consists of 4000 tetrahedrons (946 distinct vertices) filling the new irreducible wedge. With a denoting lattice constant, this corresponds to to $.05 \times (2\pi/a)$ increments for mesh points along $\langle 100 \rangle$ directions. By using a regular tetrahedral discretization of the new wedge, one obtains remarkably smooth results with relatively little coding effort.

[1] M.V. Fischetti and S.E. Laux, *Phys. Rev. B*, vol. 38, pp. 9721-9745, 1988.
[2] T. Kunikiyo *et al.*, *J. Phys.: Condens. Mat.*, vol. 3, pp. 6721-6743, 1991.
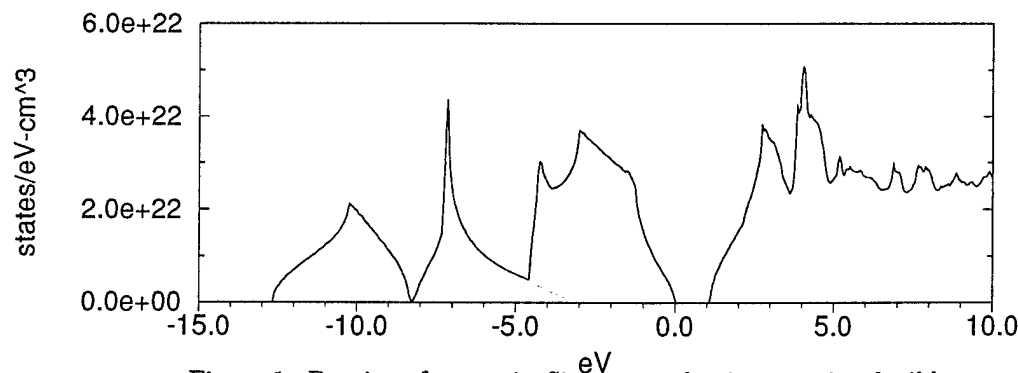[3] J.R. Chelikowsky and M.L. Cohen, *Phys. Rev. B*, vol. 14, pp. 556-582, 1976.

Figure 1: Density of states in Si computed using new irreducible wedge

A Self-Consistent Model for Quantum Well *pin* Solar Cells

S. Ramey and R. Khoie
Department of Electrical and Computer Engineering
University of Nevada, Las Vegas
Las Vegas, NV 89154
ark@ee.unlv.edu, sramey@ee.unlv.edu

We are developing a self-consistent numerical simulation model for a *pin* single-cell solar cell consisting of a $p - AlGaAs$ region, an intrinsic $i - AlGaAs/GaAs$ region with several quantum wells, and a $n - AlGaAs$ region. Our simulator solves a field-dependent Schrödinger equation self-consistently with Poisson and Drift-Diffusion equations. The emphasis is given to the study of the capture of electrons by the quantum wells, the escape of electrons from the quantum wells, and the absorption and recombination within the quantum wells. We believe this would be the first such comprehensive model ever reported.

The field-dependent Schrödinger equation is solved using the transfer matrix method.[1] The eigenfunctions and eigenenergies obtained are used to calculate the escape rate of electrons from the quantum wells,[2] and the non-radiative recombination rates of electrons at the boundaries of the quantum wells. These rates together with the capture rates of electrons by the quantum wells[3] are then used in a self-consistent numerical Poisson-Drift-Diffusion solver. The resulting field profiles are then used in the field-dependent Schrödinger solver, and the iteration process continues until convergence is reached. The flow chart of our simulator is depicted in Fig. 1.

In a $p-AlGaAs$ $i-AlGaAs/GaAs$ $n-AlGaAs$ cell with aluminum mole fraction of 0.3, with one 100 $A°$-wide 284 meV-deep quantum well, the eigenenergies with zero field are 36meV, 136meV, and 267meV, for the first, second and third subbands, respectively. The corresponding wavefunctions are shown in Fig. 2. With an electric field of 50 KV/cm, the eigenenergies are shifted to 58meV, 160meV, and 282meV, respectively, and the amplitudes of the eigenfunctions are amplified as illustrated in Fig. 3. Using the eigenenergies, the rate of thermionic escape of electrons from the $GaAs$ Γ-valley, as a function of electric field, is calculated and plotted in Fig. 4.

In our presentation, we will discuss the predictions of our model, focusing on the influence of the rate of capture of electrons by the wells, the rate of escape of electrons from the wells and the rate of non-radiative recombination at the boundaries of the wells, on the current-voltage characteristics of the device. In particular, we will relate the depth, width, and number of the quantum wells within the *i*-region to the conversion efficiency and fill factor of the solar cells. We will also compare our simulation results with those reported by theoretical[4] and experimental[5] researchers.

[1] B. Jonsson and S. Eng, *IEEE J. Quantum Electron.*, vol. QE-26, no. 11, pp. 2025-2035, 1990.
[2] D. Moss, T. Ido, H. Sano, *IEEE J. Quantum Electron.*, vol. QE-30, no. 4, pp. 1015-1026, 1994.
[3] E. Rosencher, et. al., *IEEE Trans. on Quantum Electron.*, vol. 30, no. 12, pp. 2875-2888, 1994.
[4] N. G. Anderson, *J. Appl. Phys.*, vol. 78, no. 3, pp. 1850-1861, 1995.
[5] F. W. Ragay, et. al., *12th European Community Photovoltaic Solar Energy Conference*, pp. 1429-1433, April 1994.
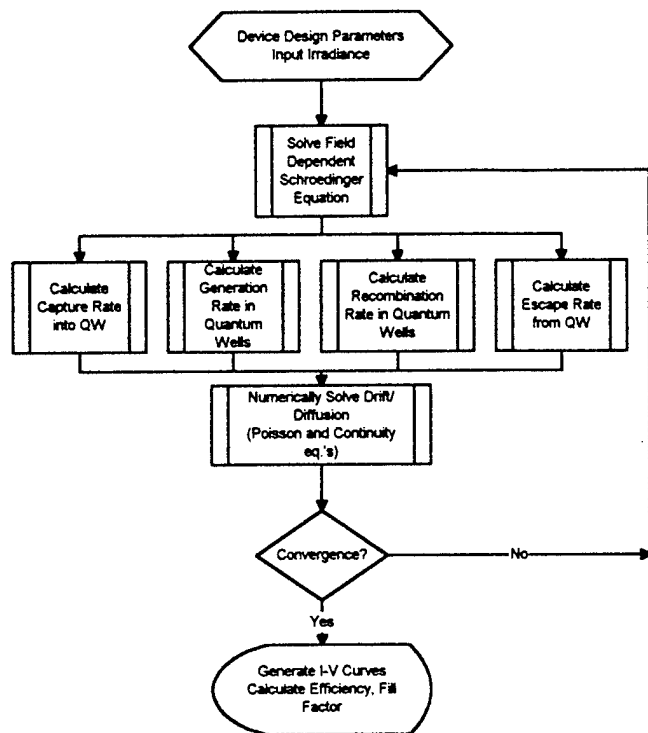
Figure 1: Flow chart of the simulation model.

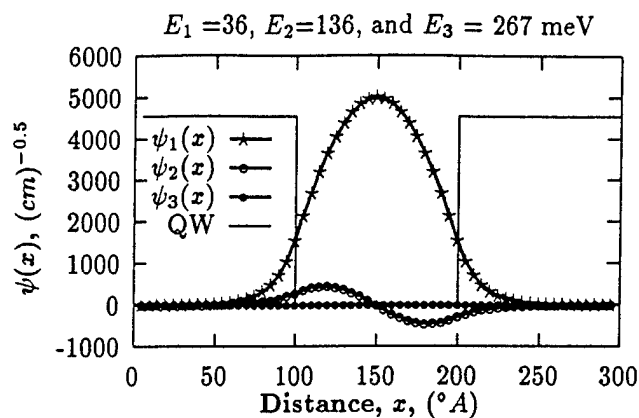Figure 2: Eigenfunctions of a 100 $A°$-wide 284 meV-deep quantum well with no field. The $GaAs$ region extends from 100 $A°$ to 200 $°A$.
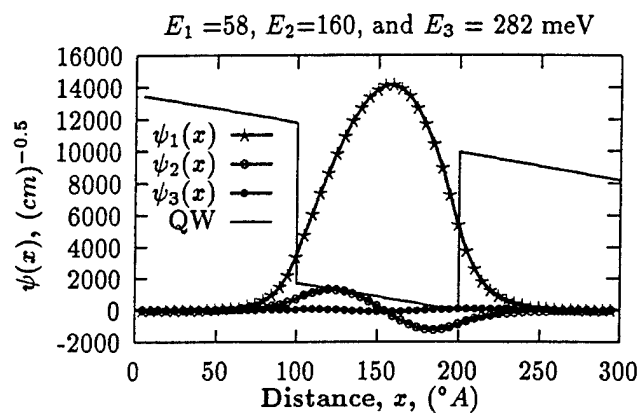

Figure 3: Eigenfunctions of a 100 $A°$-wide 284 meV-deep quantum well with 50 KV/cm field. The $GaAs$ region extends from 100 $A°$ to 200 $A°$.
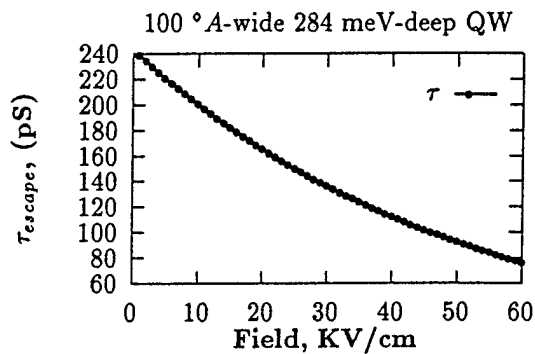

Figure 4: The thermionic escape rate of electrons from the $GaAs$ Γ-valley as a function of electric field.

Hydrodynamic (HD) Simulations of N-Channel MOSFET's with a Computationally Efficient Inversion Layer Quantization Model

Haihong Wang, Wei-Kai Shih, Susan Green, Scott Hareland,
Christine Maziar, and Al Tasch
Microelectronics Research Center, The University of Texas at Austin
Austin, TX 78712, USA
(512)471-8838, (512)471-5625 (fax)
haihong@thor.mer.utexas.edu

The quantum mechanical treatment of silicon MOSFET inversion layers is essential for accurate simulation of devices scaled down to the deep submicron region. It is well known that a high transverse electric field at the Si/SiO_2 interface leads to a large energy band bending, which can cause quantization of the inversion layer carriers in the direction perpendicular to the interface [1]. Self-consistent solutions of the Schrodinger and Poisson equations have been adopted by a number of researchers to investigate the two-dimensional nature of electrons in inversion layers [2]-[3]. However, from the point of view of the device design engineer, less computationally expensive approaches are necessary. Van Dort's simple quantum model [4] and three subband quantization model (3SB) [5] have been implemented in drift-diffusion simulation tools and have facilitated the extraction of device structure parameters (such as the physical oxide thickness) and the prediction of device electrical behavior (such as threshold voltage and capacitance). On the other hand, hydrodynamic (HD) simulation is showing advantages over drift-diffusion simulation by its ability to simulate velocity overshoot phenomena, which is pronounced in carrier transport study for short channel devices. In this paper, we present, for the first time, HD simulation results with a 3SB model included using UT-MINIMOS [6].

Since the electron temperature (or average energy) is used as an additional variable in the HD simulation, the temperature effect should be included in the quasi-Fermi level calculation in order to obtain a correct carrier distribution. Also, due to the electron heating, the classical carrier component may play an important role in the carrier density calculation for the region near the drain edge. The quasi-Fermi level and the classical carrier component need to be calculated correctly in the 3SB model to ensure that the HD simulation converges and that the simulation results is physically correct. In our approach, the fractional electron population in the quantum domain as a function of the electron energy is first obtained from the uniform Monte Carlo (MC) simulation [7]. The fractional population is then used to calculate the sheet quantum carrier concentration (N_{qm}) and classical carrier concentration (N_{cl}) for a given total sheet carrier concentration ($N_{qm}+N_{cl}$) after the drift-diffusion solution is obtained. By knowing N_{qm} and N_{cl}, we can calculate the quasi-Fermi level and classical effective density of states. The carrier distribution along the depth direction is subsequently calculated in the 3SB model to obtain the effective intrinsic carrier density, following the similar approach of ref. [5].

An examination of the electron concentration near the source and the drain edges illustrates that the distribution at the source edge obtained from the HD 3SB calculation is almost the same as from a DD 3SB calculation. The distribution near the drain edge obtained from the HD 3SB calculation, on the other hand, differs significantly from that obtained with DD 3SB. The I_d-V_d characteristics suggest the need for both the HD treatment and the QM picture either through the use of the 3SB model or a temperature corrected van Dort model.

References:
[1] J. R. Schriffer, in *Semiconductor Surface Physics*, p. 55, 1957.
[2] F. Stern, *Phys. Rev.* B, vol. 5, no. 12, p. 4891, 1972.
[3] T. Ando *et al.*, *Rev. Mod. Phys.* vol. 54, no. 2, p. 437, 1982.
[4] M. J. van Dort *et al.*, *Solid-State Electron.*, vol. 37, no. 3, p. 411, 1994.
[5] S. A. Hareland *et al.*, *IEEE Trans. Electron Devices*, vol. 43, no. 1, p. 90, 1996.
[6] *UT-MINIMOS 5.2-3.0 Information Package*, Microelectronics Research Center, The University of Texas at Austin, 1994.
[7] Wei-Kai Shih *et al.*, *54th Annual Device Research Conference Digest*, p. 28, 1996

Study of Electron Velocity Overshoot in nMOS Inversion Layers

W.-K. Shih, S. Jallepalli, M. Rashed, C. M. Maziar and A. F. Tasch, Jr.
Microelectronics Research Center, The University of Texas at Austin
email: stone@ccwf.cc.utexas.edu; Phone:(512) 471-8838

Although non-steady state phenomena in deep-submicron silicon nMOSFETs such as velocity overshoot and non-local impact ionization have been previously investigated by Monte Carlo and analytical modeling tools, effects due to channel quantization resulting from the steep bulk band bending have often been ignored. In the local transport regime, conventional MC tools [1] have been demonstrated to reproduce the experimental inversion-layer velocity-field characteristics within a limited range of temperatures using bulk silicon band structure in conjunction with a phenomenological surface-roughness scattering model. However, the validity and accuracy of this type of approach remains questionable in the non-local transport regime, although it is generally agreed upon that the quantum effects is small in steady-state high-field transport. In this work, we attempt to address this problem by performing MC simulations that include the two-dimensional nature of the electron gas in the inversion layers. The integrated MC tool encompasses two simulation domains that divide the entire electron population into 2D and 3D components for low- and high-energy electrons, respectively. It has been validated over a wide range of temperatures, substrate doping concentrations, and both lateral and transverse effective fields (E_{eff}) [2, 3]. The integrated MC tool is applied to uniform MOS inversion layers subjected to artificial lateral field profiles that vary abruptly along the channel. The effect of the Poisson feedback has been purposely ignored in order to make a direct assessment of the non-local effect purely due to the applied field. To appreciate the importance of the quantum domain in the non-local transport regime, the fractional electron population in the 2D domain under step-like and ramp-shaped lateral field profiles is examined. It is observed that, in contrast to the uniform-field condition, the 2D electron population in the high lateral-field region remains significant (> 40%) near the overshoot regions (around

$x=0.5\mu m$ for the ramp profile and $x=0.35\mu m$ for the step profile). This finding suggests that quantization might be of importance in the non-local transport regime in spite of the presence of the high lateral fields. With the same ramped lateral field profile, we have seen that the magnitude of the overshoot decreases at higher E_{eff}. This can be qualitatively explained by the higher population in the lowest subband, which has a lower mobility at high E_{eff} due to stronger surface roughness scattering. To see the quantization effects on the velocity profile, we will also show that the purely classical simulation predicts a velocity profile comparable to that obtained by the integrated MC tool at low E_{eff}. However, the difference between them increases at higher E_{eff} as quantization becomes stronger. With the relatively low E_{eff} near the drain of realistic deep-submicron MOSFETs, the impact of channel quantization on the magnitude of velocity overshoot should be quite limited.

References

[1] E. Sangiorgi and M. R. Pinto, "A semi-empirical model of surface scattering for Monte Carlo simulation of silicon n-MOSFETs," *IEEE Trans. Electron Devices*, vol. 39, pp. 356-361, 1992.
[2] W.-K. Shih, S. Jallepalli, C.-F. Yeap, M. Rashed, C. M. Maziar, and A. F. Tasch, "A Monte Carlo study of electron transport in Silicon nMOSFET inversion layers," presented at International Workshop on Computational Electronics, Phoenix, AZ, 1995.
[3] S. Jallepalli, C.-F. Yeap, S. Krishnamurthy, C. M. Maziar, and A. F. Tasch, "Application of Hierarchical Transport Models for the Study of Deep Submicron n-MOSFETs," presented at International Workshop on Computational Electronics, Portland, OR 1994.

Study on Possible Double Peaks in Cutoff Frequency Characteristics of AlGaAs/GaAs HBTs by Energy Transport Simulation

T. Okada and K. Horio

Faculty of Systems Engineering, Shibaura Institute of Technology
307 Fukasaku, Omiya 330, Japan (TEL:81-48-687-5813, FAX:81-48-687-5198)

Usually, cutoff frequency f_T of AlGaAs/GaAs HBTs increases with the collector current I_C and begins to decrease at a certain I_C, showing a single peak. However, according to the simulation using a drift-diffusion model, f_T characteristics show a steep second peak in some cases [1],[2]. This is attributed to the fact that in the drift-diffusion approximation, electron mobility is given as a function of *local* electric field and the electron velocity versus electric field curve of GaAs shows a peak behavior. So, in this work, we have simulated f_T characteristics of AlGaAs/GaAs HBTs by using an energy transport model [3] in which electron mobility is determined by electron energy (not by local electric field) and velocity overshoot can be treated. As a result, we have found that the double peak behavior can arise also when using this model, and so we discuss here why the double peaks in f_T characteristics are observed.

Here, we consider an npn^-n^+ AlGaAs/GaAs HBT shown in Fig.1 where Al composition changes from 0.3 to 0 in the emitter and base regions. So, this is a graded band-gap base HBT. n^--collector doping density N_{C1} and its thickness L_{C1} are varied as parameters. Basic equations for electron transport are three conservation equations obtained by taking moments of the Boltzmann transport equation. If we now treat an equivalent one-valley model where an upper and a lower valleys are considered, we must give transport parameters (such as average electron mobility, energy relaxation time and upper-valley fraction) as functions of Al composition x, electron energy w_n and impurity density N. To do this, we first calculate the transport parameters (by Monte Carlo method) as a function of w_n for some representative x (0, 0.1, 0.2, 0.3) and N. Once these are available as fit curves or tables, parameters for any x between 0 and 0.3 can be obtained as functions of w_n and N by a linear extraporation method. Thus we can give the transport parameters at any mesh point and at any bias condition.

Fig.2 and Fig.3 show calculated $f_T - I_C$ curves as parameters of n^--doping density N_{C1} and n^--thickness L_{C1}, respectively. From these, we see that for lower N_{C1} (10^{16} cm^{-3} in Fig.2) and for thinner L_{C1} (0.1 μm and 0.2 μm in Fig.3), f_T characteristics show a single peak. These cases correspond to the situation that n^--layer is almost or fully depleted already at $V_{BE} = 0$ V. In other cases, two peaks are clearly seen in the f_T characteristics. In these cases, a neutral n^--region exists at $V_{BE} = 0$ V. So, we interpret the double peak behavior in the following way. The first peak arises because the depletion region in the n^--layer begins to expand due to a high injection effect and so the collector transit time increases. The fall of f_T lasts until the n^--layer becomes entirely depleted. When V_{BE} is raised further, the electric field in the n^--layer becomes lower, leading to the lower electron energy there. So, the electron velocity in the n^--layer becomes higher, resulting in the shorter collector transit time. Therefore, f_T begins to increase again. Finally, f_T decreases due to the base-push-out (Kirk) effect that results in lower electron velocity around the base/n^--collector junction and higher collector capacitance. In fact, we have acertained these phenomena by studying various profiles in the device.

In conclusion, by using the energy transport simulation, we have shown theoretically that double peaks can be seen in f_T characteristics of AlGaAs/GaAs HBTs. Physical mechanism of this behavior has been successfully explained.

[1] J.Chen *et al*, Solid-State Electron., vol.34, pp.1263-1273 (1991).
[2] K. Horio, Y. Iwatsu and H. Yanai, IEEE Trans. Electron Devices, vol.36, pp.617-624 (1989).
[3] A. Nakatani and K. Horio, Inst. Phys. Conf. Ser., vol.141, pp.633-638 (1995).
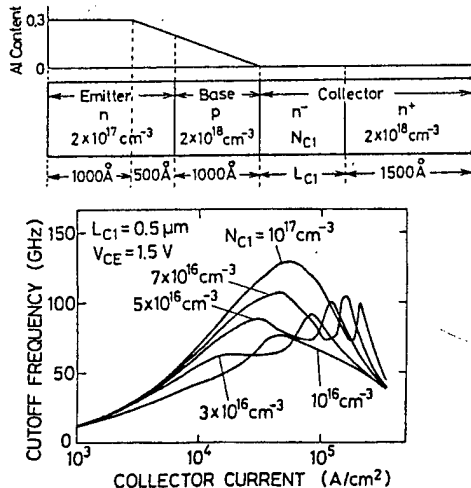
Fig.1 Device structure simulated in this study.

Fig.2 Calculated $f_T - I_C$ curves of AlGaAs/GaAs HBTs as a parameter of n^--collector doping density N_{C1}.
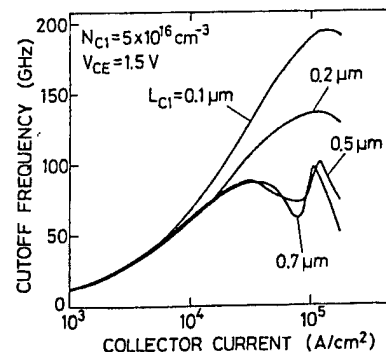

Fig.3 Calculated $f_T - I_C$ curves of AlGaAs/GaAs HBTs as a parameter of n^--layer thickness L_{C1}.

Time Dependent Hydrodynamic Model of MESFET

C. C. Lee[1], H. L. Cui[1], J. Cai[1], R. Pastore[1,2], D. Woolard[2], and D. Rhodes[2]
[1]Department of Physics and Engineering Physics
Stevens Institute of Technology, Hoboken, New Jersey 07030
e-mail: c1lee@attila.stevens-tech.edu
[2]*U.S. Army Research Laboratory,* Fort Monmouth, New Jersey 07703

Analysis of the character of non-stationary carrier motion in a submicron semiconductor device has revealed the necessity of a model which has the descriptions of nonlinear transport properties due to some special scattering interactions, carrier heating effects, etc. Traditionally, the simulation of transient behavior for a semiconductor device has been based on the drift-diffusion equation. The drift-diffusion model is a low-order approximation of the Boltzmann Transport Equation and it does not take account of the non-stationary phenomena such as carrier heating and velocity overshoot. . As a result, the drift-diffusion model is no longer applicable. We present a two-dimensional semiconductor device model based on a set of quantum mechanically derived hydrodynamic balance equations. Unlike conventional hydrodynamic models, where collisions with impurities and phonons are represented by momentum and energy relaxation times, we represented the scattering interaction in terms of a frictional force acting on the carriers and energy loss rate of the carriers. These quantities are calculated within the simulation process, as functions of the electron drift velocity, electron temperature, as well as the electron density, without an outside Monte Carlo procedure. Thus, besides the usual advantages of traditional hydrodynamic simulation approaches, the present method enjoys the added convenience of self-contained treatment of scattering.

We have applied our time-dependent hydrodynamic balance equations to the simulation of a two-dimensional submicron silicon MESFET. The initial conditions were obtained from the steady state solution with the gate voltage at 0V. Then at time t =0, the gate voltage is stepped from 0V to -0.8V. We calculated the electron drift velocity and electron temperature as functions of position along the device in the transient process. Our simulation results for the submicron MESFET are in agreement with other work in the steady state limit. However, ours is a complete, time transient simulation which should useful in predicting the frequency and time transient response of the device. Furthermore, in our work, scattering was included self-consistently, not approximated as relaxation times that are given in empirical expressions.

SHELL-FILLING EFFECTS IN CIRCULAR QUANTUM DOTS

M. Macucci

Dipartimento di Ingegneria dell'Informazione:
Elettronica, Informatica, Telecomunicazioni
Università degli Studi di Pisa
Via Diotisalvi, 2
I-56126 Pisa, Italy
Tel. +39 50 568537, FAX +39 50 568522, e-mail: `massimo@mercurio.iet.unipi.it`

and Karl Hess

Beckman Institute
*405 N Mathews   Urbana, IL 61801*

We have performed a numerical study of the shell-filling effects in a circular quantum dot, obtaining quantitative agreement with recently published experimental data by Tarucha *et al.* (PRL **77**, 3613 (1996)). Our results show that the succession of shell-filling events differs for the case of a realistic self-consistent potential from that predicted by a single-electron approximation and with an idealized parabolic potential.

Our calculations have been performed for a 2-dimensional circular quantum dot, solving the Schrödinger equation self-consistently within a mean-field approximation including exchange and correlation effects via a local density functional approach. The confinement potential is assumed to be parabolic up to a distance corresponding to the geometric dot radius, where hard walls define the outer boundary. Such a potential landscape is consistent with the experimental results for the charging energy.

The Schrödinger equation is separable into a radial and an azimuthal equation. The azimuthal equation has a trivial analytic solution, while the radial equation is solved numerically with a finite difference procedure.

The chemical potential $\mu(N)$, corresponding to the energy needed to add the N-th electron to a system with $N-1$ electrons, is computed by means of Slater's transition rule, in order to avoid the amplification of numerical errors associated with differentiations. The charging energy is then obtained as $E_C = \mu(N+1) - \mu(N)$.

In the figure we report the values of E_C obtained for dots with a geometrical radius of 90 nm and parabolic confinement potential given by $V_p = 1/2\, m^* \omega^2 r^2$, where r is the radial coordinate and $\hbar\omega = 3$ meV (solid line), 4 meV (dotted line), and 2.5 meV (dashed line). We have made these choices of parameters because $\hbar\omega = 3$ meV corresponds to the estimate given by Tarucha *et al.* and $R = 90$ nm is a value allowing quick convergence.
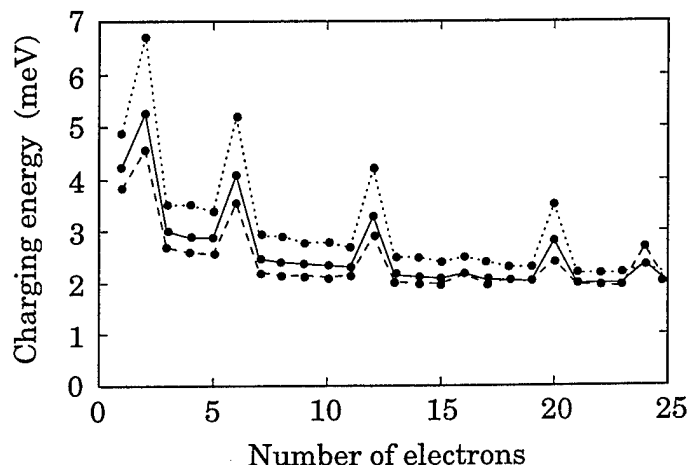
It is possible to notice that there are peaks also for $N = 16$ and $N = 24$, which are not predicted by the one-electron model, but which, at least for $N = 16$, have been observed experimentally.

MODELING OF SHOT NOISE
IN RESONANT TUNNELING STRUCTURES

G. Iannaccone

Dipartimento di Ingegneria dell'Informazione:
Università degli studi di Pisa, Via Diotisalvi 2, I-56126 Pisa, Italy
ianna@pimac2.iet.unipi.it — *phone: +39-50-568677 — fax: +39-50-568522*

Noise characterization of quantum effect devices has been the subject of increasing interest in recent years, since it provides information about the transport properties and the device structure, complementary to those given by DC characteristics and the small signal AC response.

Therefore, it is important to test the validity of the transport models used for these structures also on the ground of the correct prediction of noise properties.

In this paper, we focus on resonant tunneling devices: it is well known that the shot-noise current spectral density S in such devices is suppressed down to one half of the "full shot noise" value $S_{full} = 2qI$, obtained in the case of a purely poissonian process. Such suppression is observable when either Pauli exclusion or electrostatic repulsion are effective in introducing correlations between electrons traversing the structure, which make the process sub-poissonian.

We use a model that allows us to address noise properties of generic resonant tunneling structures in the whole range of transport regimes, from completely coherent to completely incoherent, from a wholly quantum mechanical point of view, and accounts for the combined effects of Pauli exclusion and of Coulomb repulsion. According to this model it is shown that, up to a given amount of collisions in the well, a minimum shot noise suppression factor of one half is to be expected independently of the coherence of transport.

In addition, we show that new insights about the transport properties and the geometrical structure of resonant tunneling devices can be gained from the study of the temperature dependence of the shot noise suppression factor (also called Fano factor) $\gamma \equiv S/(2qI)$, for a given bias current. This subject has received little attention from a theoretical point of view, even though a few experimental results are available.

For a diode biased in the first resonance region of the I-V curve, we show that the behaviour of the Fano factor as a function of temperature depends on whether Coulomb repulsion or Pauli exclusion is the dominant cause of shot noise suppression, and on the relative transparency of the barriers.

Our model simply explains the experimental reduction of shot noise suppression with increasing temperature observed by Ciambrone and co-workers.

Impact Ionization and Hot-Electron Injection Derived Consistently from Boltzmann Transport

Paul Hasler, Andreas G. Andreou, Chris Diorio, Bradley A. Minch, and Carver A. Mead

We develop a quantitative analytical model of the impact-ionization and hot-electron processes in MOS devices that is derived consistently from a single spatially varying hot-electron distribution function. This approach not only provides a useful circuit model, but also complements and validates numerical results from Monte Carlo simulations.

We measure hot-electron injection (gate) and impact-ionization (substrate) currents using an n-type MOSFET built with a high substrate doping ($1 \times 10^{17} cm^{-3}$) operating with subthreshold currents. In subthreshold the current current of a MOSFET is sufficiently small so that the mobile charge does not affect the surrounding electrostatics, resulting in a constant surface potential. Consequently, by operating the MOSFET in subthreshold, we obtain a high field region that is independent of the channel current; the high electric fields in the drain-to-channel depletion region accelerate channel electrons to high energies. The high substrate doping increases the threshold voltage, guaranteeing that electrons reaching the silicon-silicon-dioxide barrier will be transported to the floating gate. This higher substrate doping is consistent with a $0.3\mu m$ channel length CMOS process; thus, these effects are directly applicable to modern processes.

We begin by modeling hot-electron transport in the drain-to-channel depletion region using the spatially varying Boltzmann transport equation [1]. We derive an approximate collision-operator model for optical-phonon scattering and impact-ionization collisions. The mean free length for phonon collisions (λ) is known to be approximately constant for high energies; we eliminate the bandstructure effects by developing our model in terms of mean free lengths, rather than mean free rates. We propose the following model for the energy dependence for the impact-ionization mean-free length

$$L(E) = (1.81 \times 10^{-2} \text{nm}) \exp\left(\sqrt{\frac{119 eV}{E - .95 eV}}\right), \quad (1)$$

which is based on our experimental measurements of the impact-ionization mean free length, and corresponds to previous numerical calculations (see [2]).

Next, we analytically solve for a self-consistent distribution function using a two-step process. In the first step, we solve for the average hot-electron trajectory in energy and direction as a function of position through the depletion region. The average hot-electron trajectory is the flow line for the hyperbolic P.D.E. operator, and is related to the numerical method that Bude presented previously [3]. In this model, the average electron gains energy at the position (z_{crit}), where the phonon restoring force is equal to the energy increase due to the local electric field ($\mathcal{E}(z)$). The average energy, $E_1(z)$, that the electron gains after reaching z_{crit} is the difference between the potential from z_{crit} to the position z in the drain-to-channel depletion region, and the number of phonon collisions in this region.

In the second step, we solve for the electron distribution function around this average electron trajectory. In this coordinate system, phonon collisions diffuse the electron distribution

spatially, and impact-ionization collisions remove high-energy electrons. From this analysis, the solution for the distribution function, $f(z, E)$, is

$$f(z, E) = \exp\left(-\frac{\lambda}{z - z_{crit}}\left(\frac{E - E_1(z)}{2 E_R}\right)^2\right) a(z, E), \quad (2)$$

where E_R is the energy of an optical phonon ($E_R = 63 \text{meV}$ in Si), and $a(z, E)$ models the electrons lost to impact ionization, and is approximated by

$$a(z, E) = \exp\left(-\frac{1}{(q\mathcal{E}(z)\lambda - E_R)}\int_{E=0}^{E}\frac{\lambda}{L(E)}dE\right). \quad (3)$$

This solution shows that the assumption of a constant electron temperature is not valid at energies at which impact ionization and hot-electron injection occur.

From the electron distribution function in (2), we then calculate the probabilities of impact ionization and hot-electron injection as functions of channel current and drain-to-channel voltage (Φ_{dc}). The model of these currents simultaneously fits both the hot-electron–injection and impact-ionization nFET data. Our experimental data on the Early voltage versus Φ_{dc} show that the channel doping profile is approximately a step junction for a fixed gate voltage. The hot-electron–injection efficiency—the ratio of the injection current (I_{inj}) and the source current (I_s)—is approximately given by

$$\frac{I_{inj}}{I_s} = B_2 \exp\left(-\frac{\lambda}{d - z_{crit}}\left(\frac{E_{ox} - E_1(d)}{2 E_R}\right)^2 - \frac{7.102}{\sqrt{E_1(d)}}\right), \quad (4)$$

where λ is equal to 6.5nm, E_{ox} is the Si–SiO₂ barrier height at the drain, $B_2 = 4.55 \times 10^{-3}$, d is the width of the drain-to channel depletion region, and $\sqrt{E_1(d)} = \sqrt{\Phi_{dc}} - \sqrt{\Phi_{crit}}$. The impact-ionization efficiency—the ratio of the substrate current (I_{sub}) and the source current (I_s)—is approximately calculated as

$$\frac{I_{sub}}{I_s} = \exp\left(-\sqrt{\frac{119 eV}{E_1(d)}}R(E_1(d))\right), \quad (5)$$

where $R(E_1(d))$ is a slowly varying function. This analytic model of impact-ionization and hot-electron injection currents agrees well with experimental data. It accounts for impact ionizations in the drain-to-channel and drain regions. From measured values of α versus Φ_{dc}, our analytical model allows us to measure the energy-dependent impact-ionization collision rate from experimental data; (1) is a curve fit to these data.

REFERENCES

[1] P. Hasler, *Foundations of Learning in Analog VLSI*, Ph.D. thesis, Computation and Neural Systems, California Institute of Technology, February 1997. *Also at www.pcmp.caltech.edu/anaprose/paul.*

[2] M.V. Fischetti, S.E. Laux, and E. Crabbe, "Understanding hot-electron transport in silicon devices: Is there a shortcut?" *Journal of Applied Physics*, vol. 78 no. 2, July 1995, pp. 1058–1087.

[3] H. Budd, "Path variable formulation of the hot carrier problem," *Physical Review*, vol. 158, no. 3, June 1967, pp. 798–804.

The authors are associated with California Institute of Technology, Pasadena, CA 91125. E-mail: paul@pcmp.caltech.edu.

Comparison of Variance Reduction Schemes for Monte Carlo Semiconductor Simulation

Carl J. Wordelman,

Beckman Institute, University of Illinois at Urbana-Champaign, Urbana, Illinois 61801, USA

Andrea Pacelli,

Dipartimento di Elettronica e Informazione and CEQSE-CNR, Politecnico di Milano,
Piazza Leonardo da Vinci 32-20133 Milano, Italy

Mark G. Gray, and Thomas J. T. Kwan

Los Alamos National Laboratory, Los Alamos, NM 87545, USA

Monte Carlo semiconductor device simulation is used to gather information about regions in phase space that are too sparsely populated to use the fluid approximation. Since the number of particles in a simulation ($N \sim 10^4$) is small compared to the number of particles in a real device ($N \sim 10^8$), variance reduction or redistribution techniques are necessary. The most common class of variance reduction techniques is distribution biasing where the number and weights of particles are adjusted to populate the phase space areas of interest. The variance-reduction techniques presented here are computationally efficient methods to enhance statistics and are useful in the investigation of device reliability and degradation due to hot electrons.

In this work, we examine several distribution-biased variance reduction techniques. The multi-comb scheme [1] was adapted from neutral particle scattering and has been shown successful in resolving hot electron tails in device simulation. The non-local adaptive gathering method [2] can be used in self-consistent calculations and processes the entire ensemble instead of working locally in phase space. The technique currently used in DAMOCLES [3] selectively clones or roulettes particles to retain the population in each phase space domain. The techniques are compared for a number of test cases including a simple bulk device and a sub-micron n-MOSFET.

References

[1] M. G. Gray, T. E. Booth, T. J. T. Kwan, and C. M. Snell, "A Multi-comb Variance Reduction Scheme for Monte Carlo Semiconductor Simulators", National Laboratory Report LA-UR 96-334, 1996.

[2] A. Pacelli and U. Ravaioli, "Analysis of Variance-Reduction Schemes for Ensemble Monte Carlo Simulation of Semiconductor Devices", to appear in *Solid-State Electron.*

[3] S. E. Laux, M. V. Fischetti, D. J. Frank, "Monte Carlo analysis of semiconductor devices: The DAMOCLES program", *IBM J. Res. Develop.*, **34**, No. 4, 471. (July, 1990)

Edge Element Solution of Optical Dielectric Cavities *

A. T. Galick

Beckman Institute, University of Illinois at Urbana-Champaign, Urbana, Illinois 61801, USA

We present an efficient computational approach to the modeling of three-dimensional electromagnetic confinement to arbitrary dielectric media. The essential features of this approach are an edge element formulation which pins the unwanted static solutions at exactly zero frequency, and an iterative preconditioned Arnoldi solver for the resulting eigenvalue problem which focuses computational resources on those few low-wavenumber non-static modes which the cavity is designed to support.

Edge element spaces are ideal for electromagnetics in inhomogeneous media, since they enforce only as much continuity across interfaces as is required for **E** and **H** fields. More importantly, unlike nodal elements, ker(curl) is represented in this space. In other words, this space sits in the right place in an exact Whitney sequence for discretizing equations like that for the modes of a dielectric cavity,

$$\nabla \times \left(\mu^{-1} \nabla \times \mathbf{E} \right) = \omega^2 \epsilon \mathbf{E}.$$

This is of more than academic interest because the discretized ker(curl) remains at $\omega = 0$, where it can be removed by a preconditioner, thus eliminating the problem of "parasitic" or "spurious" modes [1].

We use a rectangular grid in the standard ordering. This avoids the problems associated with generating general 3D tessellations and assembling mass and stiffness matrices on them, and gives us banded matrices that allow the matrix operator routine to be vectorized.

In our computations we use a uniform grid in the core region. The mesh spacing grows exponentially as the lines extend far out into the cladding. Such grids both resolve rapid oscillations of higher modes in the core region and extend sufficiently far to allow the modes to decay exponentially into the cladding.

Corresponding Author:
Albert Galick, 3261 Beckman Institute, 405 N. Mathews Avenue, Urbana, IL 61801
FAX: (217) 244-4333 - e-mail: galick@uiuc.edu

References

[1] A. Bossavit. Simplicial finite elements for scattering problems in electromagnetism. *Comput. Methods Appl. Mech. Engrg.*, 76:299–316, 1989.

Inclusion of Bandstructure and Many-Body Effects in a Quantum Well Laser Simulator

F. Oyafuso, P. Von Allmen, M. Grupen, K. Hess

Beckman Institute, University of Illinois, Urbana, IL 61801

Abstract

A self-consistent eight band $\mathbf{k} \cdot \mathbf{p}$ calculation, which takes into account strain and includes Hartree, exchange, and correlation terms (determined from a local density approximation) is incorporated into a QW laser simulator (MINILASE-II). The computation is performed within the envelope function approximation for a superlattice, in which all spatially varying terms of the $\mathbf{k} \cdot \mathbf{p}$ Hamiltonian, including the exchange and correlation energies are expanded in plane waves. The $\mathbf{k} \cdot \mathbf{p}$ eigenvalue equation, and Poisson's equation are solved iteratively until self-consistency is attained. Results from the the $\mathbf{k} \cdot \mathbf{p}$ calculation are exported to MINILASE-II via a density of states and an energy dependent optical matrix element factor, which is renormalized by a Coulomb enhancement factor computed from the statically screened 2D Coulomb potential. Results will be presented for the gain spectrum and modulation response for a $Ga_{.8}In_{.2}As/Al_{.1}Ga_{.9}As$ quantum well laser.

COUPLED FREE CARRIER AND EXCITON DYNAMICS IN BULK AND QUANTUM WELL SEMICONDUCTOR MATERIALS

M. Gulia[a,b], F. Compagnone[a,d], P.E. Selbmann[c], F. Rossi[a,b], E. Molinari[a,b], P. Lugli[a,d,*]

[a] Istituto Nazionale Fisica della Materia (INFM), Italy
[b] Dipartimento di Fisica, Università di Modena, I-41100 Modena, Italy
[c] Swiss Federal Institute of Technology (EPFL) , CH-1015 Lausanne, Switzerland
[d] Dipartimento di Ingegneria Elettronica, II Università di Roma, I-00177, Roma, Italy

Non resonant optical excitation of semiconductors at energies high above the band gap is followed by a rapid relaxation of the initial non-equilibrium carrier distributions. Parallel to this process, electrons and holes may bind into excitons, leading to a rise of the excitonic luminescence. The interplay of exciton and free-carrier dynamics therefore plays a very important role, particularly in low-dimensional systems.

Even if the intrinsic process of exciton formation has been the subject of several experimental studies, the dependence of formation dynamics on the experimental conditions is not yet fully understood, and the relative influence of both acoustic and optical phonon has to be clarified [1,2].

Standard Monte Carlo simulations of the carrier dynamics cannot be used for this purpose, as they only follow the evolution of free-carrier populations; on the other hand, quantum-kinetic approaches which take into account coherent effects on a femtosecond time-scale [3] are not yet able to treat incoherent exciton phenomena occurring in the range $\sim 1 - 100$ ps.

We have therefore developed a kinetic model describing the temporal evolution of the coupled system of free carriers and excitons in the low density limit. We first calculate the probabilities associated to the relevant scattering mechanisms, including phonon-mediated exciton binding and dissociation, as well as carrier-carrier, carrier-phonon, and exciton-phonon interaction. The coupled kinetic equations of Boltzmann-type are then solved by means of an extended Ensemble Monte Carlo method which treats the phonon-assisted free carrier-exciton reactions as many-particle collisions. This enables us to study in detail the build-up of an exciton population and to perform simulations of typical time-resolved luminescence experiments in the incoherent regime.

In bulk GaAs we find that the excitation conditions strongly influence the relative exciton and free carrier populations and their time evolution in the *ps* range. The origin is the strong energy dependence of the probabilities for free-carriers to exciton transitions. In the initial stage after the excitation, the interaction of electron-hole pairs with LO-phonons leads to a fast formation of excitons with relatively large kinetic energies. The optically active states close to the exciton band edge are populated via slower relaxation processes due to scattering with acoustic phonons.

A similar picture holds for II-VI bulk materials, e.g. CdTe and CdSe, where the exciton formation processes are much faster than in GaAs.

Our novel theoretical scheme is then extended to GaAs/AlGaAs quantum wells, where we follow the evolution of appropriate populations associated to each carrier and exciton subband. Here, we find that most of excitons are rapidly created mainly via LO-phonon emission and therefore a dependence of formation time on the simulation conditions is observed. On the contrary AC-phonon assisted mechanisms have a reduced influence on the formation dynamics while their role is important for the energy relaxation of excitons towards optically active states.

[1] P.W.M. Blom et al., Phys. Rev. Lett. **71**, 3878 (1993).
[2] T.C. Damen et al., Phys. Rev. **B42**, 7434 (1990).
[3] F. Rossi, S. Haas, and T. Kuhn, Phys. Rev. Lett. **72**, 152 (1994), and refs. therein.

* Corresponding author. E-mail: lugli@roma2.infn.it Tel: +39 (6) 72594469 Fax: +39 (6) 2020519

OPTICAL AND ELECTRONIC PROPERTIES OF SEMICONDUCTOR 2D NANOSYSTEMS: SELF-CONSISTENT TIGHT-BINDING CALCULATIONS

A. Di Carlo, S. Pescetelli, A. Reale, M. Paciotti, P. Lugli*

Istituto Nazionale Fisica della Materia (INFM) and
Dipartimento di Ingegneria Elettronica, Università di Roma "Tor Vergata",
Via della Ricerca Scientifica 1, 00133 Roma (Italy)

Electronic and optical properties of semiconductor nanostructures based on homo- and heterojunctions have been investigated theoretically by means of a variety of tools. These range from *ab-initio* approaches [1], which are very precise but require a large computational effort and, consequently, are limited only to very small nanostructures, to approximate but easy-to-handle and fast methods such as for example those based on the envelope function approximation (EFA) [2]. Such an approach, and its generalizations, have been very successful, even though several problems cannot be handled easily within the EFA context, as, e.g., band mixing, indirect gap, and strain [3]. The empirical tight binding method (TB) [3] has been shown to be a valid alternative to EFA, since it improves the physical content in the description of nanostructures with respect to EFA, without requiring a much higher computational effort. So far, however, TB has been mainly used in the calculation of the electronic properties of nanostructures without taking into account self-consistent charge redistribution, which is an important requirement when we deal with real devices.

In this communication we will show that the TB method can be implemented in a self-consistent fashion and we demonstrate its suitability for the calculation of optical and electronic properties of realistic nanostructured devices. By using a recently developed theory [4] we also show how to define the susceptibility tensor, without requiring periodic boundary conditions. This makes the method suitable for nanosystems where the translational symmetry is broken at least in one direction. Self-consistent results for strained and unstrained quantum well systems, namely lattice matched quantum well and pseudomorphic high electron mobility transistor (P-HEMT), are given. Photoluminescence spectra are then calculated and the relation with selection rules of intersubband transition and light polarization is analyzed.

With respect to self-consistent EFA the method proposed is suitable to study heterojunction devices based on indirect band gap semiconductors such as Si/SiGe devices. Furthermore, the barrier high reduction due to $\Gamma - X$ mixing in heterojunction devices is fully accounted.

[1] C. H. Park and K. J. Chang, *Phys. Rev.* **B47**, 12709 (1993).
[2] G. Bastard, *Wave mechanics applied to semiconductor heterostructure*
    (Les Edition de Physique, Les Ulis Cedex, 1988).
[3] T.B. Boykin *et al. Phys. Rev.* **B43**, 4777 (1991);
    A. Di Carlo, P. Lugli, *Semicon. Sci. Technol.* **10**, 1673 (1995);
    J. N. Schulman, Y. C. Chang, *Phys. Rev.* **B31**, 2056 (1985);
[4] M. Graf and P. Vogl, *Phys. Rev.* **B51**, 4940 (1995);
    A. Di Carlo et al. Solid State Comm. **98**, 803 (1996)

* Corresponding author. E-mail: lugli@roma2.infn.it Tel: +39 (6) 72594469 Fax: +39 (6) 2020519

Transient Phenomena in High Speed Bipolar Devices

Michael S. Obrecht[*], Edwin L. Heasell, Jiri Vlach and Mohamed I. Elmasry

Department of Electrical and Computer Engineering, University of Waterloo

[*]*Siborg Systems Inc, Waterloo, Ontario, Canada*

A new numerical approach has been introduced recently [1] for the analysis of charge partitioning in semiconductor devices. A method for separating the space charge density into a true space charge density, related to the depletion capacitance, and a quasi-neutral charge density, related to the diffusion capacitance, was proposed. A method for the separation the charging current from the "pass-through" current was introduced. The latter component does not affect the charge stored inside the device and is a generalization of the commonly used transfer current, for the case of non-quasi-static transients.

Preliminary results, obtained from this analysis, are compared with the predictions of the conventional charge partitioning models. Significant discrepancies are found to arise from the simplifications necessary for analytic modeling. For example: the charge partitioning depends on the ramp speed and injection level, and the switch-on and switch-off transients are not symmetrical.

In the case of a simple pn-junction diode, in high injection, the charge partitioning of the minority charge in the quasi-neutral base varies from 0:1 to 1:1 for the ramp times from 10^{-11} to 10^{-7} s. This implies that the traditional diffusion capacitance, which is proportional to the charge partitioning, depends not only on the doping profile but also on the device switching conditions, showing that the equivalent circuit must be reconsidered.

For BJTs some of the results dependent upon the device structure, nevertheless a few general conclusions seem to be possible:

i) In low level injection charge partitioning deviates from the theoretical 1:2 collector:base partition due to 2D effects.
ii) When high level injection occurs, the resulting built-in electric field the QNB leads to a collector charge fraction that grows with V_{BE}.
iii) The ramp speed affects charge partitioning in both high and low injection level operation, by effectively reducing the collector charge fraction at faster ramp speeds.

These results demonstrate the inapplicability of the traditional circuit analysis approach, where the stored charges in p-n junctions are replaced by depletion and diffusion capacitances. It can also be erroneous to use small signal analysis, based on the quasi-steady-state solution, to extract the equivalent circuit parameters for the analysis of fast, large signal transients. The introduction of the "pass-through" current is essential for understanding the transient charge partitioning.

[1] M.S.Obrecht and E.L Heasell "A numerical analysis of transient charge partitioning", IEEE Trans. Electron Devices, vol.43, pp. 424-430, March 1996

Interaction of 2D Electrons with Acoustic Phonons near the Semiconductor Surface and its Effect on 2D Electron Transport

B. A. Glavin[1], V. I. Pipa, V. V. Mitin, M. Stroscio[†]

Department of ECE, Wayne State University, Detroit, MI 48202

[†] *US Army Research Office, Research Triangle Park, NC 27709-2211*

We consider transport of 2D electrons in a quantum well (QW) placed near the surface of a slab in which the QW is embedded. We show that conventional methods for calculating electron–phonon scattering rates are suitable only if the QW is in the bulk of the slab. Otherwise, the surface induce substantial changes of the phonon's structure which results in substantial modification of electron transport. Since in most experimental structures QWs are situated near surfaces or interfaces, the proposed effect is important in the design of modern quantum structures.

This change in electron transport characteristics arises due to the mutual conversion of LA and TA phonons upon reflection from the surface. To simulate this conversion we calculated the confined acoustic modes of a slab with finite thickness, which implicitly accounts for the mentioned reflection-stipulated conversion. Then the corresponding matrix elements for the 2D electron–phonon interaction have been obtained. It has been shown that in a particular range of temperatures, the 2D electron–phonon scattering becomes highly inelastic. To take this into account we have obtained an integral equation which determines electron mobility. This equation has been solved numerically for different parameters of the system.

We have investigated the dependence of the mobility on the distance between the QW and the surface of the slab, temperature and mechanical conditions on the slab's surface. It has been established, that the subject effect can lead to substantial change of the electron mobility. Depending on the mechanical conditions on the surface, which change drastically the acoustic mode's structure, mobility either increases (for free surface) or decreases (for clamped surface) with respect to the corresponding value for the QW placed into the bulk of the slab. The change in mobility is maximal if the QW is situated near the surface of the slab and in the range of temperatures $2s_l p_F < T < (2\hbar s_l)/d$, where p_F is the Fermi momentum of electrons, s_l is the velocity of LA waves and d is the thickness of the QW.

---

[1]Corresponding author. FAX: (313) 5771101 e-mail: glavin@ciao.eng.wayne.edu

Acoustic phonon modulation of the electron response
in tunnel-coupled quantum wells

G.Ya. Kis and F.T. Vasko[1]
Institute of Semiconductor Physics, Kiev, 252650, Ukraine
V.V. Mitin
Department of ECE, Wayne State University, Detroit, MI 48202

Modulation of the electron properties of the tunnel-coupled double quantum wells (DQWs) due to acoustic phonon pumping is considered. Linear, with respect to the phonon pumping intensity, electron response is calculated in the balance equation approximation taking into account interface roughness scattering. Phonon-induced dipole momentum (i.e. induced transverse voltage δU) and phonon-drag effect (i.e. induced in-plane current δJ) are calculated for the cases of low and high doping levels of the DQWs structures. The transverse induced voltage arises due to electron redistribution between QWs, and the phonon drag current is generated due to transmission of the in-plane component of the phonon wave vector to the electrons in the DQWs. The voltage δU can be observed under isotropic in 2D layer phonon pump, while the current δJ can be realized under excitation by the phonon beam with fixed component of the longitudinal wave vector.

The calculations are based on the quantum kinetic equation taking into account intra- and interwell electron scattering which is caused by the interface roughness (for the general case these roughness are different in left and right QWs). Non-equilibrium phonon excitation described by the phonon collision integral and then balance equation for concentration redistribution and momentum transfer have been used. The dependencies of δU and δJ versus level splitting, characteristics of phonon pump and parameters of the DQWs were presented. Numerical calculations for a typical DQWs structure parameters show that pumping phonon flux near 1 $\mu W/cm^2$ is enough for measurement of both δU and δJ (see [1], where conditions for experimental measurement δJ are presented). The possible applications of the DQWs as a sensitive phonon detectors are noted.

[1] H. Karl, W. Dietsche, A. Fischer, and K. Ploog, Phys. Rev. Lett. **61**, 2360 (1988).

---

[1] Corresponding author

Cathode Shape Influence on Subterahertz Oscillations of Ballistic Quantized Hole Current

A. N. Korshak[1,2], Z. S. Gribnikov[1,2], N. Z. Vagidov[1], S. I. Kozlovsky[1], V. V. Mitin[2]

[1]*Institute of Semiconductor Physics, Kiev, Ukraine*

[2] *Department of ECE, Wayne State University, Detroit, MI 48202*

A problem of space-charge-limited currents for bulk semiconductor is a one-dimensional (1D) transport problem which is self-consistent with a 1D Poisson equation solution. But an analogous problem for the 2D electron gas in a quantum well (QW) loses this 1D character because electrodes can be of different geometric configurations and a potential distribution near the conducting channel is greatly affected by both the electrode shape and the structure of a surrounding space. One of the simplest versions of such structure is a periodic array of parallel QWs with a spatial period $2a$ (Fig.1). The solitary well case corresponds to the limit $a/l \to \infty$. Figure 1, a, b, c, shows the considering structures with different cathode and anode shapes (quasimetallic regions are shaded) and therefore with different positions and potential structures of effective cathode regions.

Here we study an effect of electrode shape on the ballistic quantized hole transport for a periodic arrays of doped parallel p-QW's (up to the limit $a/l \to \infty$). We consider conductivity in the lowest subband of size-quantization only. A negative effective mass (NEM) region in the hole dispersion relation is a reason of a current oscillation generation in the subterahertz or terahertz ranges depending on the energy ranges for the NEM region, the base length l and the other parameters of the well and structure [1]. The electrode shape and the Fermi-energy of emitting holes affect substantially both the voltage range of the oscillations and their features. An elongation of the quasimetallic section l_1, $x_{elec} \equiv l_1$ (Fig. 1, c) leads to the significant broadening of the voltage ranges of the oscillations (both linear and nonlinear, see Fig. 2). It is due to the changes in the potential distribution in the effective cathode region and a decrease of the bypassing capacity.

Reference: [1] Z. S. Gribnikov, A. N. Korshak, N. Z. Vagidov, Z. M. Alexeeva, Proceedings of the 23rd International Conference on The Physics of Semiconductors, ed. by M. Scheffler and R. Zimmermann (World Scientific, Singapore 1996) v. 4, p. 3287-3290.
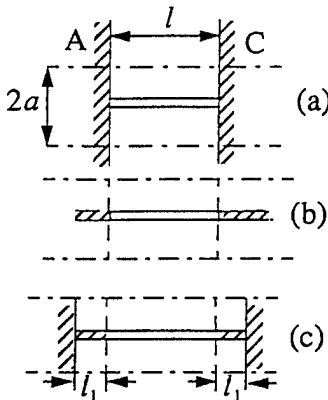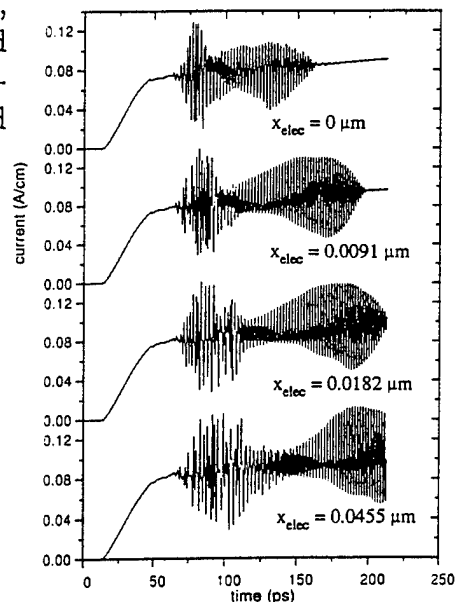
Fig. 1

Fig. 2

Transverse Patterns in the Bistable Resonant Tunneling Systems under Ballistic Lateral Electron Transport

V. A. Kochelap[1,2], B. A. Glavin[1,2], and V. V. Mitin[1]

[1]*Department of ECE, Wayne State University, Detroit, MI 48202*
[2]*Institute of Semiconductor Physics, Kiev, Ukraine, 252028*

Recently we reported a phenomenon of formation of transverse self-sustained patterns of the tunneling current and built–in charge in double barrier resonant tunneling structures with the bistable current–voltage characteristic [1]. The phenomenon arises due to the electrostatical feedback between the tunneling injection rate and electrical charge of resonant electrons accumulated in the quantum well. The patterns formation leads to a strong coupling of the tunneling current and lateral (perpendicular to the current) electron transport.

In this work we show that for the well developed bistability the lateral transport of resonant electrons has ballistic character. This gives rise to the peculiarities of the phenomenon in compare with majority of the patterns formation effects in multistable systems. The latter are usually described within diffusion–like models. To deal with patterns for the case of the ballistic transport we have developed the variational procedure for the self–consistent solution of the kinetic and Poisson equations. This method has allowed us to obtain soliton and anti–soliton patterns for the different voltages within bistable interval. The spatial scale of the obtained patterns is of the order of $v_F \tau_{es}$, where v_F is the Fermi velocity and τ_{es} is the time of tunneling escape of electrons from the quantum well. The effect of lateral dimensions of devices on the patterns is studied. Besides stationary, mobile patterns have been obtained within the same variational method. In fact, they are autowaves, switching the system from the high to low current state (or vise versa, depending on the voltage). The dependence of the velocity of the autowaves (whose characteristical value is determined by v_F) on the applied voltage has been calculated.

The following device applications of the presented phenomenon are discussed: the current switcher and new type of microwave oscillations.

[1] V. A. Kochelap, B. A. Glavin, V. V. Mitin, in *Hot Carriers in Semiconductors*, ed. by K. Hess, J.-P. Leburton, and U. Ravaioli, Plenum Press, N.Y., 1996, p.551.

SPIN – A S̲chrödinger P̲oisson Solver I̲ncluding N̲on-parabolic Bands

H. Kosina and C. Troger

Institute for Microelectronics, TU-Vienna, Gusshausstrasse 27-29, A-1040 Vienna, Austria

Phone +43/1/58801-3719, FAX +43/1/5059224, e-mail kosina@iue.tuwien.ac.at

A self-consistent Schrödinger Poisson solver has been developed capable of computing the subband structure of a quasi-two dimensional electron gas formed in silicon inversion layers or in various heterostructures. The employed model features position-dependent material parameters and a non-parabolic band structure.

In bulk semiconductors one frequently introduces non-parabolicity by using an E–$\vec{k}$ dispersion relation of the form $E(1 + \alpha E) = \hbar^2 \vec{k}^2/2m^*$, which results from the two-band Kane Model (see e.g. [1]). Such a model is expected to be accurate enough in many cases of interest and, in any case, can be used to to draw qualitative conclusions about non-parabolicity effects [2]. Assuming quantization in one dimension we replace the scalar quantities z and k_z by the operators $\mathbf{z}$ and $\mathbf{k}_z$, respectively, and end up with the following implicit definition of the kinetic energy operator $\mathbf{T}$:

$$\mathbf{T} + \mathbf{T}\,\alpha(\mathbf{z})\,\mathbf{T} = \frac{\hbar^2}{2}\left(\frac{k_x^2}{m_x(\mathbf{z})} + \frac{k_y^2}{m_y(\mathbf{z})} + \mathbf{k}_z\frac{1}{m_z(\mathbf{z})}\mathbf{k}_z\right) \tag{1}$$

The in-plane wave vector is represented by $\vec{K} = (k_x, k_y)$. Expression (1) accounts for spatially varying material parameters such that multi-layer structures can be treated properly. The one-dimensional Schrödinger equation including the kinetic energy operator defined by (1) is solved numerically. As base functions we use the eigen functions of the momentum operator, $\hbar\mathbf{k}_z$, i.e., the wave functions are represented as Fourier series, and the unknowns of the equation system are the Fourier coefficients. On the other hand, to solve Poisson's equation finite difference discretization in real-space is used in order to take advantage of the sparsity of the equation system. The repeatedly required conversions from momentum to real-space representation and vice versa are accomplished by means of the fast Fourier transform (FFT).

Each subband can be characterized by an effective mass, m_n, and a non-parabolicity factor, α_n, two parameters which are extracted by applying perturbation theory at $\vec{K} = \vec{0}$. To describe the in-plane dispersion relation it appears favorable to use again an expression of the form $\epsilon_n(1 + \alpha_n\epsilon_n) = \hbar^2\vec{K}^2/2m_n$. One consequence of non-parabolicity is that the wave functions depend on the in-pane wave vector. Their effective widths decrease with with higher in-plane momentum.

[1] G. Bastard, *Wave Mechanics Applied to Semiconductor Heterostructures* (Les Ulis, Cedex, France, 1992).

[2] J. López-Villanueva, I. Melchor, P. Cartujo, and J. Carceller, Physical Review B **48**, 1626 (1993).

ADVANTAGES OF SEMICONDUCTOR DEVICE SIMULATOR COMBINING ELECTROMAGNETIC AND ELECTRON TRANSPORT MODELS

S. M. Sohel Imtiaz, Samir M. El-Ghazaly and Robert O. Grondin

Department of Electrical Engineering
Telecommunications Research Center
Arizona State University, Tempe, AZ 85287-7206
Phone: (602) 965-5322, Fax: (602) 965-8325, Email: sme@asu.edu

Abstract

Physical simulation of semiconductor devices at high frequencies involves not only semiconductor transport issues but also electromagnetic wave propagation issues. In order to obtain the nonlinear and the large-signal characteristics of the semiconductor devices, an electromagnetic model should replace the traditional quasi-static model in the device simulator. In this paper, the advantages of a semiconductor device simulator combining an electromagnetic and an electron transport models are presented. This study is based on a semiconductor device simulator that couples a semiconductor model to the 3D time-domain solution of Maxwell's equations. The semiconductor transport model is based on the moments of the Boltzmann transport equation. The electromagnetic wave propagation effects on the millimeter-wave FETs and HEMTs are thoroughly analyzed. The use of the electromagnetic model over the convensional quasi-static model provides the actual device response at high frequencies. It also shows the nonlinear energy build-up along the device width whereas the quasi-static model provides a linear increase of energy. The exchange of energy between the electrons and the electromagnetic waves inside the semiconductor devices are observed. This model also facilitates the optimum choice of the device width in terms of the output voltage. The combined model is capable of predicting the large signal behavior of submicron devices as well. The equivalent circuit parameters are extracted at high frequencies for the transistors using a time-domain approach.

Quantum Transport and Thermoelectric Properties of InAs/GaSb Superlattices

J.-F. Lin, and D. Z.-Y. Ting†
Department of Physics
National Tsing Hua University
Hsinchu, Taiwan, R.O.C.

ABSTRACT

In recent years, artificially layered microstructures have been considered as candidates for better thermoelectrics. By studying how transport properties in these structures are affected by the quantum size effect, researchers are hoping to find mechanisms for enhancing the performance of thermoelectrics. In this work we examine quantum transport properties of the type-II broken-gap InAs/GaSb superlattice. In this structure the relevant quantized states are complex mixtures of InAs conduction-band and GaSb valence-band states, and requires the use of a multiband model for a realistic description of the band structures. At the same time, efficiency is important due to high computational demands. We use the effective bond orbital model for an accurate description of the band structures. We shall report on our theoretical study of the thermoelectric properties of this superlattice.

† Corresponding Author. 886.3.574-2518; dzt@phys.nthu.edu.tw

Multiband Quantum Transmitting Boundary Method
for Non-orthogonal Basis

G.-C. Liang, Y. A. Lin, and D. Z.-Y. Ting†
Department of Physics, National Tsing Hua University
Hsinchu, Taiwan, R.O.C.

Y.-C. Chang
Loomis Laboratory of Physics
University of Illinois at Urbana-Champaign
1110 W. Green St., Urbana, Illinois 61801

ABSTRACT

The Multiband Quantum Transmitting Boundary Method (MQTBM) [*Phys. Rev. B* **45**, 3583 (1992)] is a multiband realization of Quantum Transmitting Boundary Method originally developed by Lent and Kirkner [*J. Appl. Phys.* **67**, 6353 (1990)] for treating quantum transport in nanostructures. Thus far, MQTBM has been implemented for several realistic, empirical, multiband models, including the tight-binding model, effective bond orbital model, and the k · p method. Recently, Chang has developed a new band structure model designed for treating heterostructures using generalized planar Wannier functions (GPWF). [*Comp. Phys. Commun.* **95**(2-3), 159 (1996)]. The band structure model is as efficient and easy to use as empirical tight-binding models, and, at the same time, can be constructed directly from first principles and offers the hope for better accuracy. The method has been successfully applied to study electronic and optical properties of surface and interfaces. We implement MQTBM for this new band structure model so that it can be used to treat quantum transport problems. The present work differs from the previous MQTBM implementations in that the generalized planar Wannier functions form a non-orthogonal basis set.

† Corresponding Author. 886.3.574-2518; dzt@phys.nthu.edu.tw

Calibration of a one dimensional hydrodynamic simulator with Monte Carlo data

O. Muscato †, S. Rinaudo ‡ and P. Falsaperla †

†Dipartimento di Matematica, Viale Andrea Doria, 95125 Catania (Italy)
fax : +39-95-330094 , e-mail:*muscato@dipmat.unict.it — paolo.falsaperla@ct.infn.it*
‡ SGS-THOMSON Microelectronis,Stradale Primo Sole 50, 95121 Catania (Italy)
fax : +39-95-599686 , e-mail:*salvatore.rinaudo@st.com*

Abstract

Recent advances in technology leads to increasing high speed performance of submicrometer electron devices by the scaling of both process and geometry. In order to aid the design of these devices it is necessary to utilize powerful numerical simulation tools.

Such devices are simulated by sophysticated hydrodynamic simulators [1] which includes higher order moments of the distribution function [2]-[4]; transport coefficients are passed into the code by Monte Carlo (MC) simulations (e.g. by using the DAMOCLES code [5]).

Now the problem is how to optimize the simulator with the MC data. In this paper we shall present the code EXEMPLAR [6] based on the Least Squares Method to optimize the hydrodynamic simulator : this is a general purpose code in which it is not necessary to have the knowledge of the analytical form of the implemented model. In particular the Least Square problem is tackled by the Simplex method and Powell's method.

In order to test this code , we simulate the stationary electron flow in the one dimensional $n^+ - n - n^+$ submicron diode, which mimics the channel of a MOSFET [7].

References

[1] P. Falsaperla and M. Trovato,preprint University of Catania (1997)

[2] A.M. Anile and O. Muscato , Phys. Rev. B,**51**,16728, (1995)

[3] A.M. Anile and O. Muscato,Transp. Theory and Stat. Phys.,**25**,20,(1996)

[4] A.M. Anile, O. Muscato, Cont. Mech. Therm.,**8**,131,(1996)

[5] S.E. Laux, M.V. Fischetti and D.J. Frank,IBM J. Res. Develop.,**34**,(1990)

[6] S. Rinaudo,*A General algorithm to calibrate any kind of simulators without any knowledge about analytical form of the implemented models*, SGS-THOMSON Microelectronic, internal report (1995)

[7] C.L. Gardner,J.W. Jerome and D.J. Rose IEEE Trans.Comp. Aided Design, **CAD 8** **n.5**,501,(1989)

Hyperbolic Hydrodynamical Model of Carrier Transport in Semiconductors

Angelo Marcello Anile*

Dipartimento di Matematica, Universitá di Catania
viale A. Doria 6 - 95125 Catania, Italy

Vittorio Romano[†]

Politecnico di Bari, sede di Taranto,
Viale del Turismo 8 - 74100 Taranto, Italy

Giovanni Russo[‡]

Università dell'Aquila
Via Vetoio, loc. Coppito - 67100 L'Aquila

February 4, 1997

Abstract

An extended hydrodynamical model for carriers transport in semiconductors is presented. The model is obtained from the set of moments equations of the transport equations for electrons at the level of 13 moments with the closure relations obtained in the framework of Extended Thermodynamics [1, 2] by employing the entropy principle. The balance equations for the macroscopic variables form a hyperbolic system for values of heat flux and stress tensor which are routinely encountered in the simulation of semiconductor devices of interest for industrial purposes. In the present paper we model the productions as relaxations terms. A more general expression is under current investigation [3].

A suitable numerical scheme, developed in [4, 5], has been successfully applied to the present model. It is based on the splitting method between relaxation and convection and allows an easy implementation in numerical codes. For the convective steps we used the Nessyahu-Tadmor [6] scheme for quasilinear hyperbolic systems in divergence form. It is a second order shock capturing methods and does not require the analytical expressions of the eigenvalues and eigenvectors of the jacobian matrix of fluxes. The latter property is crucial because explicit expressions for the eigenvalues and

---

*e-mail anile@dipmat.unict.it

[†]e-mail romano@dipmat.unict.it

[‡]e-mail russo@univaq.it

eigenvectors are not available for the balance equations of Extended Thermodynamics. For the relaxation part a suitable combinations of implicit Euler steps assures a global second order accuracy.

In particular we present the simulation of a $n^+ - n - n^+$ silicon diode.

The numerical results shows a uniform accuracy in all the fields (energy density, velocity, particle number, heat flux) within a reasonable degree of tolerance and could be employed for a systematic use as a CAD tool.

References

[1] I. Müller e T. Ruggeri, *Extended Thermodynamics*, Springer-Verlag, Berlin, (1993).

[2] D. Jou, J. Casas-Vazquez e G. Lebon, *Extended Irreversible Thermodynamics*, Springer-Verlag, Berlin, (1993).

[3] A.Anile, V.Romano, G.Russo, *Testing closure relations for hydrodynamical models of carrier transport in semiconductors*, preprint.

[4] V. Romano and G. Russo, *Numerical solution for hydrodynamical models of semiconductors*, submitted to IEEE trans. on CAD (1996).

[5] F. Liotta and G. Russo, *Second Order Splitting Shemes for Balance Law with Relaxation*, in preparation.

[6] H. Nessyahu e E. Tadmor, J. Comp. Phys., **Vol. 87**, n. 2 . pp 408-463

A hydrodynamical model for transport in semiconductors without free parameters

P. Falsaperla and M. Trovato

*Dipartimento di Fisica, Università di Catania,
Corso Italia 57, I-95129, Catania, Italy.*

e-mail: *falsaperla@ct.infn.it – trovato@ct.infn.it*

We have developed a totally self-consistent hydrodynamical method for the study of transport phenomena in semiconductors, based on the Principle of Maximum Entropy.

Using moments of the Boltzmann transport equation one can obtain a hierarchy of equations for a given set of macroscopic fields. With the Principle of Maximum Entropy it is possible to express the distribution function through these fields. As a consequence, all the unknown constitutive functions (fluxes and collisional productions) can be completely fixed according to the physical characteristics of the simulated system, i.e. band structure and scattering processes. Then, contrary to other hydrodynamical models, our model does not contain free parameters (transport coefficients), i.e. parameters depending on the geometry and working conditions of the devices. The presence of these free parameters has always been a limit to a practical use of HD models, because, in general, they have to be determined in each case on the base of Monte Carlo simulations or experimental data.

We have applied our model to the simulation of some submicron devices, obtaining results comparable with Monte Carlo ones, with the remarkable advantage of a reduction of the computation time by several orders of magnitude.

Modeling of Poly-Silicon Carrier Transport with Explicit Treatment of Grains and Grain Boundaries

Edwin C. Kan and Robert W. Dutton

CIS-X 334, Stanford University, Stanford, CA 94305-4075

Phone: (415)723-9796, Fax: (415)725-7731, Email: kan@gloworm.stanford.edu

Poly-silicon devices such as TFT for SRAM, LCD and image sensor, and high-value resistance in analog circuit, have recently received much attention in consideration with its integration capability [1]. The carrier transport in poly-Si is conventionally modeled by the average grain size, since more than tens of grains usually exist within the device area of interest [1]. However, with the aggressive scaling of VLSI technology, TFT for SRAM and high resistance poly-Si resistors may have only a few grains within the device. Discrete effects from the limited number of grains may be important and explicit treatment of transport within grains and grain boundaries will be necessary.

If the grain size in poly-Si is still larger than 100 Å, deviation from single-crystal Si transport (based on the periodic potential approximation) within grains may be neglible. Bandtail transport [2] within grains can be used as the next level of approximation. Intuitively, the grain boundary can be modeled by interface trapped charge and the carrier transport across the grain boundary can be expressed by thermionic emission. This approach has been taken in [3], although a Monte Carlo simulation is used. The drift-diffusion model is much more computationally efficient and numerically stable, and thus we have chosen to implement the grain boundary treatment under the drift-diffusion model. The electron concentration profiles for a poly-Si resistor with various levels of interface trapped charge is shown in Fig. 1. Alternatively, since dopant diffusion in grain boundaries is usually 100 to 1000 times faster than in grains, the grain boundary can be modeled by delta dope and the carrier transport across the grain boundary can be treated by diffusion. A similar comparison is shown in Fig. 2.

The transport models for poly-Si will be first benchmarked with the poly-Si resistance measurement for various temperatures. Applications of these new models to TFT and their respective effects will also be presented in the conference.

[1] T. Kamins, *Polycrystalline Silicon for Integrated Circuit Applications*, Kluwer Academic, 1988.

[2] T. Serikawa, et. al., *Proc. of Intl. Conf. Solid State Dev. and Mat.*, Osaka, 1995, p. 662.

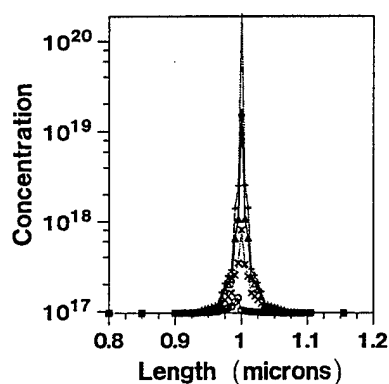[3] T. Shimatani and M. Koyanagi, *IEDM Tech. Dig.*, p. 297, 1995.

Fig. 1: electron concentration of a poly-Si resistor with $10^{17} cm^{-3}$ arsenic doping and one grain boundary in the center. The grain boundary is modeled by interface trapped charge and the carrier transport across the grain boundary is by thermionic emission.
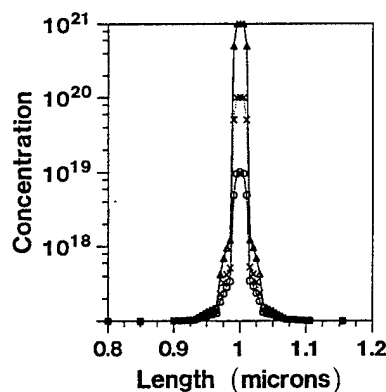
Fig. 2: same device as in Fig. 1. The grain boundary is modeled by delta dope and the carrier transport across the grain boundary is by diffusion.

Formulation of the Boltzmann Equation
as a
Multi-Mode Drift-Diffusion Equation

Kausar Banoo, Farzin Assad, and Mark Lundstrom
(765) 494-3515 / (765) 494-6441 (FAX) / lundstro@purdue.edu
School of Electrical and Computer Engineering
Purdue University, West Lafayette, Indiana 47907

The conventional, drift-diffusion transport model has proven to be remarkably robust, but more rigorous transport models are being used with increasing frequency as MOSFET channel lengths shrink towards sub-0.1 µm dimensions. It is difficult, however, to easily move through steps of the hierarchy because the various methods are formulated so differently. In this poster, we introduce an original formulation of the Boltzmann equation and show that it promises to provide a full description of transport from the drift-diffusion level to the full Boltzmann level while being applicable on a general, unstructured grid.

If we discretize k-space into bins, then we can inquire as to the population of each bin, $n_i(\mathbf{r})$, and the current, $J_i(\mathbf{r})$, carried by each bin (here, $\mathbf{r}$ is a vector in position space and i labels the bin in momentum space). One can show that the bin currents and populations are related by

$$\vec{J}(\mathbf{r}) = -[\mu]\vec{n}\,\mathcal{E} - [D]\nabla\vec{n}, \tag{1}$$

where $\vec{J}$ and $\vec{n}$ are M x 1 vectors in the M-dimensional momentum space, and $[\mu]$ and $[D]$ are M x M mobility and diffusion coefficient matrices. The mobility and diffusion coefficient matrices are related by

$$[D][\mu]^{-1} = [E], \tag{2}$$

where [E] is an "Einstein matrix." Equation (1) is not a complete description of transport, it must be augmented by

$$\nabla \bullet \vec{J} = [G]\vec{n} - [R]\vec{n} + [S]\vec{n}, \tag{3}$$

where S(r) is an explicit source or sink of carriers (due to R-G processes, optical excitation, etc.) and [G] and [R] are M x M matrices that describe the "generation" and "recombination" of current in a bin due to in-scattering and out-scattering from/to other bins.

Equations (1) - (3) are an original re-formulation of the Boltzmann equation. Their advantage comes from the fact that the $[\mu]$, [D] matrices are field-independent and can be directly related to the scattering matrix of an infinitesimally thin slab. As a consequence, they can be pre-computed and stored. (The same applies to [G], [R] and [S].) The advantage of this technique over scattering matrices is that no assumptions about a spatial discretization are made; the resulting equations are in differential form. By summing the currents in all bins, eq. (1) can be re-expressed as a conventional macroscopic DD equation. By using coarse description of momentum space (e.g. spherical harmonics), off-equilibrium transport can be treated. Finally, by using a fine discretization of k-space, the full Boltzmann equation can be solved. Since it is written in drift-diffusion form, well-developed numerical methods should be applicable at each level of the hierarchy. The approach, therefore, provides a unified description of transport from a macroscopic level to a very detailed level.

In this poster we present the formulation, discuss how the mobility matrix and other matrices are evaluated from scattering matrices, and discuss solution methods for the bulk and for devices.

Modeling of Hot Carrier Effects in Semiconductor Lasers

Valery I. Tolstikhin and Theo G. van de Roer

Faculty of Electrical Engineering, Telecommunication Technology and Electromagnetics, Eindhoven University of Technology, P.O. Box 513, 5600 MB Eindhoven, The Netherlands

Hot carrier effects are becoming generally accepted as an important factor in semiconductor lasers, particularly in the long-wavelength ones. Such phenomena as a saturation of gain and enhancement of Auger recombination, intervalence band absorption and leakage currents, which eventually limit the device performance, e.g. direct modulation speed, all are attributed to the carrier heating within the laser active layer (AL). On the other hand, gain-switching via controllable heating of the AL electron-hole plasma seems to be a very promising new option for a high-speed modulation. Despite of the hot carrier effects are emerging to be critical for modern lasers and potentially useful for new generation devices, neither physics behind them is completely understood nor comprehensive model of a semiconductor laser under the carrier heating conditions is developed so far. Particularly, carrier transport over the laser structure resulting in a carrier and energy injection into the AL remains still poorly investigated. In the present paper, on the basis of the earlier proposed approach which considers the laser AL as a nonequilibrium system consisting of the thermalized carriers, LO-phonons and guided photons [1], the physical models of a dual - carrier and energy - injection are discussed with respect to some laser devices with both the bulk and quantum well ALs.

In a conventional double heterostructure laser diode with the bulk AL, the energy injection rate, Q, is a predetermined function of the carrier injection rate, J, which is found analytically assuming the thermionic mechanism of the electron transport over the heterojunction and close-fitting space charge regions. An approach employed to solve the relevant transport problem takes into account the injection current dependent band bending at either heterojunction and the real space transfer of electrons via the side (L, X) valleys.

In a bulk AL three-terminal laser structure, recently proposed for a high-speed, low-chirp modulation using variable carrier heating [2], the electron contribution to Q can be tuned independently on J, via controllable change the energy of injected electrons, ε_{cJ}, which ultimately is the destiny of this structure. Here, the transport problem for hot electrons travelling over the high electric field region just above the AL is solved numerically, by using the hydrodynamic approach and also the Monte Carlo simulator. All the relevant scattering mechanisms as well as nonparabolicity of the multi-valley conduction band in a hot electron launcher are taken into account resulting in an accurate computation of the energy ε_{cJ} as a function of a drive voltage.

In a separate-confinement heterostructure laser diode with the quantum well AL, neither electron nor hole contributions to Q is directly related to J since the thermalization and energy relaxation of the carriers injected into the barriers is prior to their capture by the quantum well. Carrier and energy transport over the barriers is considered in dependence on the relation between the characteristic time-constants of these processes, which results in an analytically solvable dual - carrier and energy - diffusion model when the thermalization is the fastest one.

The modeling examples, including transport solutions for discussed laser structures as well as their stationary characteristics and modulation responses under the carrier heating conditions, are given for GaAlAs/GaAs, InGaAsP/InP and InGaAlAs/InP devices emitting in 0.85 or 1.55 mµ wavelengths.

References

[1]   V. I. Tolsikhin and M. Willander, *IEEE J. Quantum Electron.*, Vol. 31, pp. 814-833 (1995).
[2]   V. I. Tolsikhin and M. Willander, *Proceed. SPIE*, Vol. 2693, pp. 534-544 (1996).

Quadratic Electron Wind in Electromigration

Alfred M. Kriman,[1] R. Frankovic[2] and G. H. Bernstein[2]

[1]*Dept. of Electrical Engineering, Univ. of Notre Dame, IN (on leave from SUNY Buffalo)*

[2]*Dept. of Electrical Engineering, Univ. of Notre Dame, IN.*

Electromigration (EM), observed in liquid metal isotope separation, Blech edge displacement, and other experiments, can be understood in terms of an electron wind force acting on ions. This force is theoretically linear in the electron current density, as confirmed by the inverse first-power dependence of critical Blech length on current density. This linear dependence appears to be broadly inconsistent with studies of integrated circuit interconnect failure by EM, usually described by an Arrhenius rate law (Black's equation). A number of explanations have been offered to explain the inconsistency, all based essentially on a linear electron wind. Micron-scale Cu wires have been shown to exhibit linear electron wind (standard Blech length behavior). However, recent experiments in which EM void formation is seeded are also not explained by a linear electron wind, instead showing void formation away from the high-current regions. This paper presents calculations in support of a consistent explanation of the contradictory data. It is observed that in the interconnect experiments, the effect of linear electron wind is to produce an ion flow without accumulation. Qualitatively, Black's-Law behavior can be explained by the quadratic component of the electron wind that is dominant when the effects of the linear force cancel out. The seeded-EM experiments are simulated using two-dimensional hydrodynamics, with Schwartz-Christoffel transformations to account for the deformed initial shape of the wire. In these simulations, a quadratic electron wind reproduces the observed failure patterns. A physical basis is outlined for a quadratic component in the electron wind, based on a microscopic picture of electron-collision effects on ionic diffusion.

Semiclassical Many-body Simulation

Jae-Hyun Yu[1] and Alfred M. Kriman[2]

[1]Dept. of Electrical and Computer Engineering, SUNY Buffalo

[2]Dept. of Electrical Engineering, Univ. of Notre Dame, IN (on leave from SUNY Buffalo).

One of the principal tools of semiconductor transport simulation is the semiclassical approximation: position and momentum expectations evolving as a classical trajectory, obeying a Hamiltonian that incorporates the properties of an isolated quantum particle. Attempts to incorporate quantum many-body effects (exchange and correlation) beyond Pauli exclusion generally employ Green's-function approaches or methods of comparable difficulty. These methods are computationally expensive and are currently impractical for the simulation of realistic models of quantum devices. As an alternative, a semiclassical method has been developed which is similar in form and computational complexity to the ordinary single-particle semiclassical approximation, but which incorporates many-body corrections. These corrections are realized through momentum-dependent interparticle corrections to the potential and effective mass. This paper shows how these corrections realize Heisenberg uncertainty and the qualitative notion of "Pauli repulsion." The paper also describes simulations using this approach for two-particle, spin-dependent Coulomb scattering. "Exact" treatments that exist for these problems provide tests of the approximation, as well as constraints on it: While the general semiclassical formalism is fixed by the underlying quantum Hamiltonian, freedom in the selection of semiclassical wavepacket profile and scale defines a range of possible semiclassical Hamiltonians. Packet parameters are optimized on the basis of two-body scattering cross sections, with optimal packet size depending on the energy range simulated.

On the Numerical Simulation to a Thermistor Device

Charles Miller and Hong-Ming Yin

Department of Mathematics

University of Notre Dame

Notre Dame, IN 46556, USA.

In this paper we study the numerical simulation of a thermistor device. The mathematical model of the device consists of an elliptic and a parabolic equations which govern the electrical potential and the temperature in the device, respectively:

$$-\nabla[\sigma(u)\nabla\psi] = 0,$$
$$u_t - \nabla[k(u)\nabla u] = \sigma(u)|\nabla\psi|^2,$$

where ψ represents the electrical potential, u the tempearture, $k(u)$ and $\sigma(u)$ are the thermal and electrical conductivities, respectively.

Numerical solution will be calculated by using a finite difference method. In particular, we will show that the temperature may blow up (thermal runaway) for certain devices. The error estimate will also be discussed.

A 3D nonlinear Poisson-solver

Gyula Veszely
Departement of Electromagnetic Theory
Budapest Technical University
1521 Budapest, Hungary

The solution of the 3D nonlinear Poisson's equation is important in the modeling of semiconductor devices and quantum dashes and dots. A computer code was developed based on the finite-difference representation of the Laplace operator. The resulting equation with a matrix of 7 diagonals was solved by the generalization of the Stone's method. The algorithm is quite robust, so far no divergent example was found. Some results what are usefull in the theory of in semiconductor realized quantum dots are presented. The convergence properties of the method is examined. The maximum number of the unknowns achived so far is 120 000 on a HP APOLLO 715/33 workstation, but this number is not the upper limit.

Equilibrium Aspects of Quantum Dot Formation

István Daruka* and Albert-László Barabási**

Department of Physics, University of Notre Dame
Notre Dame, IN 46556

Self-assembling quantum dots (SAQDs) – i.e. islands with very narrow size distribution – can form in highly-mismatched heteroepitaxial growth. Although experimental interest in this area continues to be high, many important details of the process are still not understood. This talk will discuss the equilibrium aspects of heteroepitaxy in terms of an analytical model. Observed properties, such as the critical layer thickness, island size and island density, as well as two dimensional, Stranski-Krastanow, and Volmer-Weber growth modes and island ripening predicted by the model, will be described and compared with experimental results.
This work was done in collaboration with S. Lee and J. K. Furdyna.

*   Tel: 219-631-5976   Fax: 219-631-5952   E-mail: idaruka@tin.helios.nd.edu
** Tel: 219-631-5767   Fax: 219-631-5952   E-mail: alb@nd.edu

An Alternative Geometry for Quantum Cellular Automata

P. Douglas Tougaw, Paul Krause, Rachel Mueller, and Janelle Weidner
Department of Electrical and Computer Engineering
Valparaiso University
Valparaiso, IN 46383

Abstract

We examine an alternative layout geometry for the quantum cellular automata (QCA) architecture. In the traditional QCA geometry, all of the cells are placed in a single plane, so that each cell interacts with a particular neighbor along one of its edges[1-4]. By rotating the cells out of the plane, we have made it possible for neighbors to interact Coulombically along all four of their edges at once.

This increased interaction leads to a more bistable cell-cell response function for a given tunneling coefficient. In addition, the eigenvalue splitting between the ground state and the first excited state increases by 50%. This splitting of the excited state from the ground state determines the maximum operating temperature and the switching speed for QCA cells, so we also expect to see a significant improvement in those areas.

A binary wire composed of rotated cells will alternate polarization direction with each cell, so it is possible to invert a signal by including an odd number of cells in a wire. We have also designed a majority logic gate using these rotated cells, so the alternative geometry should have a functionality equivalent to that of the traditional geometry.

[1] C. S. Lent, W. Porod, P. D. Tougaw, *Appl. Phys. Lett.* **62**, 714 (1993).

[2] C. S. Lent, et al., *Nanotechnology* **4**, 49 (1993).

[3] P. D. Tougaw, C. S. Lent, W. Porod, *J. Appl. Phys.* **74**, 3558 (1993).

[4] C. S. Lent and P. D. Tougaw, *J. Appl. Phys.* **74**, 6227 (1993).

Energy Dissipation in Quantum-dot Cellular Automata

John Timler and Craig S. Lent
Department of Electrical Engineering
University of Notre Dame
Notre Dame, IN 46556

ABSTRACT

Quantum functional devices will need to be coupled in new architectures to become useful technologically in the next century. We discuss a new paradigm for computing based on connecting quantum devices in a cellular automata (CA) architecture — quantum-dot cellular automata (QCA). Computing in such a paradigm is edge-driven. Input, output, and power are delivered at the edge of the array only; no direct flow of information or energy to internal cells is required. Computing in this paradigm is also computing with the ground-state. The architecture is so designed that the ground state configuration of the array, subject to boundary conditions determined by the input, yields the computational result.

We have examined a specific realization of these ideas using two-electron cells composed of quantum dots, which is within the reach of current fabrication technology. The charge density in the cell is very highly polarized (aligned) along one of the two cell axes, suggestive of a two-state CA. The polarization of one cell induces a polarization in a neighboring cell through the Coulomb interaction in a very nonlinear fashion.[1,2] This basic interaction is exploited to make QCA wires[3] which transmit binary information encoded in the polarization state of the quantum cells. More complex devices such as adders and other digital logic gates can be constructed.[4]

We have previously examined the dynamics of QCA arrays in the regime of negligible energy dissipation for which the Schrödinger equation is an adequate description.[5] We have also demonstrated the utility of adiabatic switching of QCA arrays. Here we examine the effects of energy dissipation during the switching event itself. We model the dissipation using a coherence vector approach derived from the density matrix. Generalized Bloch equations describe the time-evolution of the cellular array. We explore the effect of dissipation on metastable bottlenecks and as a refinement of the adiabatic switching approach.

[1] Craig S. Lent, P. Douglas Tougaw, Wolfgang Porod, and Gary H. Bernstein, *Nanotechnol.* **4**, 49 (1993).

[2] Craig S. Lent and P. Douglas Tougaw, *J. Appl. Phys.*, **74**, 6227 (1993).

[3] P. Douglas Tougaw, Craig S. Lent, and Wolfgang Porod, *J. Appl. Phys.* **74**, 3558 (1993).

[4] P. Douglas Tougaw and Craig S. Lent, *J. Appl. Phys.* **75**, 1818 (1994).

[5] P. Douglas Tougaw and Craig S. Lent, *J. Appl. Phys.* **80** 4722, (1996).

WE REQUEST A POSTER PRESENTATION

Electrostatic formation of coupled quantum dots*

Per Hyldgaard[†], Henry K. Harbury[‡] and Wolfgang Porod[†]

University of Notre Dame

Notre Dame, IN 46556

Cells of coupled quantum dots may serve in a quantum-dot cellular automata system [1] depending on the single-electron charging energy E_C and inter-dot tunneling rate γ. A two-dimensional numerical study [2] demonstrated gate-controlled confinement of even just a few electrons in a single dot realized in a GaAs/AlGaAs heterostructure. We present here a *three-dimensional* numerical investigation of *coupled* quantum dots allowing estimates for both E_C and γ.

The schematics below shows a gated heterostructure realization of two coupled quantum dots. A 30–40 nm layer of delta-doped AlGaAs caps the GaAs substrate and attracts a two-dimensional electron gas at the GaAs/GaAlAs interface. A positive bias at enhancement gates 'E' combined with a negative bias at surrounding depletion gate 'D' traps electrons within an elongated quantum dot (light grey area.) The barrier gate 'B' allows a controlled transition to the pair of *coupled* dots.

We obtain for this structure the fully three-dimensional finite-element solution for the electrostatic potential on a non-uniform tetrahedral mesh assuming a Thomas-Fermi charge model. We employ Newton-Raphson iteration and solve the linerized system using the sparse-matrix quasi-minimum residual (QMR) method [3]. From the calculated potential we provide estimates for the single-electron charging energy E_C and the inter-dot tunneling rate γ.
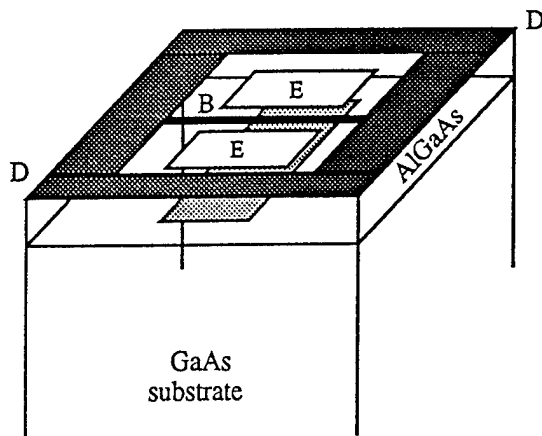
We calculate the effective electron confinement for both the extended quantum dot (light grey area) defined by enhancement gates 'E' and surrounding depletion gate 'D' as well as for the *coupled* quantum dot system arising with a finite bias at gate 'B'.

[1] C. S. Lent *et al.*, *Nanotechnology* 4, 49 (1993).

[2] M. Chen *et al.*, *J. Appl. Phys.* **78**, 1050 (1995).

[3] R. W. Freund *et al.*, *Numerische Mathematik*, **60**, 315 (1991).

"A Novel Method for Computing Particle Distributions"

Fred H. Schlereth
233 Link Hall
Syracuse University
Syracuse, NY 13244
schleret@cat.syr.edu
FAX 315-443-2583

We describe a novel method for determining the distribution of particles in scattering and absorbing media which is well suited to distributed computation. Applications include ion implantation in semiconductors and photons in dispersive media. The algorithm is based on the solution of the diffusion equation using relaxation and is based on a standard discrete approximation to the partial differential equation.

We extend the standard relaxation method by assuming the flux in each cell to be a vector of four or six components, depending on whether a 2D or 3D simulation is desired. For the 2D case, the flux in each cell is assumed to be a vector of four components. $F(i,j) = [f^n, f^e, f^s, f^w]^T$. In this case the relaxation equations for the directed flow take the following form. $4*F_{ij}(n+1) = [A_t]*[f^n_{i,j-1}(n), f^e_{i+1,j}(n), f^s_{i,j+1}(n), f^w_{i-1,j}(n)]^T$. $[A_t]$ is a transmission matrix defining the path of the particles in the medium. For example, if $[A_t]$ is the identity matrix then the radiation is constrained to flow along the path in which it was initially directed. The transmission matrix for other conditions depends on the physical mechanisms governing the flow of particles in the medium.

We have used this method to simulate photon motion in dispersive media with good results. For example, a simulation of a 3D volume of size 81x81x60 takes less than 30 minutes for an error of 0.1% and 60 minutes for an error of 0.0001% on a high speed workstation. Analysis of the code indicates that it will run with high efficiency on a parallel distributed architecture.

Nonperturbative Many Electron Approach Based on the Representation of Scattering States for Simulating Optoelectronic Devices using Laser-Assisted Field Emission

Andres J. Barrios[1], Valery G. Valeyev[2], Mark J. Hagmann[1,3], and Carolyne M. Van Vliet[1]
[1]Department of Electrical and Computer Engineering, Florida International University, Miami, FL 33199; [2]Department of Physical Electronics, Bashkir State University, 32 Frunze Str., Ufa, 450074 Russia; [3]Corresponding author, Phone: 305-348-3017, FAX: 305-348-3707, E-mail: HAGMANN@ENG.FIU.EDU

Recent simulations and preliminary experiments [1] suggest that a resonant interaction of tunneling electrons with optical fields [2] may be applied to gate field emission current at extremely high frequencies by means of amplitude modulated, pulsed, or optically-mixed lasers. Thus far, simulations of laser-assisted field emission have been limited to 1) one-particle solutions, which neglect all many-particle effects, 2) the transfer-Hamiltonian method, which is not gauge invariant and assumes that the electrons are in equilibrium at a definite temperature, 3) the nonequilibrium Keldysh Green function diagram technique applied with perturbation, which is limited to weak electromagnetic fields, and 4) density functional theory.

A new many-electron approach to the problem of tunneling in condensed systems has been described [3] which is based on the Hamiltonian of a tunnel junction in the representation of scattering states. This method is not limited to weak coupling, but may be used to calculate the elastic tunneling current explicitly for coupling of arbitrary strength. This procedure is gauge-invariant, suitable for nonequilibrium as well as equilibrium processes, and may be formulated to include the effects of electron scattering by other electrons as well as by phonons and impurities.

We have extended the earlier analysis by Valeyev [3] to include a coherent electromagnetic wave as well as the static potential at a metal surface in order to simulate laser-assisted field emission. The kinetic equation for the one-electron density matrix is derived in the formalism of the nonequilibrium Keldysh Green function diagram technique [4]. However, in the present method the full orthonormalized set of scattering states is obtained for this system without the use of perturbation. The Hamiltonian is developed in the representation of this new basis, and the current operator is constructed in terms of the one-electron scattering matrix for electron scattering on the potential profile in the presence of the electromagnetic wave. The first applications of this new method to the simulation of optoelectronic devices using laser-assisted field emission will be described.

1. M. J. Hagmann and M. Brugat, J. Vac. Sci. Technol. B 15 (in press, March/April, 1997).
2. M. J. Hagmann, J. Appl. Phys. 78, 25 (1995).
3. V. G. Valeyev, Surf. Sci. 266, 274 (1991).
4. L. V. Keldysh, Sov. Phys. JETP 20, 1018 (1965).

Electron transport in one-dimensional magnetic superlattices

Zhen-Li Ji* and D. W. L. Sprung

Department of Physics and Astronomy, McMaster University, Hamilton, Ontario, L8S 4M1 Canada

A quantum wire of uniform width with a finite number of *electric* barriers is a one-dimensional (1D) superlattice because there is no channel coupling: the longitudinal motion is strictly 1D. In this paper we consider the corresponding *magnetic* superlattice. That electron transmission is inevitably much more complex, can be understood from several viewpoints. The Lorentz force on an electron couples the longitudinal and transverse motion, leading to channel coupling that makes the problem strictly 2D. If one thinks in terms of an effective static potential, this will depend on the channel and on the electron energy.

We show, in Fig. 1, that conductance is quantized in steps of $2e^2/h$, but rather than a staircase one finds that the conductance steps up or down as the Fermi energy (E_F) is varied. Mini-bands develop but the number of maxima is not tied directly to the number N of barriers in the superlattice, as in the *electric* case [1, 2]. Further, conductance plateaus are not due to unit conductance in each open channel, but rather occur as the sum of several partially open channels. See for example the region near $9 meV$ in the figure.
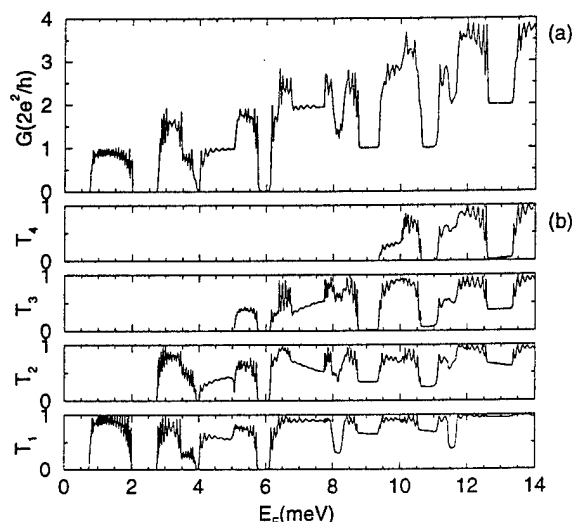

Fig. 1. (a) Conductance as a function of Fermi energy E_F for a finite period superlattice with 16 unit cells. (b) Transmission coefficients of individual modes for the magnetic modulated quantum wire.

The non-monotonic conductance quantization persists in the case of varying *magnetic* modulation amplitude B_m. The conductance plateaus step down or up by one or two units of $2e^2/h$ as B_m is increased. In contrast, the conductance for a 1D *electric* superlattice steps down monotonically as the traveling modes in the leads are blocked by the potential barriers with increasing *electric* modulation amplitude V_m. Current flows confirm that the electron transport in this *electric* superlattice is equivalent to a one-dimensional case, in contrast to the *magnetic* one, in which it is not.

This complex behaviour suggest that the experimental study of 1D *magnetic* superlattices should be very interesting. Several methods are available to produce such devices, including the laying down of patterned superconducting stripes on top of a gated device.

* Corresponding author. Electronic mail: zheji@physun.physics.mcmaster.ca FAX: (905) 546-1252

[1] D.W.L. Sprung, Hua Wu and J. Martorell, Am. J. Phys. **61**, 310 (1993).

[2] M. Leng and C. S. Lent, Phys. Rev. B **50**, 10 823 (1994).

Boundary Condition for the Modeling of Open-Circuited Devices in Non-Equilibrium

Joseph W. Parks, Jr. and Kevin F. Brennan
School of Electrical and Computer Engineering
Georgia Institute of Technology
Atlanta, GA 30332-0250

Abstract

In this paper, we introduce a boundary condition specifically designed to model open-circuited devices in a drift-diffusion/hydrodynamic device simulator. Other simulation techniques have relied on an external circuit model to regulate the current flow out of a contact thus allowing the potential to remain the controlled variable at the boundary. The limitations of these methods become apparent when modeling open-circuited devices with an exceptionally small or zero output current. In this case, using a standard ohmic-type Dirichlet boundary condition would not yield satisfactory results and attaching the device to an arbitrarily large load resistance is physically and numerically unacceptable. This proposed condition is a true current controlled boundary where the external current is the specified parameter rather than the potential. Using this model, the external current is disseminated into electron and hole components relative to their respective concentration densities at the contact. This model also allows for the inclusion of trapped interface charge and a finite surface recombination velocity at the contact.

An example of the use of this boundary condition is performed by modeling a silicon avalanche photodiode operating in the flux integrating mode for use in an imaging system. In this example, the device is biased in steady-state to just below the breakdown voltage and then open-circuited. The recovery of the isolated photodiode back to its equilibrium condition is then determined by the generation lifetime of the material, the quantity of signal and background radiation incident upon the device, and the impact ionization rates.

Positron Slowing Down in Solids

N. Bouarissa

Physics Department, University of Setif 19000 - Algeria -

Abstract :

Results are presented from an investigation of the slowing down of positrons implanted into solids. The energy loss, stopping profiles, back scattered fraction and energy distribution of positrons with incident energies up to 10 keV are stochastically modelled with a Monte-Carlo frame work. The elastic scattering cross sections have been obtained from the modified Rutherford differential cross section. To model inelastic scattering, we have used Gryzinski's excitation function expressions. For elastic processes the polar scattering angle is computed by random sampling from the differential scattering cross section. However, for the inelastic ones, it is computed from the binary collision approximation. The incident particles are followed to an energy of 20 eV. Details of the model and the information it generates are presented. Calculations with normal and oblique angles of incidence have been made for positrons impinging on semi-infinite aluminium, copper and gold. Our simulated results for positron implantation and back scattering fractions are in very good agreement with the available experimental data, which confirms the validity of our model for describing transport of slow positrons in solids.

Modeling of Mid-Infrared
Multi-Quantum Well Lasers

A.D. Andreev

A.F. Ioffe Physico-Technical Institute of RAS
St. Petersburg 194021, Russia
FAX: 7-812-2471017; Phone: 7-812-2479367
e-mail: andreev@theory.ioffe.rssi.ru

Modeling of mid-infrared (2-5 um) III-V semiconductor multi-quantum well (MQW) lasers becomes more and more actual during last years. These lasers have a wide range of applications including laser radar systems, molecular spectroscopy and remote sensing. However, practical application of mid-infrared lasers is strongly limited by low operating temperature and low quantum efficiency of these lasers. Nevertheless it is possible to considerably improve the parameters of mid-infrared lasers by choosing the optimal structure parameters (QW width, barrier heights, strain and the number of QWs). The goal of this paper is model the performance of mid-infrared lasers with the aim of structures optimization. To model the threshold characteristics of these lasers we study the following elementary processes: Auger and radiative recombination of the excess carriers, interband absorption and the processes which lead to the carrier leakage out of the active region. The rates of the Auger processes have been calculated in the framework of multiband Kane model [1], taking account of light-heavy hole mixing and non-parabolicity of electron and hole spectrum. The threshold current is shown to be very sensitive to the variation of structure parameters. At definite values of these parameters the threshold current decreases and the internal quantum efficiency increases which is due to the suppression of the Auger process. The carrier distribution between quantum wells was calculated using drift-diffusion model. It is shown that threshold current has a minimum as a function of the number of QWs. The position of this minimum depends on QW and barrier widths, strain and temperature. It is demonstrated that the limiting operation temperature of mid-infrared MQW laser can be increased by choosing the optimal structure parameters.

[1] A.D. Andreev, G.G. Zegrya, Appl. Phys. Lett, v.70, N 5 (1997)

Computation of Auger Recombination Rates in Semiconductor Quantum Wells

A.D. Andreev

A.F. Ioffe Physico-Technical Institute of RAS
St. Petersburg 194021 Russia
FAX: 7-812-2471017; Phone: 7-812-2479367
e-mail: andreev@theory.ioffe.rssi.ru

The Auger recombination (AR) process is the main mechanism of non-radiative recombination of the excess carriers in semiconductor optoelectronic devices. Theoretical investigation of such processes is very important for further improvement of the device performance and characteristics. In this paper we present a novel approach for numerical calculation of the AR rates in semiconductor quantum wells (QW). This approach is based on semi-analytical calculation of the AR matrix element which allows to considerably reduce the time of AR rate computation. To calculate the AR rate dependencies on the structure parameters and composition, the carrier wave functions and the AR matrix element have been derived in the framework of multiband Kane model [1,2]. In this paper we have used 8x8 Kane model, but the calculation procedure can be easily extended to other multiband models. The matrix element of the Auger transition is expressed through the overlap integrals between initial and final states of particles participating in the Auger process. In order to considerably reduce the computation time, the analytical formulas for the overlap integrals have been derived. It is shown that the method of overlap integrals calculation proposed in this paper allows to obtain the dependencies of the overlap integrals on the QW parameters and strain. The rates of possible AR channels have been calculated in heterostructures with strained QWs based on InGaAsP quaternary alloy. It is shown that the total AR rate essentially depends on the QW parameters (QW width, barrier heights for electrons and holes, strain), but has a weak temperature dependence.

[1] A.D. Andreev, G.G. Zegrya, Appl. Phys. Lett, v.70, N 5 (1997)

[2] G.G. Zegrya, A.D. Andreev, Appl.Phys. Lett, v. 67, N. 18, 2681 (1995)